Application to Food Standards Australia New Zealand for the Inclusion of Herbicide-Tolerant KWS20-1 Sugar Beet in *Standard 1.5.2 - Food Produced Using Gene Technology*

Submitted by:

Bayer CropScience Pty Ltd
Level 4, 109 Burwood Rd
Hawthorn, Victoria 3122

7 March, 2024

TABLE OF CONTENTS

LIST OF FIGURES

LIST OF TABLES

CHECKLIST

General Requirements (3.1.1)	Page No.
A Form of application	
☑ *Application in English*	
☑ *Executive Summary (separated from main application electronically)*	
☑ *Relevant sections of Part 3 clearly identified*	
☑ *Pages sequentially numbered*	
☑ *Electronic copy (searchable)*	
☑ *All references provided*	
☑ **B Applicant details**	*Page 1*
☑ **C Purpose of the application**	*Page 1*
D Justification for the application	
☑ *Regulatory impact information*	*Page 2*
☑ *Impact on international trade*	*Page 3*
E Information to support the application	
☑ *Data requirements*	*Page 3*
F Assessment procedure	
☑ *General*	*Page 3*
☐ *Major*	
☐ *Minor*	
☐ *High level health claim variation*	
G Confidential Commercial Information	
☑ *CCI material separated from other application material*	
☐ *Formal request including reasons*	
☐ *Non-confidential summary provided*	
H Other confidential information	
☑ *Confidential material separated from other application material*	
☐ *Formal request including reasons*	
I Exclusive Capturable Commercial Benefit	

☑ *Justification provided*	*Page 4*
J International and Other National Standards	
☑ *International standards*	*Page 4*
☑ *Other national standards*	*Page 4*
☑ **K Statutory Declaration**	*Page 4*
L Checklist/s provided with Application	
☑ *3.1.1 Checklist*	*Page xi*
☑ *All page number references from application included*	
☑ Any other relevant checklists for Sections 3.2 – 3.7	*Checklist 3.5.1*

Foods Produced using Gene Technology (3.5.1)	
☑ A.1 Nature and identity	*Page 6*
☑ A.2 History of use of host and donor organisms	*Page 7*
☑ A.3 Nature of genetic modification	*Page 10*
☑ B.1 Characterisation and safety assessment of new substances	*Page 64*
☑ B.2 New proteins	*Page 124*
☑ B.3 Other (non-protein) new sustances	*Page 161*
☑ B.4 Novel herbicide metabolites in GM herbicide-tolerant plants	*Page 161*
☑ B.5 Compositional assessment	*Page 167*
☑ C Information related to the nutritional impact of the food produced using gene technology	*Page 183*
☑ D Other information	*Page 183*

ABBREVIATIONS AND DEFINITIONS

AA	Amino acid
ADF	Acid detergent fiber
APHIS	Animal and Plant Health Inspection Service
CFR	Code of Federal Regulations
CP4 EPSPS	5-enolpyruvylshikimate-3-phosphate synthase
CPF	Cloned PCR fragments
CTP	Chloroplast transit peptide
DAP	Days after planting
DMO	Dicamba mono-oxygenase
DNA	Deoxyribonucleic acid
dw	Dry weight
DWCF	Dry weight conversion factor
E. coli	Escherichia coli
ELISA	Enzyme-linked Immunosorbent Assay
E-score	Expectation score
FA	Fatty acid
FDA	Food and Drug Adminstration (U.S.)
FFDCA	Federal Food, Drug and Cosmetic Act
FOIA	Freedom of Information Act
FSANZ	Food Standards Australia New Zealand
fw	Fresh weight
GE	Genetically engineered
GLP	Good Laboratory Practice
GRAS	Generally Recognized as Safe
ILSI	International Life Science Institute
KASP	Kompetitive Allele Specific PCR
kb	Kilobase
OECD	Organisation for Economic Co-operation and Development
PAT	Phosphinothricin N-acetyltransferase
RSR	Regulatory Status Review
T-DNA	Transfer DNA
USDA	United States Department of Agriculture
UTR	Untranslated region

PART 1 GENERAL INFORMATION

B Applicant Details

(a) Applicant's name/s	Bayer CropScience Pty Ltd
(b) Name of contact person	[redacted]
(c) Address (street and postal)	Level 4, 109 Burwood Road, Hawthorn, Victoria 3122
(d) Telephone number	[redacted]
(e) Email address	[redacted]
(f) Nature of applicant's business	Technology Provider to the Agricultural and Food Industries
(g) Details of other individuals, companies or organisations associated with the application	KWS SAAT SE & Co. KGaA Grimsehlstraße 31, D-37574 Einbeck, Germany Contact person: [redacted] Email address: [redacted] Telephone number: [redacted]

C Purpose of the Application

This application is submitted to Food Standards Australia New Zealand by Bayer CropScience Proprietary Limited on behalf of Bayer Group and KWS.

The purpose of this submission is to make an application to vary **Standard 1.5.2** – *Food Produced Using Gene Technology* of the *Australia New Zealand Food Standards Code* to seek the addition of herbicide-tolerant sugar beet KWS20-1 and products derived from herbicide-tolerant sugar beet KWS20-1 (hereafter referred to as KWS20-1 sugar beet) to Schedule 26-3 Food produced using gene technology of plant origin (see below).

Commodity	Food derived from:
Sugar beet (i.e., refined sugar)	Herbicide-tolerant KWS20-1 sugar beet

D Justification for the Application

(a) The need for the proposed change

Bayer and KWS have jointly developed biotechnology-derived sugar beet KWS20-1 that is tolerant to in-crop applications of dicamba, glufosinate and glyphosate herbicides. KWS20-1 sugar beet contains a demethylase gene from *Stenotrophomonas maltophilia* that expresses a dicamba mono-oxygenase (DMO) protein to confer tolerance to dicamba herbicide, a gene from *Streptomyces viridochromogenes* that expresses the phosphinothricin N-acetyltransferase (PAT) protein to confer tolerance to glufosinate-ammonium herbicide, and the *cp4 epsps* coding sequence isolated from *Agrobacterium* sp. strain CP4 that expresses the 5-enolpyruvylshikimate-3-phosphate synthase (CP4 EPSPS) protein to confer tolerance to glyphosate herbicide.

(b) The advantages of the proposed change over the status quo, taking into account any disadvantages

KWS20-1 sugar beet will offer growers multiple choices for effective weed management including tough-to-control and herbicide-resistant broadleaf and grass weeds. The flexibility to use combinations of any of these three herbicides representing multiple mechanisms-of-action provides an effective and more durable weed management system for sugar beet production. The best management practices for minimizing the development of herbicide-resistant weeds involve implementing diversified weed management programs, which include using multiple herbicides with different mechanisms-of-action either in mixtures, sequential application or in rotation and other recommended integrated weed management principles. Therefore, KWS20-1 sugar beet will provide sugar beet growers an efficient and flexible weed management system that enables: 1) an opportunity to delay selection for further resistance to glyphosate and other herbicides that are important in crop production; 2) excellent crop tolerance to dicamba, glufosinate and glyphosate; and 3) additional weed management tools and flexibility to enhance, maintain or improve sugar beet yield and quality to meet the growing needs of the food, feed and industrial markets.

D.1 Regulatory Impact Information

D.1.1 Costs and benefits of the application

If the proposed variation to permit the sale and use of food produced from KWS20-1 sugar beet is approved, possible affected parties may include consumers, industry sectors and government. The consumers who may be affected are those that consume food containing ingredients derived from sugar beet. Industry sectors affected may be food importers and exporters, distributors and retailers, processors and manufacturers. Lastly, government enforcement agencies may be affected.

A cost/benefit analysis quantified in monetary terms is difficult to determine. In fact, most of the impacts that need to be considered cannot be assigned a dollar value. Criteria would need to be deliberately limited to those involving broad areas such as trade, consumer information and compliance. If the proposed variation is approved:

(a) The cost and benefits to the consumers e.g. health benefits:

- There would be benefits in the broader availability of sugar beet-derived refined sugar products.
- There is unlikely to be any significant increase in the prices of foods if manufacturers are able to use comingled sugar beet-derived refined sugar products.
- Consumers wishing to do so will be able to avoid GM sugar beet-derived refined sugar products as a result of labeling requirements and marketing activities.

(b) The costs and benefits to industry and business in general, noting any specific effects on small businesses e.g. savings in production costs:

- Sellers of processed foods containing sugar beet-derived refined sugar derivatives would benefit as foods derived from KWS20-1 sugar beet would be compliant with the Code, allowing broader market access and increased choice in raw materials. Retailers may be able to offer a broader range of sugar beet-derived refined sugar products or imported foods manufactured using sugar beet derivatives.
- Possible cost to food industry as some food ingredients (i.e., refined sugar) derived from KWS20-1 sugar beet would be required to be labelled.

(c) the costs and benefits to government e.g. increased regulatory costs:

- Benefit that if KWS20-1 sugar beet was detected in food products, approval would ensure compliance of those products with the Code. This approval would ensure no potential for trade disruption on regulatory grounds.
- Approval of KWS20-1 sugar beet would ensure no potential conflict with WTO responsibilities.
- In the case of approved GM foods, monitoring is required to ensure compliance with the labeling requirements, and in the case of GM foods that have not been approved, monitoring is required to ensure they are not illegally entering the food supply. The costs of monitoring are thus expected to be comparable, whether a GM food is approved or not.

D.1.2 Impact of International Trade

If the proposed variation to permit the sale and use of food produced from KWS20-1 sugar beet was rejected it would result in the requirement for segregation of any sugar beet derived products containing KWS20-1 sugar beet-derived sugar from those containing approved sugar beet or conventional sugar beet-derived sugar, which would be likely to increase the costs of imported sugar beet-derived foods.

It is important to note that if the proposed variation is approved, KWS20-1 sugar beet will not have a mandatory introduction. The consumer will always have the right to choose not to use/consume this product.

E Information to support the application

See Part 2.

F Assessment procedure

Bayer CropScience and KWS are submitting this application in anticipation that it will fall within the General Procedure category.

G Confidential commercial information (CCI)

Any CCI information has been identified as CCI and has been treated according to the FSANZ Application Handbook 2019.

H Other confidential information

Any non CCI information that Bayer CropScience and KWS want to be treated as confidential has been treated according to the FSANZ Application Handbook 2019.

I Exclusive capturable commercial benefit

This application is likely to result in an amendment to the Code that provides exclusive benefits and therefore Bayer CropScience and KWS intend to pay the full cost of processing the application.

J International and other national standards

J.1 International standards

Bayer makes all efforts to ensure that safety assessments are aligned, as closely as possible, with relevant international standards such as the Codex Alimentarius Commission's *Principles for the Risk Analysis of Foods Derived from Modern Biotechnology* and supporting *Guideline for the Conduct of Food Safety Assessment of Foods Derived from Recombinant-DNA Plants* (Codex Alimentarius, 2009).

In addition, the composition analysis is conducted in accordance with OECD guidelines and includes the measurement of OECD-defined sugar beet nutrients and a secondary metabolite based on conventional commercial sugar beet varieties (OECD, 2002a).

J.2 Other national standards or regulations

Bayer and KWS have submitted a food and feed safety and nutritional assessment summary for KWS20-1 sugar beet to the United States Food and Drug Administration (FDA) and has also requested a Regulatory Status review (RSR) for a determination of plant pest risk potential of KWS20-1 sugar beet, including all progenies derived from crosses between KWS20-1 sugar beet and conventional sugar beet, or deregulated biotechnology-derived sugar beet by the Animal and Plant Health Inspection Service (APHIS) of the U.S. Department of Agriculture (USDA).

Consistent with our commitments to the Excellence Through Stewardship® (ETS) Program[1], regulatory submissions have been or will be made to countries that import significant food and feed products derived from North America sugar beet and have functional regulatory review processes in place.

K Statutory declaration

See Part 3.

[1] Excellence Through Stewardship is a registered trademark of Excellence Through Stewardship, Washington, DC. (http://www.excellencethroughstewardship.org)

L Checklist

The checklists can be found on page xi.

PART 2 SPECIFIC DATA REQUIREMENTS FOR FOODS PRODUCED USING GENE TECHNOLOGY

A. TECHNICAL INFORMATION ON THE FOOD PRODUCED USING GENE TECHNOLOGY

A.1 Nature and Identity of the Genetically Modified Food

A.1(a) A description of the GM organism from which the new GM food is derived

Bayer and KWS have jointly developed biotechnology-derived sugar beet KWS20-1 that is tolerant to in-crop applications of dicamba, glufosinate and glyphosate herbicides. KWS20-1 sugar beet contains a demethylase gene from *Stenotrophomonas maltophilia* that expresses a dicamba mono-oxygenase (DMO) protein to confer tolerance to dicamba herbicide, a gene from *Streptomyces viridochromogenes* that expresses the phosphinothricin N-acetyltransferase (PAT) protein to confer tolerance to glufosinate-ammonium herbicide, and the *cp4 epsps* coding sequence isolated from *Agrobacterium* sp. strain CP4 that expresses the 5-enolpyruvylshikimate-3-phosphate synthase (CP4 EPSPS) protein to confer tolerance to glyphosate herbicide.

A.1(b) Name, line number and OECD Unique Identifier of each of the new lines or strains of GM organism from which the food is derived

In accordance with OECD's "Guidance for the Designation of a Unique Identifier for Transgenic Plants" KWS20-1 sugar beet has been assigned the unique identifier KB-KWS2Ø1-6.

A.1(c) The name the food will be marketed under (if known)

Sugar beet containing the transformation event KWS20-1 will be produced in North America There are currently no plans to produce this product in Australia or New Zealand. A commercial trade name for the product has not been determined at the time of this submission and will be available prior to commercial launch of the product in North America.

A.2 History of Use of the Host and Donor Organisms

A.2(a) For the donor organism(s) from which the genetic elements are derived:

A.2(a)(i) Any known pathogenicity, toxicity or allergenicity relevance to the food

A.2(a)(i)(i) Source of the *dmo* Gene Introduced into KWS20-1 Sugar Beet

The *dmo* gene is derived from the bacterium *Stenotrophomonas maltophilia* strain DI-6, isolated from soil at a dicamba manufacturing plant (Krueger *et al.*, 1989). *S. maltophilia* is ubiquitously present in the environment (Mukherjee and Roy, 2016), including in water and dairy products (Todaro *et al.*, 2011; Okuno *et al.*, 2018; An and Berg, 2018). These bacteria have been used as an effective biocontrol agent against plant and animal pathogensis (Mukherjee and Roy, 2016), and have antibacterial activity against both gram-positive and gram-negative bacteria (Dong *et al.*, 2015). *S. maltophilia* has been found in healthy individuals without any hazard to human health (Heller *et al.*, 2016; Lira *et al.*, 2017), although these bacteria can form biofilms that become resistant to antibiotics (Berg and Martinez, 2015; Brooke *et al.*, 2017). The opportunistic pathogenicity of *S. maltophilia* is mainly associated with hosts with compromised immune systems rather than with any specific virulence genes of these bacteria. Thus, documented occurrences of *S. maltophilia* infections have been limited to immune-compromised individuals in hospital settings (Lira *et al.*, 2017).

Other than the potential to become an opportunistic pathogen in immune-compromised hosts, *S. maltophilia* is not known for human or animal pathogenicity. *S. maltophilia's* history of safe exposure has been extensively reviewed during the evaluation of several dicamba-tolerant events with no safety or allergenicity issues identified by FSANZ or other regulatory agencies (e.g., MON 88701 cotton [A1080], MON 87708 soybean [A1063], MON 87419 maize [A1118] MON 87429 maize [A1192], and MON 94100 canola [A1216]).

A.2(a)(i)(ii) Identity and Source of the *pat* Gene Introduced into KWS20-1 Sugar Beet

The *pat* gene is derived from the bacterium *Streptomyces viridochromogenes* (Wohlleben *et al.*, 1988). *Streptomyces* species are widespread in the environment and present no known allergenic or toxicity issues (Kutzner, 1981; Kämpfer, 2006), though human exposure is quite common (Goodfellow and Williams, 1983). *S. viridochromogenes* is not considered pathogenic to plants, humans or other animals (Locci, 1989; Cross, 1989; Goodfellow and Williams, 1983). *S. viridochromogenes* is widespread in the environment and the history of safe use is discussed in Hérouet *et al.* (2005). This organism has been extensively reviewed during the evaluation of several glufosinate-tolerant events (e.g., A2704-12 and A5547-127 soybean [A481], MON 87419 maize [A1118] and MON 87429 maize [A1192]) with no safety or allergenicity issues identified by FSANZ or other regulatory agencies.

A.2(a)(i)(iii) Identity and Source of the *cp4 epsps* Gene Introduced into KWS20-1 Sugar Beet

The donor organism for *cp4 epsps* is *Agrobacterium* sp. strain CP4 (Padgette *et al.*, 1996). *Agrobacterium* species are not known for human or animal pathogenicity and are not commonly allergenic (FAO-WHO, 1991; Mehrotra and Goyal, 2012; Nester, 2015). The history of safe use of the CP4 EPSPS protein from *Agrobacterium* sp. strain CP4 has been previously reviewed as a part of the safety assessment of this donor organism with FSANZ regarding glyphosate-tolerant biotech crop events of MON 89788 soybean [A592], MON 88302 canola [A1071], NK603 maize [A416], MON 88017 maize [A548], MON 87411

maize [A1097], H7-1 sugar beet [A525], J101/163 alfalfa [A575], and MON 88913 cotton [A553].

A.2(a)(i)(iv) Identity and Source of Other Genetic Material Introduced into KWS20 1 Sugar Beet

Plasmid vector PV-BVHT527462 was used for the transformation of conventional sugar beet to produce KWS20-1 sugar beet. PV-BVHT527462 contains one T-DNA delineated by Left and Right Border regions. The T-DNA contains the *dmo*, *pat and cp4 epsps* expression cassettes.

The *dmo* expression cassette is regulated by the *DaMV-1* enhancer from Dalia Mosaic Virus, *Ubq-Cm1* promoter, 5′ UTR and intron from *Cucumis melo*, the *RbcS (Ps)* targeting sequence from *Pisum sativum*, and the *guf-Mt2* 3′ untranslated region from *Medicago truncatula*. The *pat* expression cassette is regulated by the *Cab-At1* promoter and 5′ untranslated region from *Arabidopsis thaliana*, and the *Hsp20-Mt1* 3′ untranslated region from *Medicago truncatula.* The *cp4 epsps* expression cassette is regulated by the *SAM2-Cm1* intron, 5' untranslated region (UTR) and promoter from *Cucumis melo*, the *CTP2* targeting sequence from *A. thaliana* and *guf-Mt1* 3′ untranslated region from *Medicago truncatula*.

Dalia Mosaic Virus, *Cucumis melo, Pisum sativum, Medicago truncatula, and Arabidopsis thaliana* have a long history of safe use. Dalia Mosaic Virus is a species of virus within the *Caulimovirus* genus. This genus of mosaic viruses is associated with staples of the human diet, such as soybean, and their genetic elements have been utilized in GM events previously. *Cucumis melo* (melon) *Pisum sativum* (pea) have been staples of the human diet for centuries, with many cultivars being consumed directly or in a multitude of food and animal feed products. Lastly, *Medicago truncatula, and Arabidopsis thaliana* are popular model organism in legume biology, plant biology and genetics, whose genomes have been extensively studied.

A.2(a)(ii) History of use of the organism in food supply or history of human exposure to the organism through other than intended food use (e.g. as a normal contaminant)

As described in Section A.2(a)(i), *Stenotrophomonas maltophilia* is ubiquitously present in the environment (Mukherjee and Roy, 2016), including in water and dairy products (Todaro *et al.*, 2011; Okuno *et al.*, 2018; An and Berg, 2018). It has been found in healthy individuals without any hazard to human health (Heller *et al.*, 2016; Lira *et al.*, 2017), although these bacteria can form biofilms that become resistant to antibiotics (Berg and Martinez, 2015; Brooke *et al.*, 2017).

Streptomyces viridochromogenes is widespread in the environment and presents no known allergenic or toxicity issues (Kutzner, 1981; Kämpfer, 2006), though human exposure is quite common (Goodfellow and Williams, 1983). *S. viridochromogenes* is not considered pathogenic to plants, humans or other animals (Locci, 1989; Cross, 1989; Goodfellow and Williams, 1983).

Agrobacterium species are not known for human or animal pathogenicity and are not commonly allergenic (FAO-WHO, 1991; Mehrotra and Goyal, 2012; Nester, 2015). The CP4 EPSPS protein from *Agrobacterium* sp. strain CP4 is one of the most widely used biotech proteins, the history of safety use of its donor organism has been extensively reviewed and approved worldwide.

A.2(b) For the host organism into which the genes were transferred:

A.2(b)(i) Its history of safe use for food

Sugar beet is not considered a common allergenic and toxic food and there have been no known reports of allergenic reactions to the consumption of sugar beet products. During the long history of safe use of sugar beet, there have been no reported anti-nutritional or other adverse effects to human or animal health (OECD, 2002a). Sugar beet is a specialty crop which goes through rigorous processing to produce sugar, molasses and pulp in a closed-loop production-processing system. As sugar beet roots are seldom used for food or feed as such, a distinction between nutrients and anti-nutrients in a toxicological sense is not made (OECD, 2002a).

In conclusion, an assessment of sugar beet suggests that the toxic or allergenic risk to humans is likely to be extremely low.

A.2(b)(ii) The part of the organism typically used as food

Sugar beet is mainly grown for its root that is used for the production of sugar. The sugar beet root provides valuable by-products after processing, including molasses and pulp that are used primarily as feed stuffs (OECD, 2001; OECD, 2002a).

A.2(b)(iii) The types of products likely to include the food or food ingredient

The main food source from sugar beet is the sugar (sucrose) recovered from the commercial processing. World-wide production of sugar from sugar beet is approximately 36 million tons per year (Walton, 2022), with the world-wide sugar consumption from all sources at about 22.0 kg of sugar per capita from 2018-2020 (OECD-FAO, 2021).

A.2(b)(iv) Whether special processing is required to render food safe to eat

The history and uses of sugar beet products by mankind have evolved extensively since the development of the sugar beet plant. Sugar beet root is seldom used directly for food or feed, but is processed into refined sugar for food, and molasses and pulp for feed uses. Given the long history of sugar beet development and the utilization of sugar beet root processed commodities for food and feed uses, several informational sources are available that provide detailed information on sugar beet processing technology, compositional considerations and quality parameters of sugar beet. The following documents are suggested: 1) Consensus Document on Compositional Considerations for New Varieties of Sugar Beet: Key Food and Feed Nutrients and Antinutrients (OECD, 2002a) and 2) Beet – Sugar Technology (McGinnis, 1982).

The commercial production of refined sugar from sugar beet has evolved greatly since the first factory was built in 1802. Today, several factory designs are utilized, with a typical processing line described in the OECD (2002a) document. Sugar beet processing occurs as follows: the harvested roots are washed to remove dirt and debris, followed by slicing of the root into sections, referred to as cossettes. The cossettes are extracted with water for about 100 minutes, at a temperature of about 70°C. The raw juice obtained from the extraction is purified with milk of lime and carbon dioxide. The resulting precipitate material, called carbonation sludge, is removed by filtration and pressed to yield carbonation lime. The filtered juice is called thin juice and is subsequently concentrated by evaporation to form thick juice. The evaporation process is performed in multi-stage evaporators operating at temperatures of 98-130°C under varying pressures. The resultant thick juice is further concentrated to yield crystal magma from

which crystalline sugar is removed by centrifugation, separating the syrup from the crystals. The crystals are dried, cooled and stored for further use. The remaining syrup, called molasses, is mainly used as animal feed or as a fermentation substrate. The fibrous material remaining from the extracted cossettes is called wet pulp. The pulp material can be dried to remove excess water and is commonly pelleted with added molasses for animal feed (OECD, 2002a).

A.3 The Nature of the Genetic Modification

KWS20-1 sugar beet was produced by *Agrobacterium*-mediated insertion of the transfer DNA (T-DNA) contained in the transformation plasmid vector PV-BVHT527462 into the sugar beet genome. This plasmid vector contains one T-DNA, which is delineated by Right and Left Border regions. The T-DNA contains the *dmo*, *pat* and *cp4 epsps* expression cassettes and the vector backbone contains the *aadA* expression cassette. During transformation, the T-DNA was inserted into the sugar beet genome. Subsequently, traditional breeding, segregation, selection and screening were used to isolate those plants that contain the T-DNA expression cassettes.

Characterization of the DNA insert in KWS20-1 sugar beet was conducted using a combination of Southern blotting, sequencing and polymerase chain reaction (PCR). The results of this characterization demonstrate that KWS20-1 sugar beet contains one copy of the intended T-DNA containing the *dmo*, *pat* and *cp4 epsps* expression cassettes integrated at a single locus that is stably inherited over multiple generations and segregates in multiple generations according to Mendelian principles. These conclusions are based on several lines of evidence:

- Molecular characterization of KWS20-1 sugar beet by Southern blot analyses demonstrated that KWS20-1 sugar beet contains a single, intended T-DNA insert. These Southern blot analyses provided a comprehensive assessment of KWS20-1 sugar beet to determine the presence and identity of sequences derived from plasmid vector PV-BVHT527462. These analyses demonstrate that KWS20-1 sugar beet contains a single T-DNA insert with no detectable backbone.

- Directed sequencing (i.e., locus-specific PCR, DNA sequencing and analyses) performed on KWS20-1 sugar beet was used to determine the complete sequence of the single T-DNA insert from plasmid vector PV-BVHT527462, the adjacent flanking genomic DNA, and the 5' and 3' insert-to-flank junctions. This analysis confirms that the sequence and organization of the T-DNA is identical to the corresponding region in the plasmid vector PV-BVHT527462 T-DNA.

- Furthermore, the genomic organization at the insertion site in KWS20-1 sugar beet was assessed by comparing the sequences flanking the T-DNA insert in KWS20-1 sugar beet to the sequence of the insertion site in conventional sugar beet. This analysis determined that no major DNA rearrangement occurred at the insertion site in KWS20-1 sugar beet upon DNA integration; although, a seven (7) bp deletion was observed at the site of T-DNA integration in KWS20-1 sugar beet.

- Generational stability analysis by Southern blot demonstrated that the single plasmid vector PV-BVHT527462 T-DNA insert in KWS20-1 sugar beet has been maintained through five (5) breeding generations, thereby confirming the stability of the T-DNA insert in KWS20-1 sugar beet.

- Segregation analysis in three (3) generations segregating population corroborates the insert stability demonstrated by Southern blot analysis and independently establishes the nature of the T-DNA as a single chromosomal locus that shows an expected pattern of inheritance.

Taken together, the characterization of the genetic modification in KWS20-1 sugar beet demonstrates that a single copy of the intended T-DNA is stably integrated at a single locus of the sugar beet genome and that no plasmid vector PV-BVHT527462 backbone sequences are present in KWS20-1 sugar beet.

A.3(a) A description of the method used to transform the host organism

KWS20-1 sugar beet was developed through *Agrobacterium*-mediated transformation of sugar beet, based on the method described by Lindsey and Gallois (1990). Briefly, shoot segment tissues were excised from the embryos of germinated conventional seed (line 04E05B1DH05 genotype). After coculturing with *Agrobacterium* AGL1 strain carrying the transformation construct, the resultant calli were placed on selection medium containing DL-phosphinothricin (PPT) to inhibit the growth of untransformed plant cells and timentin to inhibit the overgrowth of *Agrobacterium*. The calli were then placed in media conducive to shoot development followed by a liquid overlay of selection medium and transferred to a Jiffy Carefree propagation plug for root development. Rooted plants with normal phenotypic characteristics were selected. Events which passed the advancement criteria (such as a single copy of the T-DNA insert, no presence of vector backbone, no insertion into repetitive regions or gene sequences) were selected and transferred to soil for growth and further assessment.

A single T0 plant generated through this transformation process was self-pollinated under an isolation bag to produce T1 seed. The plants of the T1 population were screened for the presence of plasmid vector PV-BVHT527462 T-DNA and absence of vector backbone sequences by Kompetitive Allele Specific PCR (KASP) and Southern blot analyses. Twelve homozygous positive T1 plants were crossed by open pollination in an isolated field to generate T2 seed. Subsequently, T2 plants homozygous for plasmid vector PV-BVHT527462 T-DNA and negative for vector backbone sequences were selected for further development and their progenies were subjected to further molecular analysis, herbicide tolerance/efficacy and phenotypic assessments. As is typical of a commercial event production and selection process, hundreds of different transformation events (regenerants) were generated in the laboratory using PV-BVHT527462. After careful selection and evaluation of these events in the laboratory, greenhouse and field, KWS20-1 was selected as the lead event based on superior agronomic, phenotypic and molecular characteristics. Studies on KWS20-1 sugar beet were initiated to further characterize the genetic insertion and the expressed products, and to establish the food and feed safety and unaltered environmental risk compared to commercial sugar beet. The major development steps of KWS20-1 sugar beet are depicted in Figure 1.

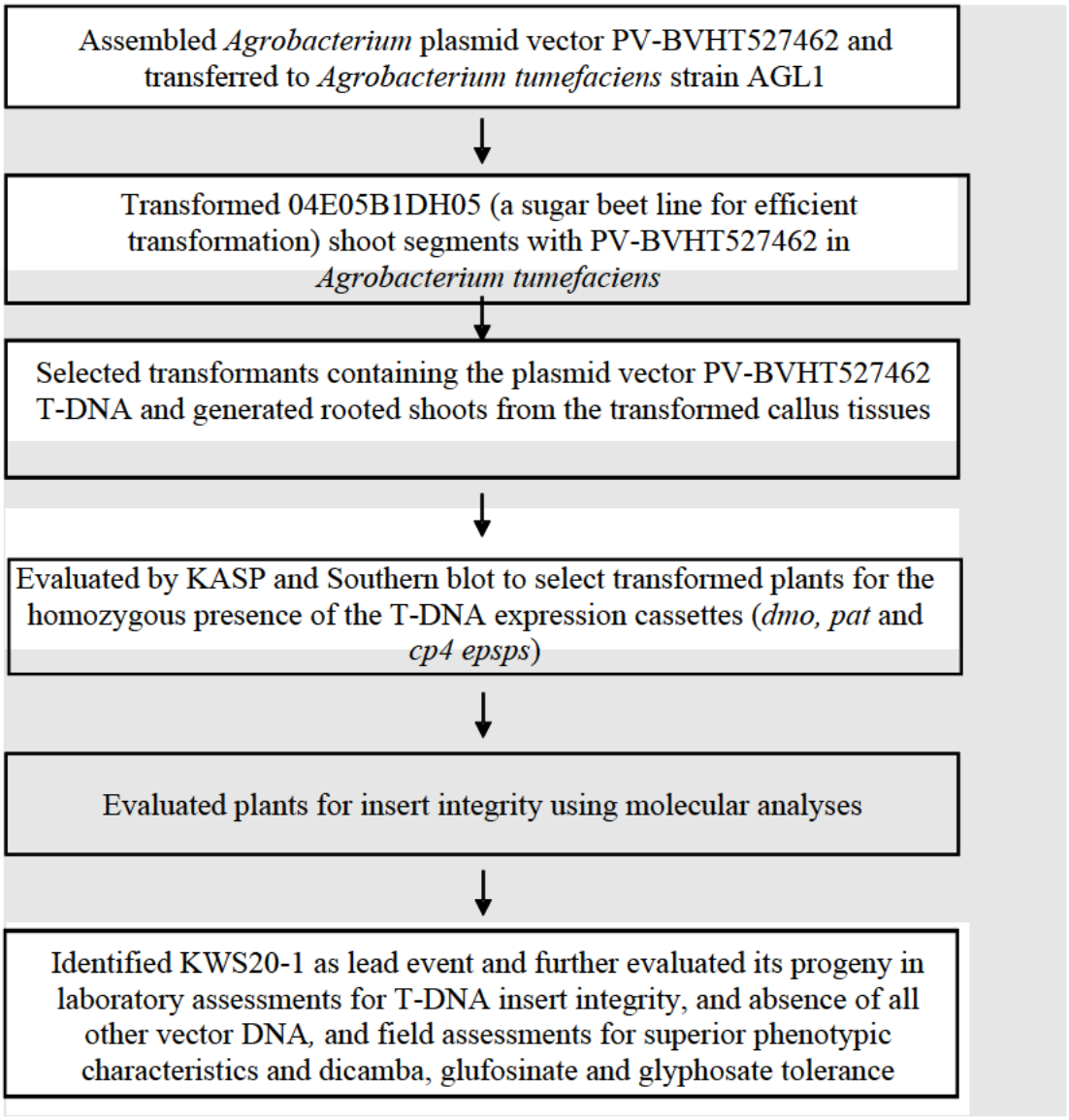

Figure 1. Schematic of the Development of KWS20-1 Sugar Beet

A.3(b) A description of the construct and the transformation vectors used, including:

A.3(b)(i) The size, source and function of all the genetic components including marker genes, regulatory and other elements

Plasmid vector PV-BVHT527462 was used for the transformation of conventional sugar beet to produce KWS20-1 sugar beet and its plasmid map is shown in A.3(b)(ii). A description of the genetic elements and their prefixes (e.g., B, T, CS, TS, P, E and OR) in PV-BVHT527462 is provided in Table 1. PV-BVHT527462 is approximately 18.9 kb and contains a single T-DNA (transfer DNA) that is delineated by Left and Right Border regions. The T-DNA contains the *dmo, pat* and *cp4 epsps* expression cassettes. During transformation, the T-DNA was inserted into the sugar beet genome. Following transformation, segregation, molecular screening and selection were used to isolate those plants that contained the *dmo, pat* and *cp4 epsps* expression cassettes and did not contain the backbone sequences from the transformation vector.

The *dmo* coding sequence in KWS20-1 sugar beet is under the regulation of a *DaMV-1* enhancer from a Dalia Mosaic Virus (DaMV) promoter region (Kuluev and Chemeris, 2007) that enhances transcription in plant cells and a *Ubq-Cm1* promoter, leader and intron for a putative ubiquitin protein gene from *Cucumis melo* which directs and regulates transcription (Hernandez-Garcia and Finer, 2014). Additionally, the *dmo* coding sequence utilizes the *guf-Mt2* 3' UTR from an expressed gene of *Medicago truncatula* of unknown function that directs polyadenylation of mRNA (Hunt, 1994).

The *pat* coding sequence is under the regulation of the *Cab-At1* promoter and 5' UTR from an *Arabidopsis thaliana* chlorophyll a/b-binding (CAB) protein that is involved in regulating gene expression (Ha and An, 1988). The *pat* coding sequence also utilizes the *Hsp20-Mt1* 3' UTR from *Medicago truncatula* (barrel medic) of a putative *Hsp20* gene encoding a heat shock protein that directs polyadenylation of the mRNA (Hunt, 1994).

The *cp4 epsps* coding sequence in KWS20-1 sugar beet is under the regulation of a *SAM2-Cm1* intron, *5′* UTR, and promoter from a *Cucumis melo SAM2* gene encoding S-adenosyl-L-methionine synthetase that directs transcription (Hernandez-Garcia and Finer, 2014).. Additionally, the sequence is regulated by the *CTP2* targeting sequence of the *ShkG* gene from *Arabidopsis thaliana* encoding the EPSPS transit peptide region that directs transport of the protein to the chloroplast (Klee *et al.*, 1987; Herrmann, 1995). The *cp4 epsps* expression cassette also utilizes the *guf-Mt1* 3' UTR sequence from an expressed gene of *Medicago truncatula* of unknown function that directs polyadenylation of mRNA (Hunt, 1994).

The backbone region of PV-BVHT527462, located outside of the T-DNA, contains two origins of replication for maintenance of the plasmid vector in bacteria (*ori-pVS1*, *ori-pBR322*) and a bacterial selectable marker gene (*aadA*).

A.3(b)(i)(i) The *dmo* Coding Sequence and DMO Protein

The *dmo* expression cassette contains the *dmo* gene encoding a precursor protein of 424 amino acids (340 amino acids encoded by the *dmo* gene; 84 amino acids encoded by *rbc*S gene (RbcS), which contains the 57 amino acids of chloroplast transit peptide (CTP) and the first 27 amino acids of the small subunit ribulose 1,5–bisphosphate carboxylase (Figure 2). KWS20-1 sugar beet-produced DMO protein results from the processing of the polypeptide in the

chloroplast to remove the RbcS but retains the 27 amino acids from the small subunit ribulose 1,5–bisphosphate carboxylase. This results in the KWS20-1 sugar beet-produced DMO protein comprised of 367 amino acids. The *dmo* open reading frame in the expression cassette encodes a precursor to the DMO protein from *S. maltophilia* (Wang *et al.*, 1997; Herman *et al.*, 2005). The expression of the DMO protein confers tolerance to dicamba herbicide.

DMO

1 MASMISSSAV TTVSRASRGQ SAAMAPFGGL KSMTGFPVRK VNTDITSITS NGGRVKCMQV

61 WPPIGKKKFE TLSYLPPLTR DSRAMLTFVR NAWYVAALPE ELSEKPLGRT ILDTPLALYR

121 QPDGVVAALL DICPHRFAPL SDGILVNGHL QCPYHGLEFD GGGQCVHNPH GNGARPASLN

181 VRSFPVVERD ALIWICPGDP ALADPGAIPD FGCRVDPAYR TVGGYGHVDC NYKLLVDNLM

241 DLGHAQYVHR ANAQTDAFDR LEREVIVGDG EIQALMKIPG GTPSVLMAKF LRGANTPVDA

301 WNDIRWNKVS AMLNFIAVAP EGTPKEQSIH SRGTHILTPE TEASCHYFFG SSRNFGIDDP

361 EMDGVLRSWQ AQALVKEDKV VVEAIERRRA YVEANGIRPA MLSCDEAAVR VSREIEKLEQ

421 LEAA

Figure 2. Deduced Amino Acid Sequence of the KWS20-1 Sugar Beet-Produced DMO Precursor Protein

The amino acid sequence of the KWS20-1 sugar beet DMO precursor protein was deduced from the full-length coding nucleotide sequence present in plasmid vector PV-BVHT527462). The RbcS and the first 27 amino acids of the small subunit ribulose 1,5–bisphosphate carboxylase are designated by the single- and double-underlined sequence, respectively. The RbcS amino acids were cleaved in the chloroplast, resulting in a KWS20-1 sugar beet-produced DMO protein with 367 amino acids that begins at the position 58.

A.3(b)(i)(ii) The *pat* Coding Sequence and PAT Protein

The *pat* expression cassette encodes for 183 amino acids. KWS20-1 sugar beet expresses an ~22.3 kDa PAT protein consisting of a single polypeptide of 182 amino acids, except for the lead methionine which is cleaved during a co-translational process in KWS20-1 sugar beet (Wehrmann *et al.*, 1996; Wohlleben *et al.*, 1988) (Figure 3). The *pat* open reading frame in the expression cassette includes sequence from *Streptomyces viridochromogenes* that encodes the PAT protein (Wehrmann *et al.*, 1996; Wohlleben *et al.*, 1988). The expression of PAT protein confers glufosinate herbicide tolerance.

PAT

```
1   MSPERRPVEI RPATAADMAA VCDIVNHYIE TSTVNFRTEP QTPQEWIDDL
51  ERLQDRYPWL VAEVEGVVAG IAYAGPWKAR NAYDWTVEST VYVSHRHQRL
101 GLGSTLYTHL LKSMEAQGFK SVVAVIGLPN DPSVRLHEAL GYTARGTLRA
151 AGYKHGGWHD VGFWQRDFEL PAPPRPVRPV TQI
```

Figure 3. Deduced Amino Acid Sequence of the KWS20-1 Sugar Beet-Produced PAT Protein

The amino acid sequence of the KWS20-1 sugar beet-produced PAT protein was deduced from the full-length coding nucleotide sequence present in plasmid vector PV-BVHT527462. The lead methionine of the PAT protein expressed by KWS20-1 sugar beet is cleaved during a co-translational process in KWS20-1 sugar beet.

A.3(b)(i)(iii) The *cp4 epsps* Coding Sequence and CP4 EPSPS Protein

The *cp4 epsps* expression cassette contains the *cp4 epsps* gene encoding a precursor protein of 531 amino acids (455 amino acids encoded by the *cp4 epsps* gene and 76 amino acids encoded by the *CTP2* gene for targeting the CP4 EPSPS protein into chloroplasts) (Figure 4). KWS20-1 sugar beet expresses an ~43.5 kDa CP4 EPSPS protein, consisting of a single polypeptide of 455 amino acids starting at the methionine position 77 (Padgette *et al.*, 1996) after a complete cleavage of the chloroplast transit peptide (CTP2). The *cp4 epsps* coding sequence is the codon optimized coding sequence of the *aroA* gene from *Agrobacterium* sp. strain CP4 encoding CP4 EPSPS (Barry *et al.*, 2001; Padgette *et al.*, 1996). The CP4 EPSPS protein is similar and functionally equivalent to endogenous plant EPSPS enzymes, but has a much-reduced affinity for glyphosate, the active ingredient in Roundup agricultural herbicides, relative to endogenous plant EPSPS (Barry *et al.*, 2001; Padgette *et al.*, 1996). The presence of this protein renders the plant tolerant to glyphosate herbicide.

CP4 EPSPS

```
1    MLHGASSRPA TARKSSGLSG TVRIPGDKSI SHRSFMFGGL ASGETRITGL
51   LEGEDVINTG KAMQAMGARI RKEGDTWIID GVGNGGLLAP EAPLDFGNAA
101  TGCRLTMGLV GVYDFDSTFI GDASLTKRPM GRVLNPLREM GVQVKSEDGD
151  RLPVTLRGPK TPTPITYRVP MASAQVKSAV LLAGLNTPGI TTVIEPIMTR
201  DHTEKMLQGF GANLTVETDA DGVRTIRLEG RGKLTGQVID VPGDPSSTAF
251  PLVAALLVPG SDVTILNVLM NPTRTGLILT LQEMGADIEV INPRLAGGED
301  VADLRVRSST LKGVTVPEDR APSMIDEYPI LAVAAAFAEG ATVMNGLEEL
```

```
351   RVKESDRLSA VANGLKLNGV DCDEGETSLV VRGRPDGKGL GNASGAAVAT

401   HLDHRIAMSF LVMGLVSENP VTVDDATMIA TSFPEFMDLM AGLGAKIELS

451   DTKAA
```

Figure 4. Deduced Amino Acid Sequence of the KWS20-1 Sugar Beet-Produced CP4 EPSPS Protein

The amino acid sequence of the KWS20-1 sugar beet-produced CP4 EPSPS protein was deduced from the full-length coding nucleotide sequence present in plasmid vector PV-BVHT527462.

A.3(b)(i)(iv) Regulatory Sequences

The transformation plasmid PV-BVHT527462 contains the *dmo, pat* and *cp4 epsps* expression cassettes, and also the expression cassette for the *aadA* selectable marker, each with their own regulatory sequences. The regulatory sequences associated with each cassette are described in Section A.2(a)(i) and Table 1.

A.3(b)(i)(v) T-DNA Border Regions

Plasmid vector PV-BVHT527462 contains Left and Right Border regions (Figure 5 and Table 1) that were derived from *A. tumefaciens* plasmids. The border regions each contain a nick site that is the site of DNA exchange during transformation (Barker *et al.*, 1983; Depicker *et al.*, 1982; Zambryski *et al.*, 1982). The border regions separate the T-DNA from the plasmid backbone region and are involved in the efficient transfer of T-DNA into the sugar beet genome.

A.3(b)(i)(vi) Genetic Elements Outside the T-DNA Border Regions

Genetic elements that exist outside of the T-DNA border regions are those that are essential for the maintenance or selection of plasmid vector PV-BVHT527462 in bacteria and are referred to as plasmid backbone. The origin of replication, *ori-pVS1*, is required for the maintenance of the plasmid in *Agrobacterium* and is derived from the plasmid pVS1 (Itoh *et al.*, 1984). The origin of replication, *ori-pBR322*, is required for the maintenance of the plasmid in *E. coli* and is derived from the plasmid vector pBR322 (Sutcliffe, 1979). The selectable marker *aadA* is the coding sequence for an aminoglycoside-modifying enzyme, 3"(9)–*O*–nucleotidyltransferase from the transposon Tn*7* (Fling *et al.*, 1985) that confers spectinomycin and streptomycin resistance in *E. coli* and *Agrobacterium* during molecular cloning. Because these elements are outside the border regions, they are not expected to be transferred into the sugar beet genome. The absence of the backbone and other unintended plasmid sequence in KWS20-1 sugar beet was confirmed by Southern blot analyses (see Section A.3(c))

Table 1. Summary of Genetic Elements in PV-BVHT527462

Genetic Element	Location in Plasmid Vector	Function (Reference)
B[1]-Right Border Region	1-357	DNA region from *Agrobacterium tumefaciens* containing the right border sequence used for transfer of the T-DNA (Depicker *et al.*, 1982; Zambryski *et al.*, 1982)
Intervening Sequence	358-401	Sequence used in DNA cloning
T[2]-*guf-Mt1*	402-901	3' UTR from an expressed gene of *Medicago truncatula* of unknown function that directs polyadenylation of mRNA (Hunt, 1994)
Intervening Sequence	902-907	Sequence used in DNA cloning
CS[3]-*cp4 epsps*	908-2275	Codon optimized coding sequence of the *aroA* gene from the *Agrobacterium* sp. strain CP4 encoding the CP4 EPSPS protein that provides herbicide tolerance (Barry *et al.*, 2001; Padgette *et al.*, 1996)
TS[4]-*CTP2*	2276-2503	Targeting sequence of the *ShkG* gene from *Arabidopsis thaliana* encoding the EPSPS transit peptide region that directs transport of the protein to the chloroplast (Klee *et al.*, 1987; Herrmann, 1995)
Intervening Sequence	2504-2512	Sequence used in DNA cloning
P[5]-*SAM2-Cm1*	2513-4516	Intron, 5′ UTR, and promoter from a *Cucumis melo SAM2* gene encoding S-adenosyl-L-methionine synthetase which directs transcription (Hernandez-Garcia and Finer, 2014)
Intervening Sequence	4517-4522	Sequence used in DNA cloning
E[6]-*DaMV-1*	4523-4854	Enhancer from a Dalia Mosaic Virus (DaMV) promoter region (Kuluev and Chemeris, 2007) that enhances transcription in plant cells
Intervening Sequence	4855-4864	Sequence used in DNA cloning
P-*Ubq-Cm1*	4865-7475	Promoter, leader and intron for a putative ubiquitin protein gene from *Cucumis melo* which directs and regulates transcription (Hernandez-Garcia and Finer, 2014)
Intervening Sequence	7476-7486	Sequence used in DNA cloning
TS-*RbcS (Ps)*	7487-7738	Targeting sequence and the first 27 amino acids from *Pisum sativum* (pea) rbcs gene family encoding the small subunit ribulose 1.5 bisphosphate carboxylase protein that is expressed in the chloroplast (Fluhr *et al.*, 1986)
CS-*dmo*	7739-8761	Codon optimized coding sequence for the dicamba mono-oxygenase (DMO) protein of *Stenotrophomonas maltophilia* that confers dicamba resistance (Wang *et al.*, 1997; Herman *et al.*, 2005)
Intervening Sequence	8762-8767	Sequence used in DNA cloning
T-*guf-Mt2*	8768-9267	3' UTR from an expressed gene of *Medicago truncatula* of unknown function that directs polyadenylation of mRNA (Hunt, 1994)
Intervening Sequence	9268-9273	Sequence used in DNA cloning
P-*Cab-At1*	9274-10661	Promoter and leader from an *Arabidopsis thaliana* chlorophyll a/b-binding (CAB) protein that is

		involved in regulating gene expression (Ha and An, 1988)
Intervening Sequence	10662-10667	Sequence used in DNA cloning
CS-*pat*	10668-11219	Codon optimized coding sequence from *Streptomyces viridochromogenes* for the phosphinothricin N-acetyltransferase (PAT) protein that confers tolerance to glufosinate (Wehrmann *et al.*, 1996; Wohlleben *et al.*, 1988)
Intervening Sequence	11220-11227	Sequence used in DNA cloning
T-*Hsp20-Mt1*	11228-11727	3' UTR sequence from *Medicago truncatula* (barrel medic) of a putative *Hsp20* gene encoding a heat shock protein that directs polyadenylation of the mRNA (Hunt, 1994)
Intervening Sequence	11728-11779	Sequence used in DNA cloning
B-Left Border Region	11780-12221	DNA region from *Agrobacterium tumefaciens* containing the left border sequence used for transfer of the T–DNA (Barker *et al.*, 1983)
Intervening Sequence	12222-12229	Sequence used in DNA cloning
OR[7]-*ori-pVS1*	12230-15986	Origin of replication from plasmid pVS1 for maintenance of plasmid in *Agrobacterium* (Itoh *et al.*, 1984)
Intervening sequence	15987-16174	Sequence used in DNA cloning
CS-*rop*	16175-16366	Coding sequence for repressor of primer protein from the ColE1 plasmid for maintenance of plasmid copy number in *E. coli* (Giza and Huang, 1989)
Intervening Sequence	16367-16793	Sequence used in DNA cloning
OR-*ori-pBR322*	16794-17378	Origin of replication from plasmid pBR322 for maintenance of plasmid in *E. coli* (Sutcliffe, 1979)
Intervening Sequence	17379-17908	Sequence used in DNA cloning
aadA	17909-18797	Bacterial promoter, coding sequence, and 3' UTR for an aminoglycoside-modifying enzyme, 3"(9) *–O–* nucleotidyltransferase from the transposon *Tn7* (Fling *et al.*, 1985) that confers spectinomycin and streptomycin resistance
Intervening Sequence	18798-18933	Sequence used in DNA cloning

[1] B, Border
[2] T, Transcription termination sequence
[3] CS, Coding sequence
[4] TS, Targeting sequence
[5] P, Promoter
[6] E, Enhancer
[7] OR, Origin of replication

A.3(b)(ii) A detailed map of the location and orientation of all genetic elements contained within the construct and vector, including the location of relevant restriction sites

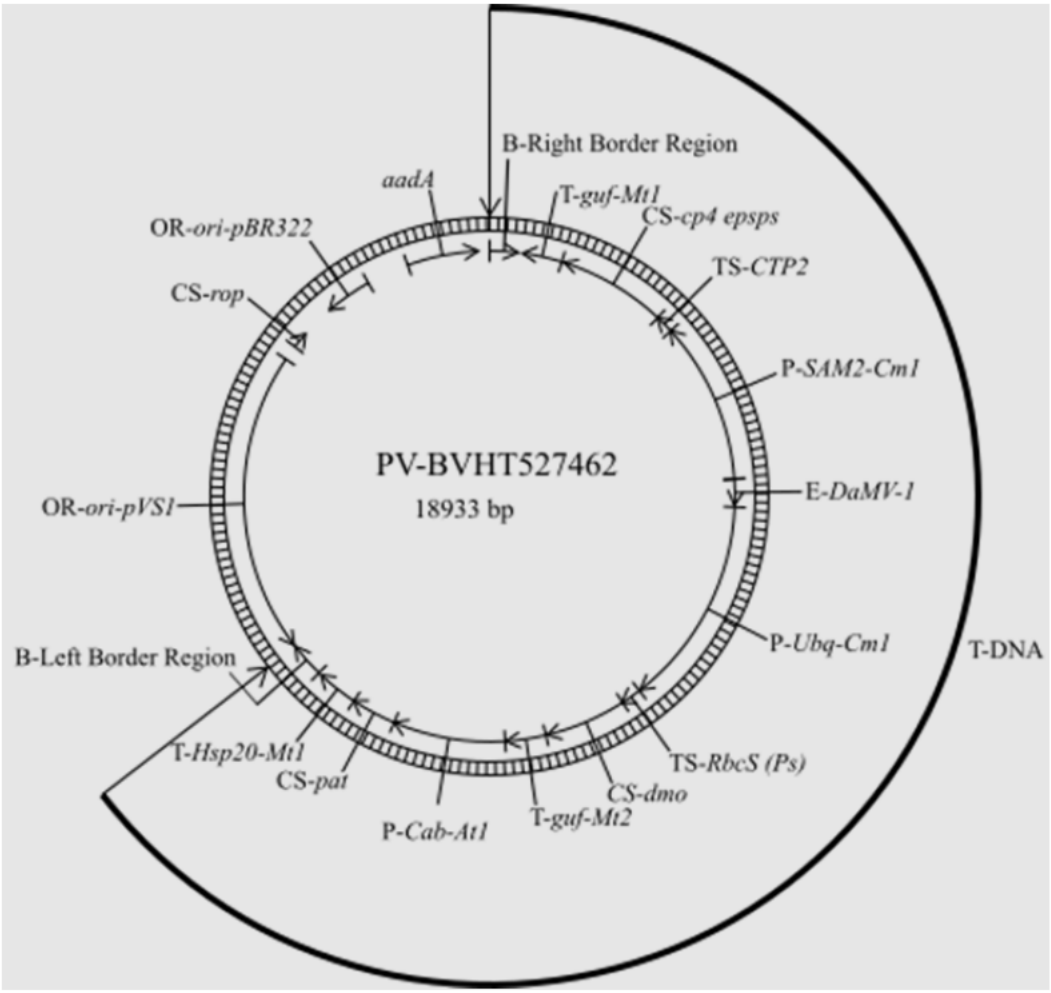

Figure 5. Circular Map of PV-BVHT527462

A circular map of plasmid vector PV-BVHT527462 used to develop KWS20-1 sugar beet is shown. PV-BVHT527462 contains a single T-DNA. Genetic elements are shown on the exterior of the map.

A.3(c) A full molecular characterisation of the genetic modification in the new organism, including:

This section describes the methods and results of a comprehensive molecular characterisation of the genetic modification present in KWS20-1 sugar beet. It provides information on the DNA insertion(s) into the plant genome of KWS20-1 sugar beet, and additional information regarding the arrangement and stability of the introduced genetic material. The information provided in this section addresses the relevant factors in Codex Plant Guidelines, Section 4, paragraphs 30, 31, 32, and 33 (Codex Alimentarius, 2009).

A multi-faceted approach was taken to characterize the genetic modification that produced KWS20-1 sugar beet. The results confirmed that KWS20-1 sugar beet contains a single, intact copy of the expected T-DNA insert, at a single locus within the sugar beet genome that is stably integrated at a single locus over multiple generations and is inherited according to Mendelian principles in the segretating populations of three generations (see Section A.3(e)). The results confirmed that no plasmid vector backbone sequences are detected in KWS20-1 sugar beet. These conclusions are based on several lines of evidence: 1) Southern blot analyses to assay the entire sugar beet genome for the presence of DNA derived from plasmid vector PV-BVHT527462, and to confirm that a single copy of T-DNA was inserted at a single site that is stably inherited; 2) DNA sequencing analyses to determine the exact sequence of the inserted DNA and a comparison to the T-DNA sequence in PV-BVHT527462 to confirm that only the expected sequences were integrated; 3) a comparison of the DNA flanking T-DNA to the sequence of the insertion site in conventional sugar beet to identify any rearrangements that occurred at the insertion site during transformation; and 4) analysis of a segregating population of KWS20-1 sugar beet to confirm that the T-DNA insertion is inherited in a predictable pattern following Mendelian principles. Taken together, the characterization of the genetic modification demonstrates that a single copy of the T-DNA was inserted at a single locus of the sugar beet genome.

A.3(c)(i) Identification of all transferred genetic material and whether it has undergone any rearrangements

The Southern blot analysis confirmed that the T-DNA reported in Figure 6 represents the only detectable insert in KWS20-1 sugar beet. Additionally, Figure 6 is a linear map depicting restriction sites within the insert as well as within the known sugar beet genomic DNA immediately flanking the insert in KWS20-1 sugar beet. The linearized map of plasmid vector PV-BVHT527462 annotated with the probes used in the Southern blot analysis is presented in Figure 7. Based on the linear map of the insert and the plasmid map, a table summarizing the expected DNA segments for Southern analyses is presented in Table 2. The genetic elements integrated in KWS20-1 sugar beet are summarized in Table 3. The generations used are depicted in the breeding history shown in Figure 12.

For details, please refer to Appendix 1.

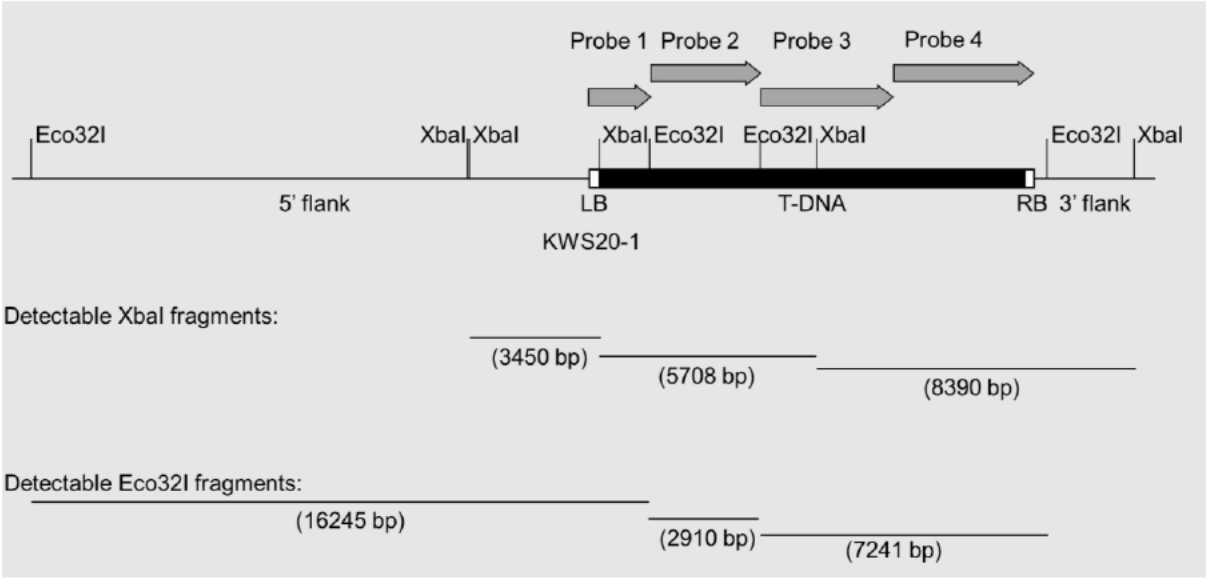

Figure 6. Detectable XbaI and Eco32I Digestion Fragments

A schematic representation of the plasmid vector PV-BVHT527462 T-DNA sequence inserted in KWS20-1 sugar beet is presented. The black horizontal bar indicates the position of the T-DNA, the 5' and 3' flanking regions, as well as restriction nuclease sites for XbaI and Eco32I are indicated. LB and RB mark the Left and Right T-DNA Borders, respectively. The fragments resulting from XbaI and Eco32I digestion that can be detected by at least one of the four T-DNA probes are presented underneath.

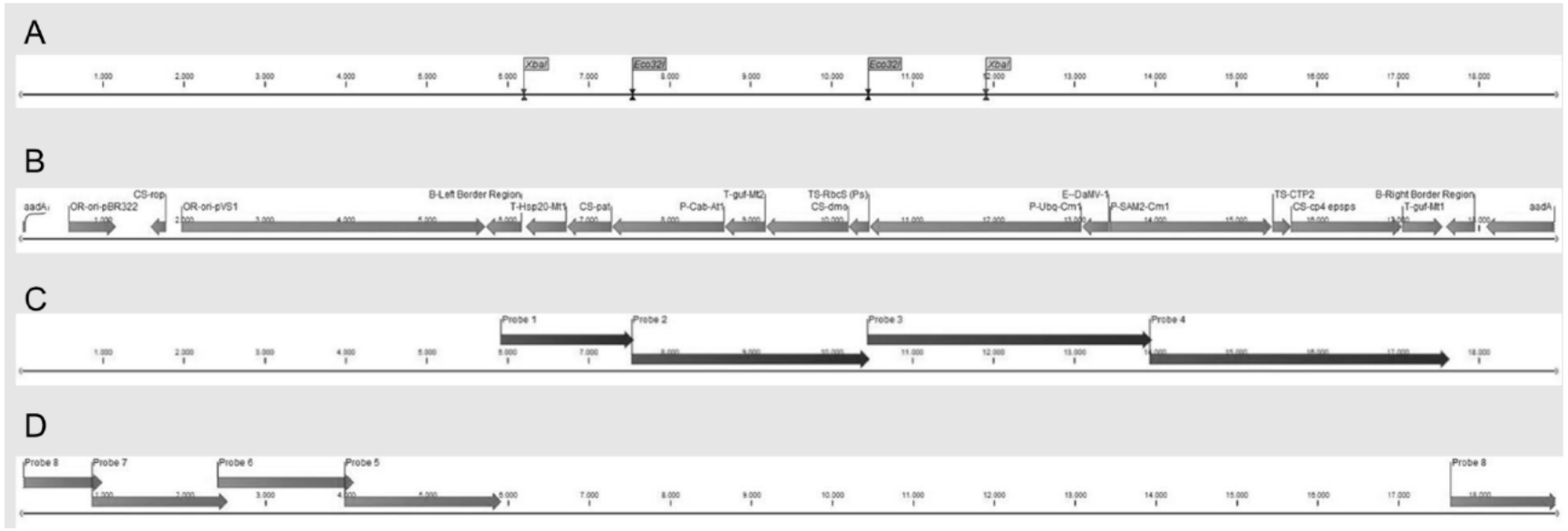

Figure 7. Linearized Map of Plasmid PV-BVHT527462 (18933 bp)

A, the restriction sites for enzymes XbaI and Eco32I. B, the position of functional elements. C, the position of T-DNA probes 1, 2, 3 and 4. D, position of backbone probes 5, 6, 7 and 8.

Table 2. Summary Chart of the Expected DNA Segments Based on Hybridizing Probes and Restriction Enzymes Used in KWS20-1 Sugar Beet Analysis

Southern Blot Figure		Figure 9, Figure 10, Figure 20, Figure 21	Figure 11, Figure 12, Figure 22, Figure 23	Figure 13, Figure 14
Probe Used		1 and 3	2 and 4	5, 6, 7 and 8
Probing Target	Digestion Enzyme	Expected Band Sizes (kb) on Each Southern Blot		
Plasmid Vector PV-BVHT527462	XbaI	13.2, 5.7	13.2, 5.7	13.2
	Eco32I	16.0	16.0, 2.9	16.0
Probe Templates	N/A	None	None	1.9, 1.7, 1.7, 2.3
Conventional Near-isogenic Control (04E05B1DH05)	XbaI	None	None	None
	Eco32I	None	None	None
KWS20-1 Sugar Beet	XbaI	8.4, 5.7, 3.5	8.4, 5.7	None
	Eco32I	16.2, 7.2	7.2, 2.9	None

Table 3. Summary of Genetic Elements in KWS20-1 Sugar Beet

Genetic Element*	Location in Sequence**	Function (Reference)
5' Flanking DNA	1-1000**	DNA sequence flanking the 5' end of the insert
B[1]-Left Border Region**	1001-1259	DNA region from *Agrobacterium tumefaciens* containing the left border sequence used for transfer of the T–DNA (Barker *et al.*, 1983)
Intervening Sequence	1260-1311	Sequence used in DNA cloning
T[2]-*Hsp20-Mt1*	1312-1811	3' UTR sequence from *Medicago truncatula* (barrel medic) of a putative *Hsp20* gene encoding a heat shock protein that directs polyadenylation of the mRNA (Hunt, 1994)
Intervening Sequence	1812-1819	Sequence used in DNA cloning
CS[3]-*pat*	1820-2371	Codon-optimized coding sequence from *Streptomyces viridochromogenes* for the phosphinothricin N-acetyltransferase (PAT) protein that confers tolerance to glufosinate (Wehrmann *et al.*, 1996; Wohlleben *et al.*, 1988)
Intervening Sequence	2372-2377	Sequence used in DNA cloning
P[4]-*Cab-At1*	2378-3765	Promoter and leader from an *Arabidopsis thaliana* chlorophyll a/b-binding (CAB) protein that is involved in regulating gene expression (Ha and An, 1988)
Intervening Sequence	3766-3771	Sequence used in DNA cloning
T-*guf-Mt2*	3772-4271	3' UTR from an expressed gene of *Medicago truncatula* of unknown function that directs polyadenylation of mRNA (Hunt, 1994)
Intervening Sequence	4272-4277	Sequence used in DNA cloning
CS-*dmo*	4278-5300	Codon optimized coding sequence for the dicamba mono-oxygenase (DMO) protein of *Stenotrophomonas maltophilia* that confers dicamba resistance (Wang *et al.*, 1997; Herman *et al.*, 2005)
TS[5]-*RbcS (Ps)*	5301-5552	Targeting sequence and the first 27 amino acids from *Pisum sativum* (pea) *rbcs* gene family encoding the small subunit ribulose 1.5 bisphosphate carboxylase protein that directs transport of the protein to the chloroplast (Fluhr *et al.*, 1986)
Intervening Sequence	5553-5563	Sequence used in DNA cloning
P-*Ubq-Cm1*	5564-8174	Promoter, leader and intron for a putative ubiquitin protein gene from *Cucumis melo*, which directs and regulates transcription (Hernandez-Garcia and Finer, 2014)

Intervening Sequence	8175-8184	Sequence used in DNA cloning
E[6]-*DaMV-1*	8185-8516	Enhancer from a Dalia Mosaic Virus (DaMV) promoter region (Kuluev and Chemeris, 2007) that enhances transcription in plant cells
Intervening Sequence	8517-8522	Sequence used in DNA cloning
P-*SAM2-Cm1*	8523-10526	Intron, 5′ UTR, and promoter from a Cucumis melo *SAM2* gene encoding S-adenosyl-L-methionine synthase, which directs transcription (Hernandez-Garcia and Finer, 2014)
Intervening Sequence	10527-10535	Sequence used in DNA cloning
TS-*CTP2*	10536-10763	Targeting sequence of the ShkG gene from *Arabidopsis thaliana* encoding the EPSPS transit peptide region that directs transport of the protein to the chloroplast (Klee *et al.*, 1987; Herrmann, 1995)
CS-*cp4 epsps*	10764-12131	Codon optimized coding sequence of the *aroA* gene from the *Agrobacterium* sp. strain CP4 encoding the CP4 EPSPS protein that provides glyphosate tolerance (Barry *et al.*, 2001; Padgette *et al.*, 1996)
Intervening Sequence	12132-12137	Sequence used in DNA cloning
T-*guf-Mt1*	12138-12637	3' UTR from an expressed gene of *Medicago truncatula* of unknown function that directs polyadenylation of mRNA (Hunt, 1994)
Intervening Sequence	12638-12681	Sequence used in DNA cloning
B-Right Border Region[***]	12682-12722	DNA region from *Agrobacterium tumefaciens* containing the right border sequence used for transfer of the T-DNA (Zambryski *et al.*, 1982)
3' Flanking DNA	12723-13722	DNA sequence flanking the 3' end of the insert

[*] Although flanking sequences and intervening sequences are not functional genetic elements, they comprise a portion of the sequence.
[**] Numbering refers to the sequence of the insert in KWS20-1 sugar beet and adjacent DNA.
[***] The sequences in KSW20-1 sugar beet Left and Right Border Regions were truncated compared to the sequences in PV BVHT527462.
[1] B, Border region
[2] T, Transcription termination sequence
[3] CS, Coding sequence
[4] P, Promoter
[5] TS, Targeting sequence
[6] E, Enhancer

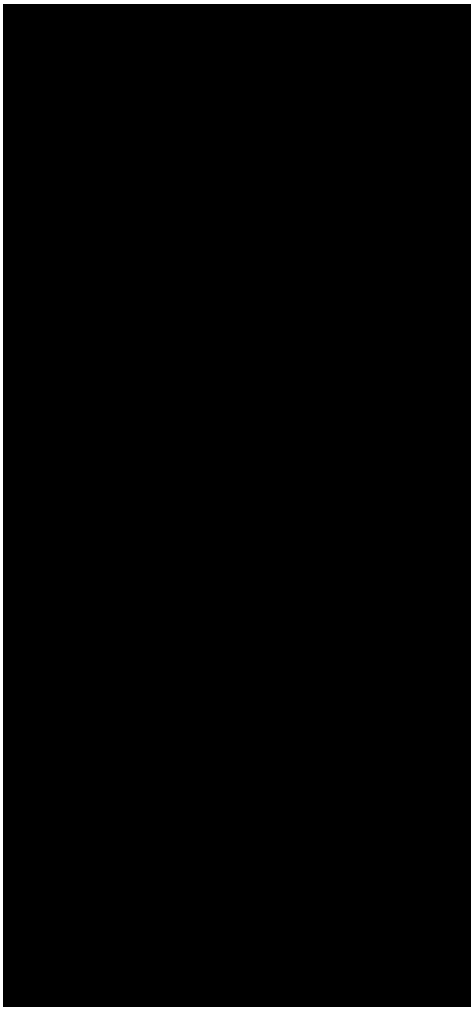

Figure 8. Breeding History of KWS20-1 Sugar Beet

A.3(c)(ii) A determination of number of insertion sites, and the number of copies at each insertion site

The number of inserted DNA sequences from plasmid vector PV-BVHT527462 in KWS20-1 sugar beet was assessed by Southern blot analysis of KWS20-1 sugar beet genomic DNA using the T2 generation (Figure 8). Figure 6 is a linear map depicting restriction sites within the insert as well as within the known sugar beet genomic DNA immediately flanking the insert in KWS20-1 sugar beet. The linearized map of PV-BVHT527462 annotated with the probes used in the Southern blot analysis is presented in Figure 7. Based on the linear map of the insert and the plasmid map, a table summarizing the expected DNA segments for Southern analyses is presented in Table 2. The genetic elements integrated in KWS20-1 sugar beet are summarized in Table 3.

For details, please refer to Appendix 1.

A.3(c)(ii)(i) Southern Blot Analysis to Determine Insert and Copy Number in KWS20-1 Sugar Beet

The copy number and insertion site of the T-DNA was assessed by digesting KWS20-1 sugar beet genomic DNA with the restriction enzyme XbaI or Eco32I and hybridizing Southern blots with probes that span the T-DNA (Figure 6). Each restriction digest is expected to produce a specific banding pattern on the Southern blots (Table 2).

The restriction enzyme XbaI cuts twice within the T-DNA and again within each of the known genomic DNA sequences flanking the 5′ and 3′ ends of the T-DNA (Figure 6). Therefore, if the T-DNA sequences are present at a single integration site in KWS20-1 sugar beet, the digestion with XbaI was expected to generate three segments with expected sizes of ~8.4 kb, ~5.7 kb and ~3.5 kb (Figure 6 and Table 2). The ~8.4 kb band represents the 3’ flanking region and the Right Border-end of the inserted T-DNA (Figure 6). The ~5.7 kb band represents the inner T-DNA fragment (Figure 6). The ~3.5 kb band represents the 5’ flanking region and the Left Border-end of the inserted T-DNA.

The restriction enzyme Eco32I cuts twice within the T-DNA and again within the known genomic DNA outside the 5′ and 3′ ends of the T-DNA (Figure 6). Therefore, if T-DNA sequences are present at a single integration site in KWS20-1 sugar beet, the digestion with Eco32I was expected to generate three segments with expected sizes of ~16.2 kb, ~2.9 kb and ~7.2 kb (Figure 6 and Table 2). The ~16.2 kb band represents the 5’ flanking region and the Left Border-end of the inserted T-DNA (Figure 6). The ~2.9 kb band represents the inner T-DNA fragment and the ~7.2 kb band represents the 3’ flanking region and the Right Border-end of the inserted T-DNA.

In the Southern blot analyses performed, each Southern blot contained a negative and a positive control. Conventional near-isogenic control genomic DNA digested with either the restriction enzyme XbaI or Eco32I was used as a negative control to determine if the probes hybridized to any endogenous sugar beet sequences. As a positive control on the Southern blots, plasmid vector PV-BVHT527462 digested with the restriction enzyme XbaI or Eco32I was mixed with predigested conventional near-isogenic control DNA. The positive hybridization control was spiked at 0.1 and 1 genome equivalence to demonstrate sufficient sensitivity of the Southern blot. Individual Southern blots were hybridized with the following probe combinations: probes 1 and 4, and probes 2 and 4 (refer to Figure 6 and Table 2). Duplicated samples that consisted of equal

amounts of digested DNA were run on agarose gels. One set of samples was run for a longer period of time (long run) than the second set (short run). The long run allows for greater resolution of large molecular weight DNA, whereas the short run allows the detection of small molecular weight DNA. The results of this analysis are shown in Figure 9, Figure 10, Figure 11 and Figure 12.

Probes 1 and 3

Conventional near-isogenic control DNA digested with the restriction enzyme XbaI (Figure 9, lane 3; Figure 10, lane 3) or Eco32I (Figure 9, lane 8; Figure 10, lane 8) and hybridized with probes 1 and 3 (Figure 6) produced no detectable hybridization bands as expected for the negative control. Conventional near-isogenic control DNA digested with XbaI and spiked with XbaI-digested plasmid vector PV-BVHT527462 DNA produced two expected size bands at ~13.2 kb and ~5.7 kb (Figure 9, lanes 4 and 5; Figure 10, lanes 4 and 5). Eco32I-digested conventional near-isogenic control DNA spiked with Eco32I-digested plasmid vector PV-BVHT527462 DNA produced a single expected size band at ~16.0 kb (Figure 9, lanes 9 and 10; Figure 10, lanes 9 and 10). These results indicate that the probes are hybridizing to their target sequences.

KWS20-1 sugar beet DNA samples digested with XbaI produced three bands at ~8.4 kb, ~5.7 kb and ~3.5 kb (Figure 9, lane 2; Figure 10, lane 2). The ~8.4 kb band represents the 3' flanking region and the Right Border-end of the inserted T-DNA, detected by probe 3 (Figure 6). The ~5.7 kb band represents the inner T-DNA fragment detected by both probes 1 and 3 (Figure 6). The ~3.5 kb band represents the 5' flanking region and the Left Border-end of the inserted T-DNA, detected by probe 1 (Figure 6). Digestion with Eco32I produced two bands at ~16.2 kb and ~7.2 kb (Figure 9, lane 7; Figure 10, lane 7). The ~16.2 kb band represents the 5' flanking region and the Left Border-end of the inserted T-DNA, detected by probe 1 (Figure 6). The ~7.2 kb band represents the 3' flanking region and the Right Border-end of the inserted T-DNA, detected by probe 3 (Figure 6). The band number and band migration observed on the insert and copy number blots, judged by comparing to the migration of the marker bands, are consistent with the expected bands and their theoretical sizes (Figure 6 and Table 2).

No additional bands were detected using probes 1 and 3. Based on the results presented in Figure 9 and Figure 10, it was concluded that the T-DNA sequences covered by probes 1 and 3 reside at a single integration locus as one copy in KWS20-1 sugar beet.

Probes 2 and 4

Conventional near-isogenic control DNA digested with the restriction enzyme XbaI (Figure 11, lane 3; Figure 12, lane 3) or Eco32I (Figure 11, lane 8; Figure 12, lane 8) and hybridized with probes 2 and 4 (Figure 6) produced no detectable hybridization bands as expected for the negative control. Conventional near-isogenic control DNA digested with XbaI and spiked with XbaI-digested plasmid vector PV-BVHT527462 DNA produced two expected size bands at ~13.2 kb and ~5.7 kb (Figure 11, lanes 4 and 5; Figure 12, lanes 4 and 5). Eco32I-digested conventional near-isogenic control DNA spiked with Eco32I-digested plasmid vector PV-BVHT527462 DNA produced two expected size bands at ~16.0 kb and ~2.9 kb (Figure 11, lanes 9 and 10; Figure 12, lanes 9 and 10). These results indicate that the probes are hybridizing to their target sequences.

KWS20-1 sugar beet DNA samples digested with XbaI produced two bands at ~8.4 kb and ~5.7 kb (Figure 11, lane 2; Figure 12, lane 2). The ~8.4 kb band represents the 3' flanking region and the Right Border-end of the inserted T-DNA, detected by probe 4. The ~5.7 kb band represents the inner T-DNA fragment detected by probe 2. Digestion with Eco32I produced two bands at ~7.2 kb and ~2.9 kb (Figure 11, lane 7; Figure 12, lane 7). The ~7.2 kb band represents the 3' flanking region and the Right Border-end of the inserted T-DNA, detected by probe 4. The ~2.9 kb band represents the inner T-DNA fragment detected by probe 2. The band number and band migration observed on the insert and copy number blots, judged by comparing to the migration of the marker bands, are consistent with the expected bands and their theoretical sizes (Figure 6 and Table 2).

No additional bands were detected using probes 2 and 4. Based on the results presented in Figure 11 and Figure 12, it was concluded that the T-DNA sequences covered by probes 2 and 4 reside at a single integration locus as one copy in KWS20-1 sugar beet.

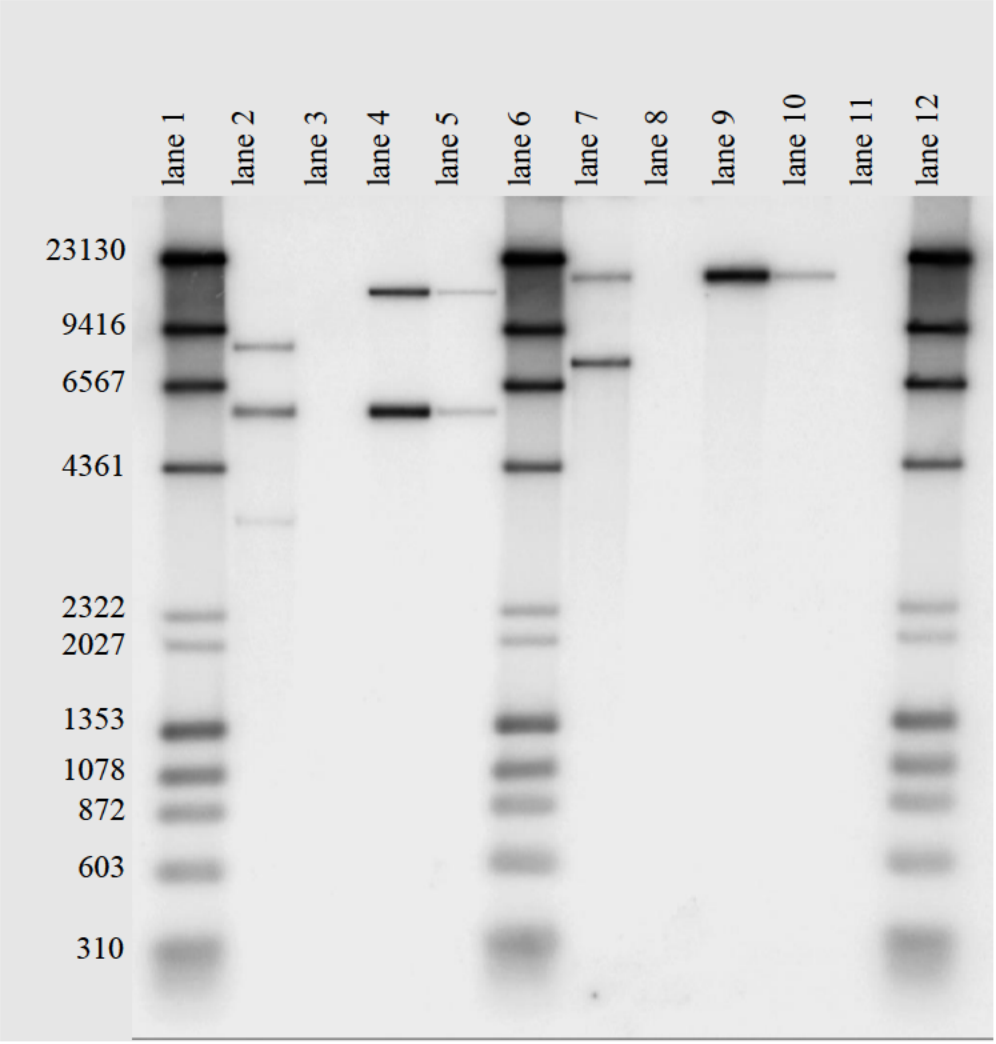

Figure 9. Southern Blot Analysis of KWS20-1 Sugar Beet: T-DNA Insert and Copy Number Analysis - Probes 1 and 3 (Long Run)

Lane 1: Molecular Size Marker
Lane 2: KWS20-1 sugar beet digested with XbaI
Lane 3: Near-isogenic control digested with XbaI
Lane 4: Near-isogenic control spiked with PV-BVHT527462 - 1 copy digested with XbaI
Lane 5: Near-isogenic control spiked with PV-BVHT527462 - 1/10 copy digested with XbaI
Lane 6: Molecular Size Marker
Lane 7: KWS20-1 sugar beet digested with Eco32I
Lane 8: Near-isogenic control digested with Eco32I
Lane 9: Near-isogenic control spiked with PV-BVHT527462 - 1 copy digested with Eco32I
Lane 10: Near-isogenic control spiked with PV-BVHT527462 - 1/10 copy digested with Eco32I
Lane 11: Empty
Lane 12: Molecular Size Marker

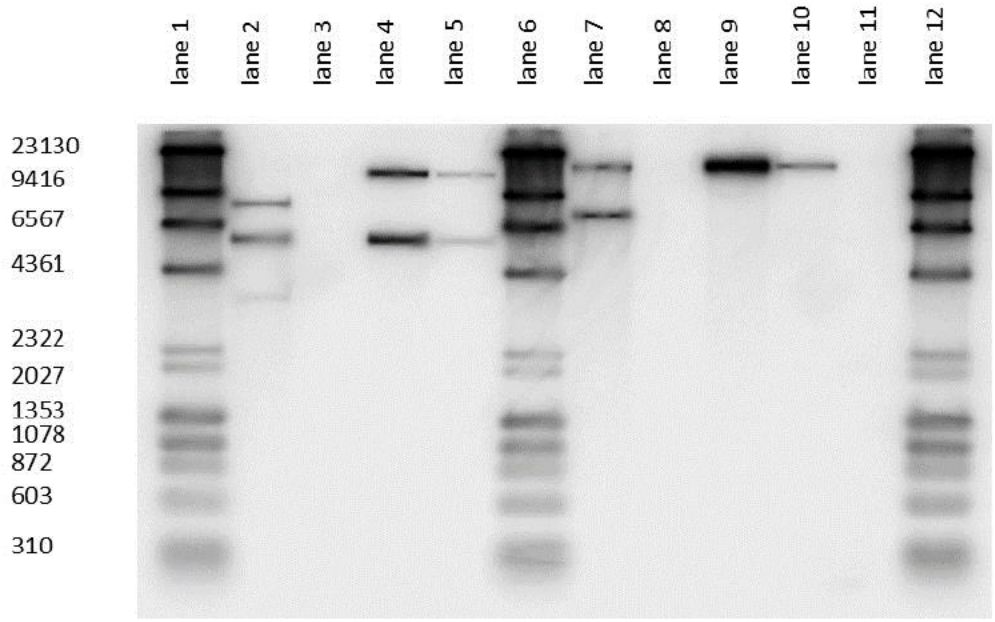

Figure 10. Southern Blot Analysis of KWS20-1 Sugar Beet: T-DNA Insert and Copy Number Analysis - Probes 1 and 3 (Short Run)

Lane 1: Molecular Size Marker
Lane 2: KWS20-1 sugar beet digested with XbaI
Lane 3: Near-isogenic control digested with XbaI
Lane 4: Near-isogenic control spiked with PV-BVHT527462 - 1 copy digested with XbaI
Lane 5: Near-isogenic control spiked with PV-BVHT527462 - 1/10 copy digested with XbaI
Lane 6: Molecular Size Marker
Lane 7: KWS20-1 sugar beet digested with Eco32I
Lane 8: Near-isogenic control digested with Eco32I
Lane 9: Near-isogenic control spiked with PV-BVHT527462 - 1 copy digested with Eco32I
Lane 10: Near-isogenic control spiked with PV-BVHT527462 - 1/10 copy digested with Eco32I
Lane 11: Empty
Lane 12: Molecular Size Marker

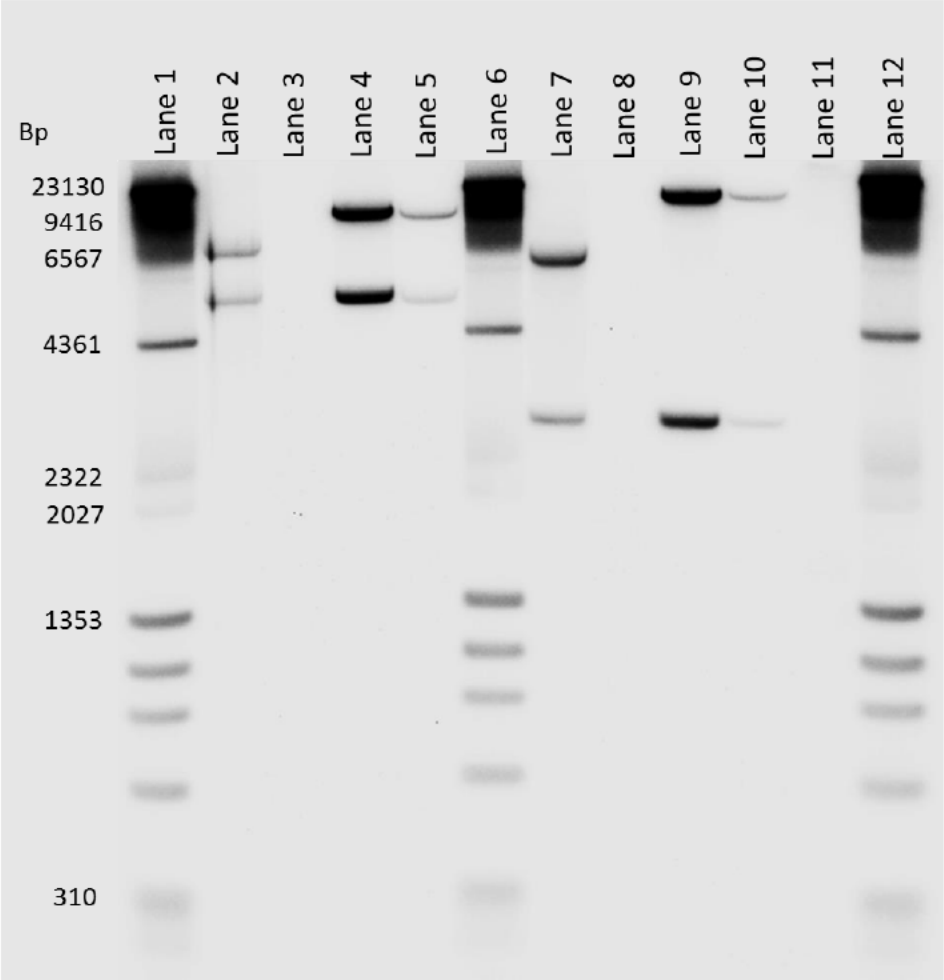

Figure 11. Southern Blot Analysis of KWS20-1 Sugar Beet: T-DNA Insert and Copy Number Analysis - Probes 2 and 4 (Long Run)

Lane 1: Molecular Size Marker
Lane 2: KWS20-1 sugar beet digested with XbaI
Lane 3: Near-isogenic control digested with XbaI
Lane 4: Near-isogenic control spiked with PV-BVHT527462 - 1 copy digested with XbaI
Lane 5: Near-isogenic control spiked with PV-BVHT527462 - 1/10 copy digested with XbaI
Lane 6: Molecular Size Marker
Lane 7: KWS20-1 sugar beet digested with Eco32I
Lane 8: Near-isogenic control digested with Eco32I
Lane 9: Near-isogenic control spiked with PV-BVHT527462 - 1 copy digested with Eco32I
Lane 10: Near-isogenic control spiked with PV-BVHT527462 - 1/10 copy digested with Eco32I
Lane 11: Empty
Lane 12: Molecular Size Marker

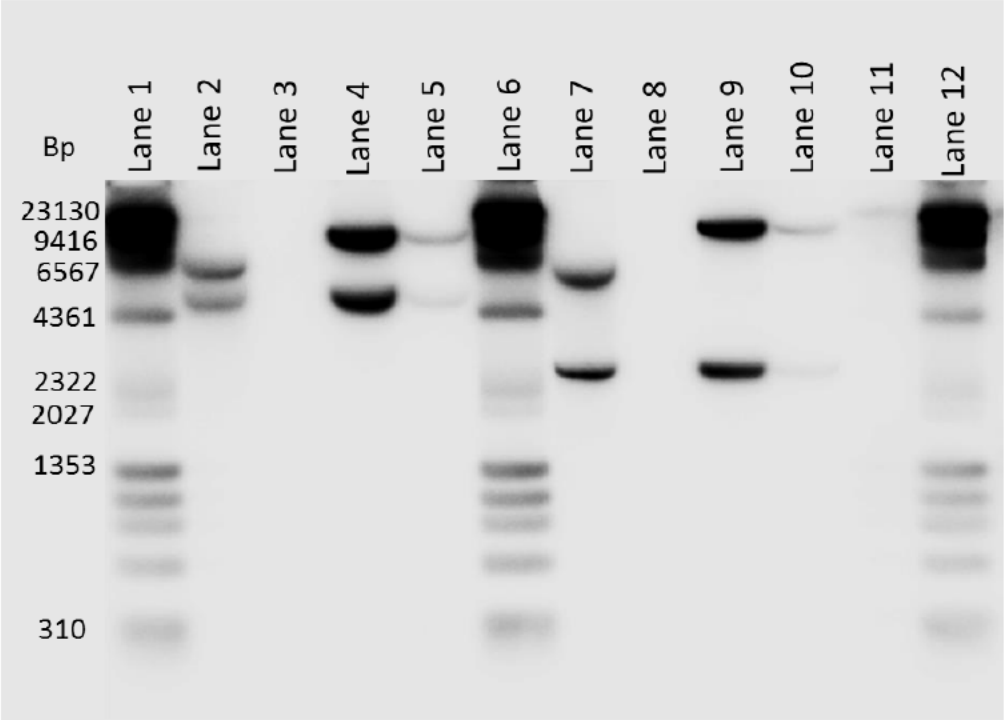

Figure 12. Southern Blot Analysis of KWS20-1 Sugar Beet: T-DNA Insert and Copy Number Analysis - Probes 2 and 4 (Short Run)

Lane 1: Molecular Size Marker
Lane 2: KWS20-1 sugar beet digested with XbaI
Lane 3: Near-isogenic control digested with XbaI
Lane 4: Near-isogenic control spiked with PV-BVHT527462 - 1 copy digested with XbaI
Lane 5: Near-isogenic control spiked with PV-BVHT527462 - 1/10 copy digested with XbaI
Lane 6: Molecular Size Marker
Lane 7: KWS20-1 sugar beet digested with Eco32I
Lane 8: Near-isogenic control digested with Eco32I
Lane 9: Near-isogenic control spiked with PV-BVHT527462 - 1 copy digested with Eco32I
Lane 10: Near-isogenic control spiked with PV-BVHT527462 - 1/10 copy digested with Eco32I
Lane 11: Empty
Lane 12: Molecular Size Marker

.

A.3(c)(ii)(ii) Southern Blot Analysis to Determine Presence or Absence of Plasmid Vector PV-BVHT527462 Backbone in KWS20-1 Sugar Beet

To determine the presence or absence of plasmid vector PV-BVHT527462 backbone sequences, KWS20-1 sugar beet and conventional near-isogenic control genomic DNA were digested with the restriction enzyme XbaI or Eco32I and Southern blots were hybridized with probes that span the plasmid vector backbone sequence (Figure 7). As a positive control on the Southern blots, digested plasmid vector PV-BVHT527462 and probe templates generated from PV-BVHT527462 were used. Approximately 1 and 0.1 genome equivalent of PV-BVHT527462 digested with the restriction enzyme XbaI or Eco32I was mixed with predigested conventional control DNA. As an additional positive control, probe templates (Figure 7, probes 5-8) generated from PV-BVHT527462 were run on the gel. The blot was hybridized with probes 5-8 (Figure 7). If backbone sequences are present in KWS20-1 sugar beet, then probing with backbone probes should result in hybridizing bands. Duplicated samples that consisted of equal amounts of digested DNA were run on agarose gels. One set of samples was run for a longer period of time (long run) than the second set (short run). The long run allows for greater resolution of large molecular weight DNA, whereas the short run allows the detection of small molecular weight DNA. The results of this analysis are shown in Figure 13 and Figure 14.

Conventional near-isogenic control DNA digested with the restriction enzyme XbaI or Eco32I (Figure 13, lanes 3 and 8; Figure 14, lanes 3 and 8) and hybridized simultaneously with the probes 5, 6, 7 and 8 (Figure 7) spanning the entire backbone sequence of plasmid vector PV-BVHT527462 showed no detectable hybridization bands, as expected for the negative control. The positive controls, conventional near-isogenic control DNA digested with XbaI and spiked with XbaI-digested plasmid vector PV-BVHT527462 DNA, produced a single hybridizing band with the expected approximate size of ~13.2 kb (Figure 13, lanes 4 and 5; Figure 14, lanes 4 and 5). The plasmid positive controls, conventional near-isogenic control DNA digested with Eco32I and spiked with Eco32I-digested plasmid vector PV-BVHT527462 DNA, produced a single hybridizing band with the expected approximate size of ~16 kb (Figure 13, lanes 9 and 10; Figure 14, lanes 9 and 10). All four individual probe fragments hybridized with the expected molecular weights (Figure 13, lanes 11-14; Figure 14, lanes 11-14). Detection of the spiked controls and individual probes indicates that the probes hybridized to their target sequences. No hybridizing bands were observed for the KWS20-1 sugar beet genomic DNA (Figure 13, lanes 2 and 7; Figure 14, lanes 2 and 7). These data indicate KWS20-1 sugar beet contains no detectable backbone sequences from plasmid vector PV-BVHT527462.

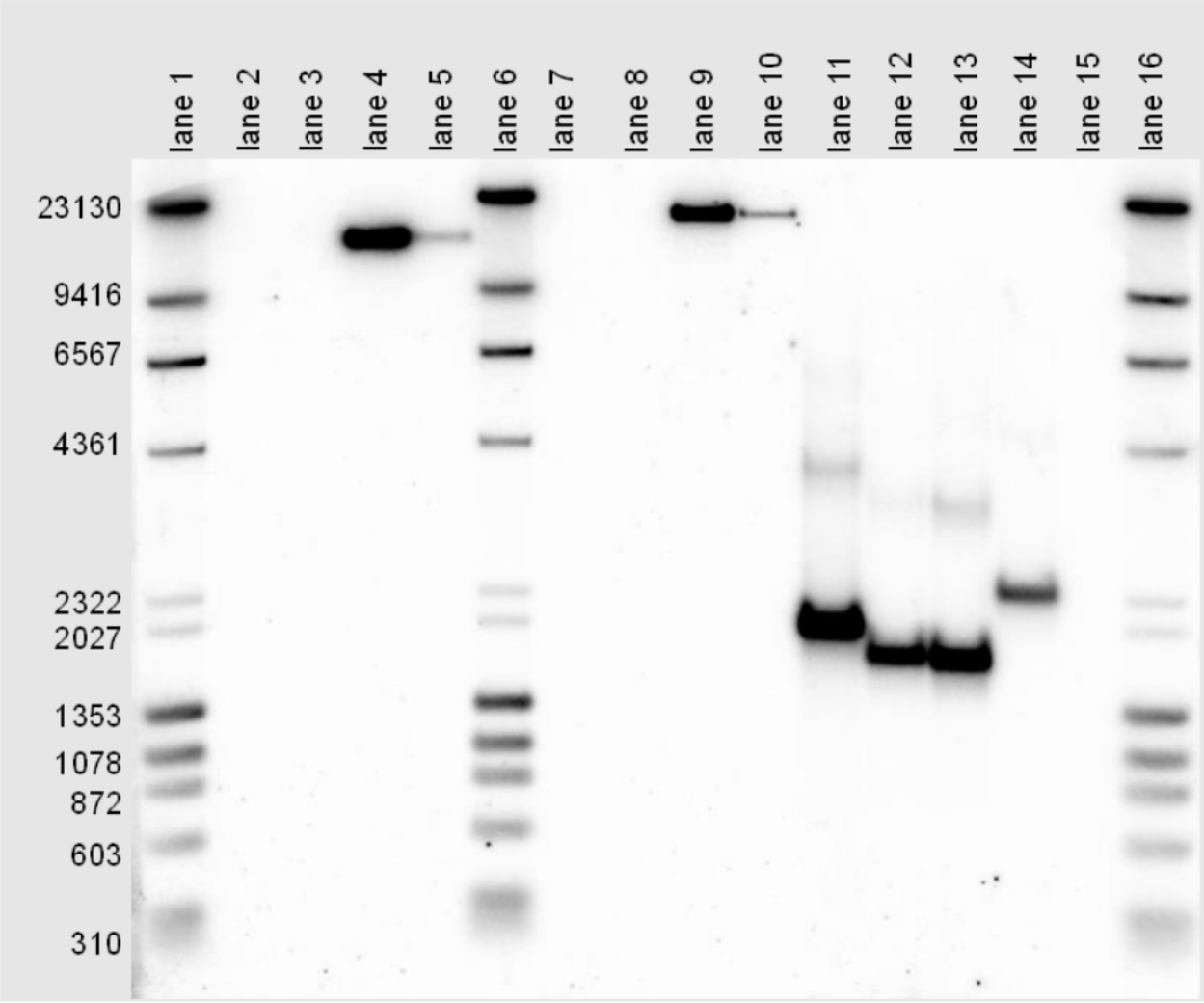

Figure 13. Southern Blot Analysis of KWS20-1 Sugar Beet: Determination of Presence or Absence of PV-BVHT527462 Backbone Sequences - Probes 5, 6, 7 and 8 (Long Run)

Lane 1: Molecular Size Marker
Lane 2: KWS20-1 sugar beet digested with XbaI
Lane 3: Near-isogenic control digested with XbaI
Lane 4: Near-isogenic control spiked with PV-BVHT527462 - 1 copy digested with XbaI
Lane 5: Near-isogenic control spiked with PV-BVHT527462 - 1/10 copy digested with Xba I
Lane 6: Molecular Size Marker
Lane 7: KWS20-1 sugar beet digested with Eco32I
Lane 8: Near-isogenic control digested with Eco32I
Lane 9: Near-isogenic control spiked with PV-BVHT527462 - 1 copy digested with Eco32I
Lane 10: Near-isogenic control spiked with PV-BVHT527462 - 1/10 copy digested with Eco32I
Lane 11: Near-isogenic control + Probe 5
Lane 12: Near-isogenic control + Probe 6
Lane 13: Near-isogenic control + Probe 7
Lane 14: Near-isogenic control + Probe 8
Lane 15: Empty
Lane 16: Molecular Size Marker

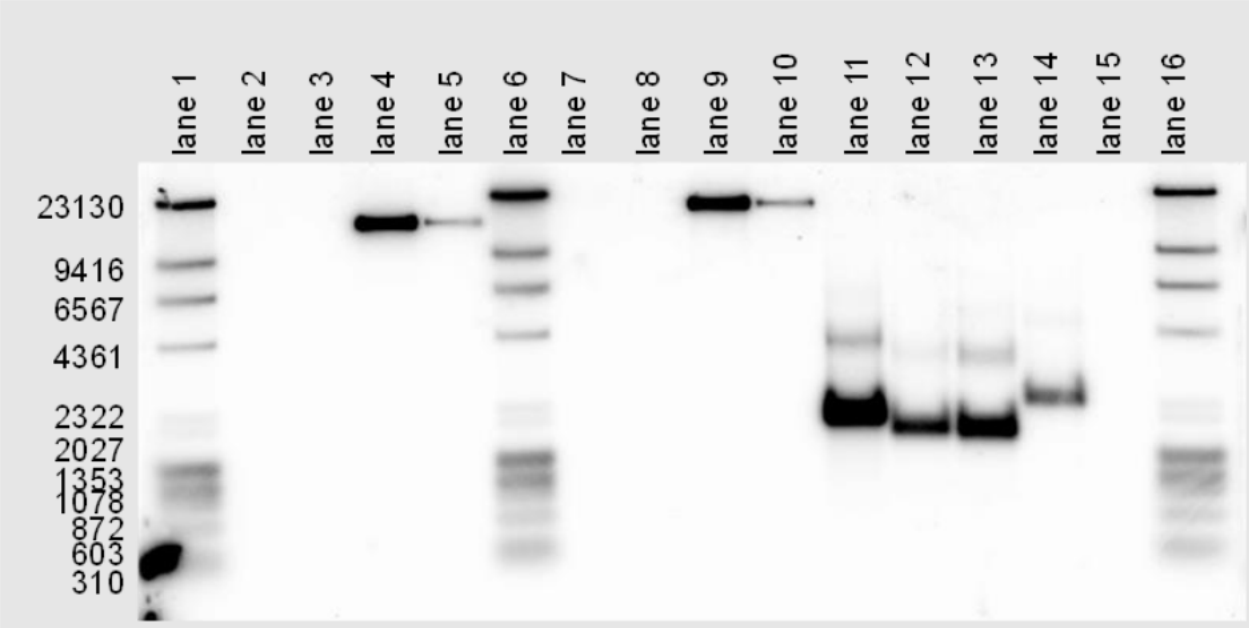

Figure 14. Southern Blot Analysis of KWS20-1 Sugar Beet: Determination of Presence or Absence of PV-BVHT527462 Backbone Sequences - Probes 5, 6, 7 and 8 (Short Run)

Lane 1: Molecular Size Marker
Lane 2: KWS20-1 sugar beet digested with XbaI
Lane 3: Near-isogenic control digested with XbaI
Lane 4: Near-isogenic control spiked with PV-BVHT527462 - 1 copy digested with XbaI
Lane 5: Near-isogenic control spiked with PV-BVHT527462 - 1/10 copy digested with Xba I
Lane 6: Molecular Size Marker
Lane 7: KWS20-1 sugar beet digested with Eco32I
Lane 8: Near-isogenic control digested with Eco32I
Lane 9: Near-isogenic control spiked with PV-BVHT527462 - 1 copy digested with Eco32I
Lane 10: Near-iosgenic control spiked with PV-BVHT527462 - 1/10 copy digested with Eco32I
Lane 11: Near-isogenic control + Probe 5
Lane 12: Near-isogenic control + Probe 6
Lane 13: Near-isogenic control + Probe 7
Lane 14: Near-isogenic control + Probe 8
Lane 15: Empty
Lane 16: Molecular Size Marker

A.3(c)(iii) Full DNA sequence of each insertion site, including junction regions with the host DNA

A.3(c)(iii)(i) Organization and Sequence of the Insert and Adjacent DNA in KWS20-1 Sugar Beet

The organization of the elements within the DNA insert and the adjacent genomic DNA was assessed using directed DNA sequence analysis. PCR primers were designed to amplify overlapping regions of the KWS20-1 sugar beet genomic DNA that span the entire length of the insert and the adjacent DNA flanking the insert (Figure 15 and Figure 16). The 5′ flanking region of the T-DNA insertion site is highly GC-rich making direct sequencing of PCR products over this region technically difficult. To overcome this limitation, a TOPO-TA cloning step was added to generate cloning vectors containing the DNA fragments covering this area (Fragments CPF 141/147, Figure 15). This strategy allows sequencing with standardized primers under optimal conditions, improving the sequencing output. The amplified or cloned PCR products were subjected to DNA sequencing analyses. The results of this analysis confirm that the KWS20-1 sugar beet T-DNA insert is 11,722 bp and that each genetic element within the T-DNA is intact compared to plasmid vector PV-BVHT527462 (Figure 17 and Figure 18). The border regions both contain small terminal deletions with the remainder of the inserted border regions being identical to the sequence in PV-BVHT527462. The sequence and organization of the insert was also shown to be identical to the corresponding T-DNA of plasmid vector PV-BVHT527462 as intended. This analysis also shows that only T-DNA elements (described in Table 3) were present. In addition, 1000 base pairs flanking the 5′ end of the KWS20-1 sugar beet insert (Table 3, bases 1-1000) and 1000 base pairs flanking the 3′ end of the KWS20-1 sugar beet insert (Table 3, bases 12723-13722) were determined.

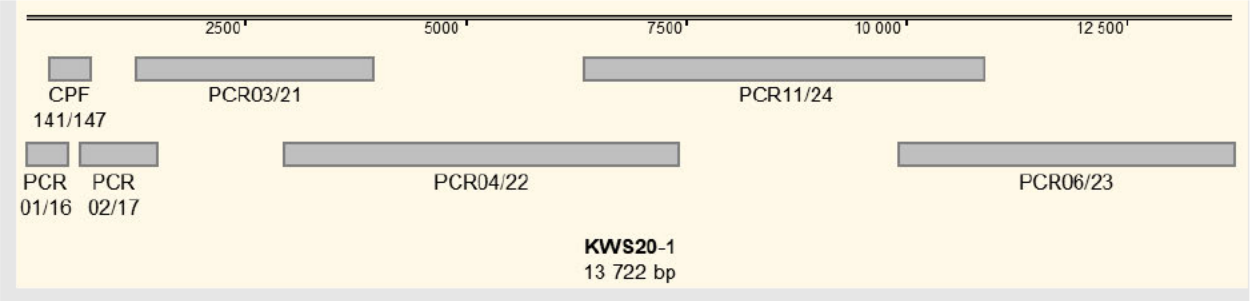

Figure 15. Illustration of PCR Amplicons and Cloned PCR Fragments (CPF) Covering the KWS20-1 Sugar Beet T-DNA Insert and Its Flanking Regions

DNA are represented by the top black line with the length indicated in base pairs. Bases pairs 1-1000 represent the 5' flanking DNA, base pairs 1001- 12722 represent the KWS20-1 sugar beet T-DNA insert and base pairs 12723-13722 represent the 3' flanking DNA. Depicted below the KWS20-1 sugar beet DNA line are the sequenced PCR and cloned PCR fragments. The relative coverage of each sequenced fragment is presented in grey. Each depicted PCR fragment and cloned PCR fragment (CPF) represent two replicate fragments, and their names are indicated (e.g., PCR replicates PCR01 and PCR16 are labeled as "PCR01/16").

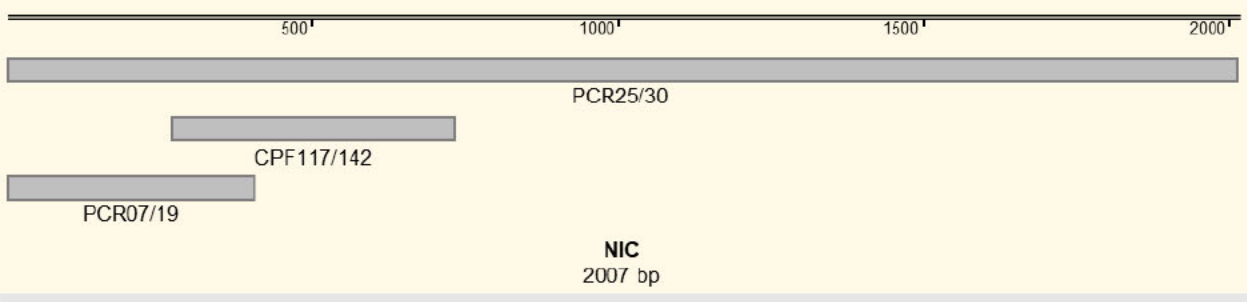

Figure 16. Illustration of PCR Amplicons and Cloned PCR Fragments (CPF) Covering the Position in the Near-isogenic Control Corresponding to the KWS20-1 Sugar Beet T-DNA Insert and Its Flanking Regions

Native sugar beet DNA are represented by the top black line with the length indicated in base pairs. Depicted below the sugar beet DNA line are the sequenced PCR and cloned PCR fragments. The relative coverage of each sequenced fragment is presented in grey. Each depicted PCR fragment and cloned PCR fragment (CPF) represent two replicate fragments, and their names are indicated (e.g., PCR replicates PCR07 and PCR19 are labeled as "PCR07/19").

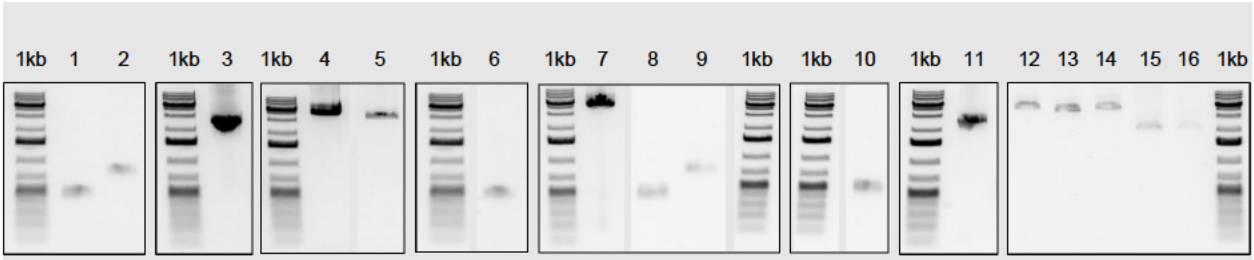

1 kb DNA Ladder

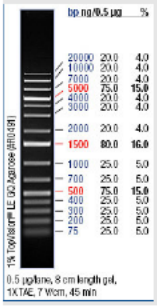

Lane no.	PCR product	Lane no.	PCR product
1	PCR01	9	PCR17
2	PCR02	10	PCR19
3	PCR03	11	PCR21
4	PCR04	12	PCR22
5	PCR06	13	PCR23
6	PCR07	14	PCR24
7	PCR11	15	PCR25
8	PCR16	16	PCR30

Figure 17. Overlapping PCR Analysis Across the Insertion Site and Insert in KWS20-1 Sugar Beet

PCR was performed on both KWS20-1 sugar beet genomic DNA and the conventional near-isogenic control genomic DNA using multiple pairs of primers to generate overlapping PCR fragments from KWS20-1 sugar beet and conventional near-isogenic control DNA for sequencing analysis. To verify the PCR products, a portion of each PCR was loaded on the gel. Lane designations are shown in the accompanying table. The relative position of the amplicons is depicted in Figure 15 (e.g., PCR replicates PCR01 and PCR16 are present in Figure 17, lanes 1 and 8, that are depicted in Figure 15 as fragment "PCR01/16") and Figure 16 (e.g., PCR replicates PCR07 and PCR19 are present in Figure 17, lanes 6 and 10, that are depicted in Figure 16 as "PCR07/19").

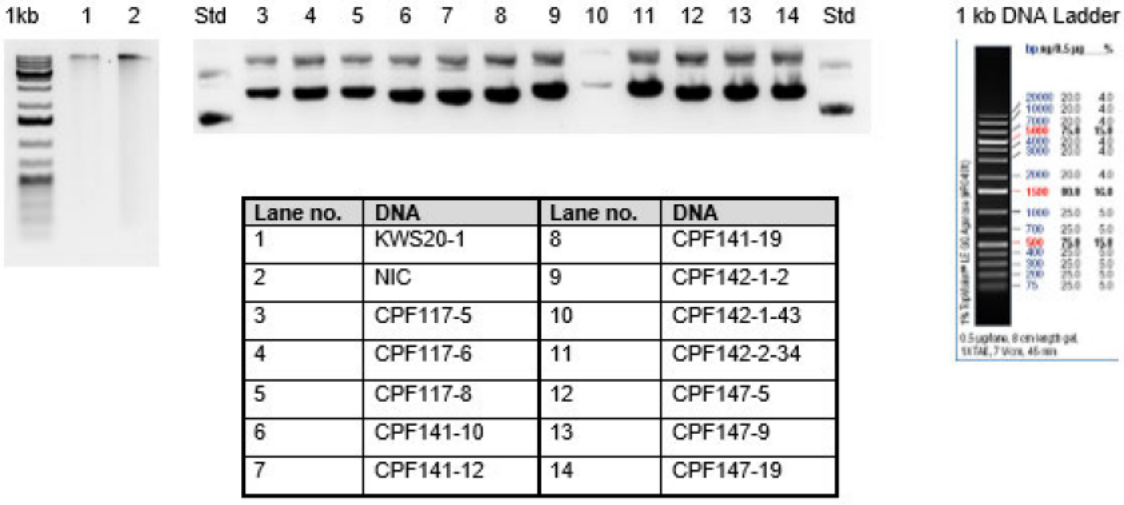

Lane no.	DNA	Lane no.	DNA
1	KWS20-1	8	CPF141-19
2	NIC	9	CPF142-1-2
3	CPF117-5	10	CPF142-1-43
4	CPF117-6	11	CPF142-2-34
5	CPF117-8	12	CPF147-5
6	CPF141-10	13	CPF147-9
7	CPF141-12	14	CPF147-19

Figure 18. Clones Generated for Insertion Site and Flanking DNA Analyses

The 5′ flanking region of the KWS20-1 sugar beet T-DNA insertion site is highly GC-rich. In order to sequence this region, several PCR fragments were cloned. To verify the clones, a portion of each uncut plasmid was loaded on the gel. Lane designations are shown in the accompanying table. The relative position of the cloned PCR fragments (CPFs) are depicted in Figure 15 and Figure 16. In Figure 18, CPF141-10, CPF141-12, CPF141-19 and CPF147-5, CPF147-9, CPF147-19 are three technical replicates of "CPF141" and "CPF147", respectively. These CPFs are labeled in Figure 15 as "CPF141/147". Likewise, in Figure 18, CPF117-5, CPF117-6, CPF117-8 and CPF142-1-2, CPF142-1-43 and CPF142-2-34 are three technical replicates of "CPF117" and "CPF142", respectively. These CPFs are labeled in Figure 16 as "CPF117/142".

Lanes 1-2: Purified undigested gDNA, 1µl loaded per lane;
Lanes 3-14: Purified undigested CPF samples, 5µl loaded per lane; Std = 200 ng pGEM standard; 1kb = 0.25 µg 1kb DNA Ladder.

A.3(c)(iii)(ii) PCR and DNA Sequence Analysis of the KWS20-1 Sugar Beet Insertion Site

PCR and sequence analysis were performed on genomic DNA extracted from the conventional near-isogenic control to examine the insertion site in conventional sugar beet. Several PCRs were conducted and the PCR for the primary amplicon was performed with one primer specific to the genomic DNA sequence flanking the 5′ end of the KWS20-1 sugar beet insert paired with a second primer specific to the genomic DNA sequence flanking the 3′ end of the insert (PCR25/30, Figure 16). Two additional fragments were generated covering the 5′ region in order to generate quality sequence over the GC-rich region (PCR07/19 and CPF117/142, Figure 16). A sequence comparison between the PCR product generated from the conventional near-isogenic control and the sequence generated from the 5′ and 3′ flanking sequences of KWS20-1 sugar beet indicates that seven (7) bases of the sugar beet genomic DNA were deleted during integration of the T-DNA. Such changes are common during plant transformation (Anderson *et al.*, 2016) and these changes presumably resulted from double-stranded break repair mechanisms in the plant during *Agrobacterium*-mediated transformation process (Salomon and Puchta, 1998). The remainder of the sugar beet genomic DNA sequences flanking the insert in KWS20-1 sugar beet are identical to the conventional control.

A.3(c)(iv) A map depicting the organisation of the inserted genetic material at each insertion site

PCR and DNA sequence analyses performed on KWS20-1 sugar beet and the conventional near-isogenic control determined the organisation of the genetic elements within the insert as given in Figure 19

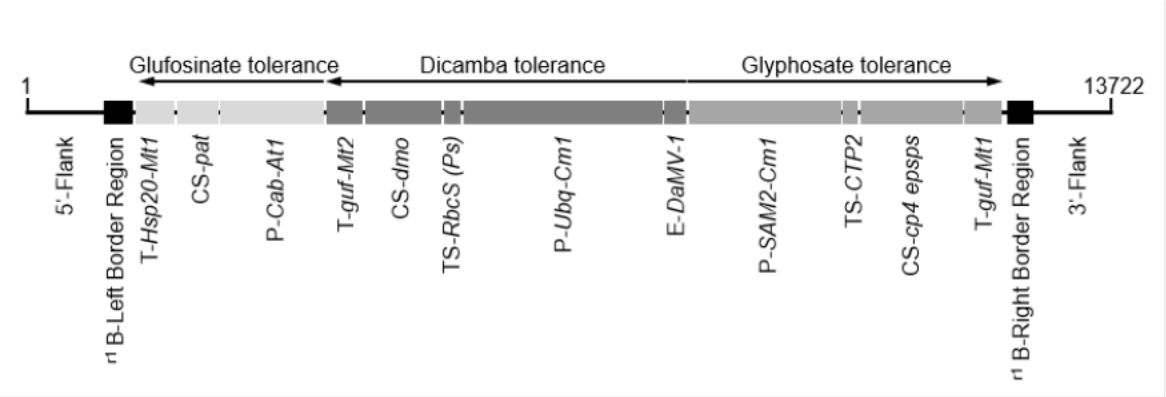

Figure 19. Schematic Representation of the Insert and Flanking Sequences in KWS20-1 Sugar Beet

The scheme represents 13,722 base pairs (1-13,722), which include 1000 base pairs from each of the two flanking regions, together with the full T-DNA. The genetic elements on the T-DNA are indicated. The regions responsible for the expression of each of the three herbicide-tolerance traits are presented in different shades of grey and the respective reading directions on the DNA are indicated. This schematic diagram may not be drawn to scale.

r1Superscript in Left and Right Border Regions indicate that the sequence in KWS20-1 sugar beet was truncated compared to the sequences in PV-BVHT527462.

A.3(c)(v) Details of an analysis of the insert and junction regions for the occurrence of any open reading frames (ORFs)

In addition to the bioinformatic analysis conducted on KWS20-1 sugar beet-produced DMO, PAT and CP4 EPSPS protein sequences (Sections B.2(a)(i) and B.2(b)(ii)), bioinformatic analyses were also performed on the KWS20-1 sugar beet T-DNA insert and flanking genomic DNA sequences to assess the potential for allergenicity, toxicity or biological activity of putative polypeptides encoded by all six reading frames present in the KWS20-1 sugar beet T-DNA insert, as well as ORFs spanning the 5' and 3' T-DNA insert-flanking sequence junctions. These various bioinformatic evaluations are depicted in Figure 20 diting. ORFs spanning the 5' flanking sequence DNA-inserted DNA junctions and 3' flanking sequence DNA-inserted DNA junctions were translated from stop codon to stop codon in all six reading frames (three forward reading

frames and three reading frames in reverse complement orientation)[2]. Putative polypeptides of eight amino acids or greater from each reading frame were then compared to toxin, allergen and all proteins databases using bioinformatic tools. Similarly, the entire KWS20-1 sugar beet T-DNA insert sequence was translated in all six reading frames (three forward reading frames and three reading frames in reverse complement orientation) and the resulting deduced amino acid sequence was subjected to bioinformatic analyses. There are no analytical data that indicate any putative polypeptides/proteins subjected to bioinformatic evaluation other than the KWS20-1 sugar beet-produced DMO, PAT and CP4 EPSPS proteins which are part of the T-DNA insert sequence analysis are produced. Moreover, the data generated from these analyses confirm that even in the highly unlikely occurrence that a translation product other than KWS20-1 sugar beet-produced DMO, PAT and CP4 EPSPS proteins were derived from frames 1 to 6 of the insert DNA, or the ORFs spanning the insert junctions, they would not share a sufficient degree of sequence similarity with other proteins to indicate they would be potentially allergenic, toxic or have other safety implications. Therefore, there is no evidence for concern regarding the relatedness of putative polypeptides from KWS20-1 sugar beet to known toxins, allergens or biologically-active putative peptides.

A.3(c)(v)(i) Bioinformatics Evaluation of the T-DNA Insert Reading Frames in KWS20-1 Sugar Beet

Bioinformatic analyses were performed to assess the potential of toxicity, allergenicity or biological activity of any putative peptides encoded by translation of reading frames 1 through 6 of the inserted DNA in KWS20-1 sugar beet (Figure 20).

The FASTA sequence alignment tool was used to assess structural relatedness between the query sequences and any protein sequences in the AD_2022, TOX_2022 and PRT_2022 databases. Structural similarities shared between each putative polypeptide with each sequence in the database was examined. The extent of structural relatedness was evaluated by detailed visual inspection of the alignment, the calculated percent identity and alignment length as 35% or greater identity in 80 or greater amino acids to ascertain if alignments exceeded Codex (Codex Alimentarius, 2009) thresholds for FASTA searches of the AD_2022 database, and the *E*-score. Alignments having an *E*-score less than 1×10^{-5} are deemed significant because they may reflect shared structure and function among sequences. In addition to structural similarity, each putative polypeptide was screened for short polypeptide matches using a pair-wise comparison algorithm. In these analyses, eight contiguous and identical amino acids were defined as immunologically-relevant, where eight represents the typical minimum sequence length likely to represent an immunological epitope (Silvanovich *et al.*, 2006) and evaluated against the AD_2022 database.

[2] An evaluation of sequence translated from stop codon to stop codon represents the most conservative approach possible for flank junction analysis as it does not take into consideration that a start codon is necessary for the production of a protein sequence.

The results of the search comparisons showed that no relevant structural similarity to known allergens and toxins were observed for any of the putative polypeptides when compared to proteins in the allergen (AD_2022) or toxin (TOX_2022) databases. When subjected to a sliding 8-mer search of the AD_2022 database, frame 6 yielded a single 8-mer match to AEV41413.1, described as Allergen beta-1,3-glucanase from *Hevea brasiliensis* (Pará rubber tree), a candidate latex allergen. However, this 8-mer is located in the predicted signal peptide of AEV41413.1, which would be cleaved off in the mature protein (Torres *et al.*, 2015). Therefore, the match to the 8-mer of AEV41413.1 would not result in an increased allergy risk in KWS20-1 sugar beet. Furthermore, the only expected translation products from the T-DNA insert in KWS20-1 sugar beet are DMO, PAT and CP4 EPSPS, which are encoded on frame 4, frame 5 and frame 2, respectively. There is no evidence to suggest that the putative peptide containing a single 8-mer match to AEV41413.1 is produced *in planta*. No short (i.e., eight-amino acid) polypeptide matches were shared between the putative polypeptides from frames 1-5 and proteins in the allergen database.

When the frames were used to query the PRT_2022 database, the results of these analyses positively identified the following genetic elements within the KWS20-1 sugar beet T-DNA: (1) all alignments to frame 1 were punctuated with stop codons in the query sequence and required gaps to optimize the alignment. As a result, it is unlikely any of these alignments reflect conserved structure and, therefore, do not indicate potential for adverse biological activity; (2) frame 2 top alignment was to AQN08360.1, which corresponds to "Sequence 17 from patent U.S. 9365863". This alignment represents the self-identification of the CTP2 and CP4 EPSPS present in KWS20-1 sugar beet; (3) frame 3 did not yield an alignment with an *E*-score of ≤1e-5; (4) frame 4 top alignment was to AJM44845.1, which corresponds to "Sequence 28 from patent U.S. 8791325". This alignment represents the self-identification of DMO present in KWS20-1 sugar beet. A second region of alignments is represented by ABO87585.1, which corresponds to "inclusion body matrix protein, partial" from Dahlia mosaic virus (DaMV). This alignment displayed 100% identity over 111 amino acids, with an *E*-score of 3.5e-39. Alignments to this region were expected and correspond to the DaMV enhancer present in KWS20-1 sugar beet. A third region of alignments is represented by ADT45325.1, which corresponds to "Sequence 1 from patent U.S. 7838729". This alignment displayed 100% identity over 84 amino acids, with an *E*-score of 5.1e-28. Alignments to this region were also expected and correspond to the *TS-RbcS* element present in KWS20-1 sugar beet; (5) frame 5 top alignment was to CAA00269.1, which corresponds to "phosphinothricin resistance". This alignment represents the self identification of PAT present in KWS20-1 sugar beet; and (6) all alignments to frame 6 were punctuated with stop codons in the query sequence and required gaps to optimize the alignment. As a result, it is unlikely any of these alignments, other than the expected sequences in KWS20-1 sugar beet, reflect conserved structure and therefore do not indicate potential for adverse biological activity. No other relevant sequence similarities between the six reading frames translated from the KWS20-1 sugar beet T-DNA were observed with allergens, toxins or other biologically-active proteins of concern.

Taken together, these data demonstrate the lack of relevant similarities between known allergens or toxins for putative peptides derived from all six reading frames from the inserted DNA sequence of KWS20-1 sugar beet. As a result, in the unlikely event that a translation product other than DMO, PAT and CP4 EPSPS proteins was derived from reading frames 1 to 6, these putative polypeptides are not expected to be cross-reactive allergens, toxins or display adverse biological activity.

A.3(c)(v)(ii) Bioinformatics Evaluation of the DNA Sequences Flanking the 5′ and 3′ Junctions of the KWS20-1 Sugar Beet Insert: Assessment of Putative Peptides

Analyses of putative polypeptides encoded by DNA spanning the 5' and 3' genomic junctions of the KWS20-1 sugar beet inserted DNA were performed using a bioinformatic comparison strategy. The purpose of the assessment is to evaluate the potential for novel open reading frames (ORFs) that may have homology to known allergens, toxins or proteins that display adverse biological activity. Sequences spanning the 5' and 3' genomic DNA-insert DNA junctions (Figure 20) were translated from stop codon (TGA, TAG, TAA) to stop codon in all six reading frames. Putative polypeptides from each reading frame, that were eight amino acids or greater in length, were compared to AD_2022, TOX_2022 and PRT_2022 databases using FASTA and to the AD_2022 database using an eight-amino acid sliding window search. A total of 10 putative polypeptide sequences were compared to allergen (AD_2022), toxin (TOX_2022) and all protein (PRT_2022) databases using bioinformatic tools.

The FASTA sequence alignment tool was used to assess structural relatedness between the query sequences and any protein sequences in the AD_2022, TOX_2022 and PRT_2022 databases. Structural similarities shared between each putative polypeptide with each sequence in the database were examined. The extent of structural relatedness was evaluated by detailed visual inspection of the alignment, the calculated percent identity, alignment length, as 35% or greater identity in 29 or more amino acids in an $\geq$80 amino acid overlap to ascertain if alignments exceeded Codex Alimentarius (Codex Alimentarius, 2009) thresholds for FASTA searches of the AD_2022 database, and the *E*-score. Alignments having an *E*-score less than 1×10^{-5} are deemed significant because they may reflect shared structure and function among sequences. In addition to sequence similarity, each putative polypeptide was screened for short polypeptide matches using a pair-wise comparison algorithm. In these analyses, eight contiguous and identical amino acids were defined as immunologically-relevant, where eight represents the typical minimum sequence length likely to represent an immunological epitope (Silvanovich *et al.*, 2006).

The analysis performed using the 10 putative peptide sequences translated from junctions is theoretical. The results of these bioinformatic analyses indicate that no structurally-relevant sequence similarities were observed between the translated putative flank junction derived sequences and allergens, toxins or biologically-active proteins. Likewise, other than translation of DMO, PAT and CP4 EPSPS, no evidence exists to indicate that any other sequence from the KWS20-1 sugar beet T-DNA junctions is translated. Rather, the results of these bioinformatic analyses indicate that in the unlikely occurrence that any of the putative flank-junction sequences analyzed herein is found *in planta*, or translation of sequence other than the intended protein products was to occur, none would share significant similarity or identity to known allergens, toxins or other biologically-active proteins that could affect human or animal health.

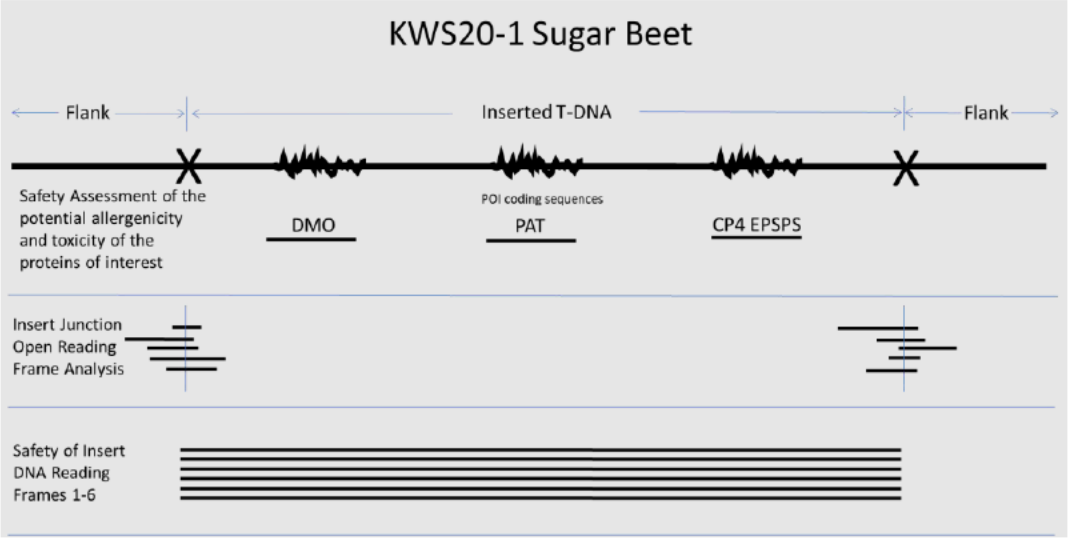

Figure 20. Schematic Summary of KWS20-1 Sugar Beet Bioinformatic Analyses

A.3(c)(v)(iii) Bioinformatic Evaluation of Putative Open Reading Frames of KWS20-1 Sugar Beet Insert and Flanking Sequences Summary and Conclusions

A conservative bioinformatic assessment of potential allergenicity, toxicity and adverse-biological activity for putative polypeptides derived from different reading frames of the entire insert of KWS20-1 sugar beet or that span the 5' and 3' insert junctions was conducted. There are no analytical data that indicate any putative polypeptides subjected to bioinformatic evaluation are produced by KWS20-1 sugar beet. Moreover, the data generated from these analyses confirm that even in the highly unlikely occurrence that a translation product other than KWS20-1 sugar beet-produced DMO, PAT and CP4 EPSPS proteins were derived from frames 1 to 6 of the insert DNA, or the ORFs spanning the insert junctions, they would not share a sufficient degree of sequence similarity with other proteins to indicate they would be potentially allergenic, toxic or have other safety implications. Furthermore, no short (i.e., eight-amino acid) polypeptide matches were shared between any of the putative polypeptides and proteins in the allergen database. Therefore, there is no evidence for concern regarding the putative polypeptides for KWS20-1 sugar beet relatedness to known toxins, allergens or biologically-active putative peptides.

For details, please refer to Appendix 3 and Appendix 4.

A.3(d) A description of how the line or strain from which food is derived was obtained from the original tranformant (i.e. provide a family tree or describe the breeding process) including which generations have been used for each study

KWS20-1 sugar beet was derived from a single plant transformant of breeding line 04E05B1DH05, from which the near-isogenic control was derived. The near-isogenic control was used as the conventional sugar beet comparator to support the safety assessment of KWS20-1 sugar beet. KWS20-1 sugar beet and the conventional near-isogenic control have similar genetic backgrounds with the exception of the *dmo*, *pat* and *cp4 epsps* expression cassettes, thus, the effect of the *dmo*, *pat* and *cp4 epsps* expression cassettes and the expressed DMO, PAT and CP4 EPSPS

proteins can be assessed in an unbiased manner in comparative safety assessments. Where appropriate, commercial reference sugar beet materials were used to establish a range of variability or responses representative of commercial sugar beet.

For more details, see KWS20-1 sugar beet breeding history Figure 8.

A.3(e) Evidence of the stability of the genetic changes, including:

A.3(e)(i) The pattern of inheritance of the transferred gene(s) and the number of generations over which this has been monitored

In order to demonstrate the stability of the T-DNA insert present in KWS20-1 sugar beet through multiple generations, Southern blot analysis was performed using DNA obtained from five breeding generations of KWS20-1 sugar beet. For reference, the breeding history of KWS20-1 sugar beet is presented in Figure 8, and the specific generations tested are indicated in the figure legend. The T2 generation was used for the molecular characterization analyses shown in Sections A.3(c)(ii) and A.3(c)(iii). To analyze stability, four additional generations were evaluated by Southern blot analysis and compared to the fully characterized T2 generation. Genomic DNA, isolated from each of the selected generations of KWS20-1 sugar beet and the conventional near-isogenic control, was digested and probed with the T-DNA specific probes (1 and 3, 2 and 4) as described in Section A.3(c)(ii). Any instability associated with the T-DNA insert would be detected as novel bands within the fingerprint on the Southern blot. The Southern blot has the same positive hybridization controls as described in Section A.3(c)(ii). The results are shown in Figure 21, Figure 22, Figure 23 and Figure 24.

Probes 1 and 3

Conventional near-isogenic control DNA digested with the restriction enzyme XbaI (Figure 21, lane 5) or Eco32I (Figure 21, lane 12) and hybridized with probes 1 and 3 (Figure 21) produced no detectable hybridization bands, as expected for the negative control. Conventional near-isogenic control DNA digested with XbaI and spiked with XbaI-digested plasmid vector PV-BVHT527462 DNA produced two expected size bands at ~13.2 kb and ~5.7 kb (Figure 21, lanes 6 and 7). Eco32I-digested conventional control DNA spiked with Eco32I-digested plasmid vector PV-BVHT527462 DNA produced a single expected size band at ~16.0 kb (Figure 21, lanes 13 and 14). Likewise, conventional near-isogenic control DNA digested with the restriction enzyme XbaI (Figure 22, lane 4) or Eco32I (Figure 22, lane 10) and hybridized with probes 1 and 3 (Figure 22) produced no detectable hybridization bands, as expected for the negative control. Conventional near-isogenic control DNA digested with XbaI and spiked with XbaI-digested plasmid vector PV-BVHT527462 DNA produced two expected size bands at ~13.2 kb and ~5.7 kb Figure 22, lanes 5 and 6). Eco32I-digested conventional control DNA spiked with Eco32I-digested plasmid vector PV-BVHT527462 DNA produced a single expected size band at ~16.0 kb (Figure 22, lanes 11 and 12). Collectively, these results indicate that each probe is hybridizing to its target sequence.

Digestion of KWS20-1 sugar beet genomic DNA from multiple generations (T2, T3, T4) with the restriction enzyme Xba1 and hybridized with probes 1 and 3 (Figure 6) produced three bands at ~8.4 kb, ~5.7 kb and ~3.5 kb (Figure 21, lanes 2-4). The ~8.4 kb band represents the 3' flanking region and the Right Border-end of the inserted T-DNA (Figure 6). The ~5.7 kb band represents

the inner T-DNA fragment (Figure 6). The ~3.5 kb band represents the 5' flanking region and the Left Border-end of the inserted T-DNA (Figure 6). Digestion with Eco32I produced two bands at ~16.2 kb and ~7.2 kb (Figure 21, lanes 9-11). The ~16.2 kb band represents the 5' flanking region and the Left Border-end of the inserted T-DNA (Figure 6). The ~7.2 kb band represents the 3' flanking region and the Right Border-end of the inserted T-DNA (Figure 6).

Likewise, digestion of KWS20-1 sugar beet genomic DNA from the T1 and T5 generations with the restriction enzyme Xba1 and hybridized with probes 1 and 3 (Figure 6) produced three bands at ~8.4 kb, ~5.7 kb and ~3.5 kb (Figure 22, lanes 2 and 3). The ~8.4 kb band represents the 3' flanking region and the Right Border-end of the inserted T-DNA (Figure 6). The ~5.7 kb band represents the inner T-DNA fragment (Figure 6). The ~3.5 kb band represents the 5' flanking region and the Left Border-end of the inserted T-DNA (Figure 6). Digestion with Eco32I produced two bands at ~16.2 kb and ~7.2 kb (Figure 22, lanes 8 and 9). The ~16.2 kb band represents the 5' flanking region and the Left Border-end of the inserted T-DNA (Figure 6). The ~7.2 kb band represents the 3' flanking region and the Right Border-end of the inserted T-DNA (Figure 6).

Probes 2 and 4

Conventional near-isogenic control DNA digested with the restriction enzyme XbaI (Figure 23, lane 5) or Eco32I (Figure 23, lane 12) and hybridized with probes 2 and 4 (Figure 23) produced no detectable hybridization bands, as expected for the negative control. Conventional near-isogenic control DNA digested with XbaI and spiked with XbaI-digested plasmid vector PV-BVHT527462 DNA produced two expected size bands at ~13.2 kb and ~5.7 kb (Figure 23, lanes 6 and 7). Eco32I-digested conventional control DNA spiked with Eco32I-digested plasmid vector PV-BVHT527462 DNA produced two expected size bands at ~16.0 kb and ~2.9 kb (Figure 23, lanes 13 and 14). Likewise, conventional near-isogenic control DNA digested with the restriction enzyme XbaI (Figure 24, lane 4) or Eco32I (Figure 24, lane 10) and hybridized with probes 2 and 4 (Figure 24) produced no detectable hybridization bands, as expected for the negative control. Conventional near-isogenic control DNA digested with XbaI and spiked with XbaI-digested plasmid vector PV-BVHT527462 DNA produced two expected size bands at ~13.2 kb and ~5.7 kb (Figure 24, lanes 5 and 6). Eco32I-digested conventional control DNA spiked with Eco32I-digested plasmid vector PV-BVHT527462 DNA produced two expected size bands at ~16.0 kb and ~2.9 kb (Figure 24, lanes 11 and 12). Collectively, these results indicate that each probe is hybridizing to its target sequence.

Digestion of KWS20-1 sugar beet genomic DNA from multiple generations (T2, T3, T4) with the restriction enzyme Xba1 and hybridized with probes 2 and 4 (Figure 6) produced two bands at ~8.4 kb and ~5.7 kb (Figure 23, lanes 2-4). The ~8.4 kb band represents the 3' flanking region and the Right Border-end of the inserted T-DNA (Figure 6). The ~5.7 kb band represents the inner T-DNA fragment (Figure 6). Digestion with Eco32I produced two bands at ~7.2 kb and ~2.9 kb (Figure 23, lanes 9-11). The ~16.2 kb band represents the 5' flanking region and the Left Border-end of the inserted T-DNA, detected by probe 2 (Figure 6). The ~7.2 kb band represents the 3' flanking region and the Right Border-end of the inserted T-DNA, detected by probe 4 (Figure 6).

Likewise, digestion of KWS20-1 sugar beet genomic DNA from the T1 and T5 generations with the restriction enzyme Xba1 and hybridized with probes 2 and 4 (Figure 6) produced two bands at ~8.4 kb and ~5.7 kb (Figure 24, lanes 2 and 3). The ~8.4 kb band represents the 3' flanking region and the Right Border-end of the inserted T-DNA (Figure 6). The ~5.7 kb band represents the inner T-DNA fragment (Figure 6). Digestion with Eco32I produced two bands at ~7.2 kb and ~2.9 kb (Figure 24, lanes 8 and 9). The ~16.2 kb band represents the 5' flanking region and the Left Border-end of the inserted T-DNA, detected by probe 2 (Figure 6). The ~7.2 kb band represents the 3' flanking region and the Right Border-end of the inserted T-DNA, detected by probe 4 (Figure 6).

The fingerprint of the Southern blot signals from multiple generations, T1, T2, T3, T4 and T5 (Figure 21, lanes 2-4 and 9-11; Figure 22, lanes 2-3 and 8-9; Figure 23, lanes 2-4 and 9-11; Figure 24, lanes 2-3 and 8-9), of KWS20-1 sugar beet is consistent with the fully characterized KWS20-1 sugar beet generation T2 (Figure 9, lanes 2 and 7; Figure 10, lanes 2 and 7). No unexpected bands were detected.

These results demonstrate that the single locus of integration characterized in the T2 generation of KWS20-1 sugar beet is found in five breeding generations of KWS20-1 sugar beet, confirming the stability of the insert. This comprehensive Southern blot analysis from multiple generations supports the conclusion that KWS20-1 sugar beet contains a single, stable T-DNA insert.

For details, please refer to Appendix 1 and Appendix 2.

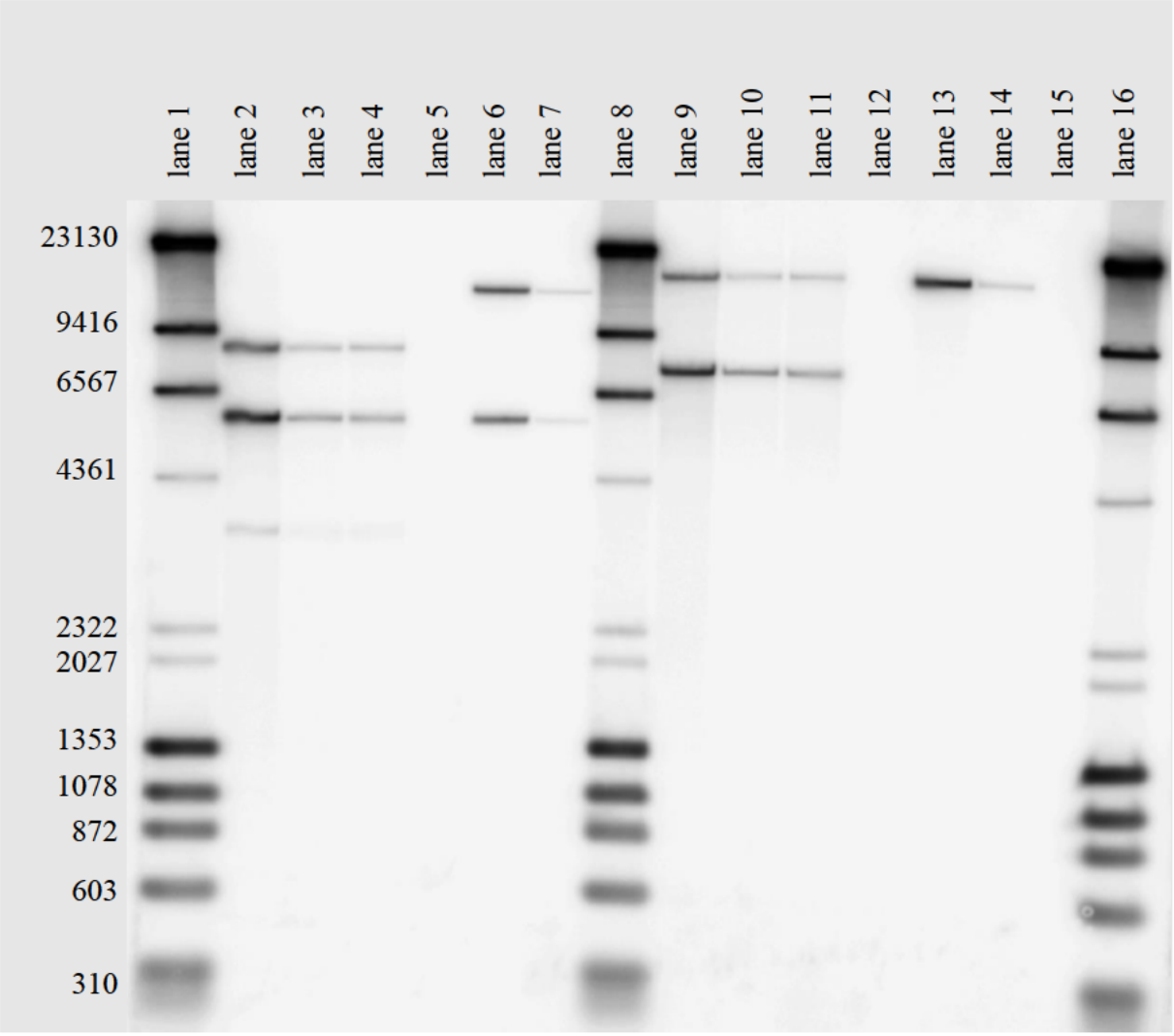

Figure 21. Southern Blot Analysis of KWS20-1 Sugar Beet: T-DNA Insert Stability in Multiple (T2-T4) Generations – Probes 1 and 3

Lane 1: Molecular Size Marker
Lane 2: KWS20-1 sugar beet (T2) digested with XbaI
Lane 3: KWS20-1 sugar beet (T3) digested with XbaI
Lane 4: KWS20-1 sugar beet (T4) digested with XbaI
Lane 5: Near-isogenic control digested with XbaI
Lane 6: Near-isogenic control spiked with PV-BVHT527462 – 1 copy digested with XbaI
Lane 7: Near-isogenic control spiked with PV-BVHT527462 – 1/10 copy digested with XbaI
Lane 8: Molecular Size Marker
Lane 9: KWS20-1 sugar beet (T2) digested with Eco32I
Lane 10: KWS20-1 sugar beet (T3) digested with Eco32I
Lane 11: KWS20-1 sugar beet (T4) digested with Eco32I
Lane 12: Near-isogenic control digested with Eco32I
Lane 13: Near-isogenic control spiked with PV-BVHT527462 – 1 copy digested with Eco32I
Lane 14: Near-isogenic control spiked with PV-BVHT527462 – 1/10 copy digested with Eco32I
Lane 15: Empty
Lane 16: Molecular Size Marker

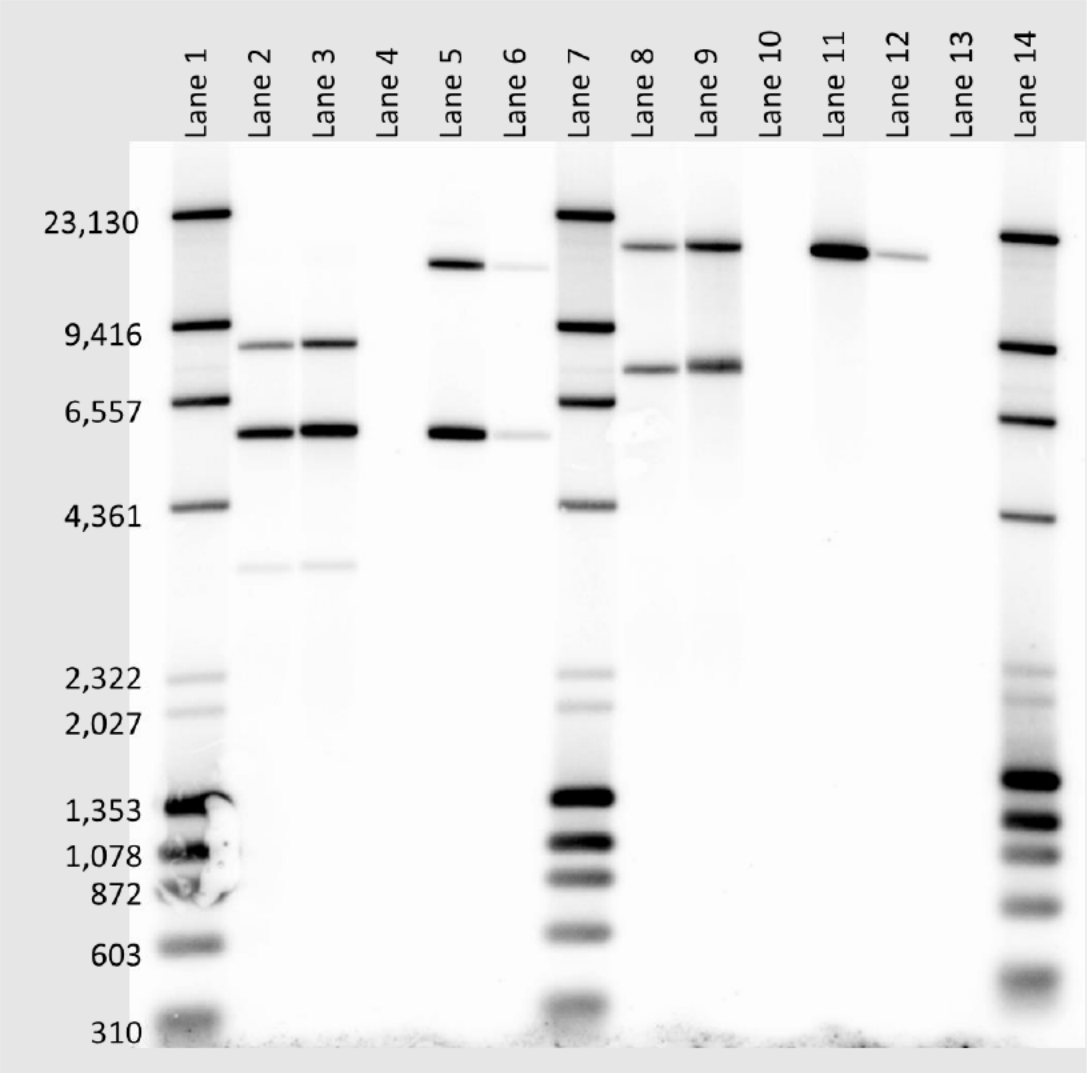

Figure 22. Southern Blot Analysis of KWS20-1 Sugar Beet: T-DNA Insert Stability in the T1 and T5 Generations – Probes 1 and 3

Lane 1: Molecular Size Marker
Lane 2: KWS20-1 sugar beet (T1) digested with XbaI
Lane 3: KWS20-1 sugar beet (T5) digested with XbaI
Lane 4: Near-isogenic control digested with XbaI
Lane 5: Near-isogenic control spiked with PV-BVHT527462 – 1 copy digested with XbaI
Lane 6: Near-isogenic control spiked with PV-BVHT527462 – 1/10 copy digested with XbaI
Lane 7: Molecular Size Marker
Lane 8: KWS20-1 sugar beet (T1) digested with Eco32I
Lane 9: KWS20-1 sugar beet (T5) digested with Eco32I
Lane 10: Near-isogenic control digested with Eco32I
Lane 11: Near-isogenic control spiked with PV-BVHT527462 – 1 copy digested with Eco32I
Lane 12: Near-isogenic control spiked with PV-BVHT527462 – 1/10 copy digested with Eco32I
Lane 13: Empty
Lane 14: Molecular Size Marker

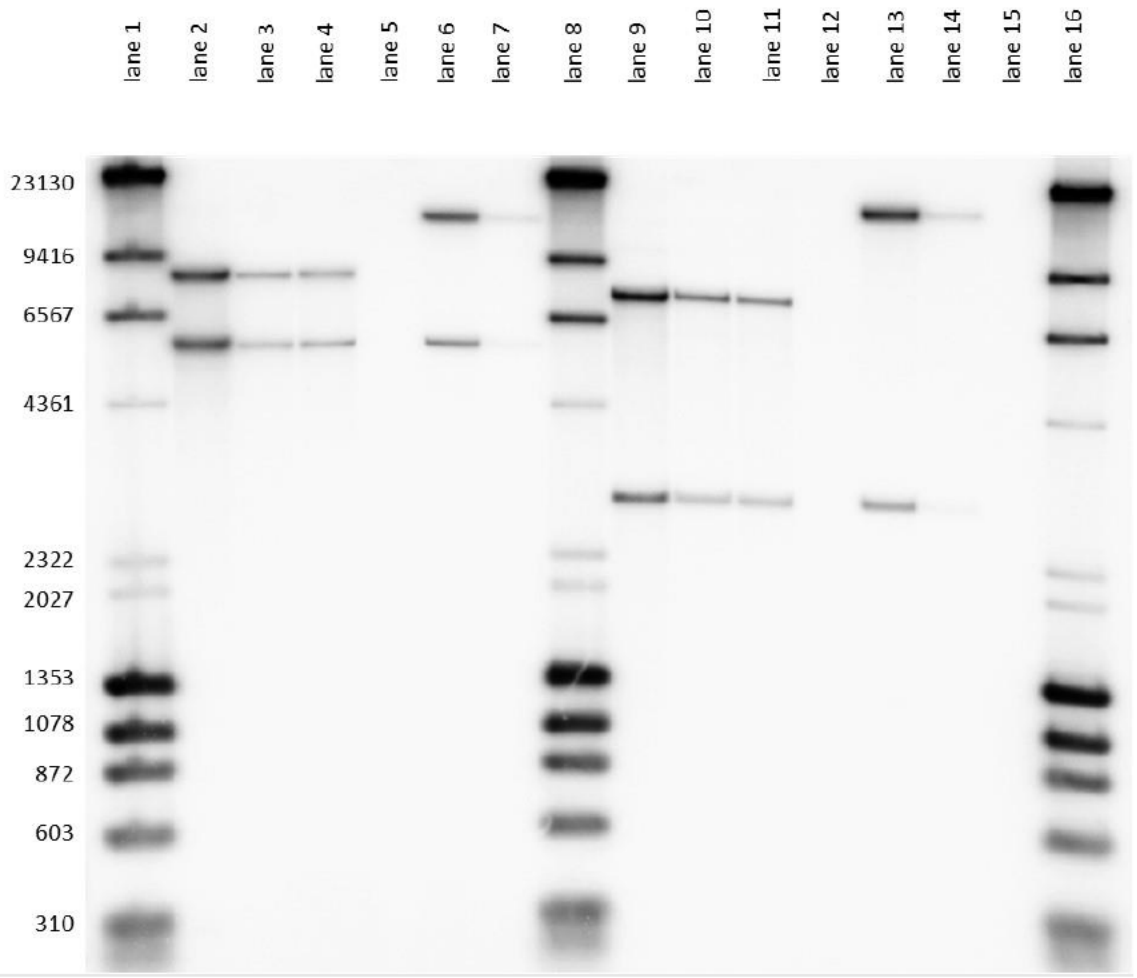

Figure 23. Southern Blot Analysis of KWS20-1 Sugar Beet: T-DNA Insert Stability in Multiple (T2-T4) Generations – Probes 2 and 4

Lane 1: Molecular Size Marker
Lane 2: KWS20-1 sugar beet (T2) digested with XbaI
Lane 3: KWS20-1 sugar beet (T3) digested with XbaI
Lane 4: KWS20-1 sugar beet (T4) digested with XbaI
Lane 5: Near-isogenic control digested with XbaI
Lane 6: Near-isogenic control spiked with PV-BVHT527462 – 1 copy digested with XbaI
Lane 7: Near-isogenic control spiked with PV-BVHT527462 – 1/10 copy digested with XbaI
Lane 8: Molecular Size Marker
Lane 9: KWS20-1 sugar beet (T2) digested with Eco32I
Lane 10: KWS20-1 sugar beet (T3) digested with Eco32I
Lane 11: KWS20-1 sugar beet (T4) digested with Eco32I
Lane 12: Near-isogenic control digested with Eco32I
Lane 13: Near-isogenic control spiked with PV-BVHT527462 – 1 copy digested with Eco32I
Lane 14: Near-isogenic control spiked with PV-BVHT527462 – 1/10 copy digested with Eco32I
Lane 15: Empty
Lane 16: Molecular Size Marker

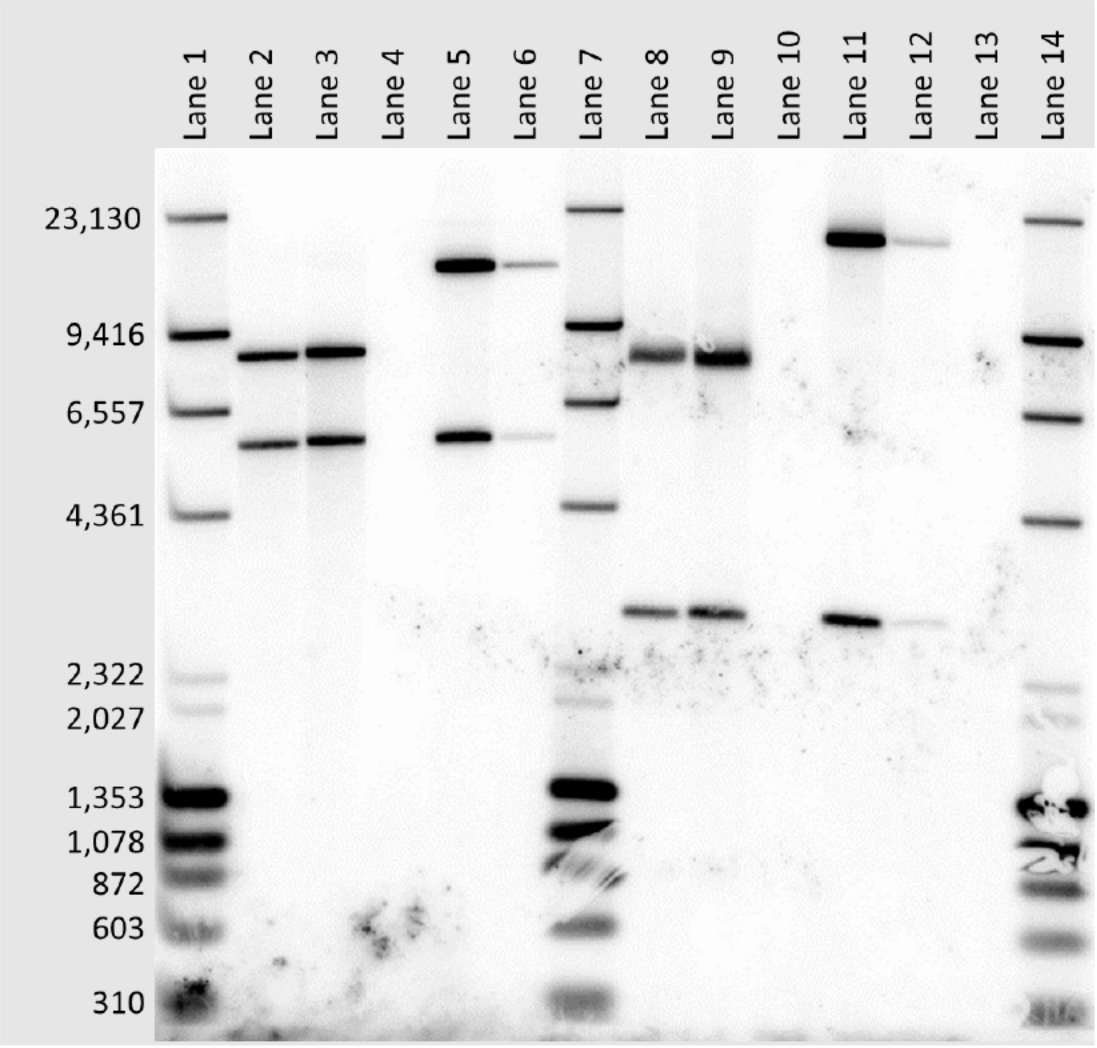

Figure 24. Southern Blot Analysis of KWS20-1 Sugar Beet: T-DNA Insert Stability in the T1 and T5 Generations – Probes 2 and 4

Lane 1: Molecular Size Marker
Lane 2: KWS20-1 sugar beet (T1) digested with XbaI
Lane 3: KWS20-1 sugar beet (T5) digested with XbaI
Lane 4: Near-isogenic control digested with XbaI
Lane 5: Near-isogenic control spiked with PV-BVHT527462 − 1 copy digested with XbaI
Lane 6: Near-isogenic control spiked with PV-BVHT527462 − 1/10 copy digested with XbaI
Lane 7: Molecular Size Marker
Lane 8: KWS20-1 sugar beet (T1) digested with Eco32I
Lane 9: KWS20-1 sugar beet (T5) digested with Eco32I
Lane 10: Near-isogenic control digested with Eco32I
Lane 11: Near-isogenic control spiked with PV-BVHT527462 − 1 copy digested with Eco32I
Lane 12: Near-isogenic control spiked with PV-BVHT527462 − 1/10 copy digested with Eco32I
Lane 13: Empty
Lane 14: Molecular Size Marker

A.3(e)(ii) The pattern of inheritance and expression of the phenotype over several generations and, where appropriate, across different environments

A.3(e)(ii)(i) Inheritance of the Genetic Insert in KWS20-1 Sugar Beet

The KWS20-1 sugar beet T-DNA resides at a single locus within the sugar beet genome of genotype 04E05B1DH05 and therefore should be inherited according to Mendelian principles of inheritance. Genotypic segregation data were recorded to assess the inheritance and stability of the KWS20-1 sugar beet T-DNA using Chi square (χ^2) analysis across generations. The χ^2 analysis is based on comparing the observed segregation ratio to the expected segregation ratio according to Mendelian principles.

The KWS20-1 sugar beet breeding path for generating segregation data is described in Figure 24. A single transformed T0 plant was self-pollinated to generate T1 seed. The resultant T1 plants were tested and those positive for the KWS20-1 sugar beet T-DNA were identified by KASP analysis in the T1 segregating population. Homozygous positive T1 plants were crossed by open pollination in an isolated field to give rise to T2 seed. A single homozygous positive T2 plant was crossed by hand in the greenhouse, a traditional breeding method, to a conventional sugar beet line (i.e., 07R027B108DH06) that does not contain the KWS20-1 sugar beet T-DNA insert to produce BC0 seed that is hemizygous for the KWS20-1 sugar beet T-DNA. The BC0 plants were self-pollinated to produce the BC0S1 generation that was tested for the presence of the KWS20-1 sugar beet T-DNA by a set of KASP assays. Initially, two dominant KASP assays were used to determine the presence or absence of the T-DNA in the segregating BC0S1 population. As a secondary assessment, two co-dominant KASP assays were used to determine the zygosity of plants in the BC0S1 generation, discriminating between homozygous positive, hemizygous positive and homozygous negative (i.e., non-transgenic) plants. Upon establishing expected zygosity in the BC0S1 population, segregation analysis was conducted in subsequent generations using only dominant qualitative PCR-based assays. A single hemizygous positive BC0 plant was crossed by hand in the greenhouse to a conventional sugar beet line (i.e., 07R027B108DH06) that does not contain the KWS20-1 sugar beet T-DNA insert to produce BC1 seed. A single BC1 plant that was hemizygous positive for the KWS20-1 sugar beet T-DNA was self-pollinated to produce the BC1S1 generation that was tested by qualitative PCR for the presence or absence of the KWS20-1 sugar beet T-DNA in the segregating BC1S1 population. Finally, a single hemizygous positive BC1 plant was crossed by hand in the greenhouse to a conventional sugar beet line (i.e., 19ZCXCM08679) that does not contain the KWS20-1 sugar beet T-DNA insert to produce BC2 seed. A single BC2 plant that was hemizygous for the KWS20-1 sugar beet T-DNA was self-pollinated to produce the BC2S1 generation that was tested by qualitative PCR for the presence or absence of the KWS20-1 sugar beet T-DNA in the segregating BC2S1 population.

It was expected in the BC0S1, BC1S1 and BC2S1 generations that the KWS20-1 sugar beet T-DNA would be segregating at a ratio of 3:1 (T-DNA presence to T-DNA absence, respectively) when performing an assay that tests for the presence or absence of the T-DNA (Table 4). Whereas when the BC0S1 generation that was tested with the co-dominant KASP assay to assess zygosity, a 1:2:1 ratio (homozygous positive : hemizygous positive : homozygous negative plants, respectively) was expected (Table 5) according to Mendelian inheritance principles.

A Pearson's chi square (χ^2) analysis was used to compare the observed segregation ratios of the KWS20-1 sugar beet T-DNA to the expected ratios.

The Chi square was calculated as:

$\chi^2 = \sum [(| o - e |)^2 / e]$

where o = observed frequency of the genotype or phenotype and e = expected frequency of the genotype or phenotype. The level of statistical significance was predetermined to be 5% ($\alpha = 0.05$).

The results of the χ^2 analysis of the segregating progeny of KWS20-1 sugar beet are presented in Table 4 and Table 5. The $\chi 2$ value in the BC0S1, BC1S1 and BC2S1 generations indicated no statistically significant difference between the observed and expected segregation ratios of KWS20-1 sugar beet. These results support the conclusion that the KWS20-1 sugar beet T-DNA resides at a single locus within the sugar beet genome and is inherited according to Mendelian principles of inheritance. These results are also consistent with the molecular characterization data indicating that KWS20-1 sugar beet contains a single, intact copy of the T-DNA inserted at a single locus in the sugar beet genome.

For details, please refer to Appendix 1 and Appendix 5.

Figure 25. Breeding Path for Generating Segregation Data for KWS20-1 Sugar Beet

Table 4. Segregation of KWS20-1 Sugar Beet Based on Presence or Absence of the Inserted T-DNA

Generation	Total Plants	Observed[1]		Expected[2]		χ^2	p-value
		T-DNA positive	**T-DNA negative**	**T-DNA positive**	**T-DNA negative**		
BC0S1*	200	154	46	150	50	0.427	0.514
BC1S1**	200	150	50	150	50	0.000	1.000
BC2S1**	200	154	46	150	50	0.427	0.514

[1] Segregating BC0S1, BC1S1 and BC2S1 plants were tested for the presence of the KWS20-1 sugar beet T-DNA.
[2] The BC0S1, BC1S1 and BC2S1 plants were expected to be segregating for the KWS20-1 sugar beet T-DNA at a ratio of 3:1 (presence : absence, respectively) according to Mendelian inheritance principles.
*BC0S1 KWS20-1 sugar beet generation was tested for presence or absence of the KWS20-1 T-DNA using a dominant KASP assay.
** BC1S1 and BC2S1 KWS20-1 sugar beet generatins were tested for presence or absence of the KWS20-1 T-DNA using qualitative PCR.

Table 5. Segregation of KWS20-1 Sugar Beet Based on Zygosity of the Inserted T-DNA

Generation	Total Plants	Observed[1]			Expected[2]			χ^2	p-Value
		Homo-zygous positive	**Hemi-zygous positive**	**Homo-zygous negative**	**Homo-zygous positive**	**Hemi-zygous positive**	**Homo-zygous negative**		
BC0S1	200	50	104	46	50	100	50	0.480	0.787

[1] Segregating BC0S1 plants were tested for the presence of the KWS20-1 sugar beet T-DNA by a co-dominant KASP assay.
[2] The zygosity of the BC0S1 plants was expected to be segregating for the KWS20-1 sugar beet T-DNA at a ratio of 1:2:1 (homozygous positive : hemizygous positive : homozygous negative, respectively) according to Mendelian inheritance principles.

A.3(e)(ii)(ii) Expression of the Genetic Insert

In order to assess the presence of the DMO, PAT and CP4 EPSPS proteins in KWS20-1 sugar beet across multiple breeding generations, western blot analysis was conducted on leaf tissue collected from generations T2, T3 and T4 of KWS20-1 sugar beet, using leaf tissue of the conventional near-isogenic control as a negative control.

The presence of the DMO protein was demonstrated in three breeding generations of KWS20-1 sugar beet using western blot analysis. The *E. coli*-produced DMO protein standard (5 ng) was used as a reference for the positive identification of the DMO protein (Figure 26, lane 3). The presence of the DMO protein in leaf tissue samples of KWS20-1 sugar beet was determined by visual comparison of the bands detected in the three breeding generations (Figure 26, lanes 5-7) to the *E. coli*-produced DMO protein reference standard. The KWS20-1 sugar beet-produced DMO protein migrated indistinguishably from that of the *E. coli*-produced protein standard analyzed on the same western blot. Additional higher molecular weight protein bands were observed (Figure 26, lanes 5-7) and are related to a small population of partially aggregated KWS20-1 sugar beet produced-DMO protein as dimers and trimers. Nevertheless, as expected, the DMO protein was not detected in the conventional near-isogenic control leaf extract (Figure 26, lane 8).

The presence of the PAT protein was demonstrated in three breeding generations of KWS20-1 sugar beet using western blot analysis. The *E. coli*-produced PAT protein standard (5 ng) was used as a reference for the positive identification of the PAT protein (Figure 27, lane 3). The presence of the PAT protein in leaf tissue samples of KWS20-1 sugar beet was determined by visual comparison of the bands detected in the three breeding generations (Figure 27, lanes 5-7) to the *E. coli*-produced PAT protein reference standard. The KWS20-1 sugar beet-produced PAT protein migrated indistinguishably from that of the *E. coli*-produced protein standard analyzed on the same western blot. An additional higher molecular weight protein band was observed (Figure 27, lanes 5-7) and is related to a small population of partially aggregated PAT protein as dimers. Nevertheless, as expected, the PAT protein was not detected in the conventional near-isogenic control leaf extract (Figure 27, lane 8).

The presence of the CP4 EPSPS protein was demonstrated in three breeding generations of KWS20-1 sugar beet using western blot analysis. The *E. coli*-produced CP4 EPSPS protein standard (5 ng) was used as a reference for the positive identification of the CP4 EPSPS protein (Figure 28, lane 3). The presence of the CP4 EPSPS protein in leaf tissue samples of KWS20-1 sugar beet was determined by visual comparison of the bands detected in the three breeding generations (Figure 28, lanes 5-7) to the *E. coli*-produced CP4 EPSPS protein reference standard. The KWS20-1 sugar beet-produced CP4 EPSPS protein migrated indistinguishably from that of the *E. coli*-produced protein standard analyzed on the same western blot. As expected, the CP4 EPSPS protein was not detected in the conventional near-isogenic control leaf extract (Figure 28, lane 8).

For details, please refer to Appendix 6.

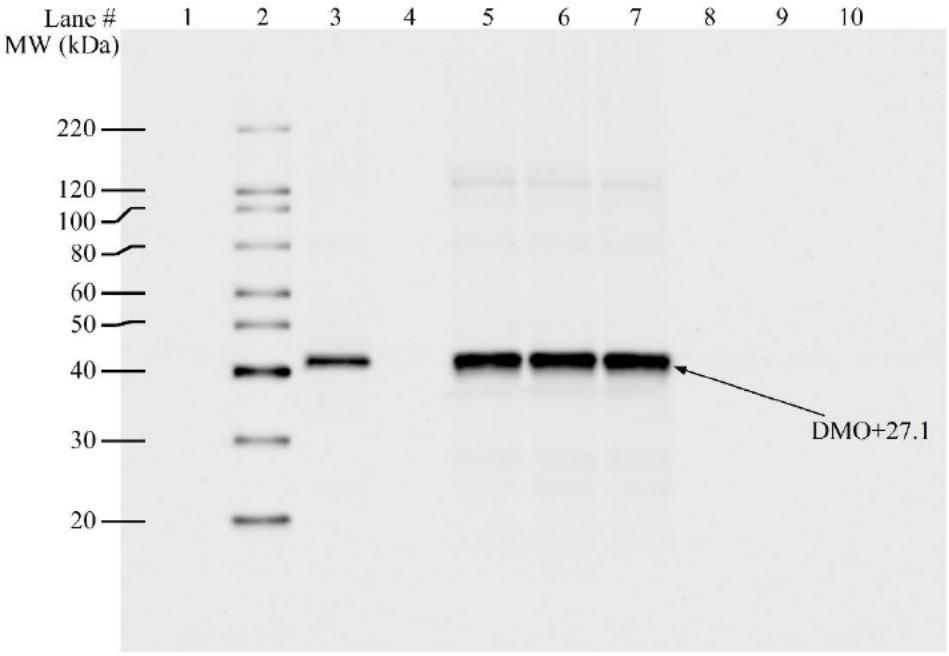

Figure 26. Presence of the DMO Protein in Multiple Generations of KWS20-1 Sugar Beet

Blot probed with monoclonal anti-DMO primary antibody and HRP conjugated anti-mouse IgG secondary antibodies. The image with an exposure time of five seconds is shown. The approximate MWs (kDa) of the MagicMark XP Western Standards are shown on the left. Lane designations are as follows:

Lane	Description	Amount Loaded
1	Precision Plus Protein Standards	5 µl
2	MagicMark XP Western Standard	1 µl
3	*E. coli*-produced DMO protein	5 ng
4	Empty	N/A
5	KWS20-1 sugar beet, T2	5 µl
6	KWS20-1 sugar beet, T3	5 µl
7	KWS20-1 sugar beet, T4	5 µl
8	Near-isogenic control	5 µl
9	Empty	N/A
10	Empty	N/A

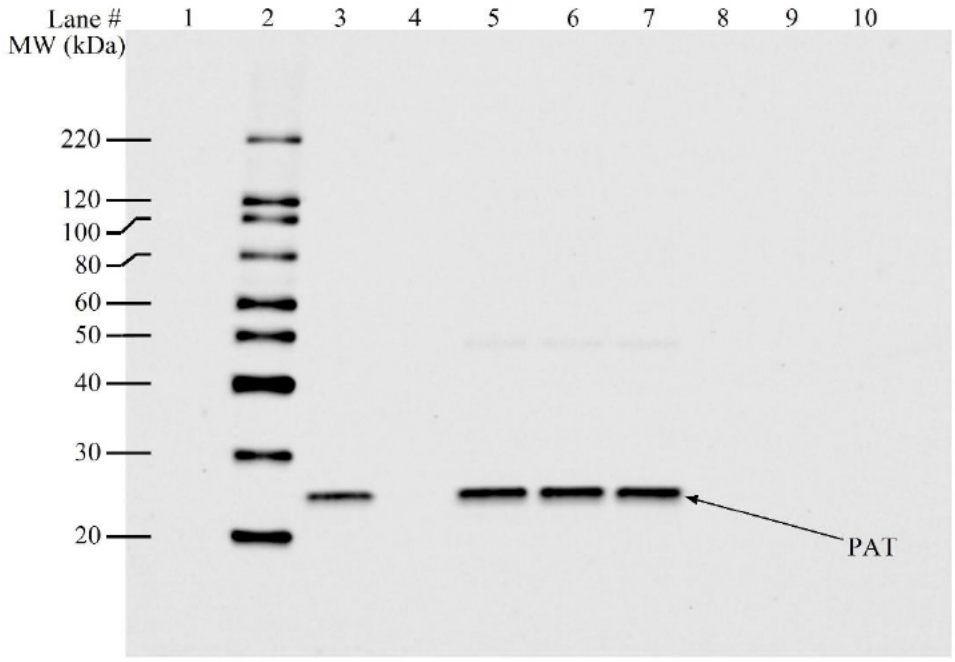

Figure 27. Presence of the PAT Protein in Multiple Generations of KWS20-1 Sugar Beet

Blot probed with monoclonal anti-PAT primary antibody and HRP conjugated anti-mouse IgG secondary antibodies. The 13-second exposure image is shown. The approximate MWs (kDa) of the MagicMark XP Western Standards are shown on the left. Lane designations are as follows:

Lane	Description	Amount Loaded
1	Precision Plus Protein Standards	5 µl
2	MagicMark XP Western Standard	1 µl
3	*E. coli*-produced PAT protein	5 ng
4	Empty	N/A
5	KWS20-1 sugar beet, T2	5 µl
6	KWS20-1 sugar beet, T3	5 µl
7	KWS20-1 sugar beet, T4	5 µl
8	Near-isogenic control	5 µl
9	Empty	N/A
10	Empty	N/A

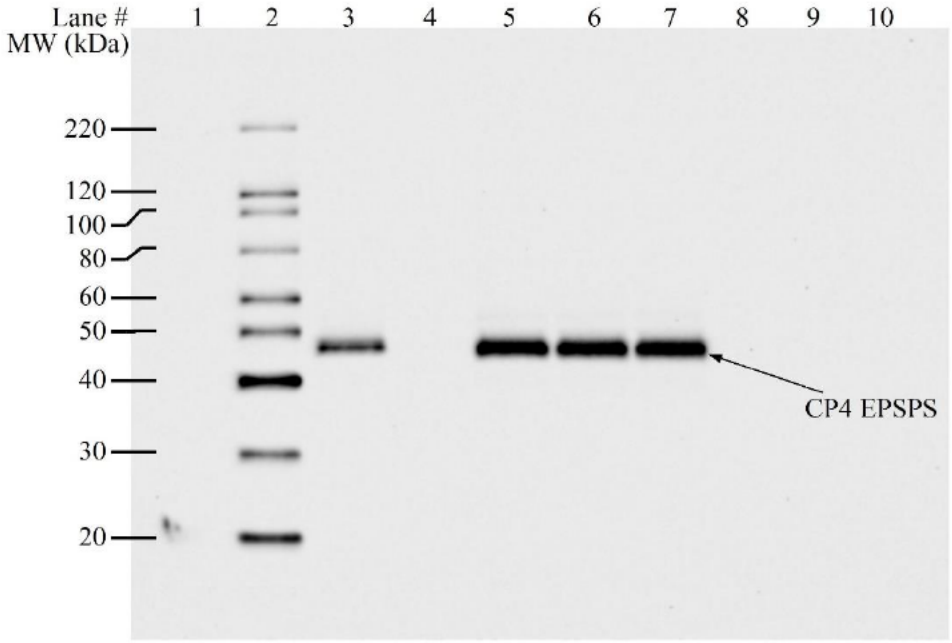

Figure 28. Presence of the CP4 EPSPS Protein in Multiple Generations of KWS20-1 Sugar Beet

Blot probed with polyclonal anti-CP4 EPSPS primary antibodies and HPR conjugated anti-goat IgG secondary antibodies. The 13-second exposure image is shown. The approximate MWs (kDa) of the MagicMark XP Western Standards are shown on the left. Lane designations are as follows:

Lane	Description	Amount Loaded
1	Precision Plus Protein Standards	5 µl
2	MagicMark XP Western Standard (1/4 dilution)	1 µl
3	*E. coli*-produced CP4 EPSPS protein	5 ng
4	Empty	N/A
5	KWS20-1 sugar beet, T2	5 µl
6	KWS20-1 sugar beet, T3	5 µl
7	KWS20-1 sugar beet, T4	5 µl
8	Near-isogenic control	5 µl
9	Empty	N/A
10	Empty	N/A

A.3(f) An analysis of the expressed RNA transcripts, where RNA interference has been used

Not relevant for this product.

B. CHARACTERISATION AND SAFETY ASSESSMENT OF NEW SUBSTANCES

B.1 Characterisation and Safety Assessment of New Substances

B.1(a) Full description of the biochemical and phenotypic effects of all new substances (e.g. a protein or an untranslated RNA) that are expressed in the new GM organism, including their levels and site of accumulation, particularly in edible portions

B.1(a)(i) Description, mode-of-action, and specificity of DMO, PAT, and CP4 EPSPS proteins expressed in KWS20-1 sugar beet

B.1(a)(i)(i) DMO Protein Expressed in KWS20-1 Sugar Beet

B.1(a)(i)(i)(i) General Description

Wild type DMO was initially purified from *Stenotrophomonas maltophilia* (*S. maltophilia*) strain DI-6 (Palleroni and Bradbury, 1993; Herman *et al.*, 2005), isolated from soil at a dicamba manufacturing plant (Krueger *et al.*, 1989). DMO is targeted to the chloroplast by a chloroplast transit peptide (CTP) to allow co-localization with the endogenous reductase and ferredoxin enzymes that supply electrons for the DMO demethylation reaction as described by Behrens *et al.* (2007). In the construction of the plasmid vector PV-BVHT527462 used in the development of KWS20-1 sugar beet, a transit peptide coding sequence from *Pisum sativum* (pea) Rubisco gene (*RbcS*) was joined to the *dmo* coding sequence to enable transport of the produced protein to the sugar beet chloroplast (Klee *et al.*, 1987; Herrmann, 1995). This coding sequence results in the production of a precursor protein consisting of the DMO protein, a transit peptide and an intervening sequence (IS), and is referred to as the KWS20-1 sugar beet DMO precursor protein. Typically, transit peptides are precisely removed from the precursor protein following delivery to the targeted plastid (della-Cioppa *et al.*, 1986) resulting in the full length protein. However, there are examples in the literature of alternatively processed forms of a protein targeted to a plant's chloroplast (Clark and Lamppa, 1992; Behrens *et al.*, 2007). Such alternative processing is observed with the DMO precursor protein produced in KWS20-1 sugar beet. Data from N-terminal sequencing analysis of the KWS20-1 sugar beet-produced DMO indicate that processing of the DMO precursor protein expressed in KWS20-1 sugar beet produced one isoform of the processed DMO protein, termed DMO+27.1 (Figure 29). The determined amino acid sequence of DMO+27.1 is identical to wild-type DMO protein from the DI-6 strain of *S. maltophilia* (Herman *et al.*, 2005), except for a leucine at position 2, plus 27 additional amino acids on its N-terminus derived from RbcS and IS. Therefore, the term "KWS20-1 sugar beet-produced DMO protein" will be used to refer to the DMO+27.1 protein and distinctions will only be made in this dossier where necessary.

With some minor differences that do not impact functionality, DMO protein produced in KWS20-1 sugar beet is also present in MON 88701 cotton [A1080], MON 87708 soybean [A1063], MON 87419 maize [A1118], MON 87429 maize [A1192] and MON 94100 canola [A1216] submitted to FSANZ. The safety of these proteins has also been reviewed and approved in numerous other countries (e.g., Canada, Colombia, Japan, Korea, Mexico and Taiwan for MON 88701 cotton; Brazil, Canada, China, the European Union, Indonesia, Japan, Korea, Mexico,

Philippines, Taiwan and Vietnam for MON 87708 soybean)[3]. Except for minor amino acid differences at the N-terminus (e.g., residual amino acids from the CTP) of the KWS20-1 sugar beet-produced DMO protein, the amino acid sequence of the mature DMO protein in KWS20-1 sugar beet is identical to the mature DMO protein (i.e., blue regions in Figure 29) expressed in MON 87419 corn, MON 87429 maize, MON 88701 cotton and MON 94313 soybean. These minor amino differences between the DMO proteins expressed in KWS20-1 sugar beet, MON 88701 cotton, MON 87419 maize, MON 87429 maize, MON 94100 canola, MON 87708 soybean and MON 94313 soybean are not anticipated to have an effect on the structure of the catalytic site, functional activity, immunoreactivity or specificity of the protein (D'Ordine *et al.*, 2009; Dumitru *et al.*, 2009).

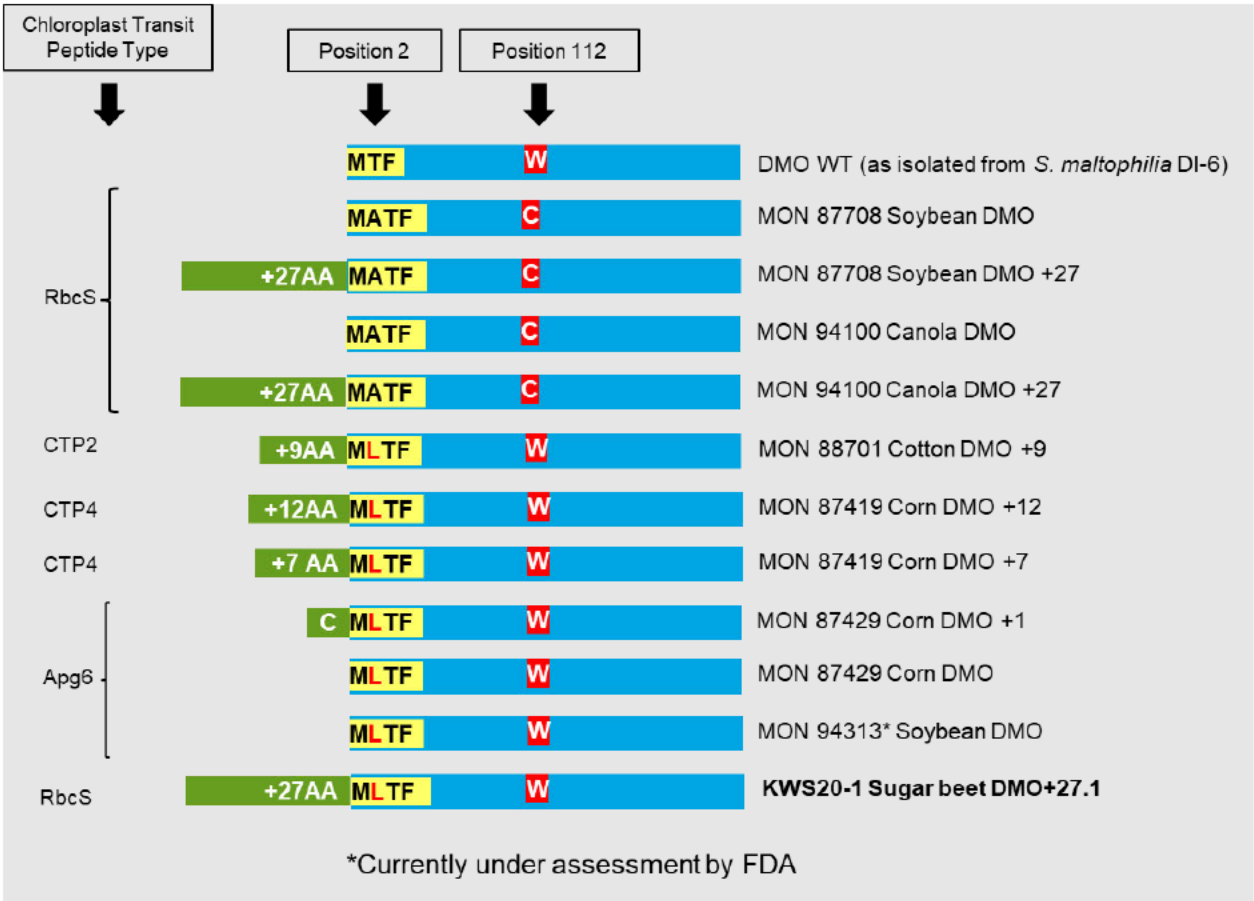

Figure 29. Forms of DMO Protein and Their Relationship to the Wild-Type DMO Protein

Protein sequence alignment of DMO proteins in *Stenotrophomonas maltophilia*, MON 87708 soybean, MON 94100 canola, MON 88701 cotton, MON 87419 corn, MON 87429 corn, MON 94313 soybean and KWS20-1 sugar beet. Blue indicates regions with 100% sequence identity to the wild type DMO. Insertion

[3] Source Biotechnology Industry Organization BIOTradeStatus database (http://www.biotradestatus.com/).

of a single alanine or leucine amino acid at position 2 from the N-terminus is indicated in the yellow box (A or L), and a single tryptophan to cysteine amino acid change at position 112 is indicated in red (C or W). RbcS, CTP2/4, and APG6 are chloroplast transit peptide sequences.

B.1(a)(i)(i)(ii) Mode-of-Action

KWS20-1 sugar beet contains a demethylase gene from *S. maltophilia* that expresses a DMO protein. As a mono-oxygenase protein, the DMO protein is part of the larger oxygenase family of enzymes that incorporate one or two oxygen atoms into substrates and are widely distributed in many universal metabolic pathways (Harayama *et al.*, 1992). DMO is a Rieske-type non-heme iron oxygenase and is part of a three component system comprised of a reductase, a ferredoxin, and a terminal oxygenase, which in this case is the DMO protein. In KWS20-1 sugar beet, these three proteins work together to catalyze the demethylation of the broadleaf herbicide dicamba to the non-herbicidal compound 3,6-dichlorosalicylic acid (DCSA) and formaldehyde, thus conferring dicamba resistance (Chakraborty *et al.*, 2005). This three-component redox system is presented in Figure 30.

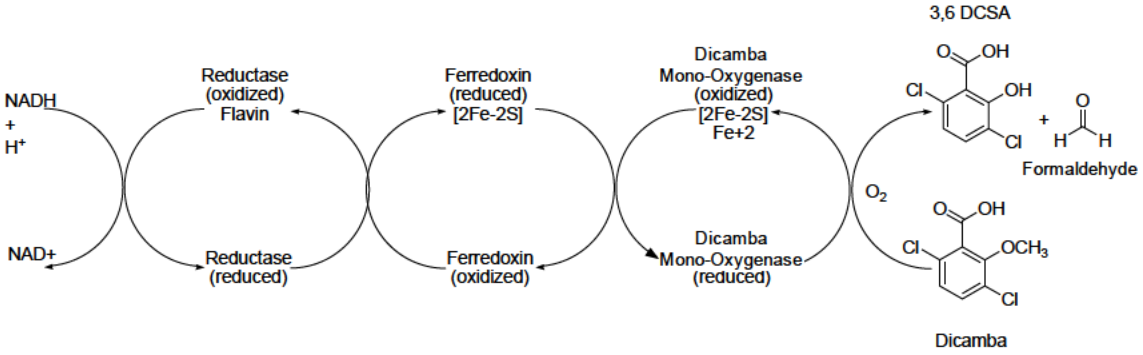

Figure 30. Three Components of the DMO Oxygenase System

Depicted is the electron transport chain that starts with NADH and ends with DMO resulting in the demethylation of dicamba to form DCSA.

The crystal structure of a C-terminal histidine tagged DMO protein, which is identical to wild-type DMO except for an additional alanine at position two and a C-terminal polyhistidine tag has been solved (D'Ordine *et al.*, 2009; Dumitru *et al.*, 2009). The addition of a polyhistidine tag fused to the N- or C-terminus of a protein of interest is commonly used as a tool to aid in protein purification (Hochuli *et al.*, 1988). The crystal structure of active DMO was determined to be a trimer comprised of three identical DMO monomers (D'Ordine *et al.*, 2009; Dumitru *et al.*, 2009). Each DMO monomer contains a Rieske [2Fe-2S] cluster domain and a non-heme iron center domain (D'Ordine *et al.*, 2009; Dumitru *et al.*, 2009) that are typical of all Rieske-type mono-oxygenases (Ferraro *et al.*, 2005). To catalyze the demethylation of dicamba, electrons transferred from NADH are shuttled through endogenous reductase and ferredoxin to the terminal DMO protein. The electrons are received by the Rieske [2Fe-2S] cluster of one DMO protein molecule in the trimer and transferred to the non-heme iron center at the catalytic site of an adjacent DMO protein molecule in the trimer (D'Ordine *et al.*, 2009; Dumitru *et al.*, 2009), where it reductively activates oxygen to catalyze the final demethylation of dicamba. Electron transport from the Rieske [2Fe-2S] cluster domain to the non-heme iron center domain cannot occur within a monomer since the distance is too great (D'Ordine *et al.*, 2009; Dumitru *et al.*, 2009). As a result of the demethylation reaction, the non-herbicidal compound DCSA and formaldehyde are formed from dicamba. DCSA is a known metabolite found in cotton, soybean, soil, and livestock whose safety has been evaluated by the FAO-WHO and EPA (FAO-WHO, 2011a; FAO-WHO, 2011b; U.S. EPA, 2009). The other reaction product, formaldehyde, is found naturally in many plants and edible fungi at levels up to several hundred ppm (Tashkov, 1996; Adrian-Romero *et al.*, 1999). Thus, neither DCSA nor formaldehyde generated by the action of DMO on dicamba pose a significant food or feed safety risk.

B.1(a)(i)(i)(iii) Specificity

The substrate specificity of DMO expressed in KWS20-1 sugar beet was evaluated to understand potential interactions DMO may have with endogenous compounds structurally similar to dicamba that are found in plants. The literature indicates the specificity of DMO for dicamba is due to the specific interactions that occur at the catalytic site between the substrate and the protein (D'Ordine *et al.*, 2009; Dumitru *et al.*, 2009). Dicamba interacts with amino acids in the catalytic site of DMO through the carboxylate moiety, the ring structure and the chlorine atoms of dicamba, which are primarily involved in orienting the substrate in the catalytic site. These chlorine atoms are required for catalysis to occur (D'Ordine *et al.*, 2009; Dumitru *et al.*, 2009). The compound 2-methoxy benzoic acid (*o*-anisic acid), which is identical in structure to dicamba except for the absence of chlorines, was tested as a potential substrate of DMO by two independent laboratories (D'Ordine *et al.*, 2009; Dumitru *et al.*, 2009). No significant turnover was detected under standard assay conditions using HPLC or through liquid chromatography/mass spectrometry methods where picomole levels of products can be observed. Given the limited existence of chlorinated compounds with structures similar to dicamba in plants and other eukaryotes (Gribble, 2010), it is unlikely that DMO produced in KWS20-1 sugar beet will catalyze the conversion of endogenous compounds.

The potential for DMO to metabolize endogenous plant compounds was evaluated previously through *in vitro* experiments in support of MON 87708 soybean [A1063]. A set of potential endogenous substrates was selected for evaluation based on structural similarity of the compounds to dicamba and their presence in cotton, maize, or soybean (Janas *et al.*, 2000; Buchanan *et al.*,

2000; Schmelz *et al.*, 2003; Lege *et al.*, 1995). The potential substrates tested were *o*-anisic acid (2-methoxybenzoic acid), vanillic acid (4-hydroxy-3-methoxybenzoic acid), syringic acid (3,5-dimethoxy-4-hydroxybenzoic acid), ferulic acid [3-(4-hydroxy-3-methoxy-phenyl) prop-2-enoic acid] and sinapic acid [3-(4-hydroxy-3,5-dimethoxyphenyl)prop-2-enoic acid] (Figure 31). The assay mixture included NADH, reductase, ferredoxin and DMO. Dicamba was first used as a positive control to demonstrate that the assay system was functional. The disappearance of potential substrates and the formation of potential oxidation products were monitored using liquid chromatography-ultraviolet (LC-UV) and liquid chromatography-mass spectrometry (LC-MS). None of the tested substrates, except dicamba, were metabolized by the histidine tagged DMO in these *in vitro* experiments.

A literature survey was conducted to search for endogenous compounds in sugar beet that are structurally similar to dicamba (e.g., phenyl carboxylic acids containing methoxy moieties and chlorine moieties). The search was conducted using SciFinder with the following key words: sugar beet, phenolic compounds. In the literature, no phenyl compounds with chlorine moieties were identified in sugar beet. As discussed above, plant-endogenous compounds containing methoxy and phenyl carboxylic acid moieties and structurally similar to dicamba have been experimentally examined and determined not to be potential substrates for the DMO enzymatic proteins produced by MON 87708 soybean, as has *o*-anisic acid, the plant-endogenous compound that has the greatest structural similarity to dicamba.

In a similar experimentation, *o*-anisic acid was assayed by *E. coli*-produced KWS20-1 sugar beet DMO Similar to the results previously reported for MON 87708 soybean DMO in that the DCSA product was observed using dicamba as the substrate, whereas no demethylated products were observed with *o*-anisic acid as the substrate confirming that the KWS20-1 sugar beet DMO did not catabolize *o*-anisic acid. The lack of endogenous substrate compounds in sugar beet together with the previously reported enzymatic assessment results for MON 87708 soybean [A1063], MON 87429 maize [A1192] and MON 94313 soybean [A1276, under assessment], along with the current assessment for KWS20-1 sugar beet, demonstrate that the KWS20-1 sugar beet-produced DMO is active and has a high specificity for dicamba as a substrate and is unlikely to react with endogenous sugar beet compounds.

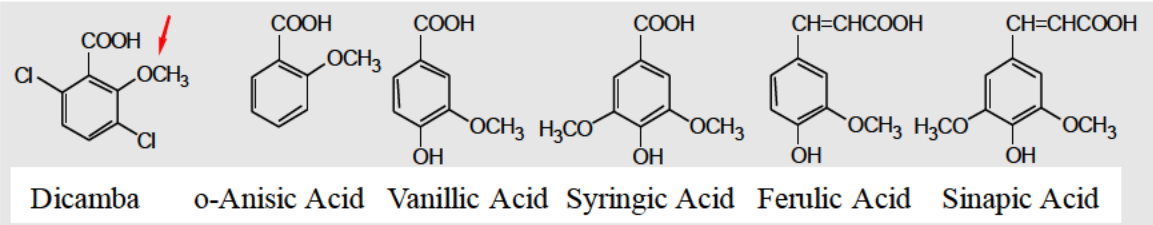

Figure 31. Dicamba and Potential Endogenous Substrates Tested through Previous *In Vitro* Experiments with DMO

The arrow indicates methyl group removed by DMO.

B.1(a)(i)(ii) PAT Protein Expressed in KWS20-1 Sugar Beet

B.1(a)(i)(ii)(i) General Description

PAT proteins conferring tolerance to glufosinate herbicide (2amino4(hydroxymethylphosphinyl) butanoic acid) have been isolated from two separate species of *Streptomyces*, *S. hygroscopicus* (Thompson *et al.*, 1987) and *S. viridochromogenes* (Wohlleben *et al.*, 1988). The PAT protein isolated from *S. hygroscopicus* is encoded by the *bar* gene, and the PAT protein isolated from *S. viridochromogenes* is encoded by the *pat* gene. Both PAT (*bar*) and PAT (*pat*) proteins are comprised of 183 amino acids which share 85% identity at the amino acid level (Wehrmann *et al.*, 1996). Based on previous studies (Wehrmann *et al.*, 1996) that have extensively characterized PAT proteins produced from both the *bar* and *pat* genes, OECD recognizes both the proteins to be equivalent with regard to function and safety (OECD, 1999). In addition, the EPA has issued a tolerance exemption for the PAT protein regardless of the encoding gene or crop (U.S. EPA, 1997). The safety of PAT proteins present in biotechnology-derived crops has been extensively assessed (Hérouet *et al.*, 2005; ILSI-CERA, 2011), leading to a conclusion that there is a reasonable certainty of no harm resulting from the consumption of PAT proteins in human food or animal feed (Hérouet *et al.*, 2005).

The PAT protein produced in KWS20-1 sugar beet is encoded by the *pat* gene and is identical to the wild type PAT (*pat*) protein encoded by *S. viridochromogenes*, except for the first methionine that is removed due to co-translational processing in KWS20-1 sugar beet. N-terminal methionine cleavage is common and naturally occurs in the vast majority of proteins (Meinnel and Giglione, 2008).. The resulting KWS20-1 sugar beet-produced PAT protein in a single polypeptide of 182 amino acids that has an apparent molecular weight of ~22.3 kDa. The PAT protein in KWS20-1 sugar beet is identical to the PAT protein expressed in several commercially available glufosinate-tolerant products.

B.1(a)(i)(ii)(ii) Mode-of-Action

The mode-of-action for PAT protein has been extensively assessed, as numerous glufosinate-tolerant products have been reviewed by the FSANZ (A2704-12 and A5547-127 soybean [A481], MON 87419 maize [A1118] and MON 87429 maize [A1192], including the PAT protein produced in KWS20-1 sugar beet is an enzyme classified as an acetyltransferase that acetylates glufosinate in the presence of acetyl-CoA to form the non-herbicidal compound N-acetyl glufosinate.

Glufosinate is a racemic mixture of the D- and L-forms of phosphinothricin. The herbicidal activity of glufosinate results from the binding of L-phosphinothricin to glutamine synthetase (OECD, 1999; OECD, 2002c). Glutamine synthetase is responsible for the assimilation of ammonia generated during photorespiration. The binding of L-phosphinothricin to glutamine synthetase results in the inactivation of glutamine synthetase and a subsequent toxic build-up of ammonia within the plant, resulting in death of the plant (Manderscheid and Wild, 1986; Wild and Manderscheid, 1984; OECD, 1999; OECD, 2002c). Thus, expression of the PAT protein in KWS20-1 sugar beet results in the ability to convert L-phosphinothricin to the non-herbicidal N-acetyl-L-phosphinothricin, thus conferring glufosinate resistance to the crop.

B.1(a)(i)(ii)(iii) Specificity

The PAT protein expressed in KWS20-1 sugar beet is highly specific for glufosinate. Enzyme assays have demonstrated that the PAT protein is unable to acetylate other common L-amino acids that are structurally similar to L-phosphinothricin, and substrate competition assays showed no inhibition of glufosinate acetylation in the presence of high concentrations of L-amino acids that are structurally similar to L-phosphinothricin (including the glufosinate analog L-glutamate) (Wehrmann *et al.*, 1996). Recent metabolic profiling reported some non-specific PAT-mediated acetylation of two amino acids (aminoadipate and tryptophan) in senescent leaf extracts from *A. thaliana* and also in PAT-expressing soybean (Christ *et al.*, 2017). However, the activity level for these two amino acids was very low relative to the activity for glufosinate, indicating that PAT has a very high level of specificity for the herbicidal molecule (Christ *et al.*, 2017).

B.1(a)(i)(iii) CP4 EPSPS Expressed in KWS20-1 Sugar Beet

B.1(a)(i)(iii)(i) General Description

The *cp4 epsps* expression cassette in KWS20-1 sugar beet contains the *cp4 epsps* gene encoding a precursor protein of 531 amino acids (i.e., 455 amino acids encoded by the *cp4 epsps* gene and 76 amino acids encoded by the *CTP2* gene for targeting the CP4 EPSPS protein into chloroplasts). Expression of the *cp4 epsps* gene in KWS20-1 sugar beet results in a single polypeptide chain of 455 amino acids starting at the methionine position 77 (Padgette *et al.*, 1996) with an apparent molecular weight of ~43.5 kDa after a complete cleavage of the chloroplast transit peptide (CTP2). The *cp4 epsps* expression cassette contains a codon optimized coding sequence of the *aroA* gene from the soil bacterium *Agrobacterium* sp. strain CP4 that expresses the CP4 EPSPS protein (Barry *et al.*, 2001; Padgette *et al.*, 1996). The CP4 EPSPS protein expressed in KWS20-1 sugar beet is identical in structure and function to the CP4 EPSPS protein expressed in Roundup Ready[Ò]products across several crops, including soybean, maize, canola, cotton, sugar beet and alfalfa.

B.1(a)(i)(iii)(ii) Mode-of-Action

The 5-enolpyruvylshikimate-3-phosphate synthase (EPSPS) family of enzymes is ubiquitous in plants and microorganisms and their properties have been well studied. Bacterial and plant EPSPS enzymes are mono-functional with molecular mass ranging from 44-48 kD (Kishore *et al.*, 1988). EPSPS is a key enzyme involved in aromatic amino acid biosynthesis and catalyzes a reaction where the enolpyruvyl group from phosphoenol pyruvate (PEP) is transferred to the 5-hydroxyl of shikimate-3-phosphate (S3P) to form 5-enolpyruvylshikimate-3-phosphate (EPSP) and inorganic phosphate (Alibhai and Stallings, 2001). Shikimic acid is a substrate for the biosynthesis of aromatic amino acids (phenylalanine, tryptophan and tyrosine) and other aromatic molecules that are necessary for plant growth. The shikimic acid pathway and EPSPS enzymes are ubiquitous to plants and microorganisms, but absent in mammals, fish, birds, reptiles and insects (Alibhai and Stallings, 2001). The CP4 EPSPS protein expressed in KWS20-1 sugar beet is structurally similar and functionally identical to endogenous plant EPSPS enzymes, but has a much reduced affinity

[®] Roundup Ready is a registered trademark of the Bayer Group.

for glyphosate, the active ingredient in Roundup® agricultural herbicides, relative to endogenous plant EPSPS (Sikorski and Gruys, 1997). In conventional plants, glyphosate blocks the biosynthesis of EPSP, thereby depriving plants of essential amino acids (Steinrücken and Amrhein, 1980; Haslam, 1993). In Roundup Ready plants, which are tolerant to Roundup agricultural herbicides, requirements for aromatic amino acids and other metabolites are met by the continued action of the CP4 EPSPS enzyme in the presence of glyphosate (Padgette *et al.*, 1996).

The KWS20-1 sugar beet-produced CP4 EPSPS protein is similar to EPSPS proteins consumed in a variety of food and feed sources. CP4 EPSPS protein is homologous to EPSPS proteins naturally present in plants, including food and feed crops (e.g., maize and soybean) and fungal and microbial food sources such as baker's yeast (*Saccharomyces cerevisiae*), all of which have a history of safe consumption (Padgette *et al.*, 1996; Harrison *et al.*, 1996). The CP4 EPSPS protein in KWS20-1 sugar beet is also produced in several glyphosate-tolerant crops previously rev iewed by the FSANZ (e.g., H7-1 sugar beet [A525], J101 and J163 alfalfa [A575]; MON 88017 maize [A548], MON 89788 soybean [A592], MON 87429 [A1192] maize and MON 88302 canola [A1071].

B.1(a)(i)(iii)(iii) Specificity

EPSPS enzymes, including the KWS20-1 sugar beet-produced CP4 EPSPS protein, are highly specific for their substrates. The only known substrates of any biological significance for EPSPS enzymes are S3P and PEP. Glyphosate is not enzymatically modified by EPSPS. Shikimic acid was shown to be a very poor substrate for EPSPS enzyme, requiring much higher concentrations to observe turnover by the enzyme than for S3P (Gruys *et al.*, 1992). Methyl shikimate, quinic acid and dihydroshikimic acid did not serve as substrates for the EPSPS enzyme (Franz *et al.*, 1997). As with most physiological pathways, there is tight regulation of metabolic flux through the shikimic acid pathway. Pathway flux is regulated both transcriptionally and post-transcriptionally (Maeda and Dudareva, 2012; Tzin *et al.*, 2012). The first enzyme in the pathway, 3-dexoy-D-arabino-heptulosonate 7-phosphate synthase (DAHPS), has been identified as the key regulatory checkpoint for the flux through the pathway, with a possible secondary checkpoints at shikimate kinase and chorismate synthase (Maeda and Dudareva, 2012; Tzin *et al.*, 2012). Plants, therefore, have mechanisms to regulate flux through the shikimate pathway irrespective of EPSPS synthase activity levels. Due to both the high substrate specificity of EPSPS enzymes and lack of a role as a regulatory enzyme in the shikimic acid pathway, there is no likely mechanism for the modification of endogenous plant constituents due to the expression of CP4 EPSPS.

® Roundup is a registered trademark of the Bayer Group.

B.1(a)(ii) Characterisation of the DMO, PAT and CP4 EPSPS proteins from KWS20-1 sugar beet

B.1(a)(ii)(i) Characterisation of the DMO Protein

The safety assessment of crops derived through biotechnology includes characterization of the physicochemical and functional properties and confirmation of the safety of the introduced protein(s). For the safety data generated using the *E. coli*-produced DMO protein to be applied to the KWS20-1 sugar beet-produced DMO protein (plant-produced DMO), the equivalence of the plant- and *E. coli*-produced proteins must first be demonstrated. To assess the equivalence between the KWS20-1 sugar beet-produced DMO and *E. coli*-produced DMO proteins, a small quantity of the KWS20-1 sugar beet-produced DMO protein was purified from KWS20-1 sugar beet leaf. The KWS20-1 sugar beet-produced DMO protein was characterized and the equivalence of the physicochemical characteristics and functional activity between the KWS20-1 sugar beet-produced and *E. coli*-produced DMO proteins was assessed using a panel of six analytical tests; as shown in Table 6. Taken together, these data provide a detailed characterization of the KWS20-1 sugar beet-produced DMO protein and establish the equivalence of the KWS20-1 sugar beet-produced DMO and *E. coli*-produced DMO proteins. With establishment of equivalence, conclusions derived from digestibility, heat susceptibility and oral acute toxiciology studies conducted with *E. coli*-produced DMO protein are applicable to KWS20-1 sugar beet-produced DMO protein.

For details, please refer to Appendix 7.

Table 6. Summary of KWS20-1 Sugar Beet-Produced DMO Protein Identity and Equivalence

Analytical Test Assessment	Analytical Test Outcome
N-terminal sequence	The expected N-terminal sequence for KWS20-1 sugar beet-produced DMO was observed by Nano LC-MS/MS[1]
Nano LC-MS/MS[1]	Nano LC-MS/MS[1] analysis of trypsin digested peptides from KWS20-1 sugar beet-produced DMO protein yielded peptide masses consistent with expected peptide masses from the theoretical trypsin digest of the amino acid sequence
Western blot analysis	KWS20-1 sugar beet-produced DMO protein identity was confirmed using a western blot probed with antibodies specific for DMO protein. Immunoreactive properties of the KWS20-1 sugar beet-produced DMO and the *E. coli*-produced DMO proteins were shown to be equivalent
Apparent molecular weight (MW)	Electrophoretic mobility and apparent molecular weight of the KWS20-1 sugar beet-produced DMO and the *E. coli*-produced DMO proteins were shown to be equivalent
Glycosylation analysis	Glycosylation status of KWS20-1 sugar beet-produced DMO and *E. coli*-produced DMO proteins were shown to be equivalent

Functional activity	Functional activity of the KWS20-1 sugar beet-produced DMO and the *E. coli*-produced DMO proteins were shown to be equivalent

[1] Nano LC-MS/MS = Nanoscale liquid chromatography coupled to tandem mass spectrometry

B.1(a)(ii)(i)(i) Results of the N-terminal Sequencing Analysis

N-terminal sequencing was performed on the DMO protein. The expected sequence for the DMO protein deduced from the *dmo* gene present in KWS20-1 sugar beet was observed. The N-terminal sequence for KWS20-1 sugar beet-produced DMO protein was consistent with the N-terminal sequence for the *E. coli*-produced DMO protein observed by LC-MS/MS analysis (Figure 32). Hence, the sequence information confirms the identity of the DMO protein isolated from the leaf tissue of KWS20-1 sugar beet.

Amino Acids Residue # from the N-terminus	→	1	2	3	4	5	6	7	8	9	10	11	12	13	14	15
E. coli-produced DMO sequence	→	M	Q	V	W	P	P	I	G	K	K	K	F	E	T	L
		|	|	|	|	|	|	|	|	|	|	|	|	|	|	|
Expected DMO Sequence	→	M	Q	V	W	P	P	I	G	K	K	K	F	E	T	L
		|	|	|	|	|	|	|	|	|	|	|	|	|	|	|
KWS20-1 Sugar Beet Experimental Sequence	→	M	Q	V	W	P	P	I	G	K	K	K	F	E	T	L

Figure 32. N-terminal Sequence of the KWS20-1 Sugar Beet-Produced DMO Protein

The experimental sequence obtained from the KWS20-1 sugar beet produced DMO was compared to the expected DMO sequence deduced from the *dmo* gene present in KWS20-1 sugar beet. The *E. coli*-produced DMO protein sequence above was derived from the reference substance COA (lot 129834). The single letter International Union of Pure and Applied Chemistry-International Union of Biochemistry (IUPAC-IUB) amino acid code is: M, methionine; Q, glutamine; V, valine; W, tryptohpan; P, proline; I, isoleucine; G, glycine; K, lysine; F, phenylalanine; E, glutamic acid; T, threonine; L, leucine.

B.1(a)(ii)(i)(ii) Results of the DMO Protein Mass Fingerprint Analysis

The identity of the DMO protein was confirmed by Nano LC-MS/MS analysis of peptide fragments produced by a trypsin digestion of the KWS20-1 sugar beet-produced DMO protein.

There were 39 unique peptides identified that corresponded to the expected masses of the trypsin-digested sequence of KWS20-1 sugar beet-produced DMO (Table 7). The identified masses were used to assemble a peptide map of the DMO protein (Figure 33). The experimentally determined coverage of KWS20-1 sugar beet-produced DMO protein was 86% (316 out of 367 amino acids). This analysis further confirms the identity of KWS20-1 sugar beet-produced DMO protein.

There were 45 unique peptides identified that corresponded to the expected masses of trypsin-digested *E. coli*-produced DMO protein (Table 8) by LC-MS/MS analysis during the protein characterization. The identified masses were used to assemble a peptide coverage map of the DMO protein (Figure 33). The experimentally determined coverage of the *E. coli*-produced DMO protein was 85% (315 out of 367 amino acids). This analysis further confirms the identity of *E. coli*-produced DMO protein and equivalence to the KWS20-1 sugar beet-produced DMO protein.

Table 7. Summary of the Tryptic Masses Identified for KWS20-1 Sugar Beet-Produced DMO Protein Using Nano LC-MS/MS[1]

Experimental Mass[2]	Calculated Mass[3]	Difference[4]	Fragment[5]	Sequence[6]
1068.5793	1068.5790	0.0003	1 - 9	MQVW...PIGK
1196.6736	1196.6740	-0.0004	1 - 10	MQVW...IGKK
923.5224	923.5229	-0.0005	2 - 9	QVWPPIGK
1691.9608	1691.9610	-0.0002	10 - 23	KKFE...PLTR
1563.8664	1563.8661	0.0003	11 - 23	KFET...PLTR
1435.7716	1435.7711	0.0005	12 - 23	FETL...PLTR
852.4529	852.4528	0.0001	27 - 33	AMLTFVR
2976.5506	2976.5531	-0.0025	27 - 52	AMLT...PLGR
2142.1100	2142.1109	-0.0009	34 - 52	NAWY...PLGR
1274.7225	1274.7234	-0.0009	53 - 63	TILD...ALYR
1759.9045	1759.9039	0.0006	64 - 79	QPDG...CPHR
832.4444	832.4443	0.0001	126 - 132	SFPVVER
2722.3233	2722.3214	0.0019	133 - 157	DALI...FGCR
719.3601	719.3602	-0.0001	158 - 163	VDPAYR
1468.6406	1468.6405	0.0001	164 - 176	TVGG...CNYK
3459.6468	3459.6452	0.0016	164 - 193	TVGG...YVHR
1993.0210	1993.0204	0.0006	177 - 193	LLVD...YVHR
1107.4950	1107.4945	0.0005	194 - 203	ANAQ...AFDR
1505.7215	1505.7222	-0.0007	194 - 206	ANAQ...RLER
1915.0098	1915.0084	0.0014	204 - 220	LERE...ALMK
1516.7800	1516.7807	-0.0007	207 - 220	EVIV...ALMK
2668.4194	2668.4180	0.0014	207 - 232	EVIV...LMAK
1169.6483	1169.6478	0.0005	221 - 232	IPGG...LMAK
1585.9017	1585.9014	0.0003	221 - 235	IPGG...KFLR
1427.6802	1427.6793	0.0009	236 - 248	GANT...NDIR
1855.8971	1855.8965	0.0006	236 - 251	GANT...RWNK
2188.1411	2188.1350	0.0061	249 - 268	WNKV...GTPK
1759.9183	1759.9178	0.0005	252 - 268	VSAM...GTPK
855.4198	855.4199	-0.0001	269 - 275	EQSIHSR
2396.0865	2396.0856	0.0009	276 - 296	GTHI...GSSR
1592.7138	1592.7141	-0.0003	297 - 310	NFGI...GVLR
1029.5616	1029.5607	0.0009	311 - 319	SWQA...ALVK
1401.7277	1401.7252	0.0025	311 - 322	SWQA...KEDK
1285.6888	1285.6878	0.0010	320 - 330	EDKV...AIER
913.5238	913.5233	0.0005	323 - 330	VVVEAIER
2292.1005	2292.0990	0.0015	333 - 353	AYVE...AAVR
859.4776	859.4763	0.0013	354 - 360	VSREIEK
1271.6615	1271.6608	0.0007	357 - 367	EIEK...LEAA
772.3965	772.3967	-0.0002	361 - 367	LEQLEAA

[1] All imported values were rounded to four decimal places.
[2] Only experimental masses that matched calculated masses with the highest scores are listed in the table.
[3] The calculated mass is the exact molecular mass calculated from the matched peptide sequence.
[4] The calculated difference = experimental mass – calculated mass
[5] Position refers to amino acid residues within the predicted KWS20-1 sugar beet-produced DMO sequence as depicted in Figure 33.
[6] For peptide matches greater than nine amino acids in length, the first four residues and last four residues are shown separated by three dots (...).

Table 8. Summary of the Tryptic Masses Identified for the *E. coli*-Produced DMO Protein Using LC-MS/MS[1]

Experimental Mass[2]	Calculated Mass[3]	Difference[4]	Fragment[5]	Sequence[6]
1054.5632	1054.5634	-0.0002	1 - 9	MQVW...PIGK
1182.6591	1182.6583	0.0008	1 - 10	MQVW...IGKK
923.5234	923.5229	0.0005	2 - 9	QVWPPIGK
1051.6180	1051.6178	0.0002	2 - 10	QVWP...IGKK
1691.9572	1691.9610	-0.0038	10 - 23	KKFE...PLTR
1563.8669	1563.8661	0.0008	11 - 23	KFET...PLTR
1435.7719	1435.7711	0.0008	12 - 23	FETL...PLTR
836.4571	836.4578	-0.0007	27 - 33	AMLTFVR
2142.1134	2142.1109	0.0025	34 - 52	NAWY...PLGR
1274.7248	1274.7234	0.0014	53 - 63	TILD...ALYR
1759.9059	1759.9039	0.0020	64 - 79	QPDG...CPHR
832.4437	832.4443	-0.0006	126 - 132	SFPVVER
3536.7610	3536.7551	0.0059	126 - 157	SFPV...FGCR
2722.3256	2722.3214	0.0042	133 - 157	DALI...FGCR
3423.6612	3423.6710	-0.0098	133 - 163	DALI...PAYR
719.3601	719.3602	-0.0001	158 - 163	VDPAYR
1468.6404	1468.6405	-0.0001	164 - 176	TVGG...CNYK
1993.0218	1993.0204	0.0014	177 - 193	LLVD...YVHR
1107.4941	1107.4945	-0.0004	194 - 203	ANAQ...AFDR
1505.7229	1505.7222	0.0007	194 - 206	ANAQ...RLER
1899.0152	1899.0135	0.0017	204 - 220	LERE...ALMK
1500.7873	1500.7858	0.0015	207 - 220	EVIV...ALMK
2652.4253	2652.4230	0.0023	207 - 232	EVIV...LMAK
1169.6482	1169.6478	0.0004	221 - 232	IPGG...LMAK
1585.9004	1585.9014	-0.0010	221 - 235	IPGG...KFLR
1427.6793	1427.6793	0.0000	236 - 248	GANT...NDIR
3581.8137	3581.8089	0.0048	236 - 268	GANT...GTPK
2172.1400	2172.1401	-0.0001	249 - 268	WNKV...GTPK
1743.9240	1743.9229	0.0011	252 - 268	VSAM...GTPK
2581.3342	2581.3322	0.0020	252 - 275	VSAM...IHSR
855.4200	855.4199	0.0001	269 - 275	EQSIHSR
2396.0838	2396.0856	-0.0018	276 - 296	GTHI...GSSR
4966.3677	4966.3443	0.0234	276 - 319	GTHI...ALVK
1576.7225	1576.7192	0.0033	297 - 310	NFGI...GVLR
1029.5614	1029.5607	0.0007	311 - 319	SWQA...ALVK
1401.7230	1401.7252	-0.0022	311 - 322	SWQA...KEDK
2297.2357	2297.2379	-0.0022	311 - 330	SWQA...AIER
1285.6866	1285.6878	-0.0012	320 - 330	EDKV...AIER
1441.7911	1441.7889	0.0022	320 - 331	EDKV...IERR

Experimental Mass[2]	Calculated Mass[3]	Difference[4]	Fragment[5]	Sequence[6]
913.5237	913.5233	0.0004	323 - 330	VVVEAIER
1069.6240	1069.6244	-0.0004	323 - 331	VVVE...IERR
2448.2031	2448.2002	0.0029	332 - 353	RAYV...AAVR
2292.0976	2292.0990	-0.0014	333 - 353	AYVE...AAVR
1271.6616	1271.6608	0.0008	357 - 367	EIEK...LEAA
772.3968	772.3967	0.0001	361 - 367	LEQLEAA

[1] All imported values were rounded to four decimal places. Data were from a previous characterization of *E. coli*-produced DMO.
[2] Only experimental masses that matched calculated masses with the highest scores are listed in table.
[3] The calculated mass is the exact molecular mass calculated from the matched peptide sequence.
[4] The calculated difference = experimental mass – calculated mass
[5] Position refers to amino acid residues within the predicted *E. coli*-produced DMO sequence as depicted in Figure 33.
[6] For peptide matches greater than nine amino acids in length the first four residues and last four residues are shown separated by dots (…).

(A)

```
1   MQVWPPIGKK KFETLSYLPP LTRDSRAMLT FVRNAWYVAA LPEELSEKPL
51  GRTILDTPLA LYRQPDGVVA ALLDICPHRF APLSDGILVN GHLQCPYHGL
101 EFDGGGQCVH NPHGNGARPA SLNVRSFPVV ERDALIWIWP GDPALADPGA
151 IPDFGCRVDP AYRTVGGYGH VDCNYKLLVD NLMDLGHAQY VHRANAQTDA
201 FDRLEREVIV GDGEIQALMK IPGGTPSVLM AKFLRGANTP VDAWNDIRWN
251 KVSAMLNFIA VAPEGTPKEQ SIHSRGTHIL TPETEASCHY FFGSSRNFGI
301 DDPEMDGVLR SWQAQALVKE DKVVVEAIER RRAYVEANGI RPAMLSCDEA
351 AVRVSREIEK LEQLEAA
```

(B)

```
1   MQVWPPIGKK KFETLSYLPP LTRDSRAMLT FVRNAWYVAA LPEELSEKPL
51  GRTILDTPLA LYRQPDGVVA ALLDICPHRF APLSDGILVN GHLQCPYHGL
101 EFDGGGQCVH NPHGNGARPA SLNVRSFPVV ERDALIWIWP GDPALADPGA
151 IPDFGCRVDP AYRTVGGYGH VDCNYKLLVD NLMDLGHAQY VHRANAQTDA
201 FDRLEREVIV GDGEIQALMK IPGGTPSVLM AKFLRGANTP VDAWNDIRWN
251 KVSAMLNFIA VAPEGTPKEQ SIHSRGTHIL TPETEASCHY FFGSSRNFGI
301 DDPEMDGVLR SWQAQALVKE DKVVVEAIER RRAYVEANGI RPAMLSCDEA
351 AVRVSREIEK LEQLEAA
```

Figure 33. Peptide Map of the KWS20-1 Sugar Beet-Produced and *E. coli*-Produced DMO Proteins

(A). The amino acid sequence of the KWS20-1 sugar beet-produced DMO protein was deduced from the *dmo* gene present in KWS20-1 sugar beet. Boxed regions correspond to peptides that were identified from the KWS20-1 sugar beet-produced DMO protein sample using LC-MS/MS. In total, 86% coverage (316 out of 367 amino acids) of the expected protein sequence was covered by the identified peptides.

(B). The amino acid sequence of the *E. coli*-produced DMO protein was deduced from the *dmo* gene that is contained on the expression plasmid pMON421813. Boxed regions correspond to peptides that were

identified from the *E. coli*-produced DMO protein sample using LC-MS/MS. In total, 85% coverage (315 out of 367 amino acids) of the expected protein sequence was covered by the identified peptides.

B.1(a)(ii)(i)(iii) Results of Western Blot Analysis of the DMO Protein Isolated from Leaf of KWS20-1 Sugar Beet and Immunoreactivity Comparison to *E. coli*-Produced DMO Protein

Western blot analysis was conducted using an anti-DMO antibody as additional means to confirm the identity of the DMO protein isolated from the leaf of KWS20-1 sugar beet and to assess the equivalence of the immunoreactivity of the KWS20-1 sugar beet-produced and *E. coli*-produced DMO proteins.

The results showed that immunoreactive bands with the same electrophoretic mobility were present in all lanes loaded with the KWS20-1 sugar beet-produced (Figure 34, lanes 8-13) and *E. coli*-produced (Figure 34, lanes 2-7) DMO proteins. For each amount loaded, comparable signal intensity was observed between the KWS20-1 sugar beet-produced and *E. coli*-produced DMO protein bands. As expected, the signal intensity increased with increasing load amounts of the KWS20-1 sugar beet-produced and *E. coli*-produced DMO proteins, thus supporting identification of KWS20-1 sugar beet-produced DMO protein. One other band migrating at ~130 kDa was also observed. This band was observed in lanes with higher load amounts and, therefore, may represent an aggregation of the KWS20-1 sugar beet-produced DMO occurring during sample preparation.

To compare the immunoreactivity of the KWS20-1 sugar beet-produced and the *E. coli*-produced DMO proteins, densitometric analysis was conducted on bands that migrated to the expected apparent MW for the DMO protein (~38 kDa). The signal intensity (reported in OD) of the band of interest in lanes loaded with KWS20-1 sugar beet-produced and *E. coli*-produced DMO proteins was measured (Table 9). Because the mean signal intensity of the KWS20-1 sugar beet-produced DMO protein band was within ±35% of the mean signal intensity of the *E. coli*-produced DMO protein, the KWS20-1 sugar beet-produced and *E. coli*-produced DMO proteins were determined to have equivalent immunoreactivity.

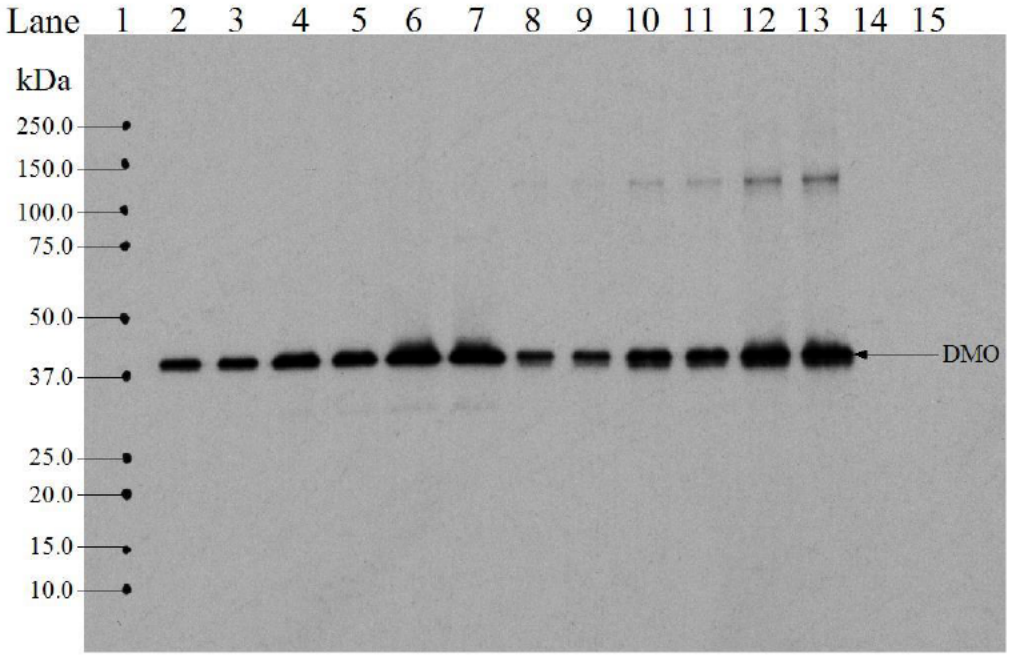

Figure 34. Western Blot Analysis of the KWS20-1 Sugar Beet-Produced and *E. coli*-Produced DMO Proteins

Aliquots of the KWS20-1 sugar beet-produced and *E. coli*-produced DMO proteins were subjected to SDS-PAGE and electrotransferred to a nitrocellulose membrane. Proteins were detected using a mouse anti-DMO monoclonal antibody as the primary antibody. Immunoreactive bands were visualized using HRP-conjugated secondary antibodies and an ECL system. The 4-minute exposure is shown. The approximate MWs (kDa) of the standards are shown on the left. Lane designations are as follows:

Lane	Sample	Amount (ng)
1	Precision Plus Protein™ Standards	-
2	*E. coli*-produced DMO	1.0
3	*E. coli*-produced DMO	1.0
4	*E. coli*-produced DMO	2.5
5	*E. coli*-produced DMO	2.5
6	*E. coli*-produced DMO	5.0
7	*E. coli*-produced DMO	5.0
8	KWS20-1 sugar beet-produced DMO	1.0
9	KWS20-1 sugar beet-produced DMO	1.0
10	KWS20-1 sugar beet-produced DMO	2.5
11	KWS20-1 sugar beet-produced DMO	2.5
12	KWS20-1 sugar beet-produced DMO	5.0
13	KWS20-1 sugar beet-produced DMO	5.0
14	Blank	-
15	Blank	-

Table 9. Comparison of Immunoreactive Signals between KWS20-1 Sugar Beet-Produced and *E. coli*-Produced DMO Proteins

Mean Signal Intensity from KWS20-1 Sugar Beet-Produced DMO[1] (OD)	Mean Signal Intensity from *E. coli*-Produced DMO[1] (OD)	Acceptance Limits[2] (OD)
5,138.75	6,006.04	3,903.93 – 8,108.15

[1] Each value represents the mean of six values (n = 6).
[2] The acceptance limits are for the KWS20-1 sugar beet-produced DMO protein and are based on the interval between -35% (6006.04 × 0.65 = 3903.93) and +35% (6006.04 × 1.35 = 8108.15) of the mean of the *E. coli*-produced DMO signal intensity across all loads.

B.1(a)(ii)(i)(iv) Results of the DMO Protein Molecular Weight and Purity Analysis

For molecular weight analysis, the KWS20-1 sugar beet-produced and the *E. coli*-produced DMO proteins were subjected to SDS-PAGE. Following electrophoresis, the gel was stained with Brilliant Blue G-Colloidal stain and analyzed by densitometry (Figure 35). The KWS20-1 sugar beet-produced DMO protein (Figure 35, lanes 3-8) migrated to the same position on the gel as the *E. coli*-produced DMO protein (Figure 35, lane 2) and the apparent molecular weight was calculated to be ~38.3 kDa (Table 10). Because the experimentally determined apparent MW of the KWS20-1 sugar beet-produced DMO protein was within the preset acceptance limits for equivalence (Table 11, 37.8–39.0 kDa), the KWS20-1 sugar beet-produced and *E. coli*-produced DMO proteins were determined to have equivalent apparent molecular weights.

The purity of the KWS20-1 sugar beet-produced DMO protein was calculated based on the six lanes loaded on the gel (Figure 35, lanes 3-8). The average purity was determined to be 87% (Table 10).

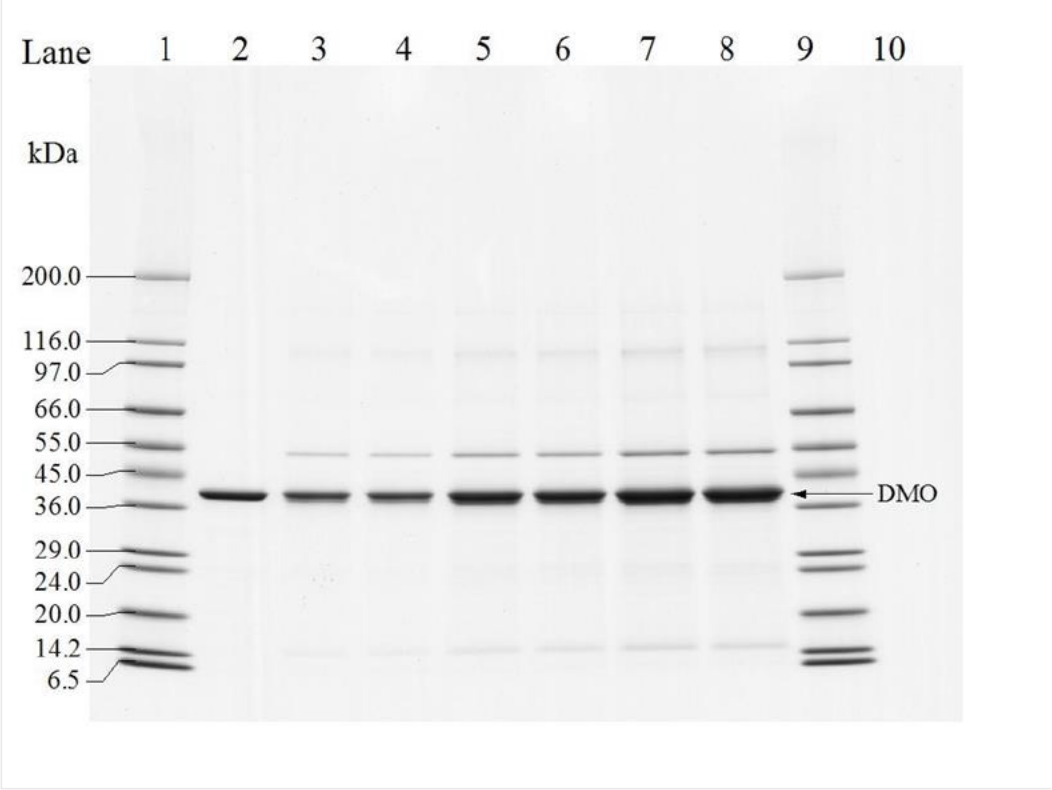

Figure 35. Molecular Weight and Purity Analysis of the KWS20-1 Sugar Beet-Produced DMO Protein

Aliquots of the KWS20-1 sugar beet-produced and the *E. coli*-produced DMO proteins were subjected to SDS-PAGE and the gel was stained with Brilliant Blue G-Colloidal stain. The MWs (kDa) are shown on the left and correspond to the standards loaded in lanes 1 and 9. Lane designations are as follows:

Lane	Sample	Amount (µg)
1	SigmaMarker Wide Range	NA
2	*E. coli*-produced DMO	1.0
3	KWS20-1 sugar beet-produced DMO	1.0
4	KWS20-1 sugar beet-produced DMO	1.0
5	KWS20-1 sugar beet-produced DMO	2.0
6	KWS20-1 sugar beet-produced DMO	2.0
7	KWS20-1 sugar beet-produced DMO	3.0
8	KWS20-1 sugar beet-produced DMO	3.0
9	SigmaMarker Wide Range	NA
10	Blank	

Table 10. Apparent Molecular Weight and Purity Analysis of the KWS20-1 Sugar Beet-Produced DMO Protein

	Apparent MW[1] (kDa)	Purity[2] (%)
Average (n=6)	38.3	87

[1]Final MW was rounded to one decimal place.
[2]Average % purity was rounded to the nearest whole number.

Table 11. Molecular Weight Comparison Between the KWS20-1 Sugar Beet- and *E. coli*-Produced DMO Proteins

Apparent MW of KWS20-1 Sugar Beet-produced DMO Protein (kDa)	Apparent MW of *E. coli*-produced DMO Protein[1] (kDa)	Acceptance Limits[2] (kDa)
38.3	38.4	37.8 – 39.0

[1] See Appendix 7 for the apparent MW of the *E. coli*-produced DMO protein.
[2] Data obtained for the *E. coli*-produced DMO protein was used to generate the prediction interval (Appendix 7).

B.1(a)(ii)(i)(v) DMO Glycosylation Analysis

Some eukaryotic proteins can be post-translationally modified by the addition of carbohydrate moieties (Rademacher *et al.*, 1988). To test whether the DMO protein was glycosylated when expressed in the leaf tissue of KWS20-1 sugar beet, the KWS20-1 sugar beet-produced DMO protein was subjected to SDS-PAGE, transferred to a membrane and the membrane was analyzed using an ECL™ glycoprotein detection method. Transferrin, a glycosylated protein, was used as a positive control in the assay. To assess equivalence of the KWS20-1 sugar beet-produced and *E. coli*-produced DMO proteins, the *E. coli*-produced DMO protein was also analyzed.

A clear glycosylation signal was observed at the expected molecular weight (~ 80 kDa) in the lanes containing the positive control, transferrin, and the band intensity increased with increasing concentration (Figure 36, Panel A, lanes 3-4), demonstrating that the assay performed as expected. In contrast, no glycosylation signal was observed in the lanes containing the KWS20-1 sugar beet-produced DMO protein (Figure 36, Panel A, lanes 9 and 10) or the *E. coli*-produced DMO protein (Figure 36, Panel A, lanes 6 and 7).

To confirm that KWS20-1 sugar beet-produced and *E. coli*-produced DMO proteins were appropriately loaded for glycosylation analysis, a second membrane with identical loadings and transfer time was stained with Coomassie Blue R250 for protein detection (Figure 36, Panel B). Both the KWS20-1 sugar beet-produced (Figure 36, Panel B, lanes 9 and 10) and *E. coli*-produced (Figure 36, Panel B, lanes 6 and 7) DMO proteins were detected. These data indicate that the glycosylation status of KWS20-1 sugar beet-produced DMO protein is equivalent to that of the *E. coli*-produced DMO protein and that neither is glycosylated.

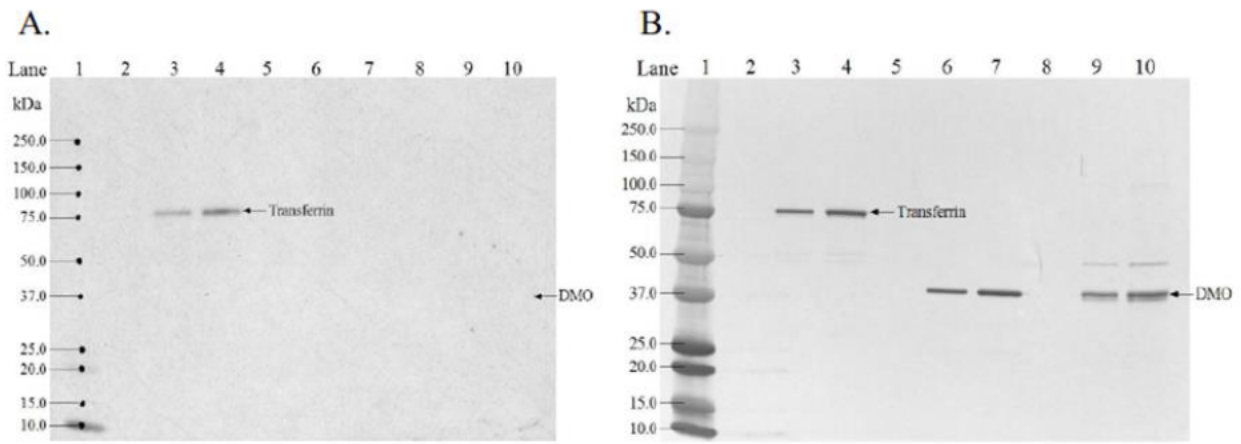

Figure 36. Glycosylation Analysis of the KWS20-1 Sugar Beet-Produced DMO Protein

Aliquots of the transferrin (positive control), *E. coli*-produced and KWS20-1 sugar beet-produced DMO proteins were subjected to SDS-PAGE and electrotransferred to a PVDF membrane. The MWs (kDa) correspond to the Precision Plus Protein™ Standards. The arrows show the expected migration of the KWS20-1 sugar beet-produced and *E. coli*-produced DMO proteins and transferrin. (A) Where present, the labeled carbohydrate moieties were detected by using ECL reagents and exposure to Hyperfilm®. The 4-minute exposure is shown. (B) An equivalent blot was stained with Coomassie Blue R-250 to confirm the presence of proteins. Lane designations are as follows:

Lane	Sample	Amount (ng)
1	Precision Plus Protein™ Standards	-
2	Blank	-
3	Transferrin (positive control)	100
4	Transferrin (positive control)	200
5	Blank	-
6	*E. coli*-produced DMO	100
7	*E. coli*-produced DMO	200
8	Blank	-
9	KWS20-1 sugar beet-produced DMO	100
10	KWS20-1 sugar beet-produced DMO	200

B.1(a)(ii)(i)(vi) DMO Functional Activity

The functional activity of the KWS20-1 sugar beet-produced DMO and *E. coli*-produced DMO proteins was determined by measuring the amount of dicamba that was converted to DSCA via HPLC separation and fluorescence detection. In this assay, activity is expressed as specific activity and reported as nmol × minute^{-1} × mg^{-1}. The KWS20-1 sugar beet-produced and *E. coli*-produced DMO proteins were considered functionally equivalent if the specific activity of both were within acceptance limits of 27.9 to 584.1 (the prediction interval calculated from data obtained for the *E. coli*-produced DMO protein activity; see Appendix 7).

The experimentally determined specific activity for the KWS20-1 sugar beet-produced and *E. coli*-produced DMO proteins are presented in Table 12. The specific activity of the KWS20-1 sugar beet-produced and *E. coli*-produced DMO proteins was determined to be 206.4 and 411.8 nmol × minute^{-1} × mg^{-1}, respectively (Table 12). Because the specific activity of the KWS20-1 sugar beet-produced and *E. coli*-produced DMO proteins were within the acceptance limits, the KWS20-1 sugar beet-produced DMO protein was considered to have equivalent functional activity to that of the *E. coli*-produced DMO protein.

Table 12. Functional Activity of the KWS20-1 Sugar Beet-Produced and *E. coli*-Produced DMO Proteins

KWS20-1 Sugar Beet-produced DMO[1] (nmol × minute^{-1} × mg^{-1})	*E. coli*-Produced DMO[1] (nmol × minute^{-1} × mg^{-1})	Acceptance Limits[2] (nmol × minute^{-1} × mg^{-1})
206.4	411.8	27.9 – 584.1

[1] Value refers to mean calculated based on n = 5 for KWS20-1 sugar beet-produced DMO and n = 4 for *E. coli*-produced DMO.

[2] Data obtained for the *E. coli*-produced DMO was used to generate a prediction interval for setting the acceptance limits (Appendix 7).

B.1(a)(ii)(i)(vii) KWS20-1 Sugar Beet DMO Protein Identity and Equivalence Conclusion

The KWS20-1 sugar beet-produced DMO protein was purified from KWS20-1 sugar beet leaf, characterized and a comparison of the physicochemical and functional properties between the KWS20-1 sugar beet-produced and the *E. coli*-produced DMO proteins was conducted following a panel of analytical tests: 1) N-terminal sequence analysis established the same amino acid identity for the KWS20-1 sugar beet-produced and *E. coli*-produced DMO proteins; 2) Nano LC-MS/MS analysis yielded peptide masses consistent with the expected peptide masses from the theoretical trypsin digest of the *dmo* gene product present in both KWS20-1 sugar beet and produced from *E. coli*; 3) the KWS20-1 sugar beet-produced and the *E. coli*-produced DMO proteins were both detected on a western blot probed with antibodies specific for DMO protein and the immunoreactive properties of both proteins were shown to be equivalent; 4) the electrophoretic mobility and apparent molecular weight of the KWS20-1 sugar beet-produced and *E. coli*-produced DMO proteins were shown to be equivalent; 5) the glycosylation status of KWS20-1 sugar beet-produced and *E. coli*-produced DMO proteins was determined to be equivalent; and 6) the functional activity of the KWS20-1 sugar beet-produced and *E. coli*-

produced DMO proteins were demonstrated to be equivalent. These results demonstrate that the KWS20-1 sugar beet-produced and the *E. coli*-produced DMO proteins are equivalent.

This demonstration of protein equivalence confirms that the *E. coli*-produced DMO protein is appropriate for use in the evaluation of the safety of the KWS20-1 sugar beet-produced DMO protein. Therefore, conclusions derived from digestibility, heat susceptibility and oral acute toxiciology studies conducted with *E. coli*-produced DMO protein are applicable to KWS20-1 sugar beet-produced DMO protein.

B.1(a)(ii)(ii) Characterisation of the KWS20-1 Sugar Beet PAT Protein

The safety assessment of crops derived through biotechnology includes characterization of the physicochemical and functional properties and confirmation of the safety of the introduced protein(s). For the safety data generated using the *E. coli*-produced PAT protein to be applied to the KWS20-1 sugar beet-produced PAT protein (plant-produced PAT), the equivalence of the plant- and *E. coli*-produced proteins must first be demonstrated. To assess the equivalence between the KWS20-1 sugar beet-produced PAT and *E. coli*-produced PAT proteins, a small quantity of the KWS20-1 sugar beet-produced PAT protein was purified from KWS20-1 sugar beet leaf tissue. The KWS20-1 sugar beet-produced PAT protein was characterized and the equivalence of the physicochemical characteristics and functional activity between the KWS20-1 sugar beet-produced and *E. coli*-produced PAT proteins was assessed using a panel of six analytical tests; as shown in Table 13. Taken together, these data provide a detailed characterization of the KWS20-1 sugar beet-produced PAT protein and establish the equivalence of the KWS20-1 sugar beet-produced PAT and *E. coli*-produced PAT proteins. With establishment of equivalence, conclusions derived from digestibility, heat susceptibility and oral acute toxicology studies conducted with *E. coli*-produced PAT protein are applicable to KWS20-1 sugar beet-produced PAT protein.

For details, please refer to Appendix 8 .

Table 13. Summary of KWS20-1 Sugar Beet-Produced PAT Protein Identity and Equivalence

Analytical Test Assessment	Analytical Test Outcome
N-terminal sequence	The expected N-terminal sequence for KWS20-1 sugar beet-produced PAT was observed by Nano LC-MS/MS[1]
Nano LC-MS/MS[1]	Nano LC-MS/MS[1] analysis of trypsin digested peptides from KWS20-1 sugar beet-produced PAT protein yielded peptide masses consistent with expected peptide masses from the theoretical trypsin digest of the amino acid sequence
Western blot analysis	KWS20-1 sugar beet-produced PAT protein identity was confirmed using a western blot probed with antibodies specific for PAT protein. Immunoreactive properties of the KWS20-1 sugar beet-produced PAT and the *E. coli*-produced PAT proteins were shown to be equivalent
Apparent molecular weight (MW)	Electrophoretic mobility and apparent molecular weight of the KWS20-1 sugar beet-produced PAT and the *E. coli*-produced PAT proteins were shown to be equivalent
Glycosylation analysis	Glycosylation status of KWS20-1 sugar beet-produced PAT and *E. coli*-produced PAT proteins were shown to be equivalent

Functional activity	Functional activity of the KWS20-1 sugar beet-produced PAT and the *E. coli*-produced PAT proteins were shown to be equivalent

[1] Nano LC-MS/MS = Nanoscale liquid chromatography coupled to tandem mass spectrometry

B.1(a)(ii)(ii)(i) Results of the N-terminal Sequencing Analysis

N-terminal sequencing was performed on the PAT protein. The expected sequence for the PAT protein deduced from the *pat* gene present in KWS20-1 sugar beet was observed. The removal of the initiator methionine (M) was expected for the KWS20-1 sugar beet-produced PAT protein, which is expressed in the cytoplasm. The cleavage of the N-terminal methionine from proteins *in vivo* by methionine aminopeptidase is thought to occur in all organisms (Bradshaw *et al.*, 1998; Giglione *et al.*, 2004) and is observed with high frequency when the second amino acid residue is a serine (Frottin *et al.*, 2006), as is the case for the PAT protein. Furthermore, the initiator methionine for the closely related PAT (*bar*) protein (85% overall amino acid sequence identity, and 100% identity for the first seven amino acid residues at the N-terminus) was also removed when expressed in biotechnology-derived cotton (Wang *et al.*, 2013). The N-terminal sequence for KWS20-1 sugar beet-produced PAT protein was consistent with the N-terminal sequence for the *E. coli*-produced PAT protein observed by LC-MS/MS analysis (Figure 37). Hence, the sequence information confirms the identity of the PAT protein isolated from the leaf tissue of KWS20-1 sugar beet.

Amino Acids Residue # from the N-terminus	→	1	2	3	4	5	6	7	8	9	10	11	12	13	14	15
E. coli-produced PAT Sequence	→	M	S	P	E	R	R	P	V	E	I	R	P	A	T	A
		|	|	|	|	|	|	|	|	|	|	|	|	|	|	|
PAT sequence	→	M	S	P	E	R	R	P	V	E	I	R	P	A	T	A
			|	|	|	|	|	|	|	|	|	|	|	|	|	|
KW20-1 sugar beet-produced PAT sequence	→	-	S	P	E	R	R	P	V	E	I	R	P	A	T	A

Figure 37. N-Terminal Sequence of the KWS20-1 Sugar Beet-Produced PAT Protein

The experimental sequence obtained from the KWS20-1 sugar beet-produced PAT was compared to the PAT sequence deduced from the *pat* gene present in KWS20-1 sugar beet. The removal of the initiator methionine (M) was expected for the KWS20-1 sugar beet-produced PAT protein which is expressed in the cytoplasm. The sequence of the N-terminus of the KWS20-1 sugar beet-produced PAT protein was obtained by Nano LC-MS/MS peptide analysis (trypsin digest). The single letter International Union of Pure and Applied Chemistry - International Union of Biochemistry (IUPAC-IUB) amino acid code is M, methionine; S; serine; P, proline; E, glutamic acid; R, arginine; V, valine; I, isoleucine; A, alanine; T, threonine. The sequence of the N-terminus of the *E. coli*-produced PAT protein is from a previous characterization.

B.1(a)(ii)(ii)(ii) Results of the PAT Protein Mass Fingerprint Analysis

The identity of the PAT protein was confirmed by Nano LC-MS/MS analysis of peptide fragments produced by a trypsin digestion of the KWS20-1 sugar beet-produced PAT protein.

There were 20 unique peptides identified that corresponded to the expected masses of the trypsin-digested sequence of KWS20-1 sugar beet-produced PAT (Table 14). The identified masses were used to assemble a peptide map of the PAT protein (Figure 38). The experimentally determined coverage of the KWS20-1 sugar beet-produced PAT protein was 99% (182 out of 183 amino acids). This analysis further confirms the identity of KWS20-1 sugar beet-produced PAT protein.

There were 11 unique peptides identified that corresponded to the expected masses of trypsin-digested *E. coli*-produced PAT protein (Table 15) by MALDI-TOF MS analysis during a previous characterization of this protein. The identified masses were used to assemble a peptide map of the PAT protein (Figure 38). The experimentally determined coverage of the *E. coli*-produced PAT protein was 87% (159 out of 183 amino acids). This analysis further confirms the identity of *E. coli*-produced PAT protein and equivalence to the KWS20-1 sugar beet-produced PAT protein.

Table 14. Summary of the Tryptic Masses Identified for KWS20-1 Sugar Beet-Produced PAT Protein Using Nano LC-MS/MS

Experimental Mass[1]	Calculated Mass[2]	Diff[3]	Fragment[4]	Sequence[5]
487.2391	487.2390	0.0001	2 - 5	SPER
3615.7905	3615.7926	-0.0021	6 - 37	RPVE...VNFR
1855.8606	1855.8588	0.0018	38 - 52	TEPQ...DLER
2368.1324	2368.1295	0.0029	38 - 56	TEPQ...LQDR
530.2807	530.2813	-0.0006	53 - 56	LQDR
2886.5072	2886.5068	0.0004	53 - 78	LQDR...GPWK
3113.6491	3113.6451	0.0040	53 - 80	LQDR...WKAR
2374.2337	2374.2361	-0.0024	57 - 78	YPWL...GPWK
1925.8919	1925.8908	0.0011	81 - 96	NAYD...VSHR
439.2290	439.2292	-0.0002	97 - 99	HQR
1414.8178	1414.8184	-0.0006	100 - 112	LGLG...HLLK
896.4060	896.4062	-0.0002	113 - 120	SMEAQGFK
1521.8529	1521.8515	0.0014	121 - 135	SVVA...PSVR
1129.5893	1129.5880	0.0013	136 - 145	LHEA...YTAR
445.2648	445.2649	-0.0001	146 - 149	GTLR
935.5194	935.5188	0.0006	146 - 154	GTLR...AGYK
508.2644	508.2645	-0.0001	150 - 154	AAGYK
1970.9300	1970.9289	0.0011	150 - 166	AAGY...FWQR
1480.6759	1480.6749	0.0010	155 - 166	HGGW...FWQR
1931.0639	1931.0629	0.0010	167 - 183	DFEL...VTQI

[1] Only experimental masses that matched calculated masses with the highest scores are listed in the table.
[2] The calculated mass is the relative molecular mass calculated from the matched peptide sequence.
[3] The calculated difference = experimental mass – calculated mass
[4] Position refers to amino acid residues within the predicted KWS20-1 sugar beet-produced PAT protein sequence as depicted in Figure 38.
[5] For peptide matches greater than nine amino acids in length the first four residues and last four residues are shown separated by three dots (…).

Table 15. Summary of the Tryptic Masses Identified for the *E. coli*-Produced PAT Protein Using MALDI-TOF MS

Experimental Mass[1]	Calculated Mass[2]	Difference[3]	Fragment[4]	Sequence[5]
3616.7368	3616.7766	-0.0398	6 - 37	RPVE…VNFR
1855.8205	1855.8588	-0.0383	38 - 52	TEPQ…DLER
2886.4400	2886.5068	-0.0668	53 - 78	LQDR…GPWK
2374.1822	2374.2361	-0.0539	57 - 78	YPWL…GPWK
1925.8546	1925.8908	-0.0362	81 - 96	NAYD…VSHR
2347.1682	2347.1094	0.0588	81 - 99	NAYD…RHQR
1414.7882	1414.8184	-0.0302	100 - 112	LGLG…HLLK
1521.8238	1521.8515	-0.0277	121 - 135	SVVA…PSVR
1129.5744	1129.5880	-0.0136	136 - 145	LHEA…YTAR
1480.6502	1480.6749	-0.0247	155 - 166	HGGW…FWQR
1931.0281	1931.0629	-0.0348	167 - 183	DFEL…VTQI

[1] Only experimental masses that matched calculated PAT trypsin digested masses are listed in the table. Data were from previous characterization of *E. coli*-produced PAT.
[2] The calculated mass is the exact molecular mass calculated from the matched peptide sequence.
[3] The calculated difference = experimental mass - calculated mass
[4] Position refers to amino acid residues within the predicted *E. coli*-produced PAT protein sequence as depicted in Figure 38.
[5] For peptide matches greater than nine amino acids in length, the first four residues and last four residues are shown separated by three dots (...).

(A)

1 MSPERRPVEI RPATAADMAA VCDIVNHYIE TSTVNFRTEP QTPQEWIDDL

51 ERLQDRYPWL VAEVEGVVAG IAYAGPWKAR NAYDWTVEST VYVSHRHQRL

101 GLGSTLYTHL LKSMEAQGFK SVVAVIGLPN DPSVRLHEAL GYTARGTLRA

151 AGYKHGGWHD VGFWQRDFEL PAPPRPVRPV TQI

(B)

001 MSPERRPVEI RPATAADMAA VCDIVNHYIE TSTVNFRTEP QTPQEWIDDL

051 ERLQDRYPWL VAEVEGVVAG IAYAGPWKAR NAYDWTVEST VYVSHRHQRL

101 GLGSTLYTHL LKSMEAQGFK SVVAVIGLPN DPSVRLHEAL GYTARGTLRA

151 AGYKHGGWHD VGFWQRDFEL PAPPRPVRPV TQI

Figure 38. Peptide Map of the KWS20-1 Sugar Beet-Produced and *E. coli*-Produced PAT Proteins

(A). The amino acid sequence of the KWS20-1 sugar beet-produced PAT protein was deduced from the *pat* gene present in KWS20-1 sugar beet. The initial methionine residue is not included as it was expected to be missing from the plant-produced protein. Boxed regions correspond to peptides that were identified from the KWS20-1 sugar beet-produced PAT protein sample using Nano LC-MS/MS. In total, 99% coverage (182 out of 183 amino acids) of the expected protein sequence was covered by the identified peptides.

(B). The amino acid sequence of the *E. coli*-produced PAT protein was deduced from the *pat* gene that is contained on the expression plasmid. Boxed regions correspond to peptides that were identified from the *E. coli*-produced PAT protein sample using MALDI-TOF MS in a previous characterization. In total, 87% coverage (159 out of 183 amino acids) of the expected protein sequence was covered by the identified peptides.

B.1(a)(ii)(ii)(iii) Results of Western Blot Analysis of the PAT Protein Isolated from Leaf of KWS20-1 Sugar Beet and Immunoreactivity Comparison to *E. coli*-Produced PAT Protein

Western blot analysis was conducted using a mouse anti-PAT monoclonal antibody as additional means to confirm the identity of the PAT protein isolated from the leaf of KWS20-1 sugar beet and to assess the equivalence of the immunoreactivity of the KWS20-1 sugar beet-produced and *E. coli*-produced PAT proteins.

The results showed that immunoreactive bands migrating with the same electrophoretic mobility were present in all lanes loaded with the KWS20-1 sugar beet-produced (Figure 39, lanes 9-14) or *E. coli*-produced (Figure 39, lanes 3-8) PAT proteins. For each amount loaded, comparable signal intensity was observed between the KWS20-1 sugar beet-produced and *E. coli*-produced PAT protein bands. As expected, the signal intensity increased with increasing load amounts of the KWS20-1 sugar beet-produced and *E. coli*-produced PAT proteins, thus, supporting identification of KWS20-1 sugar beet-produced PAT protein.

To compare the immunoreactivity of the KWS20-1 sugar beet-produced and the *E. coli*-produced PAT proteins, densitometric analysis was conducted on bands that migrated to the expected apparent MW for the PAT protein (~25 kDa). The signal intensity (reported in OD) of the band of interest in lanes loaded with KWS20-1 sugar beet-produced and the *E. coli*-produced PAT proteins was measured (Table 16). Because the mean signal intensity of the KWS20-1 sugar beet-produced PAT protein band was within ±35% of the mean signal intensity of the *E. coli*-produced PAT protein, the KWS20-1 sugar beet-produced and *E. coli*-produced PAT proteins were determined to have equivalent immunoreactivity.

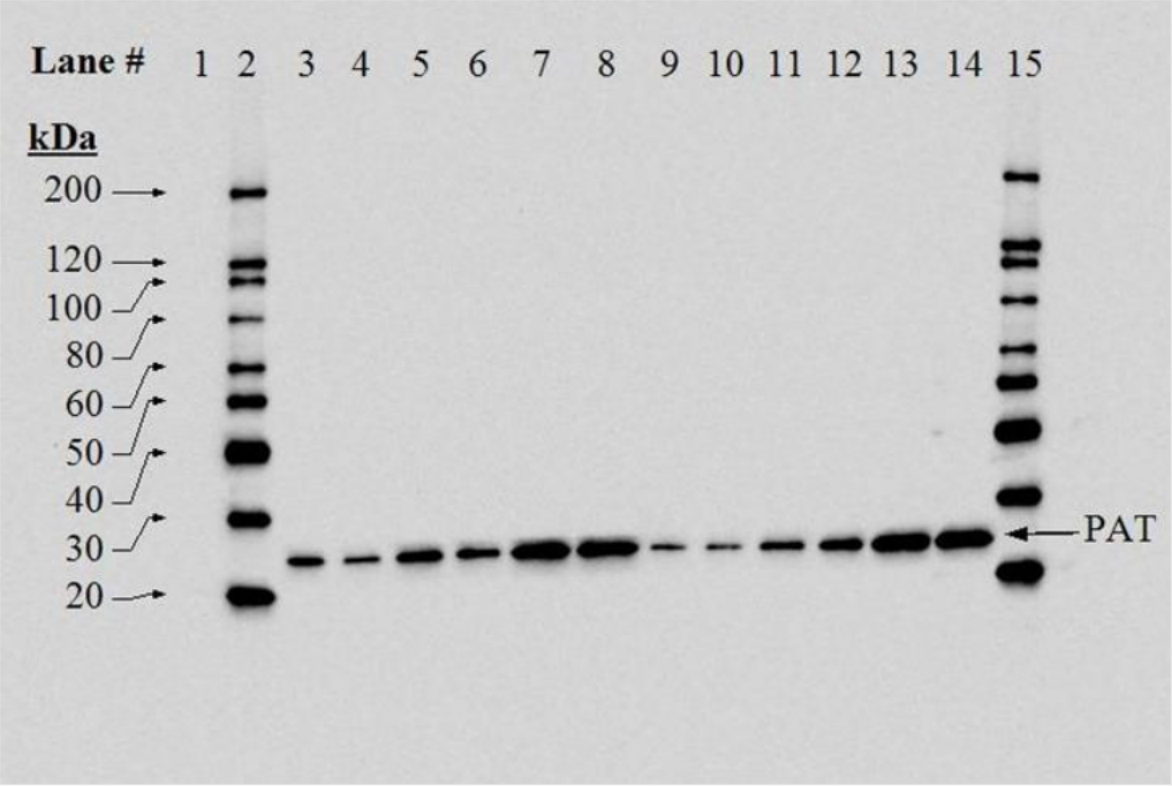

Figure 39. Western Blot Analysis of the KWS20-1 Sugar Beet-Produced and *E. coli*-Produced PAT Proteins

Aliquots of the KWS20-1 sugar beet-produced and *E. coli*-produced PAT proteins were subjected to SDS-PAGE and electrotransferred to a PVDF membrane. Proteins bound to the PVDF membrane were initially probed using a mouse anti-PAT monoclonal primary antibody. Immunoreactive bands were detected using a peroxidase conjugated anti-mouse IgG (H+L) secondary antibody and were visualized using an ECL system. The 15 second exposure is shown. The approximate MW (kDa) of the standards are shown on the left. Lane designations are as follows:

Lane	Sample	Amount (ng)
1	Precision Plus Dual Color MW marker	-
2	MagicMark™ XP Western Protein Standards	-
3	*E. coli*-produced PAT	2
4	*E. coli*-produced PAT	2
5	*E. coli*-produced PAT	4
6	*E. coli*-produced PAT	4
7	*E. coli*-produced PAT	8
8	*E. coli*-produced PAT	8
9	KWS20-1 sugar beet-produced PAT	2
10	KWS20-1 sugar beet-produced PAT	2
11	KWS20-1 sugar beet-produced PAT	4
12	KWS20-1 sugar beet-produced PAT	4
13	KWS20-1 sugar beet-produced PAT	8
14	KWS20-1 sugar beet-produced PAT	8
15	MagicMark™ XP Western Protein Standards	-

Table 16. Comparison of Immunoreactive Signals between KWS20-1 Sugar Beet-Produced and *E. coli*-Produced PAT Proteins

Mean Signal Intensity from KWS20-1 Sugar Beet-Produced PAT[1] (OD)	Mean Signal Intensity from *E. coli*-Produced PAT[1] (OD)	Acceptance Limits[2] (OD)
1265464.86	1198995.57	779347.12 – 1618644.02

[1] Each value represents the mean of six values of the immunoreactive band (n = 6).
[2] The acceptance limits are for the KWS20-1 sugar beet-produced PAT protein and are based on the interval between -35% (1198995.57 × 0.65 = 779347.12) and +35% (1198995.57 × 1.35 = 1618644.02) of the mean of the *E. coli*-produced PAT signal intensity across all loads.

B.1(a)(ii)(ii)(iv) Results of the PAT Protein Molecular Weight and Purity Analysis

For molecular weight analysis, the KWS20-1 sugar beet-produced PAT protein was separated using SDS-PAGE. Following electrophoresis, the gel was stained with Brilliant Blue G-Colloidal stain and analyzed by densitometry (Figure 40). The KWS20-1 sugar beet-produced PAT protein (Figure 40, lanes 3-8) migrated to the same position on the gel as the *E. coli*-produced PAT protein (Figure 40, lane 2) and the apparent molecular weight was calculated to be ~22.3 kDa (Table 17). Because the experimentally determined apparent MW of the KWS20-1 sugar beet-produced PAT protein was within the preset acceptance limits for equivalence (Table 18; 22.2–22.7 kDa), the KWS20-1 sugar beet-produced and *E. coli*-produced PAT proteins were determined to have equivalent apparent molecular weights.

The purity of the KWS20-1 sugar beet-produced PAT protein was calculated based on the six lanes loaded on the gel (Figure 40, lanes 3-8). The average purity was determined to be 98% (Table 17).

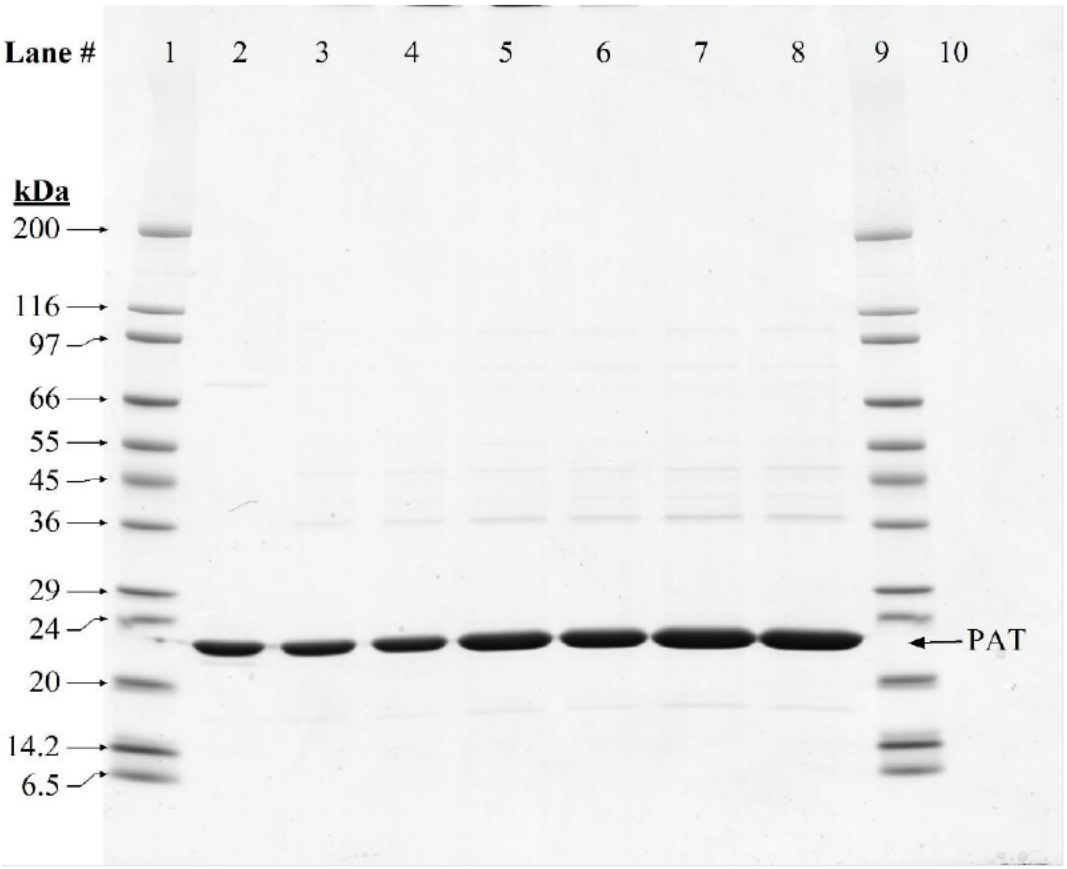

Figure 40. Molecular Weight and Purity Analysis of the KWS20-1 Sugar Beet-Produced PAT Protein

Aliquots of the KWS20-1 sugar beet-produced and the *E. coli*-produced PAT proteins were subjected to SDS-PAGE and the gel was stained with Brilliant Blue G-Colloidal stain. The MWs (kDa) are shown on the left and correspond to the standards loaded in lanes 1 and 9. Lane designations are as follows:

Lane	Sample	Amount (µg)
1	SigmaMarker™ Wide Range MW Standard	5.0
2	*E. coli*-produced PAT	1.0
3	KWS20-1 sugar beet-produced PAT	1.0
4	KWS20-1 sugar beet-produced PAT	1.0
5	KWS20-1 sugar beet-produced PAT	2.0
6	KWS20-1 sugar beet-produced PAT	2.0
7	KWS20-1 sugar beet-produced PAT	3.0
8	KWS20-1 sugar beet-produced PAT	3.0
9	SigmaMarker™ Wide Range MW Standard	5.0
10	Empty	-

Table 17. Apparent Molecular Weight and Purity Analysis of the KWS20-1 Sugar Beet-Produced PAT Protein

	Apparent MW[1] (kDa)	Purity[2] (%)
Average (n=6)	22.3	98

[1] Final MW was rounded to one decimal place.
[2] Average % purity was rounded to the nearest whole number.

Table 18. Molecular Weight Comparison Between the KWS20-1 Sugar Beet- and *E. coli*-Produced PAT Proteins

Apparent MW of KWS20-1 Sugar Beet-Produced PAT Protein (kDa)	Apparent MW of *E. coli*-Produced PAT Protein[1] (kDa)	Acceptance Limits[2] (kDa)
22.3	22.5	22.2 – 22.7

[1] See Appendix 8 for the apparent MW of the *E. coli*-produced PAT protein.
[2] Data obtained from the *E. coli*-produced PAT protein was used to generate the prediction interval (Appendix 8).

B.1(a)(ii)(ii)(v) PAT Protein Glycosylation Analysis

Some eukaryotic proteins can be post-translationally modified by the addition of carbohydrate moieties (Rademacher *et al.*, 1988). To test whether the PAT protein was glycosylated when expressed in the leaf tissue of KWS20-1 sugar beet, the KWS20-1 sugar beet-produced PAT protein was subjected to SDS-PAGE, transferred to a membrane and the membrane was analyzed using an ECL™ glycoprotein detection method. Transferrin, a glycosylated protein, was used as a positive control in the assay. To assess equivalence of the KWS20-1 sugar beet-produced and *E. coli*-produced PAT proteins, the *E. coli*-produced PAT protein, previously shown to be free of glycosylation in another equivalence assessment, was also analyzed.

A clear glycosylation signal was observed at the expected molecular weight (~ 80 kDa) in the lanes containing the positive control, transferrin, and the band intensity increased with increasing concentration (Figure 41, Panel A, lanes 3-4), demonstrating that the assay performed as expected. In contrast, no glycosylation signal was observed in the lanes containing the KWS20-1 sugar beet-produced PAT protein (Figure 41, Panel A, lanes 8 and 9) or the *E. coli*-produced PAT protein (Figure 41, Panel A, lanes 6 and 7).

To confirm that KWS20-1 sugar beet-produced and *E. coli*-produced PAT proteins were appropriately loaded for glycosylation analysis, a second membrane with identical loadings and transfer time was stained with Coomassie Blue R250 for protein detection (Figure 41, Panel B). Both the KWS20-1 sugar beet-produced (Figure 41, Panel B, lanes 8 and 9) and *E. coli*-produced (Figure 41, Panel B, lanes 6 and 7) PAT proteins were detected. These data indicate that the glycosylation status of KWS20-1 sugar beet-produced PAT protein is equivalent to that of the *E. coli*-produced PAT protein and that neither is glycosylated.

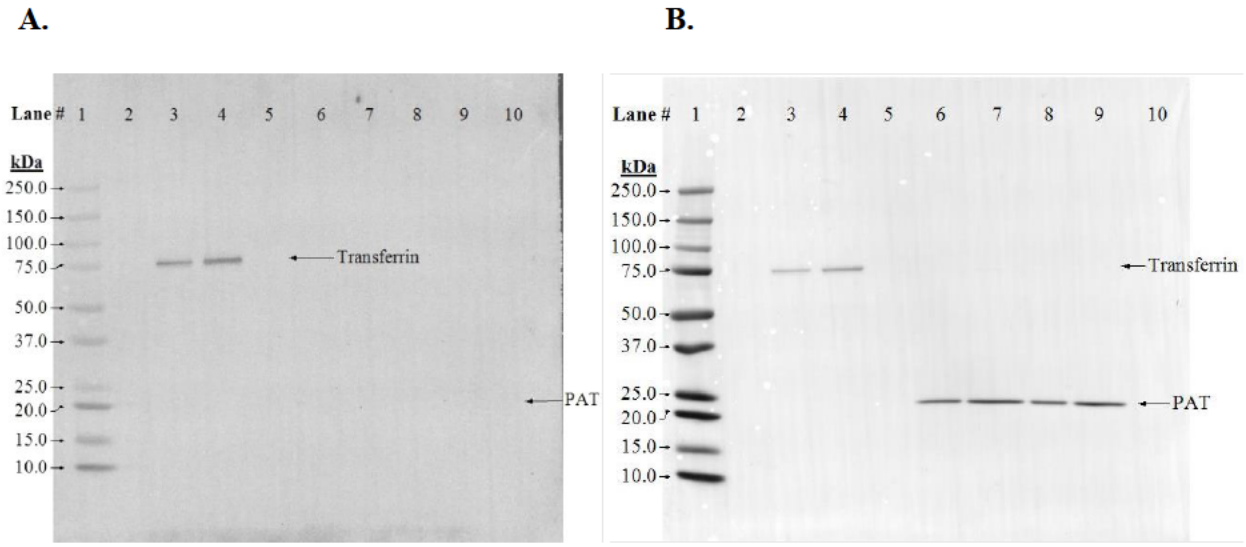

Figure 41. Glycosylation Analysis of the KWS20-1 Sugar Beet-Produced PAT Protein

Aliquots of the transferrin (positive control), *E. coli*-produced and KWS20-1 sugar beet-produced PAT proteins were subjected to SDS-PAGE and electrotransferred to a PVDF membrane. The MWs (kDa) correspond to the Precision Plus Protein™ Dual Color Standards. The arrows show the expected migration of the KWS20-1 sugar beet-produced and *E. coli*-produced PAT proteins and transferrin. (A) Where present, the labeled carbohydrate moieties were detected by addition of streptavidin conjugated to HRP followed by a luminol-based detection using ECL reagents and imaging with a ChemiDoc imager. The 2-minute exposure image is shown as an overlaid image with the MW marker on the membrane. (B) An equivalent blot was stained with Coomassie Blue R-250 to confirm the presence of proteins. Lane designations are as follows:

Lane	Sample	Amount (ng)
1	Precision Plus Protein™ Dual Color Standards	-
2	Empty	-
3	Transferrin (positive control)	100
4	Transferrin (positive control)	200
5	Empty	-
6	*E. coli*-produced PAT	100
7	*E. coli*-produced PAT	200
8	KWS20-1 sugar beet-produced PAT	100
9	KWS20-1 sugar beet-produced PAT	200
10	Empty	-

B.1(a)(ii)(ii)(vi) PAT Functional Activity

The functional activity of the KWS20-1 sugar beet-produced and *E. coli*-produced PAT proteins was determined using a Coenzyme A (CoA) release assay (Wehrmann *et al.*, 1996). PAT catalyzes the reaction of phosphinothricin (glufosinate-ammonium; PPT) with acetyl-CoA to form acetyl-PPT and free CoA. CoA released during the reaction can be monitored using the reduction of 5,5′-dithio-bis-(2-nitrobenzoic acid) (DTNB) by CoA to form the colorimetric reagent 5-thio-nitrobenzoate (TNB). In this assay, protein-specific activity is expressed as μmoles TNB released per minute at 30 °C per milligram of PAT protein. The KWS20-1 sugar beet-produced and *E. coli*-produced PAT proteins were considered to have equivalent functional activity if the specific activity of both were within acceptance limits (the prediction interval calculated from a data set based on assays conducted for the *E. coli*-produced PAT protein, Appendix **8**).

The experimentally determined specific activity for the KWS20-1 sugar beet-produced and *E. coli*-produced PAT proteins are presented in Table 19. The specific activities of KWS20-1 sugar beet-produced and *E. coli*-produced PAT proteins were 43 and 47 μmoles TNB × min^{-1} × mg^{-1}, respectively. Because the specific activities of KWS20-1 sugar beet-produced and *E. coli*-produced PAT proteins fall within the preset acceptance limits (Table 19), the KWS20-1 sugar beet-produced PAT protein was considered to have equivalent functional activity to that of the *E. coli*-produced PAT protein.

Table 19. Functional Activity of the KWS20-1 Sugar Beet-Produced and *E. coli*-Produced PAT Proteins

KWS20-1 Sugar Beet-Produced PAT[1] (μmoles × min^{-1} × mg^{-1})	*E. coli*-Produced PAT[1] (μmoles × min^{-1} × mg^{-1})	Acceptance Limits[2] (μmoles × min^{-1} × mg^{-1})
43	47	21.7 – 68.7

[1] Value refers to calculated mean based on five data points (n = 5) within each assay.
[2] Data obtained for the *E. coli*-produced PAT protein was used to generate a prediction interval for setting the acceptance limits (Appendix 8).

B.1(a)(ii)(ii)(vii) KWS20-1 Sugar Beet PAT Protein Identity and Equivalence Conclusion

The KWS20-1 sugar beet-produced PAT protein was purified from KWS20-1 sugar beet leaf, characterized and then a comparison of the physicochemical and functional properties between the KWS20-1 sugar beet-produced and the *E. coli*-produced PAT proteins was conducted following a panel of analytical tests: 1) N-terminal sequence analysis established the same amino acid identity for the KWS20-1 sugar beet-produced and *E. coli*-produced PAT proteins; 2) Nano LC-MS/MS analysis yielded peptide masses consistent with the expected peptide masses from the theoretical trypsin digest of the *pat* gene product present in both KWS20-1 sugar beet and produced from *E. coli*; 3) the KWS20-1 sugar beet-produced and the *E. coli*-produced PAT proteins were both detected on a western blot probed with antibodies specific for PAT protein and the immunoreactive properties of both proteins were shown to be equivalent; 4) the electrophoretic mobility and apparent molecular weight of the KWS20-1 sugar beet-produced and *E. coli*-produced PAT proteins were shown to be equivalent; 5) the glycosylation status of KWS20-1 sugar beet-produced and *E. coli*-produced PAT proteins was determined to be equivalent; and 6) the functional activity

of the KWS20-1 sugar beet-produced and *E. coli*-produced PAT proteins were demonstrated to be equivalent. These results demonstrate that the KWS20-1 sugar beet-produced and the *E. coli*-produced PAT proteins are equivalent.

This demonstration of protein equivalence confirms that the *E. coli*-produced PAT protein is appropriate for use in the evaluation of the safety of the KWS20-1 sugar beet-produced PAT protein. Therefore, conclusions derived from digestibility, heat susceptibility and oral acute toxiciology studies conducted with *E. coli*-produced PAT protein are applicable to KWS20-1 sugar beet-produced PAT protein.

B.1(a)(ii)(iii) Characterisation of the KWS20-1 Sugar Beet CP4 EPSPS Protein

The safety assessment of crops derived through biotechnology includes characterization of the physicochemical and functional properties and confirmation of the safety of the introduced protein(s). For the safety data generated using the *E. coli*-produced CP4 EPSPS protein to be applied to the KWS20-1 sugar beet-produced CP4 EPSPS protein (plant-produced CP4 EPSPS), the equivalence of the plant- and *E. coli*-produced proteins must first be demonstrated. To assess the equivalence between the KWS20-1 sugar beet-produced CP4 EPSPS and *E. coli*-produced CP4 EPSPS proteins, a small quantity of the KWS20-1 sugar beet-produced CP4 EPSPS protein was purified from KWS20-1 sugar beet leaf. The KWS20-1 sugar beet-produced CP4 EPSPS protein was characterized and the equivalence of the physicochemical characteristics and functional activity between the KWS20-1 sugar beet-produced and *E. coli*-produced CP4 EPSPS proteins was assessed using a panel of six analytical tests; as shown in Table 20. Taken together, these data provide a detailed characterization of the KWS20-1 sugar beet-produced CP4 EPSPS protein and establish the equivalence of the KWS20-1 sugar beet-produced CP4 EPSPS and *E. coli*-produced CP4 EPSPS proteins. With establishment of equivalence, conclusions derived from digestibility, heat susceptibility and oral acute toxiciology studies conducted with *E. coli*-produced CP4 EPSPS protein are applicable to KWS20-1 sugar beet-produced CP4 EPSPS protein.

For details, please refer to Appendix 9.

Table 20. Summary of KWS20-1 Sugar Beet-Produced CP4 EPSPS Protein Identity and Equivalence

Analytical Test	Analytical Test Outcome
N-terminal sequence	The expected N-terminal sequence for KWS20-1 sugar beet-produced CP4 EPSPS was observed by Nano LC-MS/MS[1]
Nano LC-MS/MS[1]	Nano LC-MS/MS[1] analysis of trypsin digested peptides from KWS20-1 sugar beet-produced CP4 EPSPS protein yielded peptide masses consistent with expected peptide masses from the theoretical trypsin digest of the amino acid sequence
Western blot analysis	KWS20-1 sugar beet-produced CP4 EPSPS protein identity was confirmed using a western blot probed with antibodies specific for CP4 EPSPS protein. Immunoreactive properties of the KWS20-1 sugar beet-produced CP4 EPSPS and the *E. coli*-produced CP4 EPSPS proteins were shown to be equivalent
Apparent molecular weight (MW)	Electrophoretic mobility and apparent molecular weight of the KWS20-1 sugar beet-produced CP4 EPSPS and the *E. coli*-produced CP4 EPSPS proteins were shown to be equivalent
Glycosylation analysis	Glycosylation status of KWS20-1 sugar beet-produced CP4 EPSPS and *E. coli*-produced CP4 EPSPS proteins were shown to be equivalent
Functional activity	The expected N-terminal sequence for KWS20-1 sugar beet-produced CP4 EPSPS was observed by Nano LC-MS/MS[1]

[1] Nano LC-MS/MS = Nanoscale liquid chromatography-tandem mass spectrometry

B.1(a)(ii)(iii)(i) Results of the N-terminal Sequencing Analysis

N-terminal sequencing was performed on the CP4 EPSPS protein. The expected sequence for the CP4 EPSPS protein deduced from the *cp4 epsps* gene present in KWS20-1 sugar beet was observed. A second N-terminal sequence was also observed, in which N-terminal methionine was cleaved *in vivo* from KWS20-1 sugar beet-produced CP4 EPSPS. The cleavage of the N-terminal methionine from proteins *in vivo* by methionine aminopeptidase and other aminopeptidases is common in many organisms (Wang *et al.*, 2016; Bradshaw *et al.*, 1998). The N-terminal sequencing results for KWS20-1 sugar beet-produced CP4 EPSPS protein were consistent with the sequencing results for the *E. coli*-produced CP4 EPSPS protein observed by Edman sequence analysis, corresponding to the deduced CP4 EPSPS protein beginning at amino acid position 1 (Figure 42) Hence, the sequence information confirms the identity of the CP4 EPSPS protein isolated from the leaf tissue of KWS20-1 sugar beet.

Amino Acids Residue # from the N-terminus	–	1	2	3	4	5	6	7	8	9	10	11	12	13	14	15
E. coli-produced CP4 EPSPS sequence	–	M	L	H	G	A	S	S	R	P	A	T	A	(R)	K	S
Expected CP4 EPSPS Sequence	–	M	L	H	G	A	S	S	R	P	A	T	A	R	K	S
KWS20-1 Sugar Beet Experimental Sequence	–	M	L	H	G	A	S	S	R	P	A	T	A	R	K	S

Figure 42. N-Terminal Sequence of the KWS20-1 Sugar Beet-Produced CP4 EPSPS Protein

The experimental sequence obtained from the KWS20-1 sugar beet-produced CP4 EPSPS was compared to the CP4 EPSPS sequence deduced from the *cp4 epsps* gene present in KWS20-1 sugar beet. The sequence of the N-terminus of the KWS20-1 sugar beet-produced CP4 EPSPS protein was obtained by Nano LC-MS/MS peptide analysis (trypsin digest). The sequence of the N-terminus of the *E. coli*-produced CP4 EPSPS protein was derived from the reference substance COA (lot 7779). The single letter International Union of Pure and Applied Chemistry-International Union of Biochemistry (IUPAC-IUB) amino acid code is: M, methionine; L, leucine; H, histidine; G, glycine; A, alanine; S, serine; R, arginine; P, proline; T, threonine; K, lysine; ( ), tenuous designation.

B.1(a)(ii)(iii)(ii) Results of the CP4 EPSPS Protein Mass Fingerprint Analysis

The identity of the CP4 EPSPS protein was confirmed by Nano LC-MS/MS analysis of peptide fragments produced by a trypsin digestion of the KWS20-1 sugar beet-produced CP4 EPSPS protein.

There were 57 unique peptides identified that corresponded to the expected masses of the trypsin-digested sequence of KWS20-1 sugar beet-produced CP4 EPSPS (Table 21). The identified masses were used to assemble a peptide map of the CP4 EPSPS protein (Figure 43). The experimentally determined coverage of KWS20-1 sugar beet-produced CP4 EPSPS protein was 99% (453 out of 455 amino acids). This analysis further confirms the identity of KWS20-1 sugar beet-produced CP4 EPSPS protein.

There were 28 unique peptides identified that corresponded to the expected masses of trypsin-digested *E. coli*-produced CP4 EPSPS protein (Table 22) by matrix-assisted laser desorption/ionization-time of flight (MALDI-TOF) MS analysis during the protein characterization. The identified masses were used to assemble a peptide map of the CP4 EPSPS protein (Figure 43). The experimentally determined coverage of the *E. coli*-produced CP4 EPSPS protein was 64% (291 out of 455 amino acids). This analysis further confirms the identity of *E. coli*-produced CP4 EPSPS protein and equivalence to the KWS20-1 sugar beet-produced CP4 EPSPS protein.

Table 21. Summary of the Tryptic Masses Identified for KWS20-1 Sugar Beet-Produced CP4 EPSPS Protein Using Nano LC-MS/MS[1]

Experimental Mass[2]	Calculated Mass[3]	Difference[4]	Fragment[5]	Sequence[6]
1369.6881	1369.6884	-0.0003	1 - 13	MLHG...ATAR
1222.6496	1222.6530	-0.0034	2 - 13	LHGA...ATAR
990.5470	990.5458	0.0012	14 - 23	KSSG...GTVR
862.4504	862.4509	-0.0005	15 - 23	SSGL...GTVR
528.2908	528.2908	0	24 - 28	IPGDK
1108.5980	1108.5989	-0.0009	24 - 33	IPGD...ISHR
598.3187	598.3187	0	29 - 33	SISHR
1374.6178	1374.6238	-0.006	34 - 46	SFMF...GETR
1557.8257	1557.8250	0.0007	47 - 61	ITGL...NTGK
2406.1862	2406.1883	-0.0021	47 - 69	ITGL...MGAR
850.3790	850.3789	0.0001	62 - 69	AMQAMGAR
3640.7978	3640.7944	0.0034	70 - 104	IRKE...TGCR
3371.6101	3371.6092	0.0009	72 - 104	KEGD...TGCR
3243.5213	3243.5143	0.007	73 - 104	EGDT...TGCR
2449.2105	2449.2087	0.0018	105 - 127	LTMG...SLTK
3078.5219	3078.5155	0.0064	105 - 132	LTMG...PMGR
631.3224	631.3224	0	128 - 132	RPMGR
710.4436	710.4439	-0.0003	133 - 138	VLNPLR
1497.8340	1497.8337	0.0003	133 - 145	VLNP...VQVK
789.4054	789.4055	-0.0001	139 - 145	EMGVQVK
2144.0852	2144.0896	-0.0044	139 - 157	EMGV...VTLR
1356.6999	1356.6997	0.0002	146 - 157	SEDG...VTLR
697.4489	697.4487	0.0002	152 - 157	LPVTLR
1229.6755	1229.6768	-0.0013	158 - 168	GPKT...ITYR
947.5067	947.5076	-0.0009	161 - 168	TPTPITYR
1874.9859	1874.9924	-0.0065	161 - 177	TPTP...AQVK
945.4960	945.4953	0.0007	169 - 177	VPMA...AQVK
2382.3209	2382.3192	0.0017	178 - 200	SAVL...IMTR
2992.5921	2992.5903	0.0018	178 - 205	SAVL...HTEK
628.2815	628.2816	-0.0001	201 - 205	DHTEK
2619.2253	2619.2235	0.0018	201 - 224	DHTE...DGVR
2008.9541	2008.9524	0.0017	206 - 224	MLQG...DGVR
843.4915	843.4926	-0.0011	225 - 231	TIRLEGR
473.2598	473.2598	0	228 - 231	LEGR
4388.3620	4388.3666	-0.0046	232 - 274	GKLT...NPTR
4203.2667	4203.2501	0.0166	234 - 274	LTGQ...NPTR
2198.1627	2198.1617	0.001	275 - 294	TGLI...INPR
1114.5615	1114.5618	-0.0003	295 - 305	LAGG...ADLR

1369.7269	1369.7314	-0.0045	295 - 307	LAGG...LRVR
534.3011	534.3013	-0.0002	308 - 312	SSTLK
1429.7420	1429.7413	0.0007	308 - 320	SSTL...PEDR
871.4397	871.4400	-0.0003	313 - 320	GVTVPEDR
4118.0446	4118.0340	0.0106	313 - 351	GVTV...EELR
3264.6055	3264.6046	0.0009	321 - 351	APSM...EELR
3507.7505	3507.7629	-0.0124	321 - 353	APSM...LRVK
732.3767	732.3766	0.0001	352 - 357	VKESDR
1585.8799	1585.8787	0.0012	352 - 366	VKES...NGLK
1358.7168	1358.7154	0.0014	354 - 366	ESDR...NGLK
3103.4943	3103.5092	-0.0149	354 - 382	ESDR...LVVR
871.5133	871.5127	0.0006	358 - 366	LSAV...NGLK
2616.3117	2616.3065	0.0052	358 - 382	LSAV...LVVR
1762.8064	1762.8044	0.002	367 - 382	LNGV...LVVR
628.3296	628.3293	0.0003	383 - 388	GRPDGK
2256.1496	2256.1472	0.0024	383 - 405	GRPD...LDHR
1645.8285	1645.8285	0	389 - 405	GLGN...LDHR
4399.0676	4399.0694	-0.0018	406 - 446	IAMS...LGAK
804.4225	804.4229	-0.0004	447 - 453	IELSDTK

[1] All imported values were rounded to four decimal places.
[2] Only experimental masses that matched calculated masses with the smallest differences are listed in the table.
[3] The calculated mass is the relative molecular mass calculated from the matched peptide sequence.
[4] The calculated difference = experimental mass – calculated mass
[5] Position refers to amino acid residues within the predicted KWS20-1 sugar beet-produced CP4 EPSPS protein sequence as depicted in Figure 43.
[6] For peptide matches greater than nine amino acids in length the first four residues and last four residues are shown separated by dots (…).

Table 22. Summary of the Tryptic Masses Identified for the *E. coli*-Produced CP4 EPSPS Protein Using MALDI-TOF MS[1]

Experimental Mass[2]	Calculated Mass[3]	Difference[4]	Fragment[5]	Sequence[6]
991.61	991.55	0.06	14 - 23	KSSG…GTVR
863.46	863.46	0.00	15 - 23	SSGL…GTVR
2450.32	2450.23	0.09	24 - 46	IPGD…GETR
599.32	599.33	-0.01	29 - 33	SISHR
1359.65	1359.64	0.01	34 - 46	SFMF…GETR
1558.87	1558.83	0.04	47 - 61	ITGL…NTGK
835.39	835.39	0.00	62 - 69	AMQAMGAR
3244.58	3244.52	0.06	73 - 104	EGDT…TGCR
2450.32	2450.22	0.10	105 - 127	LTMG…SLTK
616.32	616.34	-0.02	128 - 132	RPMGR
711.45	711.45	0.00	133 - 138	VLNPLR
1357.70	1357.71	-0.01	146 - 157	SEDG…VTLR
698.45	698.46	-0.01	152 - 157	LPVTLR
948.51	948.52	-0.01	161 - 168	TPTPITYR
1859.96	1860.01	-0.05	161 - 177	TPTP…AQVK
930.55	930.51	0.04	169 - 177	VPMA…AQVK
2367.28	2367.33	-0.05	178 - 200	SAVL...IMTR
629.34	629.29	0.05	201 - 205	DHTEK
1993.93	1993.97	-0.04	206 - 224	MLQG…DGVR
2183.12	2183.17	-0.05	275 - 294	TGLI…INPR
1115.56	1115.57	-0.01	295 - 305	LAGG...ADLR
872.44	872.45	-0.01	313 - 320	GVTVPEDR
733.47	733.38	0.09	352 - 357	VKESDR
1359.65	1359.72	-0.07	354 - 366	ESDR…NGLK
872.44	872.52	-0.08	358 - 366	LSAV…NGLK
1763.78	1763.81	-0.03	367 - 382	LNGV...LVVR
629.34	629.34	0.00	383 - 388	GRPDGK
1646.81	1646.84	-0.03	389 - 405	GLGN...LDHR

[1] All imported values were rounded to two decimal places.
[2] Only experimental masses that matched calculated masses with the highest scores are listed in the table.
[3] The calculated mass is the exact molecular mass calculated from the matched peptide sequence.
[4] The calculated difference = experimental mass – calculated mass
[5] Position refers to amino acid residues within the predicted *E. coli*-produced CP4 EPSPS sequence as depicted in Figure 43.
[6] For peptide matches greater than nine amino acids in length, the first four residues and last four residues are shown separated by three dots (...).

(A)

```
1   MLHGASSRPA TARKSSGLSG TVRIPGDKSI SHRSFMFGGL ASGETRITGL

51  LEGEDVINTG KAMQAMGARI RKEGDTWIID GVGNGGLLAP EAPLDFGNAA

101 TGCRLTMGLV GVYDFDSTFI GDASLTKRPM GRVLNPLREM GVQVKSEDGD

151 RLPVTLRGPK TPTPITYRVP MASAQVKSAV LLAGLNTPGI TTVIEPIMTR

201 DHTEKMLQGF GANLTVETDA DGVRTIRLEG RGKLTGQVID VPGDPSSTAF

251 PLVAALLVPG SDVTILNVLM NPTRTGLILT LQEMGADIEV INPRLAGGED

301 VADLRVRSST LKGVTVPEDR APSMIDEYPI LAVAAAFAEG ATVMNGLEEL

351 RVKESDRLSA VANGLKLNGV DCDEGETSLV VRGRPDGKGL GNASGAAVAT

401 HLDHRIAMSF LVMGLVSENP VTVDDATMIA TSFPEFMDLM AGLGAKIELS

451 DTKAA
```

(B)

```
001 MLHGASSRPA TARKSSGLSG TVRIPGDKSI SHRSFMFGGL ASGETRITGL

051 LEGEDVINTG KAMQAMGARI RKEGDTWIID GVGNGGLLAP EAPLDFGNAA

101 TGCRLTMGLV GVYDFDSTFI GDASLTKRPM GRVLNPLREM GVQVKSEDGD

151 RLPVTLRGPK TPTPITYRVP MASAQVKSAV LLAGLNTPGI TTVIEPIMTR

201 DHTEKMLQGF GANLTVETDA DGVRTIRLEG RGKLTGQVID VPGDPSSTAF

251 PLVAALLVPG SDVTILNVLM NPTRTGLILT LQEMGADIEV INPRLAGGED

301 VADLRVRSST LKGVTVPEDR APSMIDEYPI LAVAAAFAEG ATVMNGLEEL

351 RVKESDRLSA VANGLKLNGV DCDEGETSLV VRGRPDGKGL GNASGAAVAT

401 HLDHRIAMSF LVMGLVSENP VTVDDATMIA TSFPEFMDLM AGLGAKIELS

451 DTKAA
```

Figure 43. Peptide Map of the KWS20-1 Sugar Beet-Produced and *E. coli*-Produced CP4 EPSPS Proteins

(A). The amino acid sequence of the KWS20-1 sugar beet-produced CP4 EPSPS protein was deduced from the *cp4 epsps* gene present in KWS20-1 sugar beet. Boxed regions correspond to peptides that were identified from the KWS20-1 sugar beet-produced CP4 EPSPS protein sample using Nano LC-MS/MS. In total, 99% coverage (453 out of 455 amino acids) of the expected protein sequence was covered by the identified peptides.

(B). The amino acid sequence of the *E. coli*-produced CP4 EPSPS protein was deduced from the *cp4 epsps* gene that is contained on the *E. coli* expression plasmid. Boxed regions correspond to peptides that were identified from the *E. coli*-produced CP4 EPSPS protein sample using MALDI-TOF MS in a previous characterization. In total, 64% coverage (291 out of 455 amino acids) of the expected protein sequence was covered by the identified peptides.

B.1(a)(ii)(iii)(iii) Results of Western Blot Analysis of the CP4 EPSPS Protein Isolated from Leaf of KWS20-1 Sugar Beet and Immunoreactivity Comparison to *E. coli*-Produced CP4 EPSPS Protein

Western blot analysis was conducted using an anti-CP4 EPSPS antibody as additional means to confirm the identity of the CP4 EPSPS protein isolated from the leaf of KWS20-1 sugar beet and to assess the equivalence of the immunoreactivity of the KWS20-1 sugar beet-produced and *E. coli*-produced CP4 EPSPS proteins.

The results showed that immunoreactive bands migrating with the same electrophoretic mobility were present in all lanes loaded with the KWS20-1 sugar beet-produced (Figure 44, lanes 9-14) or *E. coli*-produced (Figure 44, lanes 3-8) CP4 EPSPS proteins. For each amount loaded, comparable signal intensity was observed between the KWS20-1 sugar beet-produced and *E. coli*-produced CP4 EPSPS protein bands. As expected, the signal intensity increased with increasing load amounts of the KWS20-1 sugar beet-produced and *E. coli*-produced CP4 EPSPS proteins, thus, supporting identification of KWS20-1 sugar beet-produced CP4 EPSPS protein.

To compare the immunoreactivity of the KWS20-1 sugar beet-produced and the *E. coli*-produced CP4 EPSPS proteins, densitometric analysis was conducted on bands that migrated to the expected apparent MW for the CP4 EPSPS protein (~44 kDa). The signal intensity (reported in OD) of the band of interest in lanes loaded with KWS20-1 sugar beet-produced and the *E. coli*-produced CP4 EPSPS protein was measured (Table 23). Because the mean signal intensity of the KWS20-1 sugar beet-produced CP4 EPSPS protein band was within ±35% of the mean signal intensity of the *E. coli*-produced CP4 EPSPS protein, the KWS20-1 sugar beet-produced and *E. coli*-produced CP4 EPSPS proteins were determined to have equivalent immunoreactivity.

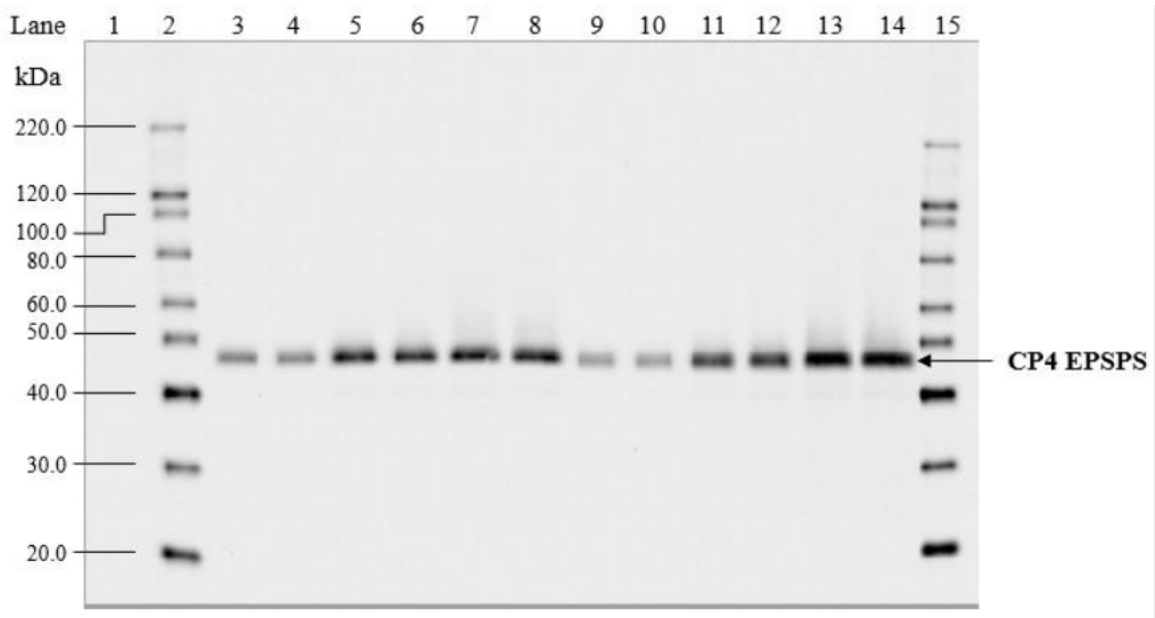

Figure 44. Western Blot Analysis of the KWS20-1 Sugar Beet-Produced and *E. coli*-Produced CP4 EPSPS Proteins

Aliquots of the KWS20-1 sugar beet-produced and *E. coli*-produced CP4 EPSPS proteins were subjected to SDS-PAGE and electrotransferred to a nitrocellulose membrane. Proteins were detected using goat anti-CP4 EPSPS polyclonal antibodies as the primary antibody. Immunoreactive bands were visualized using HRP-conjugated secondary antibody and an ECL system. The 10 second exposure is shown. The approximate MW (kDa) of the standards are shown on the left. Lane designations are as follows:

Lane	Sample	Amount (ng)
1	Precision Plus Protein™ Dual Color Standards	-
2	MagicMark™ XP Western Protein Standard	-
3	*E. coli*-produced CP4 EPSPS	1
4	*E. coli*-produced CP4 EPSPS	1
5	*E. coli*-produced CP4 EPSPS	3
6	*E. coli*-produced CP4 EPSPS	3
7	*E. coli*-produced CP4 EPSPS	5
8	*E. coli*-produced CP4 EPSPS	5
9	KWS20-1 sugar beet-produced CP4 EPSPS	1
10	KWS20-1 sugar beet-produced CP4 EPSPS	1
11	KWS20-1 sugar beet-produced CP4 EPSPS	3
12	KWS20-1 sugar beet-produced CP4 EPSPS	3
13	KWS20-1 sugar beet-produced CP4 EPSPS	5
14	KWS20-1 sugar beet-produced CP4 EPSPS	5
15	MagicMark™ XP Western Protein Standard	-

Table 23. Comparison of Immunoreactive Signals between KWS20-1 Sugar Beet-Produced and *E. coli*-Produced CP4 EPSPS Proteins

Mean Signal Intensity from KWS20-1 Sugar Beet-Produced CP4 EPSPS[1] (OD)	Mean Signal Intensity from *E. coli*-Produced CP4 EPSPS[1] (OD)	Acceptance Limits[2] (OD)
13107538.81	12163620.14	7906353.09 – 16420887.18

[1] Each value represents the mean of six values of the immunoreactive band (n = 6).
[2] The acceptance limits are for the KWS20-1 sugar beet-produced CP4 EPSPS protein and are based on the interval between -35% (12163620.14 × 0.65 = 7906353.09) and +35% (12163620.14 × 1.35 =16420887.18) of the mean of the *E. coli*-produced CP4 EPSPS signal intensity across all loads.

B.1(a)(ii)(iii)(iv) Results of the CP4 EPSPS Protein Molecular Weights and Purity Analysis

For molecular weight analysis, the KWS20-1 sugar beet-produced CP4 EPSPS protein was separated using SDS-PAGE. Following electrophoresis, the gel was stained with Brilliant Blue G-Colloidal stain and analyzed by densitometry (Figure 45). The KWS20-1 sugar beet-produced CP4 EPSPS protein (Figure 45, lanes 3-8) migrated to the same position on the gel as the *E. coli*-produced CP4 EPSPS protein (Figure 45, lane 2) and the apparent molecular weight was calculated to be ~43.5 kDa (Table 24). Because the experimentally determined apparent MW of the KWS20-1 sugar beet-produced CP4 EPSPS protein was within the preset acceptance limits for equivalence (Table 25; 42.6 – 45.1 kDa), the KWS20-1 sugar beet-produced and *E. coli*-produced CP4 EPSPS proteins were determined to have equivalent apparent molecular weights.

The purity of the KWS20-1 sugar beet-produced CP4 EPSP protein was calculated based on the six lanes loaded on the gel (Figure 45, lanes 3-8). The average purity was determined to be 99.6% (Table 24).

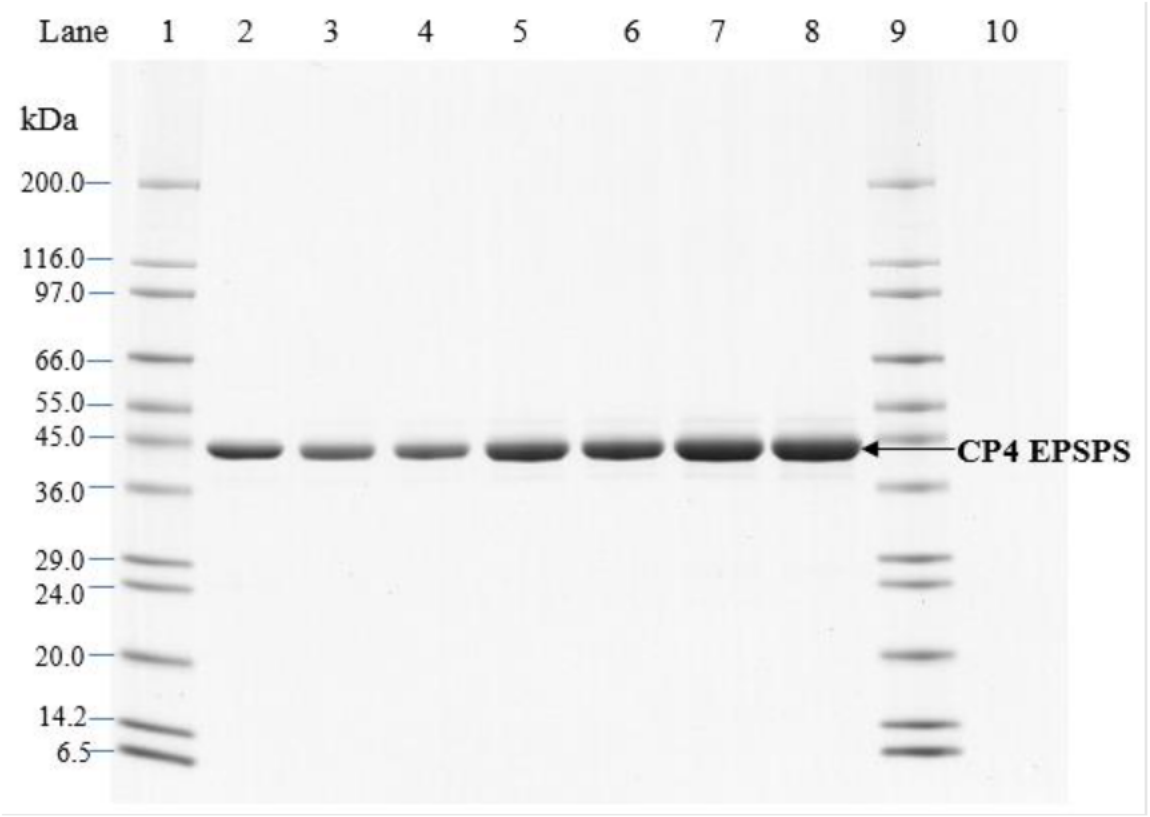

Figure 45. Molecular Weight and Purity Analysis of the KWS20-1 Sugar Beet-Produced CP4 EPSPS Protein

Aliquots of the KWS20-1 sugar beet-produced and the *E. coli*-produced CP4 EPSPS proteins were subjected to SDS-PAGE and the gel was stained with Brilliant Blue G-Colloidal stain. The MWs (kDa) are shown on the left and correspond to the standards loaded in lanes 1 and 9. Lane designations are as follows:

Lane	Sample	Amount (µg)
1	SigmaMarker™ Wide Range MW Standard	-
2	*E. coli*-produced CP4 EPSPS	1.0
3	KWS20-1 sugar beet-produced CP4 EPSPS	1.0
4	KWS20-1 sugar beet-produced CP4 EPSPS	1.0
5	KWS20-1 sugar beet-produced CP4 EPSPS	2.0
6	KWS20-1 sugar beet-produced CP4 EPSPS	2.0
7	KWS20-1 sugar beet-produced CP4 EPSPS	3.0
8	KWS20-1 sugar beet-produced CP4 EPSPS	3.0
9	SigmaMarker™ Wide Range MW Standard	-
10	Blank	-

Table 24. Apparent Molecular Weight and Purity Analysis of the KWS20-1 Sugar Beet-Produced CP4 EPSPS Protein

	Apparent MW[1] (kDa)	Purity[2] (%)
Average (n=6)	43.5	99.6

[1] Final MW was rounded to one decimal place.
[2] Average % purity was rounded to one decimal place.

Table 25. Molecular Weight Comparison Between the KWS20-1 Sugar Beet-Produced and *E. coli*-Produced CP4 EPSPS Proteins

Apparent MW of KWS20-1 Sugar Beet-Produced CP4 EPSPS Protein (kDa)	Apparent MW of *E. coli*-Produced CP4 EPSPS Protein[1] (kDa)	Acceptance Limits[2] (kDa)
43.5	43.8	42.6 – 45.1

[1] See Appendix 9 for the apparent MW of the *E. coli*-produced CP4 EPSPS protein.
[2] Data obtained for the *E. coli*-produced CP4 EPSPS protein and several plant-produced CP4 EPSPS proteins were used to generate the prediction interval (Appendix 9).

B.1(a)(ii)(iii)(vi) CP4 EPSPS Glycosylation Equivalence

Some eukaryotic proteins can be post-translationally modified by the addition of carbohydrate moieties (Rademacher *et al.*, 1988). To test whether the CP4 EPSPS protein was glycosylated when expressed in the leaf tissue of KWS20-1 sugar beet, the KWS20-1 sugar beet-produced CP4 EPSPS protein was subjected to SDS-PAGE, transferred to a membrane and the membrane was analyzed using an ECL™ glycoprotein detection method. Transferrin, a glycosylated protein, was used as a positive control in the assay. To assess equivalence of the KWS20-1 sugar beet-produced and *E. coli*-produced CP4 EPSPS proteins, the *E. coli*-produced CP4 EPSPS protein, previously shown to be free of glycosylation (Harrison *et al.*, 1996), was also analyzed.

A clear glycosylation signal was observed at the expected molecular weight (~ 80 kDa) in the lanes containing the positive control, transferrin, and the band intensity increased with increasing concentration (Figure 46, Panel A, lanes 3-4), demonstrating that the assay performed as expected. In contrast, no glycosylation signal was observed in the lanes containing the KWS20-1 sugar beet-produced CP4 EPSPS protein (Figure 46, Panel A, lanes 8 and 9) or the *E. coli*-produced CP4 EPSPS protein (Figure 46, Panel A, lanes 6 and 7).

To confirm that KWS20-1 sugar beet-produced and *E. coli*-produced CP4 EPSPS proteins were appropriately loaded for glycosylation analysis, a second membrane with identical loadings and transfer time was stained with Coomassie Blue R250 for protein detection (Figure 46, Panel B). Both the KWS20-1 sugar beet-produced (Figure 46, Panel B, lanes 8 and 9) and *E. coli*-produced (Figure 46, Panel B, lanes 6 and 7) CP4 EPSPS proteins were detected. These data indicate that the glycosylation status of KWS20-1 sugar beet-produced CP4 EPSPS protein is equivalent to that of the *E. coli*-produced CP4 EPSPS protein and that neither is glycosylated.

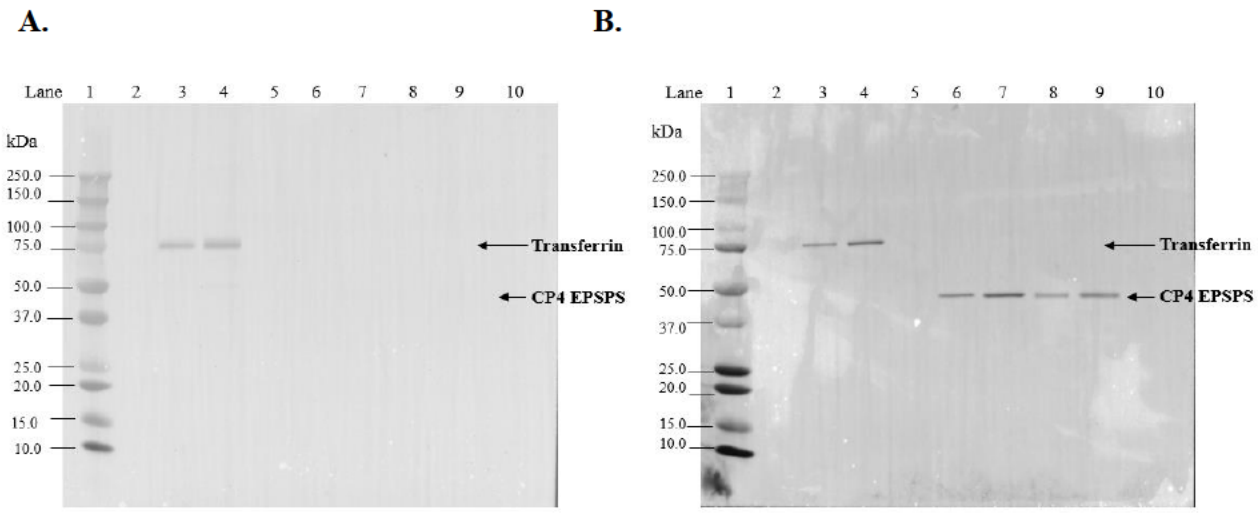

Figure 46. Glycosylation Analysis of the KWS20-1 Sugar Beet-Produced CP4 EPSPS Protein

Aliquots of the transferrin (positive control), *E. coli*-produced and KWS20-1 sugar beet-produced CP4 EPSPS proteins were subjected to SDS-PAGE and electrotransferred to a PVDF membrane. The MWs (kDa) correspond to the Precision Plus Protein™ Dual Color Standards. The arrows show the expected migration of the KWS20-1 sugar beet-produced and *E. coli*-produced CP4 EPSPS proteins and transferrin. (A) Where present, the labeled carbohydrate moieties were detected by addition of streptavidin conjugated to HRP followed by a luminol-based detection using ECL reagents and imaging with a ChemiDoc imager. The 2-minute exposure image is shown as an overlaid image with the MW marker on the membrane. (B) An equivalent blot was stained with Coomassie Blue R-250 to confirm the presence of proteins. Lane designations are as follows:

Lane	Sample	Amount (ng)
1	Precision Plus Protein™ Dual Color Standards	-
2	Blank	-
3	Transferrin (positive control)	100
4	Transferrin (positive control)	200
5	Blank	-
6	*E. coli*-produced CP4 EPSPS	100
7	*E. coli*-produced CP4 EPSPS	200
8	KWS20-1 sugar beet-produced CP4 EPSPS	100
9	KWS20-1 sugar beet-produced CP4 EPSPS	200
10	Blank	-

B.1(a)(ii)(iii)(vi) CP4 EPSPS Functional Activity

The functional activity of the KWS20-1 sugar beet-produced and *E. coli*-produced CP4 EPSPS proteins was determined using a colorimetric assay that measures formation of inorganic phosphate (Pi) from the EPSPS-catalyzed reaction between S-3-P and PEP. In this assay, protein-specific activity is expressed as units per milligram of protein (U/mg), where a unit is defined as one µmole of inorganic phosphate released from PEP per minute at 25°C. The KWS20-1 sugar beet-produced and *E. coli*-produced CP4 EPSPS proteins were considered to have equivalent functional activity if the specific activity of both were within acceptance limits of 1.96 to 7.90 U/mg (the prediction interval calculated from a data set of historically determined CP4 EPSPS protein activity; see Appendix 9).

The experimentally determined specific activity for the KWS20-1 sugar beet-produced and *E. coli*-produced CP4 EPSPS proteins are presented in Table 26. The specific activities of KWS20-1 sugar beet-produced and *E. coli*-produced CP4 EPSPS proteins were 4.05 U/mg and 4.93 U/mg of CP4 EPSPS protein, respectively. Because the specific activities of KWS20-1 sugar beet-produced and *E. coli*-produced CP4 EPSPS proteins fall within the preset acceptance limits (Table 26), the KWS20-1 sugar beet-produced CP4 EPSPS protein was considered to have equivalent functional activity to that of the *E. coli*-produced CP4 EPSPS protein.

Table 26. Functional Activity of the KWS20-1 Sugar Beet-Produced and *E. coli*-Produced CP4 EPSPS Proteins

KWS20-1 Sugar Beet-Produced CP4 EPSPS[1] (U/mg)	*E. coli*-Produced CP4 EPSPS[1] (U/mg)	Acceptance Limits[2] (U/mg)
4.05	4.93	1.96 – 7.90

[1] Value refers to calculated mean based on n = 9 which includes three replicate assays spectrophotometrically read in triplicate plate wells.

[2] Data obtained for the *E. coli*-produced CP4 EPSPS and several plant-produced CP4 EPSPS were used to generate a prediction interval for setting the acceptance limits (Appendix 9).

B.1(a)(ii)(iii)(vii) CP4 EPSPS Protein Identity and Equivalence Conclusion

The KWS20-1 sugar beet-produced CP4 EPSPS protein was purified from KWS20-1 sugar beet leaf, characterized and a comparison of the physicochemical and functional properties between the KWS20-1 sugar beet-produced and the *E. coli*-produced CP4 EPSPS proteins was conducted following a panel of analytical tests: 1) N terminal sequence analysis established the same amino acid identity for the KWS20-1 sugar beet-produced and *E. coli*-produced CP4 EPSPS proteins; 2) Nano LC-MS/MS analysis yielded peptide masses consistent with the expected peptide masses from the theoretical trypsin digest of the *cp4 epsps* gene product present in both KWS20-1 sugar beet and produced from *E. coli*; 3) the KWS20-1 sugar beet-produced and the *E. coli*-produced CP4 EPSPS proteins were both detected on a western blot probed with antibodies specific for CP4 EPSPS protein and the immunoreactive properties of both proteins were shown to be equivalent; 4) the electrophoretic mobility and apparent molecular weight of the KWS20-1 sugar

beet-produced and *E. coli*-produced CP4 EPSPS proteins were shown to be equivalent; 5) the glycosylation status of KWS20-1 sugar beet-produced and *E. coli*-produced CP4 EPSPS proteins was determined to be equivalent; and 6) the functional activity of the KWS20-1 sugar beet-produced and *E. coli*-produced CP4 EPSPS proteins were demonstrated to be equivalent. These results demonstrate that the KWS20-1 sugar beet-produced and the *E. coli*-produced CP4 EPSPS proteins are equivalent.

This demonstration of protein equivalence confirms that the *E. coli*-produced CP4 EPSPS protein is appropriate for use in the evaluation of the safety of the KWS20-1 sugar beet-produced CP4 EPSPS protein. Therefore, conclusions derived from digestibility, heat susceptibility and oral acute toxicology studies conducted with *E. coli*-produced CP4 EPSPS protein are applicable to KWS20-1 sugar beet-produced CP4 EPSPS protein.

B.1(a)(iii) Expression levels of DMO, PAT and CP4 EPSPS proteins in KWS20-1 sugar beet

The protein expression levels determined in KWS20-1 sugar beet are used to assess exposure to the introduced proteins via food or feed ingestion and potential environmental exposure. The most appropriate tissues to evaluate DMO, PAT and CP4 EPSPS protein levels are leaf/tops and root tissue samples. Levels of the introduced proteins were determined in leaf/tops and root tissue to evaluate food and feed exposure in humans and animals. Leaf/tops and root tissues are distinct above and below ground plant tissues that are important to estimate environmental exposure. The materials and methods used in the validated immunoassay are described in Appendix 10.

DMO, PAT and CP4 EPSPS protein levels in various tissues of KWS20-1 sugar beet were determined by ELISA assays. Levels of the introduced proteins were determined in relevant tissues and can be used to assess potential food and feed exposure in humans and animals. Tissues of KWS20-1 sugar beet were collected from four replicate plots planted in a randomized complete block design during the 2020 growing season from the following five U.S. field sites: Kent County, Michigan; Freeborn County, Minnesota; Bonneville County, Idaho; Power County, Idaho; and McHenry County, North Dakota. The field sites were representative of sugar beet-producing regions suitable for commercial production. Leaf [over-season leaf 1 (OSL1), over-season leaf 2 (OSL2), and Tops] and root [over-season root 1 (OSR1), over-season root 2 (OSR2), and over-season root 3 (OSR3) representing final harvest] tissue samples were collected from each replicated plot at all field sites treated with dicamba, glufosinate and glyphosate herbicides.

Tissue type[1]	Growth Stage (BBCH)[2]	Growth Stage
OSL1	17-18	V6-V8
OSL2	32-39	Up to 80% Ground Coverage
Tops	49	Harvestable Plant
OSR1	17-18	V6-V8
OSR2	32-39	Up to 80% Ground Coverage
OSR3 (Harvestable Root)	49	Harvestable Plant

[1] OSL = over-season leaf; OSR = over-season root

[2] BBCH = Biologische Bundesanstalt, Bundessortenamt und Chemische Industrie; a scale used to identify the phenological development stages of plants (Meier, 2001).

For details, please refer to Appendix 10.

B.1(a)(iii)(i) Expression Levels of DMO Protein

The ELISA results obtained for each sample were averaged across the five sites and are summarized in Table 27. The mean DMO protein level in KWS20-1 sugar beet across all sites was highest in OSL1 at 140 µg/g dry weight (dw) and lowest in OSR3 at 12 µg/g dw.

Table 27. Summary of DMO Protein Levels in Tissues from KWS20-1 Sugar Beet Produced in United States Field Trials During 2020

Tissue Type[1]	Development Stage[2]	Mean (SE) Range (µg/g fw)[3]	Mean (SE) Range (µg/g dw)[4]	LOQ/LOD (µg/g dw)[5]
OSL1	BBCH 17-18	14 (0.66) 9.6 - 20	140 (6.5) 95 - 200	0.100/0.028
OSR1	BBCH 17-18	3.4 (0.096) 2.7 - 4.0	28 (0.80) 22 - 34	0.100/0.012
OSL2	BBCH 32-39	13 (0.52) 9.1 - 18	120 (4.7) 83 - 160	0.100/0.028
OSR2	BBCH 32-39	3.7 (0.23) 1.9 - 5.7	22 (1.4) 11 - 34	0.100/0.012
Tops	BBCH 49	9.3 (0.56) 4.1 - 14	59 (3.5) 26 - 88	0.100/0.028
OSR3	BBCH 49	2.7 (0.12) 1.7 - 3.8	12 (0.53) 7.6 - 17	0.100/0.012

[1]OSL = over-season leaf, OSR = over-season root
[2]The crop development stage at which each tissue was collected.
[3]Protein levels are expressed as the arithmetic mean and standard error (SE) as microgram (µg) of protein per gram (g) of tissue on a fresh weight basis (fw). The means, SE and ranges (minimum and maximum values) were calculated for each tissue across all five sites (n=20).
[4] Protein levels are expressed as the arithmetic mean and standard error (SE) as microgram (µg) of protein per gram (g) of tissue on a dry weight basis (dw).
[5]LOQ=limit of quantitation; LOD=limit of detection

B.1(a)(iii)(ii) Expression Levels of PAT Protein

The ELISA results obtained for each sample were averaged across the five sites and are summarized in Table 28. The mean PAT protein level in KWS20-1 sugar beet across all sites was the highest in OSL1 at 25 µg/g dw and lowest in OSR3 at <LOQ (e.g., 0.125 µg/g dw for root).

Table 28. Summary of PAT Protein Levels in Tissues Collected from KWS20-1 Sugar Beet Produced in United States Field Trials During 2020

Tissue Type[1]	Development Stage[2]	Mean (SE) Range (µg/g fw)[3]	Mean (SE) Range (µg/g dw)[4]	LOQ/LOD (µg/g dw)[5]
OSL1	BBCH 17-18	2.6 (0.13) 1.7 - 3.7	25 (1.2) 16 - 36	0.313/0.113
OSR1	BBCH 17-18	0.029 (0.0033) 0.016 - 0.049	0.25 (0.028) 0.13 - 0.41	0.125/0.004
OSL2	BBCH 32-39	2.2 (0.20) 1.0 - 3.6	20 (1.8) 9.4 - 33	0.313/0.113
OSR2	BBCH 32-39	0.026 (0.0010) 0.025 – 0.027	0.16 (0.0033) 0.016 –0.049	0.125/0.004
Tops	BBCH 49	0.80 (0.071) 0.41 - 1.3	5.1 (0.45) 2.6 - 8.3	0.313/0.113
OSR3	BBCH 49	<LOQ (NA[6]) NA – NA	<LOQ (NA) NA – NA	0.125/0.004

[1]OSL = over-season leaf, OSR = over-season root
[2]The crop development stage at which each tissue was collected.
[3]Protein levels are expressed as the arithmetic mean and standard error (SE) as microgram (µg) of protein per gram (g) of tissue on a fresh weight basis (fw). The means, SE and ranges (minimum and maximum values) were calculated for each tissue across all five sites (n=20, except in OSR1 n=12 and in OSR2 n=2 because the rest of the samples were <LOQ).
[4] Protein levels are expressed as the arithmetic mean and standard error (SE) as microgram (µg) of protein per gram (g) of tissue on a dry weight basis (dw).
[5]LOQ=limit of quantitation; LOD=limit of detection
[6]NA=Not Applicable

B.1(a)(iii)(iii) Expression Levels of CP4 EPSPS Protein

The ELISA results obtained for each sample were averaged across the five sites and are summarized in Table 29. The mean CP4 EPSPS protein level in KWS20-1 sugar beet across all sites was highest in OSL1 at 590 µg/g dw and lowest in OSR3 at 100 µg/g dw.

Table 29. Summary of CP4 EPSPS Protein Levels in Tissues Collected from KWS20-1 Sugar Beet Produced in United States Field Trials During 2020

Tissue Type[1]	Development Stage[2]	Mean (SE) Range (µg/g fw)[3]	Mean (SE) Range (µg/g dw)[4]	LOQ/LOD (µg/g dw)[5]
OSL1	BBCH 17-18	60 (3.3) 33 - 87	590 (33) 320 - 850	1.250/0.776
OSR1	BBCH 17-18	52 (3.4) 32 - 81	430 (28) 270 - 680	1.250/0.460
OSL2	BBCH 32-39	56 (3.0) 40 - 87	510 (27) 370 - 790	1.250/0.776
OSR2	BBCH 32-39	46 (3.1) 24 - 71	270 (19) 140 - 420	1.250/0.460
Tops	BBCH 49	49 (1.9) 37 - 63	310 (12) 230 - 400	1.250/0.776
OSR3	BBCH 49	24 (1.3) 16 - 35	100 (5.9) 68 - 150	1.250/0.460

[1]OSL = over-season leaf, OSR = over-season root
[2]The crop development stage at which each tissue was collected.
[3]Protein levels are expressed as the arithmetic mean and standard error (SE) as microgram (µg) of protein per gram (g) of tissue on a fresh weight basis (fw). The means, SE and ranges (minimum and maximum values) were calculated for each tissue across all five sites (n=20).
[4] Protein levels are expressed as the arithmetic mean and standard error (SE) as microgram (µg) of protein per gram (g) of tissue on a dry weight basis (dw).
[5]LOQ=limit of quantitation; LOD=limit of detection

B.1(b) Information about prior history of human consumption of the new substances, if any, or their similarity to substances previously consumed in food.

Refer to Section A.2(a)(i) and A.2(a)(ii).

B.1(c) Information on whether any new protein has undergone any unexpected post-translational modification in the new host

Refer to Sections B.1(a)(ii).

B.1(d) Where any ORFs have been identified, bioinformatics analysis to indicate the potential for allergenicity and toxicity of the ORFs

Refer to Section A.3(c)(v).

B.2 New Proteins

B.2(a) Information on the potential toxicity of any new proteins, including:

B.2(a)(i) A bioinformatic comparison of the amino acid sequence of each of the new proteins to know protein toxins and anti-nutrients (e.g. protease inhibitors, lectins)

Potential structural similarities shared between the DMO, PAT and CP4 EPSPS proteins with sequences in a protein database were evaluated using the FASTA sequence alignment tool. The FASTA program directly compares amino acid sequences (i.e., primary, linear protein structure) and the alignment data may be used to infer shared higher order structural similarities between two sequences (i.e., secondary and tertiary protein structures). Proteins that share a high degree of similarity throughout the entire sequence are often homologous. Homologous proteins often have common secondary structures, common three-dimensional configuration and, consequently, may share similar functions (Caetano-Anollés *et al.*, 2009; Illergård *et al.*, 2009).

FASTA bioinformatic alignment searches using the KWS20-1 sugar beet-produced DMO, PAT and CP4 EPSPS amino acid sequence were performed with a toxin database to identify possible homology with proteins that may be harmful to human and animal health. The toxin database, TOX 2022, is a subset of sequences derived from the Swiss-Prot database (found at https://www.uniprot.org/) that was selected using a keyword search and filtered to remove likely non-toxin proteins. The TOX_2022 database contains 8,131 sequences.

An *E*-score acceptance criteria of 1×10^{-5} or less for any alignment was used to assess whether the DMO amino acid sequence shares any potential structural similarity and function with proteins from the TOX 2022 database. The *E*-score is a statistical measure of the likelihood that the observed similarity score could have occurred by chance in a search. A larger *E*-score indicates a lower degree of similarity between the query sequence and the sequence from the database. Typically, alignments between two sequences require an *E*-score of 1×10^{-5} or less to be considered to have sufficient sequence similarity to infer homology. The results of the search comparisons showed that no relevant alignments were observed against proteins in the TOX_2022 database.

The results of the bioinformatic analyses demonstrate that no structurally-relevant similarity exists between the DMO protein and any sequence in the TOX_2022 database, as no alignments displaying an *E*-score $<1\times10^{-5}$ were observed.

The results of the bioinformatic analyses demonstrate that no structurally-relevant similarity exists between the PAT protein and any sequence in the TOX_2022 database, as no alignments displaying an *E*-score $<1\times10^{-5}$ were observed.

The results of the bioinformatic analyses demonstrate that no structurally-relevant similarity exists between the CP4 EPSPS protein and any sequence in the TOX_2022 database, as no alignments displaying an *E*-score $<1\times10^{-5}$ were observed.

For details, please refer to Appendix 11, Appendix 12 and Appendix 13.

B.2(a)(ii) Information on the stability of the proteins to proteolysis in appropriate gastrointestinal model systems

Sugar beets are primarily grown for food use as sugar and are rarely used as a raw commodity (OECD, 2002a; CFIA, 2012). There are several processes that are used in sugar beet processing, including liming, carbonation, filtration, heating and crystallization (Klein *et al.*, 1998; ACSC, 2022). During the sugar refining process, sugar beet roots are processed into white sugar for food, and molasses and pulp that are used mainly for livestock feed (see Section A.2(b)).

Previous work (Klein *et al.*, 1998) has demonstrated that it is highly unlikely that any significant amount of sugar beet genomic DNA or protein are present in sugar following commercial processing. The removal and degradation of the DNA and protein from the sugar beet root materials during the manufacturing process was attributed to nucleolytic degradation of the DNA, irreversible adsorption on sludge, precipitation, denaturation and hydrolysis during alkaline pH and the high temperature carbonation steps, followed by hydrolysis at high temperatures during evaporation steps, and the physical exclusion of DNA and protein from refined sugar during crystallization. In the unlikely scenario that KWS20-1 sugar beet-produced DMO, PAT and CP4 EPSPS proteins are present in sugar derived foods, digestive fate assessments were conducted.

B.2(a)(ii)(i) Digestive Fate of the DMO Protein

Degradation of the DMO Protein by Pepsin

Degradation of the KWS20-1 sugar beet-produced DMO protein by pepsin was evaluated over time by analyzing digestion mixtures incubated for targeted time intervals following a standardized protocol validated in an international, multi-laboratory ring study (Thomas *et al.*, 2004). The assessment showed that the results of *in vitro* pepsin digestion assays using this protocol were reproducibile and consistent for determining the digestive suceptibility of a protein. This standardized *in vitro* pepsin digestion protocol utilized a physiologically-relevant acidic buffer appropriate for pepsin activity. The susceptibility of DMO protein to pepsin degradation was assessed by visual analysis of a Brilliant Blue G Colloidal stained SDS-PAGE gel and by visual analysis of a western blot probed with an anti-DMO polyclonal antibody. Both visualization methods were run concurrently with separate SDS-PAGE and western blot analyses to estimate the limit of detection (LOD) of the DMO protein for each method.

For SDS-PAGE analysis of the digestibility of the DMO protein in pepsin, the gel was loaded with 1 µg of total *E. coli*-produced DMO protein (based on pre-digestion protein concentrations) for each of the digestion samples (Figure 47, Panel A). The SDS-PAGE gel for the digestibility assessment was run concurrently with a separate SDS-PAGE gel to estimate the LOD of the DMO protein (Figure 47, Panel B). The LOD of intact DMO protein was approximately 6.3 ng (Figure 47, Panel B, lane 8). Visual examination of SDS-PAGE data showed that the intact DMO protein was digested within 0.5 min of incubation in pepsin (Figure 47, Panel A, lane 5). Therefore, based on the LOD, more than 99.4% (100% - 0.63% ≈ 99.4%) of the intact DMO protein was digested within 0.5 min of incubation in pepsin. No peptide fragment was detected at the 0.5 min or subsequent time points in the SDS-PAGE analysis.

No change in the DMO protein band intensity was observed in the absence of pepsin in the 0 min No Pepsin Control and 60 min No Pepsin Control (Figure 47, Panel A, lanes 3 and 12, respectively). This indicates that the degradation of the DMO protein was due to the proteolytic activity of pepsin and not due to instability of the protein while incubated in the pepsin stock solution. The 0 min No DMO Protein Control and 60 min No DMO Protein Control (Figure 47, Panel A, lanes 2 and 13, respectively) demonstrate that the pepsin is stable throughout the experimental phase.

For details, please refer to Appendix 14.

A.

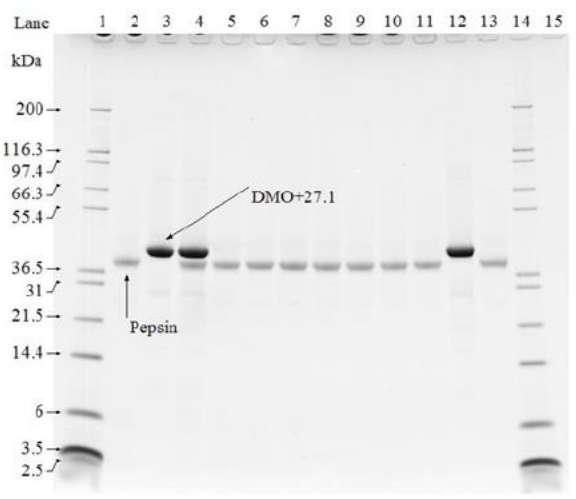

B.

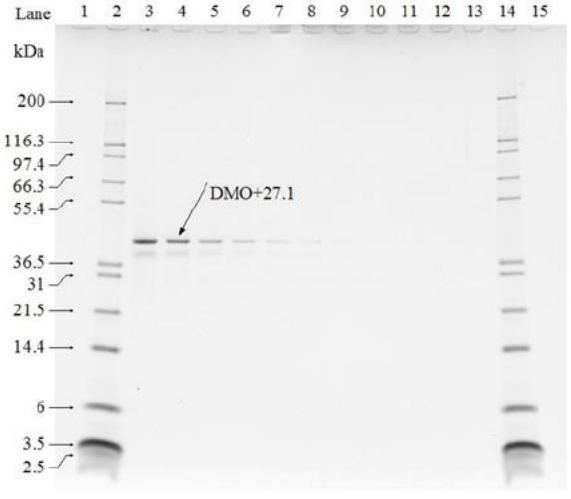

Figure 47. SDS-PAGE Analysis of the Degradation of KWS20-1 Sugar Beet-Produced DMO Protein in Pepsin

Colloidal Brilliant Blue G stained SDS-PAGE gels were used to assess the degradation of DMO protein by pepsin. Approximate molecular weights (kDa) are shown on the left of each gel and correspond to the markers loaded. In each gel, the DMO protein migrated to approximately 38.4 kDa, found above the pepsin band. Empty lanes were cropped from the images.
A: DMO protein degradation in the presence of pepsin. Based on pre-reaction protein concentrations, 1 µg of *E. coli*-produced DMO protein was loaded in each lane containing DMO protein.
B: LOD determination. Indicated amounts of the *E. coli*-produced DMO protein from the Pepsin Treated T0 sample were loaded to estimate the LOD of the DMO protein.

Lane	Sample	Incubation Time (min)
1	Mark12 MWM	-
2	0 min No DMO Protein Control	0
3	0 min No Pepsin Control	0
4	Pepsin Treated T0	0
5	Pepsin Treated T1	0.5
6	Pepsin Treated T2	2
7	Pepsin Treated T3	5
8	Pepsin Treated T4	10
9	Pepsin Treated T5	20
10	Pepsin Treated T6	30
11	Pepsin Treated T7	60
12	60 min No Pepsin Control	60
13	60 min No DMO Protein Control	60
14	Mark12 MWM	-
15	Empty	-

Lane	Sample	Amount[1] (ng)
1	Empty	-
2	Mark12 MWM	-
3	Pepsin Treated T0	200.0
4	Pepsin Treated T0	100.0
5	Pepsin Treated T0	50.0
6	Pepsin Treated T0	25.0
7	Pepsin Treated T0	12.5
8	Pepsin Treated T0	6.3
9	Pepsin Treated T0	3.1
10	Pepsin Treated T0	1.6
11	Pepsin Treated T0	0.8
12	Pepsin Treated T0	0.4
13	Pepsin Treated T0	0.2
14	Mark12 MWM	-
15	Empty	-

[1] Amount was rounded to one decimal place.

For western blot analysis of KWS20-1 sugar beet-produced DMO pepsin susceptibility, the DMO protein was loaded with approximately 5 ng per lane of total protein (based on pre-reaction total protein concentrations) for each reaction time point examined. The western blot used to assess DMO protein degradation (Figure 47, Panel A) was run concurrently with the western blot used to estimate the LOD (Figure 47, Panel B). The LOD of the DMO protein was approximately 0.155 ng (Figure 47, Panel B, lane 8). Western blot analysis demonstrated that the intact DMO protein was degraded below the LOD within 0.5 min of incubation in the presence of pepsin (Figure 47, Panel A, lane 6). Based on the western blot LOD for the DMO protein, more than 96.9% (100% - 3.1% = 96.9%) of the intact DMO protein was degraded within 0.5 min. No peptide fragments were detected at the 0.5 min or subsequent time points in the western blot analysis.

No change in the DMO protein band intensity (~38.4 kDa) was observed in the absence of pepsin in the 0 min No Pepsin Control and 60 min No Pepsin Control (Figure 47, Panel A, lanes 4 and 13, respectively). This indicates that the degradation of the DMO protein was due to the proteolytic activity of pepsin and not due to instability of the protein while incubated in the pepsin stock solution.

No immunoreactive bands were observed in 0 min No DMO Protein Control and 60 min No DMO Protein Control (Figure 47, Panel A, lanes 3 and 14, respectively). This result indicates that there was no non-specific interaction between the pepsin solution and the DMO-specific antibody under these experimental conditions.

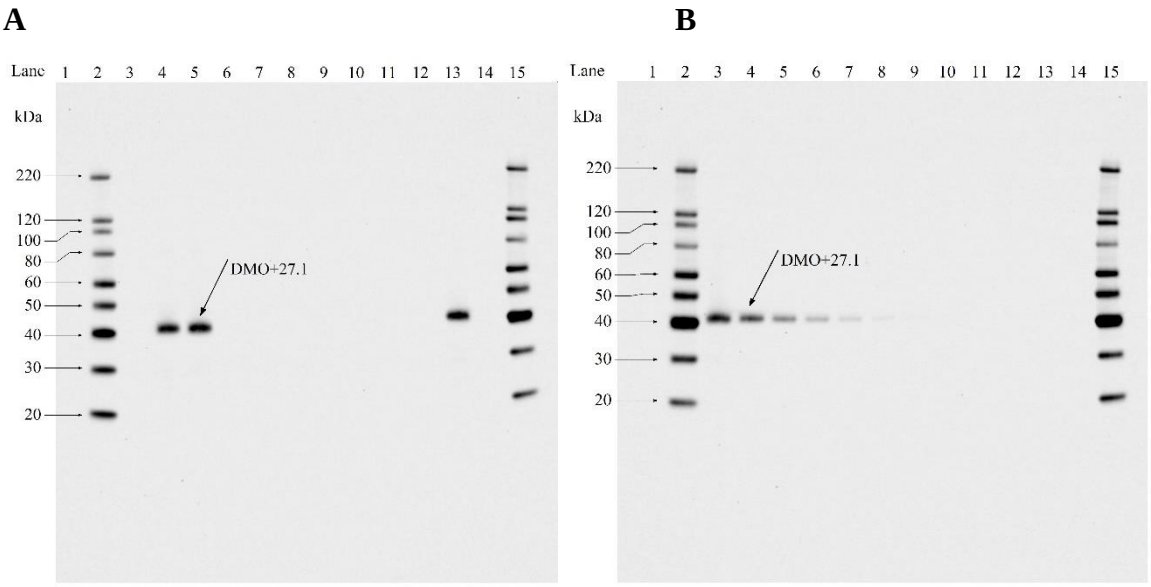

Figure 48. Western Blot Analysis of the Degradation of KWS20-1 Sugar Beet-Produced DMO Protein by Pepsin

Western blots probed with an anti-DMO antibody were used to assess the degradation of DMO by pepsin. Approximate molecular weights (kDa) are shown on the left of each gel and correspond to the MagicMark™ molecular weight marker. A 15-second exposure is shown.
A: DMO protein degradation by pepsin. Based on pre-reaction protein concentrations, 5 ng of *E. coli*-produced DMO protein was loaded in each lane containing DMO protein.
B: LOD determination. Indicated amounts of the *E. coli*-produced DMO protein from the Pepsin Treated T0 sample were loaded to estimate the LOD of the DMO protein.

Lane	Sample	Incubation Time (min)
1	Precision Plus MWM	-
2	MagicMark™ MWM	-
3	0 min No DMO Protein Control	0
4	0 min No Pepsin Control	0
5	Pepsin Treated T0	0
6	Pepsin Treated T1	0.5
7	Pepsin Treated T2	2
8	Pepsin Treated T3	5
9	Pepsin Treated T4	10
10	Pepsin Treated T5	20
11	Pepsin Treated T6	30
12	Pepsin Treated T7	60
13	60 min No Pepsin Control	60
14	60 min No DMO Protein Control	60
15	MagicMark™ MWM	-

Lane	Sample	Amount[1] (ng)
1	Precision Plus MWM	-
2	MagicMark™ MWM	-
3	Pepsin Treated T0	5.000
4	Pepsin Treated T0	2.500
5	Pepsin Treated T0	1.250
6	Pepsin Treated T0	0.625
7	Pepsin Treated T0	0.313
8	Pepsin Treated T0	0.155
9	Pepsin Treated T0	0.078
10	Pepsin Treated T0	0.040
11	Pepsin Treated T0	0.020
12	Pepsin Treated T0	0.010
13	Pepsin Treated T0	0.005
14	Pepsin Treated T0	0.003
15	MagicMark™ MWM	-

[1] Amount was rounded to three decimal places.

Degradation of the DMO protein by Pancreatin

The degradation of the KWS20-1 sugar beet-produced DMO protein by pancreatin was assessed by western blot analysis (Figure 49). The western blot used to assess the DMO protein degradation (Figure 49, Panel A) was run concurrently with the western blot used to estimate the LOD (Figure 49, Panel B) of the DMO protein. The LOD of the DMO protein was observed at approximate 0.155 ng protein loading (Figure 49, Panel B, lane 8). The LOD was used to calculate the maximum relative amount of DMO protein that could remain visually undetected after digestion, which corresponded to approximately 3.1% of the total protein loaded.

The gel used to assess degradation of the DMO protein by western blot was loaded with approximately 5 ng per lane of total protein (based on pre-reaction protein concentrations) for each reaction time point examined. Western blot analysis demonstrated that a band corresponding to the DMO protein was degraded to a level below the LOD within 5 min of incubation with pancreatin (Figure 49, Panel A, lane 5). Therefore, based on the LOD, more than 96.9% (100% - 3.1% = 96.9%) of the DMO protein was digested within 5 minutes. No peptide fragments were detected at the 5 min or subsequent time points in the western blot analysis.

No significant change in the intact DMO (~38.4 kDa) band intensity was observed in the absence of pancreatin in the 0 min No Pancreatin Control and 24 hour No Pancreatin Control (Figure 49, Panel A, lanes 3 and 13, respectively). This indicates that the degradation of the DMO protein was due to the proteolytic activity of pancreatin and not due to instability of the protein when incubated in the pancreatin stock solution over the course of the experiment. After 24 hours, the appearance of additional faint higher molecular bands (Figure 49, Panel A, lane 13) is likely due to the formation of a minor amount of DMO aggregates.

No immunoreactive bands were observed in the 0 min No DMO Protein Control and 24 hour No DMO Protein Control (Figure 49, Panel A, lanes 2 and 14, respectively), demonstrating the absence of non-specific antibody interactions with the pancreatin solution.

For details, please refer to Appendix 14.

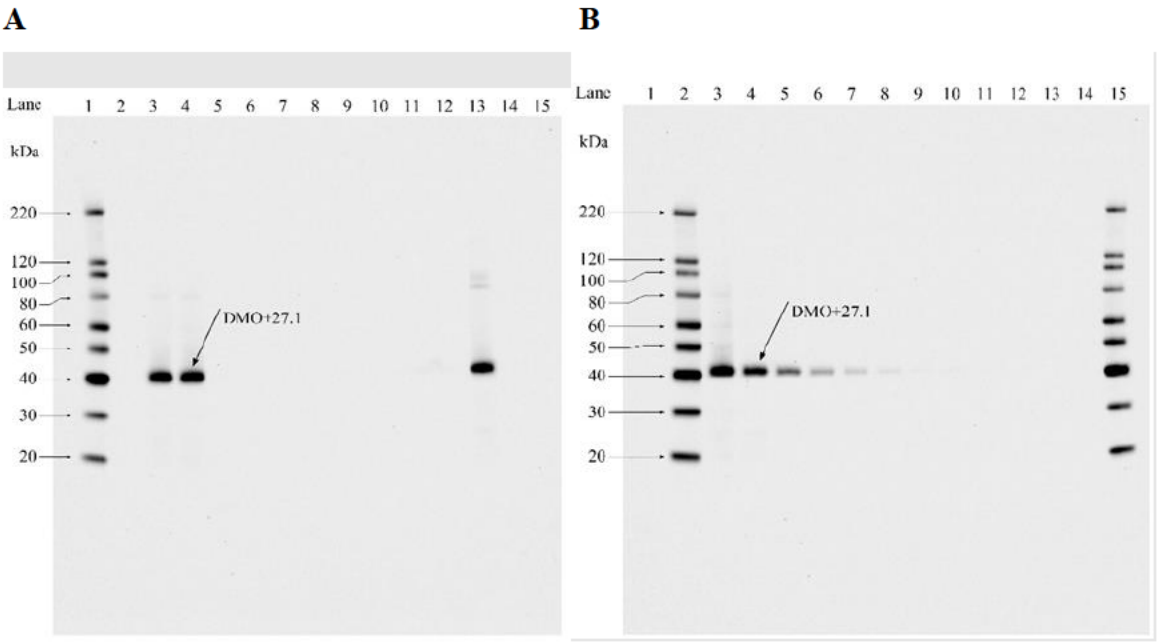

Figure 49. Western Blot Analysis of the Degradation of KWS20-1 Sugar Beet-Produced DMO Protein by Pancreatin

Western blots probed with an anti-DMO antibody were used to assess the degradation of DMO by pancreatin. Aproximate molecular weights (kDa) are shown on the left of each gel and correspond to the MagicMark™ molecular weight marker. A 15-second exposure is shown.
A: DMO protein degradation by pancreatin. Based on pre-reaction protein concentrations, 5 ng of *E. coli*-produced DMO protein was loaded in each lane containing DMO protein.
B: LOD determination. Indicated amounts of the *E. coli*-produced DMO protein from the Pancreatin Treated T0 sample were loaded to estimate the LOD of the DMO protein.

Lane	Sample	Incubation Time
1	MagicMark™ MWM	-
2	0 min No DMO Protein Control	0
3	0 min No Pancreatin Control	0
4	Pancreatin Treated T0	0
5	Pancreatin Treated T1	5 min
6	Pancreatin Treated T2	15 min
7	Pancreatin Treated T3	30 min
8	Pancreatin Treated T4	1 h
9	Pancreatin Treated T5	2 h
10	Pancreatin Treated T6	4 h
11	Pancreatin Treated T7	8 h
12	Pancreatin Treated T8	24 h
13	24 h No Pancreatin Control	24 h
14	24 h No DMO Protein Control	24 h
15	Precision Plus MWM	-

Lane	Sample	Amount[1] (ng)
1	Precision Plus MWM	-
2	MagicMark™ MWM	-
3	Pancreatin Treated T0	5.000
4	Pancreatin Treated T0	2.500
5	Pancreatin Treated T0	1.250
6	Pancreatin Treated T0	0.625
7	Pancreatin Treated T0	0.313
8	Pancreatin Treated T0	0.155
9	Pancreatin Treated T0	0.078
10	Pancreatin Treated T0	0.040
11	Pancreatin Treated T0	0.020
12	Pancreatin Treated T0	0.010
13	Pancreatin Treated T0	0.005
14	Pancreatin Treated T0	0.003
15	MagicMark™ MWM	-

[1] Amount was rounded to three decimal places.

Digestive Fate of the DMO Protein Conclusions

The susceptibility of the KWS20-1 sugar beet-produced DMO protein to degradation by either pepsin or pancreatin was evaluated. The results showed that at least 99.4% of the intact DMO protein was degraded by pepsin within 0.5 min when analyzed by SDS-PAGE and 96.9% of the intact DMO was degraded by pepsin within 0.5 min when analyzed by western blot using a DMO-specific antibody. No peptide fragment was detected at the 0.5 min or subsequent time points in the SDS-PAGE analysis. At least 96.9% of the intact DMO protein was degraded by pancreatin within 5 min when analyzed by western blot. The result that the *E. coli*-produced DMO protein is rapidly degraded by pepsin and pancreatin without the formation of stable peptide fragments contributes to the weight of evidence that the KWS20-1 sugar beet-produced DMO protein is highly unlikely to pose a meaningful risk to human or animal health.

B.2(a)(ii)(ii) Digestive Fate of the PAT Protein

Degradation of PAT Protein in the Presence of Pepsin

Degradation of the KWS20-1 sugar beet-produced PAT protein by pepsin was evaluated over time by analyzing digestion mixtures incubated for targeted time intervals following a standardized protocol validated in an international, multi-laboratory ring study (Thomas *et al.*, 2004) collected at targeted incubation time points. The susceptibility of PAT protein to pepsin degradation was assessed by visual analysis of a Brilliant Blue G-Colloidal stained SDS-PAGE gel and by visual analysis of a western blot probed with an anti-PAT polyclonal antibody. Both visualization methods were run concurrently with separate SDS-PAGE and western blot analyses to estimate the limit of detection (LOD) of the PAT protein for each method.

For SDS-PAGE analysis of the digestibility of the PAT protein in pepsin, the gel was loaded with approximately 1 µg of *E. coli*-produced total test protein (based on pre-digestion protein concentrations) for each of the digestion samples (Figure 50A). Visual examination of SDS-PAGE data showed that the intact PAT protein was completely degraded within 0.5 min of incubation in the presence of pepsin (Figure 50A, Lane 5). A peptide fragment of ~3 kDa was observed for the first 5 min of pepsin treatment with the staining intensity decreasing over time and it was completely degraded within 10 min of incubation. This ~3 kDa peptide fragment is likely a result of a partially digested protein. This is comparable with previously published safety assessments of PAT protein (Hérouet *et al.*, 2005).

No change in the PAT protein band intensity was observed in the absence of pepsin in the 0 min No Pepsin Control and 60 min No Pepsin Control samples (Figure 50A, lanes 3 and 12). This indicates that the degradation of the PAT protein was due to the proteolytic activity of pepsin and not due to instability of the protein while incubated in the pepsin test system over the course of the experiment.

The 0 min No Test Protein Control and 60 min No Test Protein Control (Figure 50A, lanes 2 and 13) demonstrated that the pepsin is stable throughout the experimental phase.

A separate SDS PAGE gel to estimate the LOD of the PAT protein was run concurrently with the SDS PAGE for the degradation assessment (Figure 50B). The LOD of the PAT protein was visually estimated to be approximately 3.6 ng (Figure 50B, lane 8). This LOD is used to calculate the maximum amount of intact PAT protein that could remain visually undetected after

degradation, which corresponded to approximately 0.4% (3.6/1000 ×100% = ~ 0.4%) of the total protein loaded. Based on that LOD, more than 99.6% (100% - 0.4% = 99.6%) of the intact PAT protein was degraded within 0.5 min of incubation in the presence of pepsin.

For details, please refer to Appendix 15.

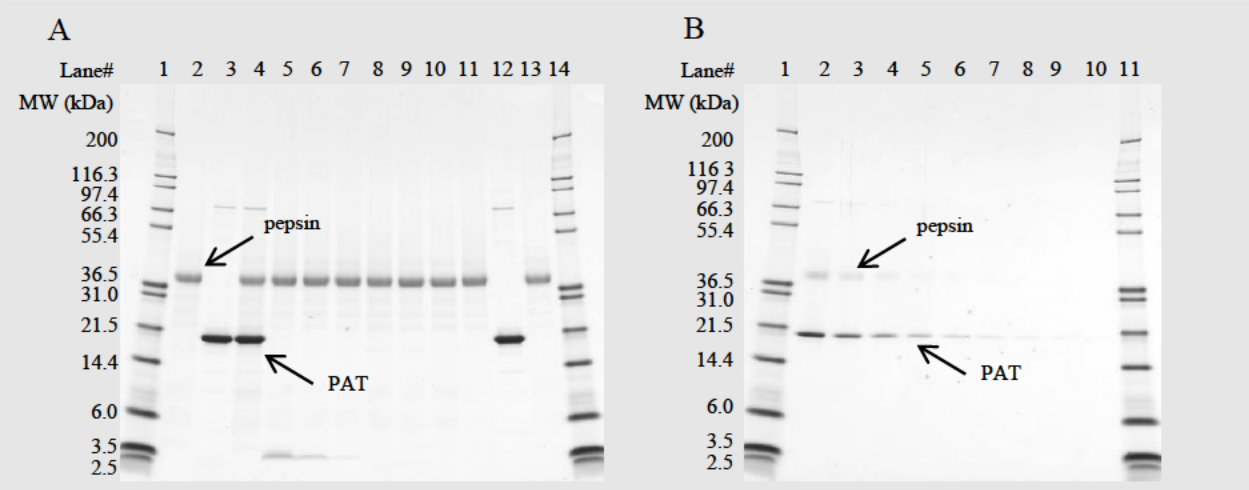

Figure 50. SDS-PAGE Analysis of the Degradation of KWS20-1 Sugar Beet-Produced PAT Protein by Pepsin

Colloidal Brilliant Blue G stained SDS-PAGE gels were used to assess the degradation of PAT protein by pepsin. Molecular weights (kDa) are shown on the left of each gel, and correspond to the markers loaded. In each gel, PAT protein migrated to approximately 21 kDa and pepsin to approximately 38 kDa. Blank lanes were cropped from the images.

A: PAT protein degradation by Pepsin. Based on pre-reaction protein concentrations, 1 µg of *E. coli*-produced PAT protein was loaded in each lane containing PAT protein.

B: LOD determination. Indicated amounts of the *E. coli*-produced PAT protein from the Pepsin Treated T0 sample were loaded to estimate the LOD of the PAT protein.

Lane	Sample	Incubation Time (min)
1	Mark 12 ™ MWM	-
2	0 min No Test Protein Control	0
3	T 0 min No Pepsin Control	0
4	Pepsin Treated T0	0
5	Pepsin Treated T1	0.5
6	Pepsin Treated T2	2
7	Pepsin Treated T3	5
8	Pepsin Treated T4	10
9	Pepsin Treated T5	20
10	Pepsin Treated T6	30
11	Pepsin Treated T7	60
12	60 min No Pepsin Control	60
13	60 min No Test Protein Control	60
14	Mark 12 ™ MWM	-

Lane	Sample	Amount (ng)
1	Mark 12 ™ MWM	-
2	Pepsin Treated T0	230
3	Pepsin Treated T0	115
4	Pepsin Treated T0	57.5
5	Pepsin Treated T0	28.8
6	Pepsin Treated T0	14.4
7	Pepsin Treated T0	7.2
8	Pepsin Treated T0	3.6
9	Pepsin Treated T0	1.8
10	Pepsin Treated T0	0.9
11	Mark 12 ™ MWM	

For western blot analysis of KWS20-1 sugar beet-produced PAT pepsin susceptibility, the *E. coli*-produced PAT protein was loaded with approximately 20 ng per lane of total protein (based on pre-reaction total protein concentrations) for each reaction time point examined. The western blot used to assess the resistance of the PAT protein to pepsin digestion (Figure 51A) was run concurrently with a western blot to estimate the LOD of the PAT protein Figure 51B). The LOD of the PAT protein was approximately 0.36 ng (Figure 51B, lane 8). The LOD was used to calculate the maximum relative amount of PAT protein that could remain visually undetected after digestion, which corresponded to approximately 1.8% (0.36/20 × 100% = 1.8%) of the total protein loaded.

Western blot analysis demonstrated that the PAT protein was degraded below the LOD within 0.5 min of incubation in the presence of pepsin (Figure 51A, lane 5). Based on the western blot LOD for the PAT protein, it can be concluded that more than 98.2% (100% - 1.8% = 98.2%) of the intact PAT protein was degraded within 0.5 min. No peptide fragments were detected at any timepoint in pepsin by western blot.

No apparent change in the PAT protein band intensity was observed in the absence of pepsin in the 0 min No Pepsin Control and 60 min No Pepsin Control samples (Figure 51A, lanes 3 and 12). This indicates that the degradation of the PATprotein was due to the proteolytic activity of pepsin and not due to instability of the protein while incubated in the pepsin test system over the course of the experiment.

No immunoreactive bands were observed in the 0 min No Protein Control and 60 min No Protein Control samples (Figure 51A, lanes 2 and 13). This result indicates that there was no non-specific interaction between the pepsin solution and the PAT specific antibody under these experimental conditions.

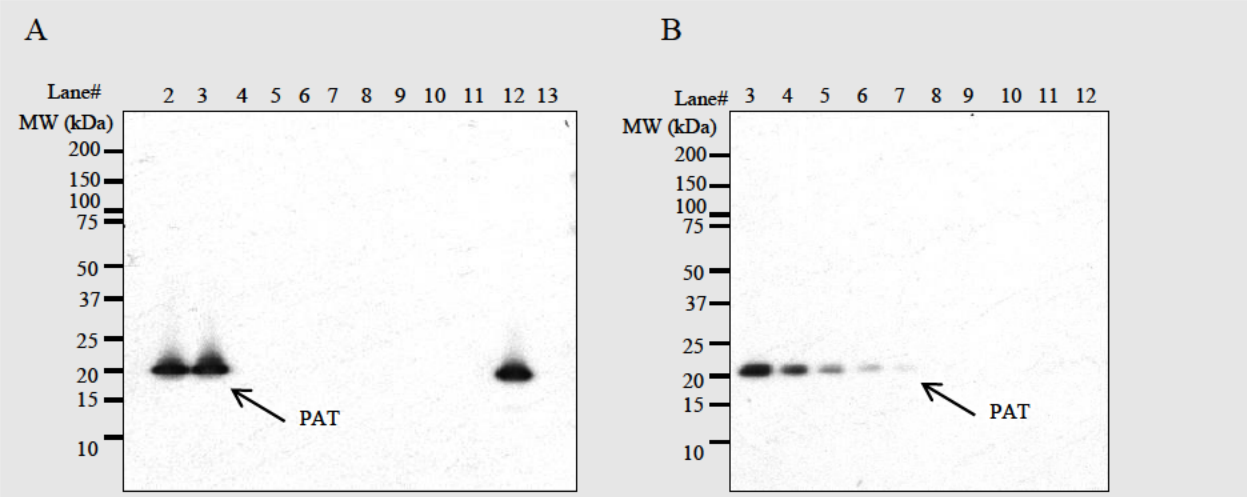

Figure 51. Western Blot Analysis of the Degradation of KWS20-1 Sugar Beet-Produced PAT Protein by Pepsin

Western blots probed with an anti-PAT antibody were used to assess the degradation of PAT by pepsin. Molecular weights (kDa) are shown on the left of each gel, and correspond to the markers loaded (cropped from images). Blank lanes were cropped from the images. A 20 sec exposure is shown.

A: PAT protein degradation by pepsin. Based on pre-reaction protein concentrations, 20 ng of *E. coli*-produced PAT protein was loaded in each lane containing PAT protein.

B: LOD determination. Indicated amounts of the *E. coli*-produced PAT protein from the Pepsin Treated T0 sample were loaded to estimate the LOD of the PAT protein.

Lane	Sample	Incubation Time (min)
1	Precision Plus ™ MWM	-
2	0 min No Test Protein Control	0
3	0 min No Pepsin Control	0
4	Pepsin Treated T0	0
5	Pepsin Treated T1	0.5
6	Pepsin Treated T2	2
7	Pepsin Treated T3	5
8	Pepsin Treated T4	10
9	Pepsin Treated T5	20
10	Pepsin Treated T6	30
11	Pepsin Treated T7	60
12	60 min No Pepsin Control	60
13	60 min No Test Protein Control	60
14	Precision Plus ™ MWM	-

Lane	Sample	Amount (ng)
1	Precision Plus ™ MWM	-
2	Empty	-
3	Pepsin Treated T0	5.8
4	Pepsin Treated T0	2.9
5	Pepsin Treated T0	1.44
6	Pepsin Treated T0	0.72
7	Pepsin Treated T0	0.36
8	Pepsin Treated T0	0.18
9	Pepsin Treated T0	0.09
10	Pepsin Treated T0	0.045
11	Pepsin Treated T0	0.022
12	Pepsin Treated T0	0.011
13	Empty	-
14	Precision Plus ™ MWM	-

Degradation of PAT Protein in the Presence of Pancreatin

The degradation of the KWS20-1 sugar beet-produced PAT protein by pancreatin was assessed by western blot analysis (Figure 52). The total loading of the *E. coli*-produced PAT protein for each timepoint examined was approximately 20 ng per lane (based on pre-reaction total protein concentrations). The western blot used to assess the PAT protein degradation (Figure 52A) was run concurrently with the western blot used to estimate the LOD (Figure 52B) of the intact PAT protein. The LOD of the PAT protein was observed at approximately the 0.17 ng protein loading (Figure 52A, lane 8). The LOD was used to calculate the maximum relative amount of the PAT protein that could remain visually undetected after digestion, which corresponded to approximately 0.9% (0.17/20 × 100% = ~0.9%) of the total protein loaded.

Western blot analysis demonstrated that a band corresponding to the PAT protein was degraded to a level below the LOD within 5 min of incubation in the presence of pancreatin (Figure 52A, lane 5), the first timepoint assessed. Therefore, based on the LOD, more than 99% (100% - 0.9% = 99.1%) of the PAT protein was degraded within 5 min. No other immunoreactive bands were detected in any other tested specimens. This is comparable with previously published safety assessments of PAT protein (Hérouet *et al.*, 2005).

No apparent change in the intact PAT band intensity was observed in the absence of pancreatin in the 0 h No Pancreatin Control and 24 h No Pancreatin Control samples (Figure 52A, lanes 3 and 13). This indicates that the degradation of all immunoreactive forms of the PAT protein was due to the proteolytic activity of pancreatin and not due to instability of the protein when incubated in the pancreatin test system over the course of the experiment.

No immunoreactive bands were observed in the 0 h No Test Protein Control and 24 h No Test Protein Control samples (Figure 52A, lanes 2 and 14), demonstrating the absence of non-specific antibody interactions with the pancreatin solution.

For details, please refer to Appendix 15.

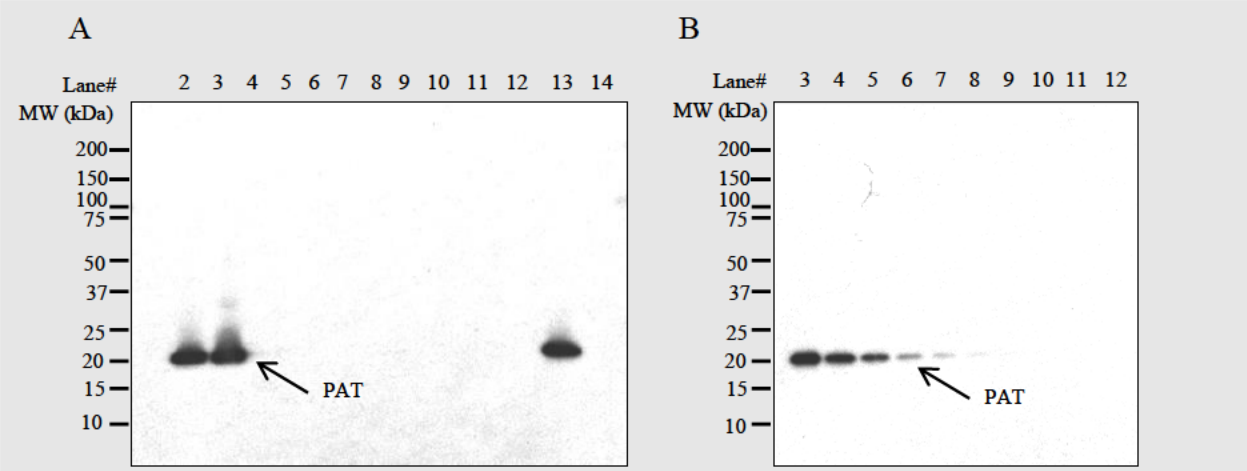

Figure 52. Western Blot Analysis of the Degradation of KWS20-1 Sugar Beet-Produced PAT Protein by Pancreatin

Western blots probed with an anti-PAT antibody were used to assess the degradation of PAT by pancreatin. Molecular weights (kDa) are shown on the left of each gel, and correspond to the markers loaded (cropped from images). Blank lanes were cropped from the images. A 15 sec exposure is shown.

A: PAT protein degradation by pancreatin. Based on pre-reaction protein concentrations, 20 ng of *E. coli*-produced PAT protein was loaded in each lane containing PAT protein.

B: LOD determination. Indicated amounts of the test *E. coli*-produced PAT protein from the T0 sample were loaded to estimate the LOD of the PAT protein.

Lane	Sample	Incubation Time
1	Precision Plus™ MWM	-
2	0 min No Test Protein Control	0
3	0 min No Pancreatin Control	0
4	Pancreatin Treated T0	0
5	Pancreatin Treated T1	5 min
6	Pancreatin Treated T2	15 min
7	Pancreatin Treated T3	30 min
8	Pancreatin Treated T4	1 hr
9	Pancreatin Treated T5	2 hr
10	Pancreatin Treated T6	4 hr
11	Pancreatin Treated T7	8 hr
12	Pancreatin Treated T8	24 hr
13	24 hr No Pancreatin Control	24 hr
14	24 hr No Test Protein Control	24 hr
15	Precision Plus™ MWM	-

Lane	Sample	Amount (ng)
1	Precision Plus™ MWM	-
2	Empty	-
3	Pancreatin Treated T0	5.6
4	Pancreatin Treated T0	2.78
5	Pancreatin Treated T0	1.39
6	Pancreatin Treated T0	0.69
7	Pancreatin Treated T0	0.35
8	Pancreatin Treated T0	0.17
9	Pancreatin Treated T0	0.087
10	Pancreatin Treated T0	0.043
11	Pancreatin Treated T0	0.022
12	Pancreatin Treated T0	0.011
13	Empty	-
14	Precision Plus™ MWM	-

Digestive Fate of the PAT Protein Conclusions

The ability of the KWS20-1 sugar beet-produced PAT protein to be degraded by pepsin and by pancreatin was evaluated. The results of the SDS-PAGE analysis demonstrate that greater than 99.6% of the intact PAT protein was degraded by pepsin within 0.5 min and at least 98.2% of the intact PAT protein was degraded by pepsin within 0.5 min when analyzed by western blot using a PAT specific antibody. SDS-PAGE analysis showed that a peptide fragment of ~3 kDa was observed in the 0.5 min time points in the presence of pepsin, but was gone by 10 min.

At least 99.1% of the intact PAT protein was degraded within 5 min during incubation with pancreatin when analyzed by western blot.

These results show that the intact PAT is rapidly degraded by pepsin and pancreatin. Rapid and complete degradation of the PAT protein by pepsin and pancreatin indicates that the PAT protein is highly unlikely to pose any safety concern to human or animal health.

B.2(a)(ii)(iii) Digestive Fate of the CP4 EPSPS Protein

Degradation of CP4 EPSPS Protein in the Presence of Pepsin

Harrison et al. (1996) demonstrated that the *E. coli*-produced CP4 EPSPS protein is rapidly degraded in simulated gastric fluids (SGF, i.e. pepsin solution). Based on western blot analysis, CP4 EPSPS protein was undetectable within 15 seconds of incubation in the presence of pepsin.

Subsequent digestive fate experiments confirmed the *in vitro* digestibility of the KWS20-1 sugar beet-produced CP4 EPSPS protein in pepsin. For SDS-PAGE analysis of the digestibility of the *E. coli*-produced CP4 EPSPS protein in pepsin, the gel was loaded with 0.5 µg of total test protein (based on pre-digestion protein concentrations) for each of the digestion samples (Figure 53A). Visual examination of SDS-PAGE data showed that the intact CP4 EPSPS protein was completely degraded within 15 seconds of incubation in the presence of pepsin (Figure 53A, lane 5).

No change in the CP4 EPSPS protein band intensity was observed in the absence of pepsin in the 0 min No Pepsin Control and 60 min No Pepsin Control samples (Figure 53A, lanes 2 and 15). This indicates that the degradation of the CP4 EPSPS protein was due to the proteolytic activity of pepsin and not due to instability of the protein while incubated in the pepsin test system over the course of the experiment.

The 0 min No Test Protein Control and 60 min No Test Protein Control (Figure 53A, lanes 3 and 14) demonstrated that the pepsin is stable throughout the experimental phase.

A separate SDS PAGE gel to estimate the LOD of the CP4 EPSPS protein was run concurrently with the SDS PAGE for the degradation assessment (Figure 53B). The LOD of intact CP4 EPSPS protein was approximately 10 ng (Figure 53B, lane 11), which corresponded to approximately 2% (10/500 ×100% = 2%) of the total protein loaded. Therefore, based on the LOD, more than 98% (100% - 2% = 98%) of the intact CP4 EPSPS protein was degraded within 15 seconds of incubation in pepsin, which is similar to the results reported by Harrison et al. (1996).

For details, please refer to Appendix 16 and Appendix 17.

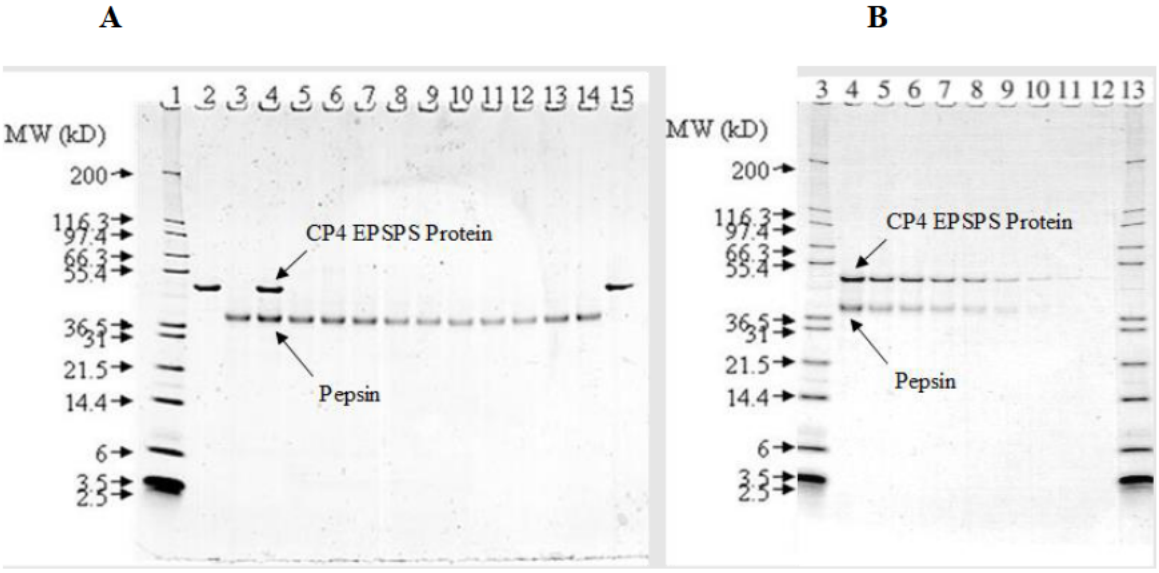

Figure 53. SDS-PAGE Analysis of the Degradation of KWS20-1 Sugar Beet-Produced CP4 EPSPS Protein by Pepsin

Colloidal Brilliant Blue G stained SDS-PAGE gels were used to assess the degradation of CP4 EPSPS protein by pepsin. Molecular weights (kDa) are shown on the left of each gel and correspond to the markers loaded. In each gel, the CP4 EPSPS protein migrated to approximately 44 kDa and pepsin to approximately 38 kDa. Empty lanes and molecular weight markers that were not visible on the gel were cropped from the images.

Panel A: CP4 EPSPS protein degradation in the presence of pepsin. Based on pre-reaction protein concentrations, 0.5 µg of *E. coli*-produced CP4 EPSPS protein was loaded in each lane containing CP4 EPSPS protein.

Panel B: LOD determination. Indicated amounts of the *E. coli*-produced CP4 EPSP protein from the Pepsin Treated T0 sample were loaded to estimate the LOD of the CP4 EPSPS protein.

Lane	Sample	Incubation Time (min)
1	Molecular Weight Marker	-
2	0 min No Pepsin Control	0
3	0 min No Test Protein Control	0
4	Pepsin Treated T0	0
5	Pepsin Treated T1	0.25
6	Pepsin Treated T2	0.5
7	Pepsin Treated T3	1
8	Pepsin Treated T4	2
9	Pepsin Treated T5	4
10	Pepsin Treated T6	8
11	Pepsin Treated T7	15
12	Pepsin Treated T8	30
13	Pepsin Treated T9	60
14	60 min Test Protein No Control	60
15	60 min No Pepsin Control	60

Lane	Sample	Amount (ng)
1	Empty	-
2	Empty	-
3	Molecular Weight Marker	-
4	Pepsin Treated T0	500
5	Pepsin Treated T0	250
6	Pepsin Treated T0	200
7	Pepsin Treated T0	150
8	Pepsin Treated T0	100
9	Pepsin Treated T0	50
10	Pepsin Treated T0	25
11	Pepsin Treated T0	10
12	Pepsin Treated T0	5
13	Molecular Weight Marker	-
14	Empty	-
15	Empty	-

For western blot analysis of the KWS20-1 sugar beet-produced CP4 EPSPS pepsin susceptibility, *E. coli*-produced CP4 EPSPS protein was loaded with approximately 1 ng per lane of total protein (based on pre-reaction total protein concentrations) for each reaction time point examined. The western blot used to assess the resistance of the CP4 EPSPS protein to pepsin digestion (Figure 54A) was run concurrently with a western blot to estimate the LOD of the CP4 EPSPS protein (Figure 54B). The LOD of intact CP4 EPSPS protein was approximately 0.05 ng (Figure 54B, lane 10). The LOD was used to calculate the maximum relative amount of CP4 EPSPS protein that could remain visually undetected after digestion, which corresponded to approximately 5% (0.05/1 ×100% = 5%) of the total protein loaded.

Western blot analysis demonstrated that the CP4 EPSPS protein was degraded below the LOD within 0.25 min (15 seconds) of incubation in the presence of pepsin (Figure 54A, lane 5). Based on the western blot LOD for the CP4 EPSPS protein, it can be concluded that more than 95% (100% - 5% = 95%) of the intact CP4 EPSPS protein was degraded within 0.25 min. No peptide fragments were detected at any timepoint in pepsin by western blot.

No apparent change in the CP4 EPSPS protein band intensity was observed in the absence of pepsin in the 0 min No Pepsin Control and 60 min No Pepsin Control samples (Figure 54A, lanes 2 and 15). This indicates that the degradation of the CP4 EPSPS protein was due to the proteolytic activity of pepsin and not due to instability of the protein while incubated in the test system over the course of the experiment.

No immunoreactive bands were observed in the 0 min No Protein Control and 60 min No Protein Control samples (Figure 54A, lanes 3 and 14). This result indicates that there was no non-specific interaction between the pepsin solution and the CP4 EPSPS-specific antibody under these experimental conditions.

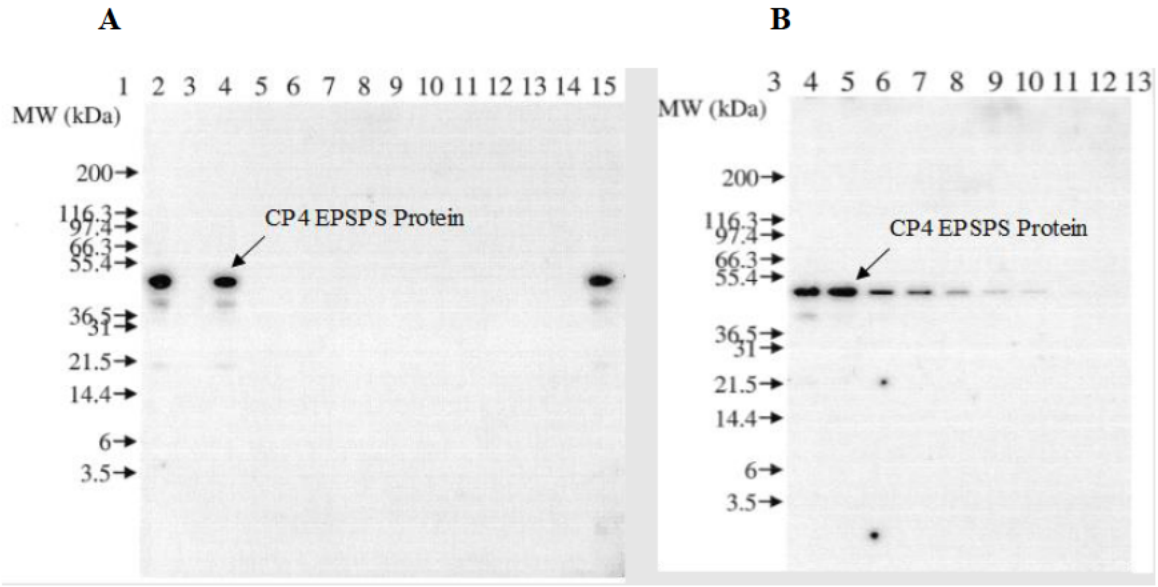

Figure 54. Western Blot Analysis of the Degradation of the KWS20-1 Sugar Beet-Produced CP4 EPSPS Protein by Pepsin

Western blots probed with an anti-CP4 EPSPS antibody were used to assess the degradation of CP4 EPSPS by pepsin. Molecular weights (kDa) are shown on the left of each gel, and correspond to the markers loaded (cropped from images). Blank lanes were cropped from the images.

Panel A: CP4 EPSPS protein degradation by pepsin. Based on total pre-reaction protein concentrations, 1 ng of *E. coli*-produced CP4 EPSPS protein was loaded in each lane containing CP4 EPSPS protein.

Panel B: LOD determination. Indicated amounts of the *E. coli*-produced CP4 EPSPS protein from the Pepsin Treated T0 sample were loaded to estimate the LOD of the CP4 EPSPS protein. Lane designations are as follows:

Lane	Sample	Incubation Time (min)
1	Molecular Weight Marker	-
2	0 min No Pepsin Control	0
3	0 min No Test Protein Control	0
4	Pepsin Treated T0	0
5	Pepsin Treated T1	0.25
6	Pepsin Treated T2	0.5
7	Pepsin Treated T3	1
8	Pepsin Treated T4	2
9	Pepsin Treated T5	4
10	Pepsin Treated T6	8
11	Pepsin Treated T7	15
12	Pepsin Treated T8	30
13	Pepsin Treated T9	60
14	60 min Test Protein No Control	60
15	60 min No Pepsin Control	60

Lane	Sample	Amount (ng)
1	Empty	-
2	Empty	-
3	Molecular Weight Marker	-
4	Pepsin Treated T0	1
5	Pepsin Treated T0	0.5
6	Pepsin Treated T0	0.4
7	Pepsin Treated T0	0.3
8	Pepsin Treated T0	0.2
9	Pepsin Treated T0	0.1
10	Pepsin Treated T0	0.05
11	Pepsin Treated T0	0.02
12	Pepsin Treated T0	0.01
13	Molecular Weight Marker	-
14	Empty	-
15	Empty	-

Degradation of CP4 EPSPS Protein in the Presence of Pancreatin

The KWS20-1 sugar beet-produced CP4 EPSPS protein degradation in pancreatin was assessed by western blot analysis. The *E. coli*-produced CP4 EPSPS protein was loaded with approximately 10 ng per lane of total protein (based on pre-reaction total protein concentrations) for each reaction time point examined. CP4 EPSPS protein standard was loaded at 5 ng and 10 ng on the same gel (Figure 55, lane 1 and 2). Greater than 50% of the CP4 EPSPS protein was degraded after a 10 min incubation in pancreatin at 37°C (Figure 55, lane 6) compared to the level detected at time zero (lane 5) and that of 5 ng load of CP4 EPSPS (lane1). No CP4 EPSPS protein was detected after incubation in pancreatin for 100 min or longer (lanes 8-10 and 12). This result is similar to the results reported by Harrison et al. (1996).

For details, please refer to Appendix 17.

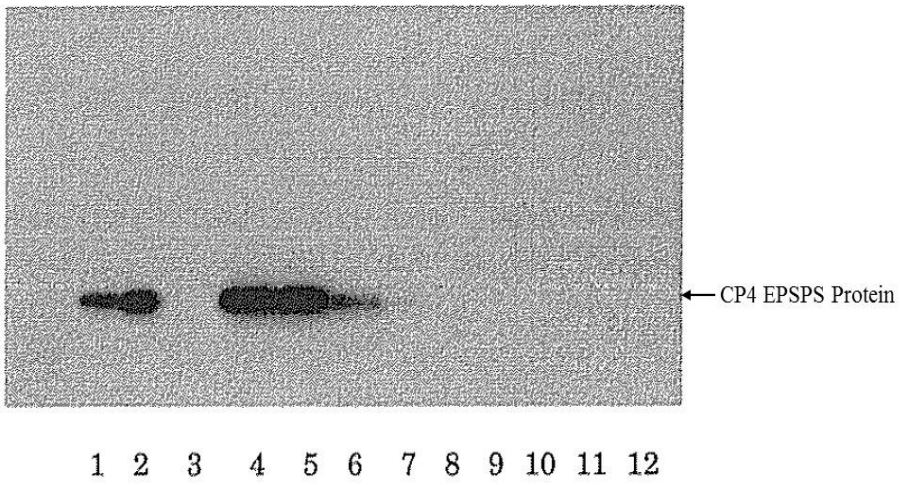

Figure 55. Western Blot Analysis of the KWS20-1 Sugar Beet-Produced CP4 EPSPS Protein Degradation in Pancreatin

The *E. coli*-produced CP4 EPSPS protein was added to pancreatin to a final concentration of 50 µg/ml, and incubated at 37°C for the designated duration as indicated below. The reactions were terminated by heating at ~100°C for 5 min before analysis by SDS-PAGE followed by western.

Lane	Sample	Incubation Time (min)
1	*E. coli*-produced CP4 EPSPS (5ng)	0
2	*E. coli*-produced CP4 EPSPS (10ng)	0
3	Pancreatin only	0
4	*E. coli*-produced CP4 EPSPS (10ng)	0
5	Pancreatin Treated T1 (10ng)	0
6	Pancreatin Treated T2 (10ng)	10
7	Pancreatin Treated T3 (10ng)	32
8	Pancreatin Treated T4 (10ng)	100
9	Pancreatin Treated T5 (10ng)	270
10	Pancreatin Treated T6 (10ng)	1181
11	Pancreatin only	1171
12	*E. coli*-produced CP4 EPSPS (10ng) + Pancreatin	1160

Digestive Fate of the CP4 EPSPS Protein Conclusions

Experiments designed to test the digestibility of the KWS20-1 sugar beet-produced CP4 EPSPS protein by pepsin were performed. Results indicate that the CP4 EPSPS protein was rapidly digested when incubated in pepsin. At least 98% of the full length CP4 EPSPS protein was digested within 15 seconds in pepsin when analyzed using Colloidal Brilliant Blue G stained SDS polyacrylamide gels. At least 95% of the CP4 EPSPS protein was digested within 15 seconds in pepsin when evaluated using western blot analysis. No proteolytic fragments were observed for samples evaluated using western blot analysis. The CP4 EPSPS protein was also rapidly digested when incubated in pancreatin. Greater than 50% of the CP4 EPSPS protein was digested within 10 minutes in pancreatin when evaluated using western blot analysis.

Results from these experiments show that the CP4 EPSPS protein is rapidly degraded by pepsin and pancreatin. Rapid degradation of the CP4 EPSPS protein in the presence of pepsin and pancreatin supports the conclusion that the CP4 EPSPS protein is highly unlikely to pose a safety concern to human and animal health.

B.2(a)(iii) An animal toxicity study if the bioinformatic comparison and biochemical studies indicate either a relationship with known protein toxins/anti-nutrients or resistance to proteolysis

Not relevant for this product.

B.2(b) Information on the potential allergenicity of any new proteins, including:

B.2(b)(i) Source of the new proteins

B.2(b)(i)(i) Identity and Source of the *dmo* Gene Introduced into KWS20-1 Sugar Beet

The *dmo* gene is derived from the bacterium *Stenotrophomonas maltophilia* strain DI-6, isolated from soil at a dicamba manufacturing plant (Krueger *et al.*, 1989). *S. maltophilia* is ubiquitously present in the environment (Mukherjee and Roy, 2016), including in water and dairy products (Todaro *et al.*, 2011; Okuno *et al.*, 2018; An and Berg, 2018). These bacteria have been used as an effective biocontrol agent against plant and animal pathogensis (Mukherjee and Roy, 2016), and have antibacterial activity against both gram-positive and gram-negative bacteria (Dong *et al.*, 2015). *S. maltophilia* has been found in healthy individuals without any hazard to human health (Heller *et al.*, 2016; Lira *et al.*, 2017), although these bacteria can form biofilms that become resistant to antibiotics (Berg and Martinez, 2015; Brooke *et al.*, 2017). The opportunistic pathogenicity of *S. maltophilia* is mainly associated with hosts with compromised immune systems rather than with any specific virulence genes of these bacteria. Thus, documented occurrences of *S. maltophilia* infections have been limited to immune-compromised individuals in hospital settings (Lira *et al.*, 2017).

Other than the potential to become an opportunistic pathogen in immune-compromised hosts, *S. maltophilia* is not known for human or animal pathogenicity. *S. maltophilia's* history of safe exposure has been extensively reviewed during the evaluation of several dicamba-tolerant events with no safety or allergenicity issues identified by FSANZ or other regulatory agencies (e.g., MON 88701 cotton [A1080], MON 87708 soybean [A1063], MON 87419 maize [A1118], MON 87429 maize [A1192] and MON 94100 canola [A1216].

B.2(b)(i)(ii) Identity and Source of the *pat* Gene Introduced into KWS20-1 Sugar Beet

The *pat* gene is derived from the bacterium *Streptomyces viridochromogenes* (Wohlleben *et al.*, 1988). *Streptomyces* species are widespread in the environment and present no known allergenic or toxicity issues (Kutzner, 1981; Kämpfer, 2006), though human exposure is quite common (Goodfellow and Williams, 1983). *S. viridochromogenes* is not considered pathogenic to plants, humans or other animals (Locci, 1989; Cross, 1989; Goodfellow and Williams, 1983). *S. viridochromogenes* is widespread in the environment and the history of safe use is discussed in Hérouet *et al.* (2005). This organism has been extensively reviewed during the evaluation of several glufosinate-tolerant events (e.g., A2704-12 and A5547-127 soybean [A481], MON 87419 maize [A1118] and MON 87429 maize [A1192]) with no safety or allergenicity issues identified by FSANZ or other regulatory agencies.

B.2(b)(i)(iii) Identity and Source of the *cp4 epsps* Gene Introduced into KWS20-1 Sugar Beet

The donor organism for *cp4 epsps* is *Agrobacterium* sp. strain CP4 (Padgette *et al.*, 1996). *Agrobacterium* species are not known for human or animal pathogenicity and are not commonly allergenic (FAO-WHO, 1991; Mehrotra and Goyal, 2012; Nester, 2015). The history of safe use of the CP4 EPSPS protein from *Agrobacterium* sp. strain CP4 has been previously reviewed as a part of the safety assessment of this donor organism with FSANZ regarding glyphosate-tolerant biotech crop events of MON 89788 soybean [A592], MON 88302 canola [A1071], NK603 maize [A416], MON 88017 maize [A548], MON 87411 maize [A1097], H7-1 sugar beet [A525], J101/163 alfalfa [A575], and MON 88913 cotton [A553].

B.2(b)(ii) A bioinformatics comparison of the amino acid sequence to known allergens

Structural similarity of the DMO, PATand CP4 EPSPS proteins to known allergens

The Codex guidelines for the evaluation of the allergenicity potential of introduced proteins (Codex Alimentarius, 2009) are based on the comparison of amino acid sequences between introduced proteins and allergens, where allergenic cross-reactivity may exist if the introduced protein is found to have at least 35% amino acid identity with an allergen over any segment of at least 80 amino acids. The Codex guideline also suggests that a sliding window search with a scientifically justified peptide size be used to identify immunologically relevant peptides in otherwise unrelated proteins. Therefore, the extent of sequence similarities between the KWS20-1 sugar beet-produced DMO, PAT and CP4 EPSPS proteins sequence and known allergens, gliadins, and glutenins was assessed using the FASTA sequence alignment tool along with an eight-amino acid sliding window search (Thomas *et al.*, 2005; Codex Alimentarius, 2009). The methods used are summarized below and detailed in Appendix 11, Appendix 12 and Appendix 13. The data generated from these analyses confirm that the KWS20-1 sugar beet-produced DMO, PAT and CP4 EPSPS proteins do not share amino acid sequence similarities with known allergens, gliadins, or glutenins.

The FASTA program directly compares amino acid sequences (i.e., primary, linear protein structure). This alignment data may be used to infer shared higher order structural similarities between two sequences (i.e., secondary and tertiary protein structures). Proteins that share a high degree of similarity throughout the entire sequence are often homologous. By definition, homologous proteins have common secondary structures, and three-dimensional configuration, and, consequently, may share similar functions. The allergen, gliadin, and glutenin protein sequence database (AD_2022) was obtained as the "COMprehensive Protein Allergen REsource" (COMPARE) database from the Health and Environmental Sciences Institute (HESI) and was used for the evaluation of sequence similarities shared between the DMO, PAT and CP4 EPSPS proteins and all proteins in the database. The AD_2022 database contains 2,463 sequences. When used to align the sequence of the introduced protein to each protein in the database, the FASTA algorithm produces an *E*-score (expectation score) for each alignment. The *E*-score is a statistical measure of the likelihood that the observed similarity score could have occurred by chance in a search. A larger *E*-score indicates a low degree of similarity between the query sequence and the sequence from the database. Typically, alignments between two sequences which have an *E*-score of less than or equal to 1×10^{-5} are considered to have meaningful homology. Results indicate that the DMO, PAT and CP4 EPSPS proteins sequences do not share meaningful similarity with sequences in the allergen database. No alignment met or exceeded the threshold of 35% identity over 80 amino acids recommended by Codex Alimentarius (2009), shared an eight amino acid match, or had an *E*-score of less than or equal to 1×10^{-5}.

The bioinformatic results demonstrated there were no biologically-relevant sequence similarities to allergens when the DMO, PAT and CP4 EPSPS proteins sequences were used as a query for a FASTA search of the AD_2022 database. Furthermore, no short (eight amino acid) polypeptide matches were shared between the DMO, PAT and CP4 EPSPS proteins sequences and proteins in the allergen database. These data show that DMO, PAT and CP4 EPSPS proteins sequences lack both structurally and immunologically relevant similarities to known allergens, gliadins, and glutenins.

For details, please refer to Appendix 11, Appendix 12 and Appendix 13.

B.2(b)(iii) The new protein's structural properties, including, but not limited to, its susceptibility to enzymatic degregation (e.g. proteolysis), heat and/or acid stability

Sugar beets are primarily grown for food use as sugar and are rarely used as a raw commodity (OECD, 2002a; CFIA, 2012). There are several processes that are used in sugar beet processing, including liming, carbonation, filtration, heating and crystallization (Klein *et al.*, 1998; ACSC, 2022). During the sugar refining process, sugar beet roots are processed into white sugar for food, and molasses and pulp that are used mainly for livestock feed (see Section A.2(b)).

Previous work (Klein *et al.*, 1998) has demonstrated that it is highly unlikely that any significant amount of sugar beet genomic DNA or protein are present in sugar following commercial processing. The removal and degradation of the DNA and protein from the sugar beet root materials during the manufacturing process was attributed to nucleolytic degradation of the DNA, irreversible adsorption on sludge, precipitation, denaturation and hydrolysis during alkaline pH and the high temperature carbonation steps, followed by hydrolysis at high temperatures during evaporation steps, and the physical exclusion of DNA and protein from refined sugar during crystallization. For the unlikely scenario that KWS20-1 sugar beet-produced DMO, PAT and CP4 EPSPS proteins are present in sugar derived foods, heat susceptibility assessments were conducted.

B.2(b)(iii)(i) Heat Susceptibility of the KWS20-1 Sugar Beet-Produced DMO Protein

Temperature can have a profound effect on the structure and function of a protein. Heat treatment is widely used in the preparation of foods containing sugar derived from sugar beet. If residual protein is present in refined sugar, it is reasonable that such heat treatment will have an effect on the functional activity and structure of the DMO protein when consumed in different food products derived from KWS20-1 sugar beet processed sugar. Therefore, an assessment of the effect of heating was conducted in the unlikely situation that the DMO protein is encountered during the preparation of foods prepared from KWS20-1 sugar beet derived sugar.

The effect of heat treatment on the activity of KWS20-1 sugar beet-produced DMO protein was evaluated using purified *E. coli*-produced DMO protein. Heat-treated samples and an unheated control sample of DMO protein were analyzed: 1) using a functional assay to assess the impact of temperature on the enzymatic activity of DMO protein; and 2) using SDS-PAGE to assess the impact of temperature on protein integrity.

Aliquots of the *E. coli*-produced DMO protein were heated to 25, 37, 55, 75 and 95°C for either 15 or 30 minutes, while a separate aliquot of DMO protein was maintained on ice for the duration of the heat treatments to serve as a temperature control. The effect of heat treatment on the activity of DMO was evaluated using a functional activity assay (Appendix 18). The effect of heat treatment on the integrity of DMO protein was evaluated using SDS-PAGE analysis of the heated and temperature control DMO protein samples.

The effects of heating on the functional activity of DMO protein are presented in Table 30 and Table 31. The DMO protein incubated at 25ºC and 37°C for 15 and 30 minutes was shown to retain functional activity; as determined by the DMO functional activity assay. The functional activity of the DMO protein incubated at 55°C for 15 and 30 minutes was reduced to 22% and 12%, respectively. However, when heated to temperatures of 75ºC or greater for 15 and

30 minutes, the DMO protein activity was reduced to 0% relative to the control sample. These results suggest that temperature has a considerable effect on the activity of DMO protein.

Analysis by SDS-PAGE stained with Brilliant Blue G Colloidal demonstrated that heat treatment to temperatures of 25, 37 and 55ºC for 15 (Figure 56, lanes 3-5) or 30 minutes (Figure 57, lanes 3-5) did not cause observable changes in the ~38 kDa DMO protein band intensity. Higher molecular weight species were visible at heat treatments of 55, 75 and 95ºC for 15 (Figure 56, lanes 5-7) and 30 minutes (Figure 57, lanes 5-7). The band intensity at ~38 kDa is greatly reduced at 95ºC for 15 minutes (Figure 56, lane 7) and 30 minutes (Figure 57, lane 7), which is likely due to aggregation of the DMO protein when exposed to high temperatures.

These data demonstrate that the DMO protein remains largely intact but behaves with a predictable tendency toward protein denaturation and loss of functional activity at elevated temperatures. Heat treatment is widely used in the preparation of foods containing sugar derived from sugar beets. Therefore, it is reasonable to conclude that in the unlikely situation that the KWS20-1 sugar beet-produced DMO protein were present in sugar, it would not be consumed as an active protein in food derived from KWS20-1 sugar beet due to standard processing practices that include heat treatment.

For details, please refer to Appendix 18.

Table 30. Functional Activity Assay of Heat-Treated KWS20-1 Sugar Beet-Produced DMO Protein after 15 Minutes at Elevated Temperatures

Treatment	Specific Activity (nmol × minute^{-1} × mg^{-1})[1]	Relative Activity (% of control sample)[2,3]
Control Treatment (wet ice)	409	100%[2]
25ºC	418	102%
37ºC	429	105%
55ºC	91	22%
75ºC	0	0%
95ºC	0	0%

[1] Mean specific activity determined from n=3.
[2] DMO protein activity of control samples was assigned 100% active.
[3] Relative Activity = [specific activity of sample/specific activity of control sample] × 100

Table 31. Functional Activity Assay of Heat-Treated KWS20-1 Sugar Beet-Produced DMO Protein after 30 Minutes at Elevated Temperatures

Treatment	Specific Activity (nmol × minute^{-1} × mg^{-1})[1]	Relative Activity (% of control sample)[2,3]
Control Treatment (wet ice)	329	100%[2]
25ºC	353	107%
37ºC	362	110%
55ºC	38	12%
75ºC	0	0%
95ºC	0	0%

[1] Mean specific activity determined from n=3.
[2] DMO protein activity of control samples was assigned 100% active.
[3] Relative Activity = [specific activity of sample/specific activity of control sample] × 100

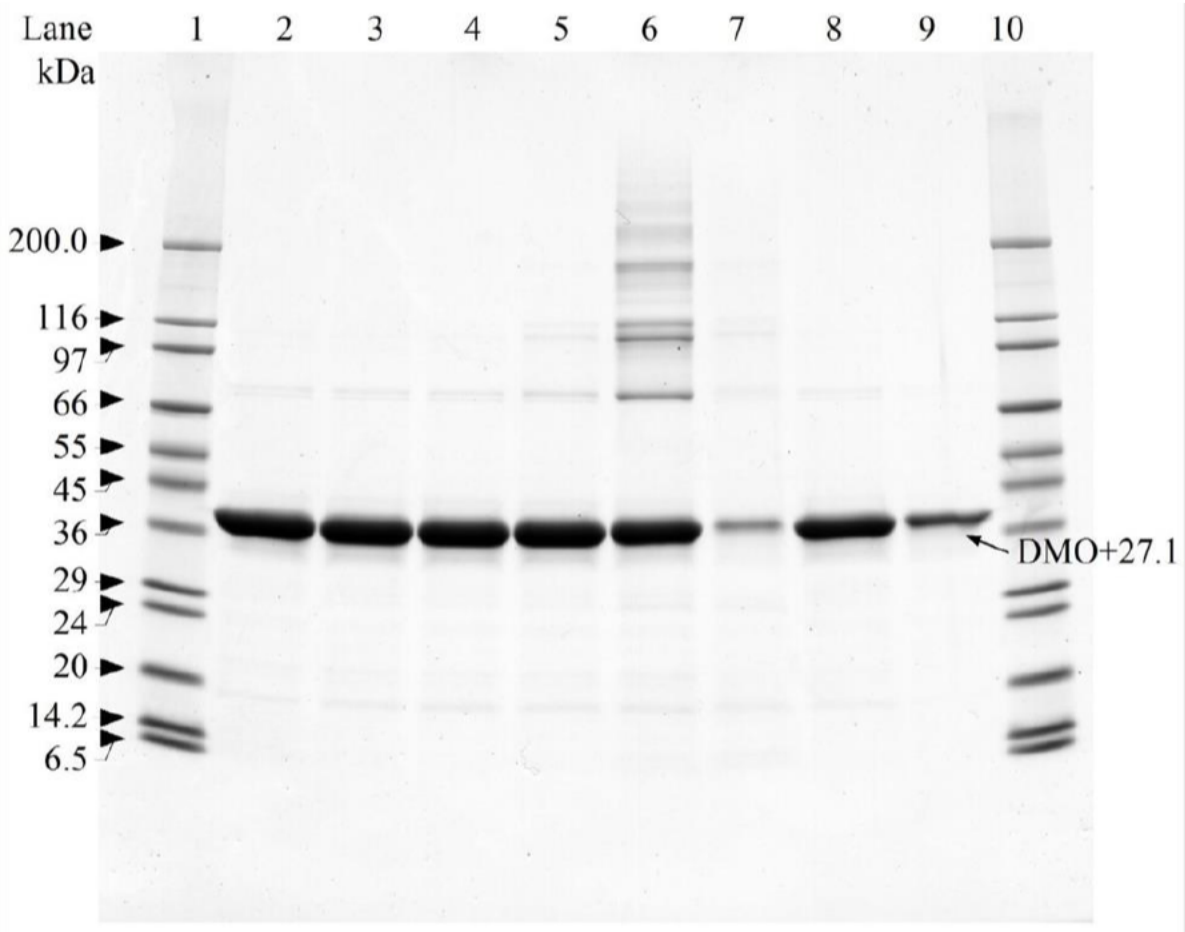

Figure 56. SDS-PAGE of KWS20-1 Sugar Beet-Produced DMO Protein Demonstrating the Effect on Protein Structural Stability After 15 Minutes at Elevated Temperatures

Heat-treated samples of *E. coli*-produced DMO (3.0 µg total protein) separated on a Tris-glycine 4-20% polyacrylamide gel under denaturing and reducing conditions. The gel was stained with Brilliant Blue G Colloidal. Approximate molecular weights (kDa) are shown on the left and correspond to molecular weight markers in lanes 1 and 10.

Lane	Description	Total Amount
1	SigmaMark Wide Range Molecular Weight Marker	-
2	*E. coli*-produced DMO Protein Control (wet ice)	3.0 µg
3	*E. coli*-produced DMO Protein 25ºC	3.0 µg
4	*E. coli*-produced DMO Protein 37ºC	3.0 µg
5	*E. coli*-produced DMO Protein 55ºC	3.0 µg
6	*E. coli*-produced DMO Protein 75ºC	3.0 µg
7	*E. coli*-produced DMO Protein 95ºC	3.0 µg
8	*E. coli*-produced DMO Protein Reference 100% Equivalence	3.0 µg
9	*E. coli*-produced DMO Protein Reference 10% Equivalence	0.3 µg
10	SigmaMark Wide Range Molecular Weight Marker	-

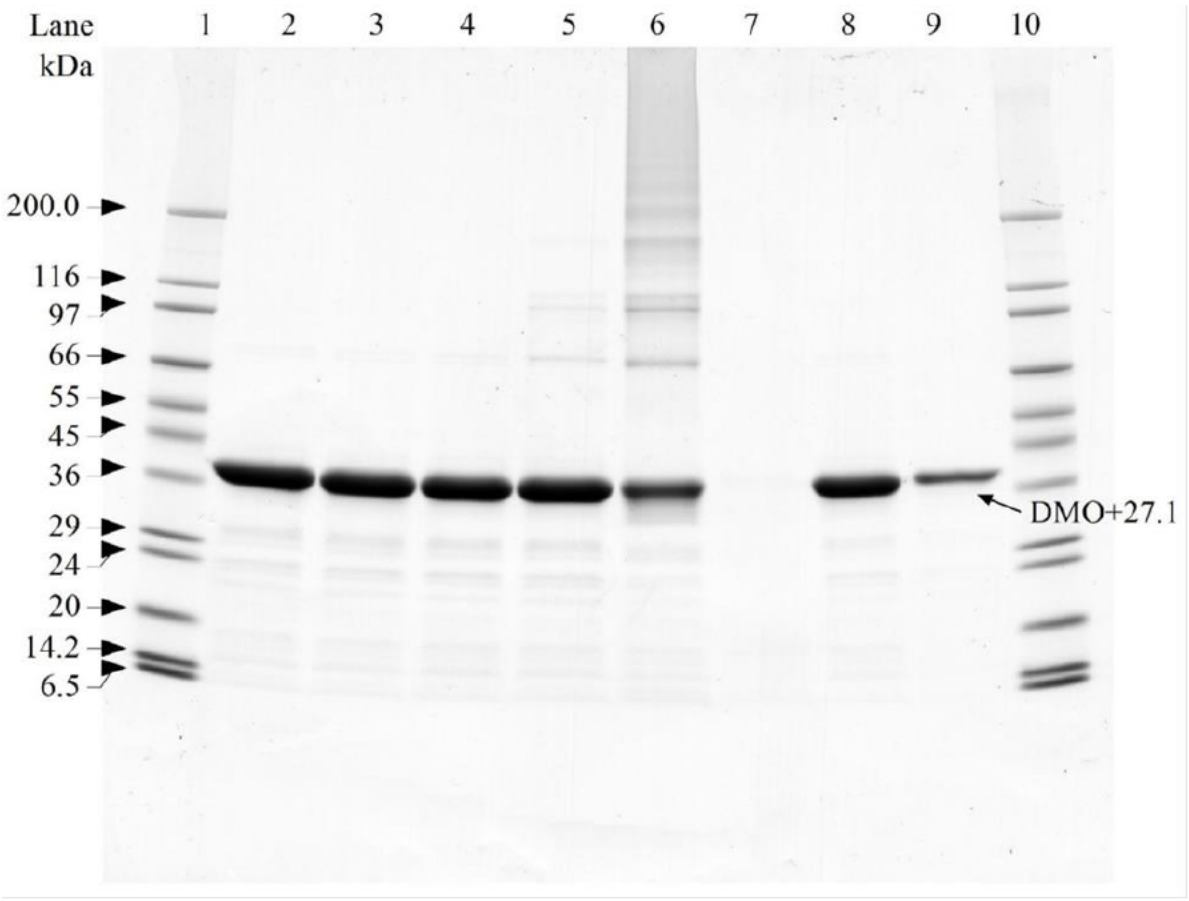

Figure 57. SDS-PAGE of KWS20-1 Sugar Beet-Produced DMO Protein Demonstrating the Effect on Protein Structural Stability After 30 Minutes at Elevated Temperatures

Heat-treated samples of *E. coli*-produced DMO (3.0 µg total protein) separated on a Tris-glycine 4-20% polyacrylamide gel under denaturing and reducing conditions. The gel was stained with Brilliant Blue G Colloidal. Approximate molecular weights (kDa) are shown on the left and correspond to molecular weight markers in lanes 1 and 10.

Lane	Description	Total Amount
1	SigmaMark Wide Range Molecular Weight Marker	-
2	*E. coli*-produced DMO Protein Control (wet ice)	3.0 µg
3	*E. coli*-produced DMO Protein 25ºC	3.0 µg
4	*E. coli*-produced DMO Protein 37ºC	3.0 µg
5	*E. coli*-produced DMO Protein 55ºC	3.0 µg
6	*E. coli*-produced DMO Protein 75ºC	3.0 µg
7	*E. coli*-produced DMO Protein 95ºC	3.0 µg
8	*E. coli*-produced DMO Protein Reference 100% Equivalence	3.0 µg
9	*E. coli*-produced DMO Protein Reference 10% Equivalence	0.3 µg
10	SigmaMark Wide Range Molecular Weight Marker	-

B.2(b)(iii)(ii) Heat Susceptibility of KWS20-1 Sugar Beet-Produced PAT Protein

Temperature can have a profound effect on the structure and function of a protein. Heat treatment is widely used in the preparation of foods containing sugar derived from sugar beet. If residual protein is present in refined sugar, it is reasonable that such heat treatment will have an effect on the functional activity and structure of the PAT protein when consumed in different food products derived from KWS20-1 sugar beet processed sugar. Therefore, an assessment of the effect of heating was conducted in the unlikely situation that the PAT protein is encountered during the preparation of foods prepared from KWS20-1 sugar beet derived sugar.

The effect of heat treatment on the activity of KWS20-1 sugar beet-produced PAT protein was evaluated using the *E. coli*-produced PAT protein. Heat-treated samples and an unheated control sample of PAT protein were analyzed: 1) using a functional assay to assess the impact of temperature on the enzymatic activity of PAT protein; and 2) using SDS-PAGE to assess the impact of temperature on protein integrity.

Aliquots of PAT protein were heated to 25, 37, 55, 75, and 95 °C for either 15 or 30 minutes, while a separate aliquot of PAT protein was maintained on ice for the duration of the heat treatments to serve as a temperature control. The effect of heat treatment on the activity of PAT protein was evaluated using a functional activity assay. The effect of heat treatment on the integrity of the PAT protein was evaluated using SDS-PAGE analysis of the heated and temperature control PAT protein samples.

The effects of heating on the functional activity of PAT are presented in Table 32 and Table 33. The functional activity of PAT protein was unaffected at 25 and 37 ºC for 15 and 30 minutes. The functional activity of the PAT protein was reduced by approximately 90% or greater relative to the activity of control PAT protein whether heated at 55°C and above for 15 or 30 min. These results suggest that temperature has a considerable effect on the functional activity of PAT protein.

Analysis by SDS-PAGE stained with Brilliant Blue G-Colloidal demonstrated that the PAT control treatment and reference standard contain a major band at ~25 kDa, corresponding to the PAT protein (Figure 58 and Figure 59, Lanes 2 and 8). No apparent decrease in the intensity of this band was observed in heat-treated PAT protein at 25, 37, 55, 75 and 95 °C for 15 minutes (Figure 58, Lanes 3-7) or 30 minutes (Figure 59, Lanes 3-7). However, PAT protein heated to 95ºC for 15 and 30 minutes (Figure 58 and Figure 59, Lane 7) showed some appearance of higher molecular weight species, which may be due to slight aggregation of the PAT protein when exposed to high temperatures.

These data demonstrate that PAT protein remains intact, but is deactivated at 55 ºC and above. This is comparable with what has been previously published on the safety assessment of PAT protein (Hérouet *et al.*, 2005). Therefore, it is reasonable to conclude that PAT protein would not be consumed as an active protein in food or feed products due to standard processing practices that include heat treatment.

For details, please refer to Appendix 19.

Table 32. Functional Activity of KWS20-1 Sugar Beet-Produced PAT Protein after 15 Minutes at Elevated Temperatures

Temperature	Specific Activity ($\mu mol \times minute^{-1} \times mg^{-1}$) [1]	Relative Activity (% of control sample) [2,3]
0 ºC (control)	24.5	100 %
25 ºC	26.7	109 %
37 ºC	26.9	110 %
55 ºC	2.8	11 %
75 ºC	0.9	4 %
95 ºC	1.1	4 %

[1] Mean specific activity determined from n=3.
[2] PAT protein activity of control samples was assigned 100 % active.
[3] Relative Activity = [specific activity of sample/specific activity of control sample] × 100

Table 33. Functional Activity of KWS20-1 Sugar Beet-Produced PAT Protein after 30 Minutes at Elevated Temperatures

Temperature	Specific Activity ($\mu mol \times minute^{-1} \times mg^{-1}$) [1]	Relative Activity (% of control sample) [2,3]
0 ºC (control)	24.5	100 %
25 ºC	31.2	127 %
37 ºC	29.8	122 %
55 ºC	1.0	4 %
75 ºC	1.1	4 %
95 ºC	1.3	5 %

[1] Mean specific activity determined from n=3.
[2] PAT protein activity of control sample was assigned 100 % active.
[3] Relative Activity = [specific activity of sample/specific activity of control sample] × 100

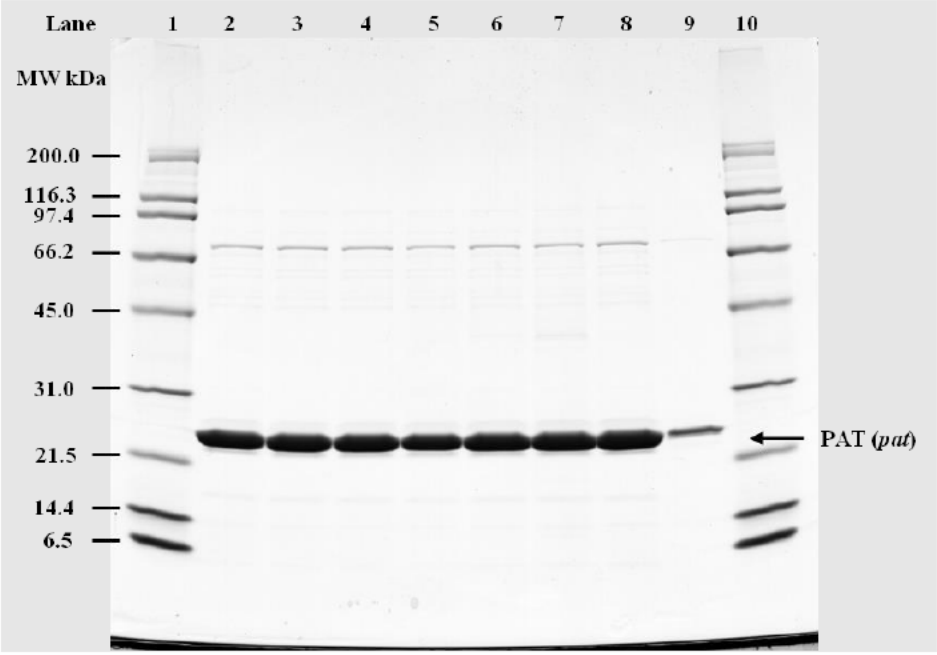

Figure 58. SDS-PAGE of KWS20-1 Sugar Beet-Produced PAT Protein Following Heat Treatment for 15 Minutes

Heat treated samples of *E. coli*-produced PAT (3.0 µg total protein) separated on a Tris-glycine 4-20 % polyacrylamide gel under denaturing and reducing conditions. The gel was stained with Brilliant Blue G-Colloidal. Molecular weights (kDa) are shown on the left and correspond to molecular weight markers in lanes 1 and 10.

Lane	Description	Total Amount
1	Broad Range™ Molecular Weight Markers	-
2	*E. coli*-produced PAT Protein Control	3.0
3	*E. coli*-produced PAT Protein 25 ºC	3.0
4	*E. coli*-produced PAT Protein 37 ºC	3.0
5	*E. coli*-produced PAT Protein 55 ºC	3.0
6	*E. coli*-produced PAT Protein 75 ºC	3.0
7	*E. coli*-produced PAT Protein 95 ºC	3.0
8	*E. coli*-produced PAT Protein Reference 100 % Equivalence	3.0
9	*E. coli*-produced PAT Protein Reference 10 % Equivalence	0.3
10	Broad Range Molecular Weight Markers	-

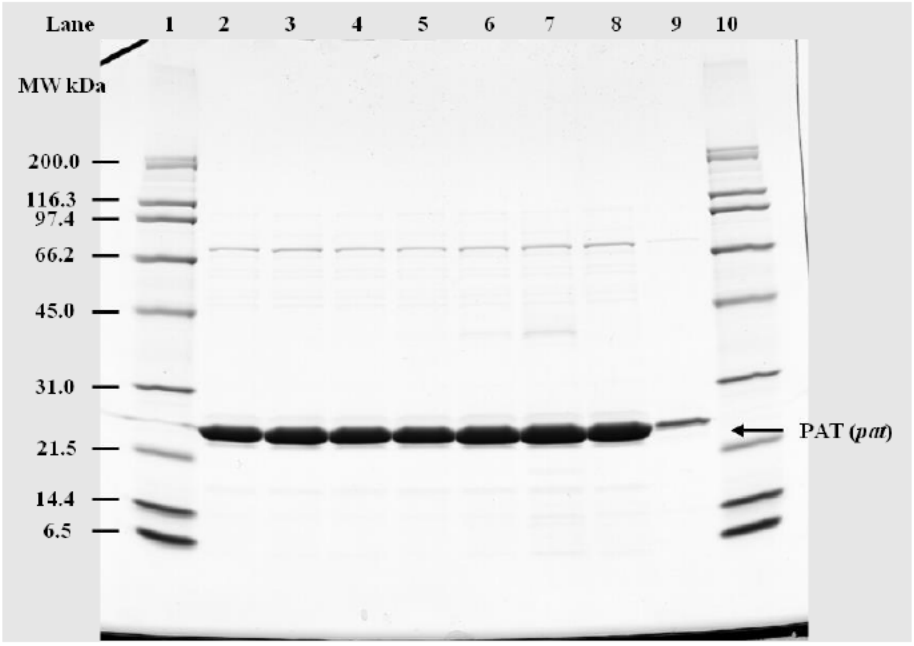

Figure 59. SDS-PAGE of KWS20-1 Sugar Beet-Produced PAT Protein Following Heat Treatment for 30 Minutes

Heat treated samples of *E. coli*-produced PAT (3.0 µg total protein) separated on a Tris-glycine 4-20 % polyacrylamide gel under denaturing and reducing conditions. The gel was stained with Brilliant Blue G-Colloidal. Molecular weights (kDa) are shown on the left and correspond to molecular weight markers in lanes 1 and 10.

Lane	Description	Total Amount
1	Broad Range™ Molecular Weight Markers	-
2	*E. coli*-produced PAT Protein Control	3.0
3	*E. coli*-produced PAT Protein 25 ºC	3.0
4	*E. coli*-produced PAT Protein 37 ºC	3.0
5	*E. coli*-produced PAT Protein 55 ºC	3.0
6	*E. coli*-produced PAT Protein 75 ºC	3.0
7	*E. coli*-produced PAT Protein 95 ºC	3.0
8	*E. coli*-produced PAT Protein Reference 100 % Equivalence	3.0
9	*E. coli*-produced PAT Protein Reference 10 % Equivalence	0.3
10	Broad Range™ Molecular Weight Markers	-

B.2(b)(iii)(iii) Heat Susceptibility of the KWS20-1 Sugar Beet-Produced CP4 EPSPS Protein

Temperature can have a profound effect on the structure and function of a protein. Heat treatment is widely used in the preparation of foods containing sugar derived from sugar beet. If residual protein is present in refined sugar, it is reasonable that such heat treatment will have an effect on the functional activity and structure of the CP4 EPSPS protein when consumed in different food products derived from KWS20-1 sugar beet processed sugar. Therefore, an assessment of the effect of heating was conducted in the unlikely situation that the CP4 EPSPS protein is encountered during the preparation of foods prepared from KWS20-1 sugar beet derived sugar.

The effect of heat treatment on the activity of KWS20-1 sugar beet-produced CP4 EPSPS protein was evaluated using the *E. coli*-produced CP4 EPSPS protein. The method for evaluating heat susceptibility is described in Appendix 20. Heat-treated samples and an unheated control sample of CP4 EPSPS protein were analyzed: 1) using a functional assay to assess the impact of temperature on the enzymatic activity of CP4 EPSPS protein; and 2) using SDS-PAGE to assess the impact of temperature on protein integrity.

Aliquots of the CP4 EPSPS protein were heated to 25, 37, 55, 75, and 95°C for either 15 or 30 minutes, while a single aliquot of the control substance was maintained on wet ice for the duration of the heat treatments. Heated CP4 EPSPS protein and unheated temperature control substance were analyzed by a CP4 EPSPS activity assay to assess the impact of temperature on the functional activity of CP4 EPSPS protein. Additionally, the protein resulting from each temperature treatment was analyzed by SDS-PAGE to assess CP4 EPSPS degradation.

The effects of heating on the functional activity of CP4 EPSPS protein are presented in Table 34 and Table 35. When heated at a temperature of 25 ºC, 37 ºC and 55 ºC with an incubation time of 15 minutes, a small reduction in CP4 EPSPS activity was observed to 81%, 84%, and 70% of control respectively. The CP4 EPSPS heated for 30 minutes showed no negative change in CP4 EPSPS activity at 25 ºC and a small reduction in activity to 88% of control at 37ºC. The CP4 EPSPS heated to 55 ºC demonstrated a reduction in CP4 EPSPS activity with 25% activity remaining relative to the control substance after the 30 minute incubation. The level of CP4 EPSPS activity following incubation at temperatures of 75 and 95ºC was below the limit of detection for incubations at both time points.

Analysis by SDS-PAGE stained with Brilliant Blue G Colloidal dye (Figure 60 and Figure 61) demonstrated that the reference standard and control substance contain one major band with an apparent molecular weight of approximately 43.8 kDa corresponding to the CP4 EPSPS protein. Results of the SDS-PAGE data for the heat treatment of the CP4 EPSPS incubated for 15 minutes and 30 minutes are illustrated in Figure 60 and Figure 61, respectively. The control substance loaded on each respective gel (Figure 60, lane 2 and Figure 61, lane 2) showed equivalent band intensity at 43.8 kDa to the 100% reference standard (Figure 60, lane 8 and Figure 61, lane 8); demonstrating that the CP4 EPSPS protein was stable on wet ice during the incubation period. No apparent decrease in band intensity of the 43.8 kDa CP4 EPSPS protein band was observed for CP4 EPSPS when heated at all temperatures for 15 minutes (Figure 60, lanes 3-7) or 30 minutes (Figure 61, lanes 3-7).

For details, please refer to Appendix 20.

Table 34. Activity of KWS20-1 Sugar Beet-Produced CP4 EPSPS After 15 Minutes at Elevated Temperatures

Temperature	Specific Activity Units/mg CP4 EPSPS[1]	Relative activity[2]
0 ºC (control substance)	6.03±0.29	100%
25 ºC	4.88±0.24	81%
37 ºC	5.08±0.33	84%
55 ºC	4.22±0.12	70%
75 ºC	Below LOD[3]	<3%
95 ºC	Below LOD[3]	<3%

[1] Mean specific activity determined from n=2.
[2] CP4 EPSPS activity of control substance was assigned 100 % active.
% CP4 EPSPS activity remaining = [specific activity of sample/specific activity of control substance] x 100
[3] LOD is defined as the value that is three times the assay blank standard deviation plus the mean of the assay blank.

Table 35. Activity of KWS20-1 Sugar Beet-Produced CP4 EPSPS After 30 Minutes at Elevated Temperatures

Temperature	Specific Activity Units/mg CP4 EPSPS	Relative activity[2]
0 ºC (control substance)	2.8 ± 0.26	100%
25 ºC	3.1 ± 0.23	110%
37 ºC	2.5 ± 0.05	88%
55 ºC	0.70 ± 0.09	25%
75 ºC	Below LOD[3]	<8%
95 ºC	Below LOD[3]	<8%

[1] Mean specific activity determined from n=2
[2] CP4 EPSPS activity of control substance was assigned 100 % active.
% CP4 EPSPS activity remaining = [specific activity of sample/specific activity of control substance] x 100
[3] LOD is defined as the value that is three times the assay blank standard deviation plus the mean of the assay blank.

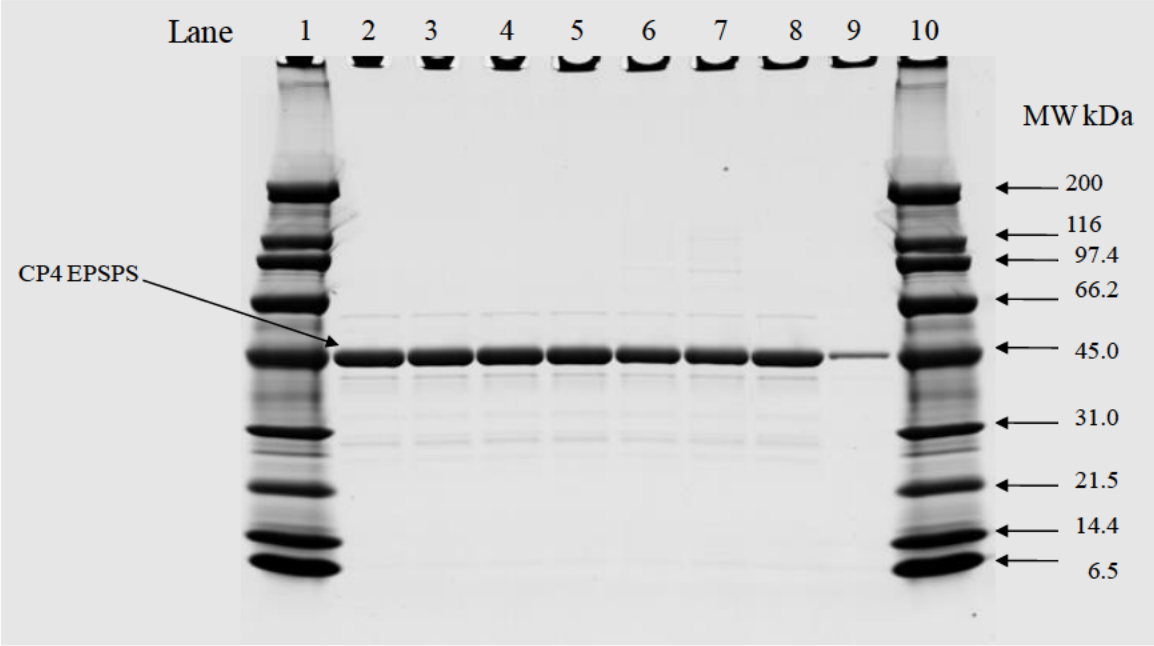

Figure 60. SDS-PAGE of KWS20-1 Sugar Beet-Produced CP4 EPSPS Protein Following Heat Treatment for 15 Minutes

Heat-treated samples of *E. coli*-produced CP4 EPSPS (3.2 µg total protein) separated on a Tris-glycine 4-20% polyacrylamide gel under denaturing and reducing conditions. Gels were stained with Brilliant Blue G Colloidal. Approximate molecular weights (kDa) are shown on the right and correspond to molecular weight markers in lanes 1 and 10.

Lane	Description	Total Amount
1	Broad Range Molecular Weight Markers	4.5 µ g
2	*E. coli*-produced CP4 EPSPS Protein Control	3.2 µ g
3	*E. coli*-produced CP4 EPSPS Protein 25 °C	3.2 µ g
4	*E. coli*-produced CP4 EPSPS Protein 37 °C	3.2 µ g
5	*E. coli*-produced CP4 EPSPS Protein 55 °C	3.2 µ g
6	*E. coli*-produced CP4 EPSPS Protein 75 °C	3.2 µ g
7	*E. coli*-produced CP4 EPSPS Protein 95 °C	3.2 µ g
8	*E. coli*-produced CP4 EPSPS Protein Reference 100% Equivalence	3.2 µ g
9	*E. coli*-produced CP4 EPSPS Protein Reference 10% Equivalence	0.32 µ g
10	Broad Range Molecular Weight Markers	4.5 µ g

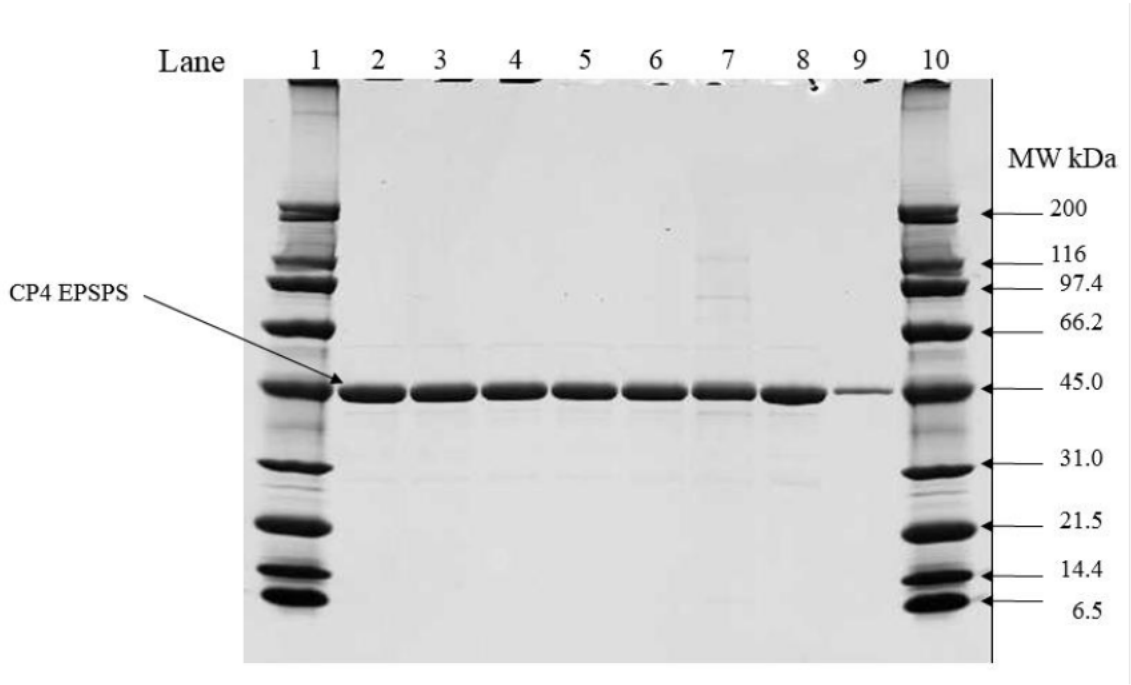

Figure 61. SDS-PAGE of KWS20-1 Sugar Beet-Produced CP4 EPSPS Protein Following Heat Treatment for 30 Minutes

Heat-treated samples of *E. coli*-produced CP4 EPSPS (3.2 µ g total protein) separated on a Tris-glycine 4-20% polyacrylamide gel under denaturing and reducing conditions. Gels were stained with Brilliant Blue G Colloidal. Approximate molecular weights (kDa) are shown on the right and correspond to molecular weight markers in lanes 1 and 10.

Lane	Description	Total Amount
1	Broad Range Molecular Weight Markers	4.5 µ g
2	*E. coli*-produced CP4 EPSPS Protein Control	3.2 µ g
3	*E. coli*-produced CP4 EPSPS Protein 25 °C	3.2 µ g
4	*E. coli*-produced CP4 EPSPS Protein 37 °C	3.2 µ g
5	*E. coli*-produced CP4 EPSPS Protein 55 °C	3.2 µ g
6	*E. coli*-produced CP4 EPSPS Protein 75 °C	3.2 µ g
7	*E. coli*-produced CP4 EPSPS Protein 95 °C	3.2 µ g
8	*E. coli*-produced CP4 EPSPS Protein Reference 100% Equivalence	3.2 µ g
9	*E. coli*-produced CP4 EPSPS Protein Reference 10% Equivalence	0.32 µ g
10	Broad Range Molecular Weight Markers	4.5 µ g

Pepsin Degradation, Pancreatin Degradation and Heat Susceptibility of the KWS20-1 Sugar Beet-Produced DMO, PAT and CP4 EPSPS Proteins – Conclusions

Previous work (Klein *et al.*, 1998) has demonstrated that it is highly unlikely that any significant amount of sugar beet genomic DNA or protein are present in sugar following commercial processing. The removal and degradation of the DNA and protein from the sugar beet root materials during the manufacturing process was attributed to nucleolytic degradation of the DNA, irreversible adsorption on sludge, precipitation, denaturation and hydrolysis during alkaline pH and the high temperature carbonation steps, followed by hydrolysis at high temperatures during evaporation steps, and the physical exclusion of DNA and protein from refined sugar during crystallization. In the unlikely scenario that KWS20-1 sugar beet-produced DMO, PAT and CP4 EPSPS proteins are present in sugar derived foods, digestive fate and heat susceptibility assessments were conducted.

Exposure to heat during food processing or cooking, and to digestive fluids is likely to have a profound effect on the structure and function of proteins. The susceptibility of a protein to heat or its degradation in the presence of pepsin and pancreatin is a factor in the assessment of its potential toxicity.

The degradation of KWS20-1 sugar beet-produced DMO, PAT and CP4 EPSPS proteins were evaluated by incubation with solutions containing pepsin and pancreatin, and the results show that KWS20-1 sugar beet-produced DMO, PAT and CP4 EPSPS proteins were readily degraded.

The effect of heat treatment on the activity of KWS20-1 sugar beet-produced DMO, PAT and CP4 EPSPS proteins was evaluated using functional assays to assess the impact of temperature on enzymatic activity, and using SDS-PAGE to assess the impact of temperature on protein integrity. The results show that KWS20-1 sugar beet-produced DMO protein was completely deactivated by heating at 75ºC or higher for 15 min or more; KWS20-1 sugar beet-produced PAT protein was substantially deactivated by heating at 55ºC and completely deactivated at 75°C or above for 15 min or more. The amount of KWS20-1 sugar beet-produced CP4 EPSPS activity remaining following heat treatment for both 15 and 30 min at 75ºC and 95ºC was below the limit of detection. Therefore, it is anticipated that exposure to functionally active KWS20-1 sugar beet-produced DMO, PAT and CP4 EPSPS proteins from the consumption of KWS20-1 sugar beet derived-sugar products is unlikely.

B.2(b)(iv) Specific serum screening where a new protein is derived from a source known to be allergenic or has sequence homology with a known allergen

Not relevant for this product.

B.2(b)(v) Information on whether the new protein(s) have a role in the elicitation of gluten-sensitive enteropathy, in cases where the introduced genetic material is obtained from wheat, rye, barley, oats, or related cereal grains

Not relevant for this product.

B.3 Other (non-protein) New Substances

Not applicable.

B.4 Novel Herbicide Metabolites in GM Herbicide-Tolerant Plants

The novel metabolites for glyphosate on sugar beet has been assessed and approved by FSANZ in application [A525], which is Bayer and KWS's first generation sugar beet product H7-1 sugar beet.

There are no novel metabolites of glufosinate or dicamba detected in treated KWS20-1 sugar beet compared to other FSANZ approved dicamba and glufosinate tolerant crops (details in A.2(a)(i)). Hence in the subsequent subsections of B.4. the magnitude of dicamba and glufosinate residues in KWS20-1 sugar beet is addressed.

B.4.(a) Dicamba Residue Study in KWS20-1 Sugar Beet

A study was conducted in the U.S. and Canada in 2020 to determine residue levels of dicamba and its major metabolites 2,5-dichloro-3-hydroxy-6-methoxybenzoic acid (5-OH dicamba), 3,6-dichloro-2-hydroxybenzoic acid (DCSA), and 2,5-dichloro-3,6-dihydroxy-benzoic acid (DCGA) in/on KWS20-1 sugar beet raw agricultural commodities (RACs) following three applications of a dicamba-based herbicide formulation.

Combined maximum application rate in the U.S. is proposed to be 2.0 lb a.i./A (2.24 kg a.i./ha). The proposed maximum application rates and corresponding application growth stages of dicamba to KWS20-1 sugar beet in the U.S. are summarized below. Any combination of application rates and timings may be used within the allowed limits for individual rates and timings as specified on the label.

Maximum Application Rates	
Combined maximum of all applications per year	2.0 lb a.i./A (2.24 kg a.i./ha)
Total of all preplant, at-planting, preemergence applications	1.0 lb a.e./acre (1.12 kg a.e./ha)
Total in-crop applications from emergence up to 10 leaves unfolded	1.0 lb a.e./acre (1.12 kg a.e./ha)
Maximum single in-crop application 0.5 lb a.e./acre	0.5 lb a.e./acre (0.56 kg a.e./ha)

Note: minimum of two weeks required between sequential applications.

The purpose of this summary is to report the residue levels of dicamba and its major metabolites 5-OH dicamba, DCSA and DCGA in/on KWS20-1 sugar beet raw agricultural commodities (RACs; roots and tops) that resulted from applications of MON 76980, a water-soluble concentrate (SL) containing 2.0 lb a.e. of dicamba per gallon. Applications of the dicamba-based herbicide

formulation, MON 76980, sold commercially as Xtendimax® with VaporGrip® Technology[4], were made to the treated plots of KWS20-1 sugar beet. Use of KWS20-1 sugar beet in this study was required to generate data that may be used to support regulatory approval of KWS20-1 sugar beet.

The field trials for the study were conducted in the U.S. and Canada at seventeen (17) sites in nine (9) states: California (Region 10); Colorado (Region 8); Idaho (Region 9 and 11); Michigan (Region 5); Minnesota (Region 5); North Dakota (Regions 5 and 7); South Dakota (Region 5); Washington (Region 11); and Wisconsin (Region 5) and one (1) providence: Alberta, Canada (Region 7). These regions were typical of the major sugar beet producing regions of North America and include the states that account for greater than 99% of the total sugar beet crop production (acreage) in the U.S.

The target application timings and rates are summarized in Table 36:

Table 36. Applications of MON 76980 to KWS20-1 Sugar Beet

Treatment	Rate as Dicamba Acid Equivalent		
	Pre-emerge Application	**Early Postemergence Application (2-4 leaves unfolded)**	**Late Postemergence Application (10 leaves unfolded)**
Control	0	0	0
Treated[1]	1.0 lb a.e./acre (1.12 kg a.e./ha) (88 fl oz MON 76980/acre)	0.5 lb a.e./acre (0.56 kg a.e./ha) (44 fl oz MON 76980/acre)	0.5 lb a.e./acre (0.56 kg a.e./ha) (44 fl oz MON 76980/acre)

[1] Treated plot is identified as Treatment 3 in the GLP study REG-2020-0051.

Actual application rates were within 5% of the target rates for all locations. The average percent of target rate across all applications and all sites was 99%.

The sugar beet root and top samples were collected at commercial maturity (BBCH 49). Samples were harvested by hand from each plot, while generally avoiding the outer rows and ends of rows. Each sample was field composited from 12 or more different locations across the entire plot. In this manner, one sample from the untreated plot was collected first, followed by the two replicate samples from the treated plot. To minimize the quantity of excessive sample tissue collected, each sugar beet root or top used for RAC sampling was quartered, and one quarter from each plant was compiled with eleven other individual quarters collected from separate plants.

Metabolism of dicamba by KWS20-1 sugar beet was demonstrated in a metabolism study. The residue of concern for tolerance setting is proposed as dicamba, DCSA, and DCGA as parent equivalents in the U.S. and Canada.

The analytical method, ME-1869-03, *Determination of Dicamba and Major Metabolites in Raw Agricultural Commodities by LC-MS/MS* with modifications, was used in this study and measured the residues of dicamba and its major metabolites, 5-OH dicamba, DCSA, and DCGA.

[4] Xtendimax® with VaporGrip® Technology is a registered trademark of Bayer Group.

The limit of quantitation (LOQ) for each analyte for each matrix (i.e., roots and tops) was determined to be 0.010 ppm in parent equivalents.

For this study, one untreated control and two treated sugar beet root and top samples from each site were analyzed.

Method performance was evaluated by use of concurrent recovery samples by fortifying each analyte for each matrix (i.e., roots and tops) at 0.010 and 0.100 ppm. The fortification levels bracketed the measured residues.

All recoveries were corrected for any interferences in corresponding controls. The overall mean of the recoveries for sugar beet roots and tops at each fortification level was within the acceptable range of 70 to 120%, and the relative standard deviation values were below 20%. The method was considered acceptable for the analysis of dicamba, 5-OH dicamba, DCSA and DCGA residues in sugar beet roots and tops.

The residues in samples collected from the treated plot in Table 36 are summarized in Table 37:

Table 37. Dicamba Residues in/on KWS20-1 Sugar Beet Raw Agricultural Commodities

Analyte	PHI (days)[1]	Treated Plot (Sugar Beet Roots)		Treated Plot (Sugar Beet Tops)	
		Median (ppm)[2]	Min-Max (ppm)[3]	Median (ppm)[2]	Min-Max (ppm)[3]
Dicamba	49-114	<0.010[4]	<0.010 - <0.010	0.0100	<0.010 - 0.0118
5-OH Dicamba	49-114	<0.010	<0.010 - <0.010	<0.010	<0.010 - <0.010
DCSA	49-114	0.0151	<0.010 - 0.0769	0.1030	<0.010 - 0.7368
DCGA	49-114	<0.010	<0.010 - 0.0293	<0.010	<0.010 - 0.0121

[1] PHI = pre-harvest interval; interval between last application and harvest (sampling) in days.
[2] Median of site averaged field sample residue values.
[3] Minimum and maximum residue range of individual field sample residue values.
[4] This method has a limit of quantitation (LOQ) of 0.010 ppm (mg/kg) for each individual analyte. Residue values <0.010 ppm are below LOQ.

The residue results indicate that the proposed U.S. EPA dicamba MRL of 0.15 ppm in sugar beet roots and of 0.9 ppm in sugar beet tops is sufficient to account for the use of dicamba on KWS20-1 sugar beets.

For details, please also refer to Appendix 21.

B.4.(b) Glufosinate Residue Study in KWS20-1 Sugar Beet

A study was conducted in the U.S. in 2020 to determine residue levels of glufosinate and its metabolites, 3-methylphosphinicopropionic acid (MPPA) and N-acetyl glufosinate (NAG), in/on KWS20-1 sugar beet raw agricultural commodities (RACs) following two applications of a glufosinate-based herbicide formulation

Combined maximum glufosinate application rate in the U.S. is 1.1 lbs a.i./acre (1.2 kg a.i./ha). Currently labeled maximum application rates and corresponding application growth stages of glufosinate to KWS20-1 sugar beet in the U.S. are summarized below. Any combination of application rates and timings may be used within the allowed limits for individual rates and timings as specified on the label.

Maximum Application Rates	
Combined maximum of all applications per year	1.1 lb a.i./acre (1.2 kg a.i./ha)
Total of all preplant, at-planting, preemergence applications	0.55 lb a.i./acre (0.62 kg a.i./ha)
Total in-crop applications from emergence up to 10 leaves unfolded	0.55 lb a.i./acre (0.62 kg a.i./ha)
Maximum single in-crop application	0.55 lb a.i./acre (0.62 kg a.i./ha)

Note: Do not apply closer than ten (10) days apart. Do not apply within sixty (60) days of harvesting sugar beets.

The purpose of this summary is to report the residue levels of glufosinate and its metabolites, MPPA and NAG, in/on KWS20-1 sugar beet raw agricultural commodities (RACs; roots and tops) that resulted from applications of MON 55620, a water-soluble concentrate (SL) containing 2.34 lb a.i. of glufosinate-ammonium per gallon. Applications of the glufosinate-based herbicide formulation, MON 55620, sold commercially as Liberty® 280 SL[5], were made to the treated plots of KWS20-1 sugar beet. Use of KWS20-1 sugar beet in this study was required to generate data that may be used to support regulatory approval of KWS20-1 sugar beet.

The field trials for the study were conducted in the U.S. at six (6) sites in five (5) states: Idaho (Region 9); Michigan (Region 5); Minnesota (Region 5); North Dakota (Region 7); and South Dakota (Region 5). These regions were typical of the major sugar beet producing regions of the U.S.

The target application timings and rates are summarized in the following table:

Table 38. Applications of MON 55620 to KWS20-1 Sugar Beet

Treatment	**Rate as Glufosinate Equivalent**	
	Pre-emerge Application	**Late Postemergence Application (10 leaves unfolded)**
Control	0	0
Treated[1]	0.55 lb a.i./acre (0.62 kg a.i./ha) (30 fl oz MON 55620/acre)	0.55 lb a.i./acre (0.62 kg a.i./ha) (30 fl oz MON 55620/acre)

[1] Treated plot is identified as Treatment 2 in the GLP study REG-2020-0053.
Actual application rates were within 5% of the target rates for all locations. The average percent of target rate across all applications and all sites was 100%.

[5] Liberty® 280 SL is a registered trademark of BASF.

The sugar beet root and top samples were collected at commercial maturity (BBCH 49). Samples were harvested by hand from each plot, while generally avoiding the outer rows and ends of rows. Each sample was field composited from 12 or more different locations across the entire plot. In this manner, one sample from the untreated plot was collected first, followed by the two replicate samples from the treated plot. To minimize the quantity of excessive sample tissue collected, each sugar beet root or top used for RAC sampling was quartered, and one quarter from each plant was compiled with eleven other individual quarters collected from separate plants.

Metabolism of glufosinate by herbicide-tolerant sugar beet was demonstrated in a metabolism study . The residue of concern for tolerance setting is proposed as glufosinate and its metabolites MPPA and NAG as parent equivalents in the U.S.

The analytical method, ME-2290-01, *Method for Determination of Glufosinate, NAG and MPPA in Various Crops Using LC-MS/MS*, was used in this study and measured the residues of glufosinate and its metabolites, MPPA and NAG.

The limit of quantitation (LOQ) for each analyte for each matrix (i.e., roots and tops) was determined to be 0.010 ppm in parent equivalents.

For this study, one untreated control and two treated sugar beet root and top samples from each site were analyzed.

Method performance was evaluated by use of concurrent recovery samples by fortifying each analyte for each matrix (i.e., roots and tops) at 0.010 and 0.100 ppm. The fortification levels bracketed the measured residues.

All recoveries were corrected for any interferences in corresponding controls. The overall mean of the recoveries for sugar beet roots and tops at each fortification level was within the acceptable range of 70 to 120%, and the relative standard deviation values were below 20%. The method was considered acceptable for the analysis of glufosinate, MPPA, and NAG residues in sugar beet roots and tops.

The residues in samples collected from the treated plot in Table 38 are summarized in Table 39.

Table 39. Glufosinate Residues in/on KWS20-1 Sugar Beet Raw Agricultural Commodities

Analyte	PHI (days)[1]	Treated Plot (Sugar Beet Roots)		Treated Plot (Sugar Beet Tops)	
		Median (ppm)[2]	Min-Max (ppm)[3]	Median (ppm)[2]	Min-Max (ppm)[3]
Glufosinate	69-107	0.0537	0.0284 - 0.1304	0.0770	0.0178 - 0.1592
MPPA	69-107	0.0154	<0.010[4] - 0.0405	0.0127	<0.010 - 0.0250
NAG	69-107	0.1427	0.0719 - 0.3201	0.2127	0.0605 - 0.5579
Total Glufosinate	69-107	0.2157	0.1103 - 0.4677	0.3109	0.0899 - 0.7421

[1] PHI = pre-harvest interval; interval between last application and harvest (sampling) in days.
[2] Median of site averaged field sample residue values.
[3] Minimum and maximum residue range of individual field sample residue values.

[4] This method has a limit of quantitation (LOQ) of 0.010 ppm (mg/kg) for each individual analyte. Residue values <0.010 ppm are below LOQ.

The residue results indicate that the existing U.S. EPA glufosinate MRLs of 0.9 ppm in sugar beet root and of 1.5 ppm in sugar beet tops (leaves) are sufficient to account for the use of glufosinate on KWS20-1 sugar beets.

The safety of glufosinate and its relevant metabolites have been assessed by U.S. EPA. U.S. EPA concluded that there is a reasonable certainty that no harm will result to the general population, or to infants and children from aggregate exposure to glufosinate residues or its metabolites.

For details, please also refer to Appendix 22.

B.5 Compositional Assessment

Food and feed safety assessments of biotechnology-derived crops follow the comparative safety assessment process (Codex Alimentarius, 2009) in which the composition of raw agricultural commodities of the biotechnology-derived crop are compared to the appropriate conventional control that has a history of safe use. For sugar beet, assessments are performed based on the general principles outlined in the OECD consensus document for sugar beet composition (OECD, 2002a).

A review of compositional assessments, that encompassed a total of seven biotechnology-derived crop traits, four maize and three soybean, nine countries, and eleven growing seasons, concluded that incorporation of biotechnology-derived agronomic traits has had little impact on crop composition compared to other sources of variation. Most compositional variation is attributable to growing region, agronomic practices, and genetic background (Harrigan *et al.*, 2010b). Numerous scientific publications have further documented the extensive variability in the concentrations of crop nutrients, anti-nutrients, and secondary metabolites that reflect the influence of environmental and genetic factors as well as extensive conventional breeding efforts to improve nutrition, agronomics and yield (Harrigan *et al.*, 2009; Ridley *et al.*, 2011; Zhou *et al.*, 2011; Harrigan *et al.*, 2010b).

Compositional equivalence between biotechnology-derived and conventional crops supports an "equal or increased assurance of the safety of foods derived from genetically modified plants" (OECD, 2002b; OECD, 2002a). OECD consensus documents on compositional considerations for new crop varieties emphasize quantitative measurements of key nutrients and known anti-nutrients or toxicants. These quantitative measurements effectively discern compositional changes that imply potential nutritional or safety (e.g., anti-nutritional) concerns. Levels of the components in raw agricultural commodities of the biotechnology-derived crop product are compared to: 1) corresponding levels in a conventional comparator, a genetically similar conventional line, grown concurrently under similar field conditions, and 2) natural ranges from data published in the scientific literature or in publically available databases (e.g., AFSI Crop Composition Database) (AFSI, 2020).. This second comparison places any potential differences between the assessed biotechnology-derived crop and its comparator in the context of the well-documented variation within and among sugar beet varieties in the concentrations of crop nutrients and the secondary metabolite. The KWS20-1 sugar beet component values were also compared to the range of values for conventional reference sugar beet grown during the 2020 season and analyzed concurrently with KWS20-1 sugar beet and its control.

This section provides a summary of the analyses conducted to evaluate key nutrients and a secondary metabolite in tops and root of KWS20-1 sugar beet compared to that of a conventional near-isogenic control sugar beet grown and harvested under similar conditions. The production of materials for compositional analyses used a sufficient variety of field trial sites, robust experimental design (i.e., randomized complete block design with four block replicates) and sensitive analytical methods that allow accurate measurement of key components that represent a range of environmental conditions typical for sugar beet production. The information provided in this section addresses relevant factors in Codex Plant Guidelines, Section 4, paragraphs 44 and 45 for compositional analyses (Codex Alimentarius, 2009).

B.5(a) Levels of key nutrients, toxicants and anti-nutrients in the food produced using gene technology compared with the levels in an appropriate comparator

Compositional Equivalence of KWS20-1 Sugar Beet to Conventional Near-Isogenic Sugar Beet

Herbicide tolerance was conferred to KWS20-1 sugar beet via *Agrobacterium*-mediated insertion of a single T-DNA gene cassette containing a demethylase gene from *Stenotrophomonas maltophilia* that expresses a dicamba mono-oxygenase (DMO) protein to confer tolerance to dicamba herbicide, a gene from *Streptomyces viridochromogenes* that expresses the phosphinothricin N-acetyltransferase (PAT) protein to confer tolerance to glufosinate-ammonium herbicide, and the *cp4 epsps* coding sequence isolated from *Agrobacterium* sp. strain CP4 that encodes the 5-enolpyruvylshikimate-3-phosphate synthase (CP4 EPSPS) protein to confer tolerance to glyphosate. Given the nature of these familiar introduced traits and the general lack of meaningful unintended compositional characteristics observed for biotechnology-derived products over the past several decades, biologically-relevant compositional changes in KWS20-1 sugar beet were not expected (Brune *et al.*, 2021). Tops and root samples were harvested from KWS20-1 sugar beet, a conventional near-isogenic control and conventional commerical reference varieties grown at five sites in the United States during 2020 under agronomic field conditions typical for the different growing regions. The field sites were planted in a randomized complete block design with four blocks per site. KWS20-1 sugar beet plots were treated with glyphosate, dicamba and glufosinate herbicides.

The compositional analysis provided a comprehensive comparative assessment of the levels of key nutrients and a secondary metabolite in tops and root of KWS20-1 sugar beet and the conventional near-isogenic control. The evaluation of KWS20-1 sugar beet followed considerations relevant to the compositional quality of sugar beet as defined by the OECD consensus document (OECD, 2002a). Harvested tops samples were assessed for moisture and levels of nutrients including proximates (protein, total fat and ash), carbohydrates by calculation and crude fiber (Table 40). Harvested root samples were assessed for moisture and levels of nutrients including protein and 18 amino acids (Table 41); sucrose and fiber (crude fiber and pectin) (Table 42); total fat and carbohydrates by calculation (Table 43); ash and minerals (phosphorus, potassium and sodium) (Table 44); and the secondary metabolite oleanolic acid (Table 45). In all, 36 different components were analyzed.

Of the 36 measured components, one component (sodium in root) had more than 50% of the observations fall below the assay limit of quantitation (LOQ) and was excluded from statistical analyses. Moisture values for tops and root were measured for conversion of components from fresh to dry weight, but were not statistically analyzed. Therefore, 33 components were statistically analyzed (five in tops and 28 in root).

The statistical comparisons of KWS20-1 sugar beet to the conventional near-isogenic control were based on compositional data combined across all field sites. Statistically significant differences were identified at the 5% level ($\alpha = 0.05$). A statistically significant difference between KWS20-1 sugar beet and the conventional near-isogenic control does not necessarily imply biological relevance from a food safety perspective. Therefore, any statistically significant difference observed between KWS20-1 sugar beet and the conventional near-isogenic control was evaluated

further to determine whether the detected difference indicated a biologically-relevant compositional change or supported a conclusion of compositional equivalence, as follows:

Step 1 – Determination of the Magnitude of Difference between Test (KWS20-1 Sugar Beet) and the Conventional Near-Isogenic Control Means

The difference in means between KWS20-1 sugar beet and the conventional near-isogenic control was determined for use in subsequent steps.

Step 2 – Assessment of the Difference in the Context of Natural Variation within the Conventional Control across Multiple Sites

The difference between KWS20-1 sugar beet and the conventional near-isogenic control was evaluated in the context of variation within the conventional control germplasm grown across multiple sites (i.e., variation due to environmental influence) by determining the range of replicate values for the conventional control sugar beet (range value = maximum value minus the minimum value). A mean difference less than the variability observed due to natural environmental variation within the single, closely related germplasm, is typically not a food safety concern (Venkatesh *et al.*, 2014).

Step 3 – Assessment of the Difference in the Context of Natural Variation Due to Multiple Sources

The relative impact of KWS20-1 sugar beet on composition was also evaluated in the context of sources of natural variation, such as environmental and germplasm influences. This assessment determined whether the component mean value of KWS20-1 sugar beet was within the natural variability defined by conventional reference sugar beet also grown during the 2020 season and analyzed concurrently with KWS20-1 and control sugar beet and/or the AFSI Crop Composition Database ((AFSI, 2020); Table 46) values. This naturally occurring variability is important in assessing the biological relevance to food safety of statistically significant differences in composition between KWS20-1 sugar beet and the conventional near-isogenic control.

These evaluations of natural variation are important as crop composition is known to be greatly influenced by environment and variety (Harrigan *et al*., 2010a). Although used in the comparative assessment process, detection of statistically significant differences between KWS20-1 sugar beet and the conventional near-isogenic control mean values does not necessarily imply a meaningful contribution by KWS20-1 sugar beet to compositional variability. Only if the impact of KWS20-1 sugar beet on levels of components is large relative to natural variation inherent to conventional sugar beet would the difference in composition be potentially meaningful from a food safety and nutritional perspective. Differences between KWS20-1 sugar beet and the conventional near-isogenic control that are within the observed natural variation for sugar beet are not meaningful and, therefore, these comparative data support a conclusion of compositional equivalence.

Compositional Analysis of KWS20-1 Sugar Beet Compared to the Conventional Near-Isogenic Sugar Beet

Compositional analysis was conducted on the tops and root of KWS20-1 sugar beet and its conventional near-isogenic control and conventional commercial reference varieties grown at five sites in the U.S. during 2020. In all, 36 different analytical components were measured. Of these, one component (sodium in root) had more than 50% of the observations below the assay limit of quantitation (LOQ) and was excluded from statistical analysis. Moisture values for tops and root were measured for conversion of components from fresh to dry weight but were not statistically analyzed. Therefore, 33 components were statistically analyzed (five in tops and 28 in root).

There were no statistically significant differences ($p<0.05$) for 25 of the 33 components analyzed (Table 40 to Table 45). No statistical differences ($p<0.05$) were observed for components in sugar beet tops. There were eight components in root (lysine, proline, serine, threonine, total fat, ash, phosphorus and potassium) that showed a statistically significant difference ($p<0.05$) between KWS20-1 sugar beet and its conventional near-isogenic control sugar beet.

Based on the step-wise assessment of evaluating a statistically significant difference in a compositional component, the mean differences between KWS20-1 sugar beet and the conventional near-isogenic control sugar beet for the four amino acids (lysine, proline, serine and threonine) were determined. In addition, since total amino acids measured in root are predominantly derived from hydrolysis of protein, the relative magnitude of differences (percent change relative to the control) in amino acid levels between KWS20-1 sugar beet and its conventional near-isogenic control sugar beet were assessed relative to those in protein. The relative magnitude of the difference in mean protein values for KWS20-1 sugar beet and the conventional near-isogenic control sugar beet was 7.05%, and the relative magnitudes of the differences for the amino acids that had statistically significant differences were similar to that for protein and ranged from 3.82% (proline) to 6.13% (serine) (Table 41).

Likewise, the mean differences between KWS20-1 sugar beet and the conventional near-isogenic control sugar beet for total fat, ash, phosphorus and potassium components were determined. For total fat, the difference was 0.14% dw (Table 43). For ash, the difference was -0.32% dw (Table 44). For the two minerals, the differences ranged from -0.11% dw (potassium) to -0.013% dw (phosphorus) (Table 44).

For these components that showed a statistically significant difference ($p<0.05$) between KWS20-1 sugar beet and its conventional near-isogenic control sugar beet, the mean difference was less than the conventional near-isogenic control range values. The KWS20-1 sugar beet mean component values were also within the range of values for conventional reference sugar beet (i.e., 14 unique conventional sugar beet reference varieties; four references at each of five locations) grown during the 2020 season and analyzed concurrently with the KWS20-1 and control sugar beet and/or the AFSI Crop Composition Database values ((AFSI, 2020); Table 46).

These data indicate that the statistically significant differences observed were not biologically meaningful from a food safety and nutritional perspective. These results support the conclusion that KWS20-1 sugar beet was not a major contributor to variation in component levels in sugar

beet tops or root and confirmed the compositional equivalence of KWS20-1 sugar beet to its conventional near-isogenic control sugar beet in levels of these components.

For details, please refer to Appendix 23.

Conclusions

Compositional analysis was conducted on tops and root of KWS20-1 sugar beet and its conventional near-isogenic control sugar beet grown at five sites in the United States during the 2020 field season. Of the 33 components statistically assessed, 25 demonstrated no statistically significant differences ($p<0.05$) between KWS20-1 sugar beet and its conventional near-isogenic control sugar beet. A total of eight components (lysine, proline, serine, threonine, total fat, ash, phosphorus and potassium for root) showed a statistically significant difference ($p<0.05$) between KWS20-1 sugar beet and the conventional near-isogenic control sugar beet. For these components, the mean difference in component values between KWS20-1 sugar beet and its conventional near-isogenic control sugar beet was less than the range of the conventional near-isogenic control values. Additionally, the KWS20-1 sugar beet mean component values with significant differences were within the range of values for conventional reference sugar beet also grown at five locations in 2020 and/or the AFSI-CCDB.

These results support the overall conclusion that KWS20-1 sugar beet was not a major contributor to variation in component levels in tops or root and confirmed the compositional equivalence of KWS20-1 sugar beet to its conventional near-isogenic control sugar beet in levels of these components. The statistically significant differences observed were not compositionally meaningful from a food safety perspective.

Table 40. Summary of Sugar Beet Tops Proximates, Carbohydrates by Calculation, and Fiber for KWS20-1 Sugar Beet and Its Conventional Near-Isogenic Control

				Difference (Test minus Control)	
Component (%dw)[1]	KWS20-1 sugar beet Mean (S.E.)[2] Range	Control Mean (S.E.) Range	Control Range Value[3]	Mean (S.E.)	p-Value
Protein	13.78 (1.04) 9.01 – 27.31	13.72 (1.04) 7.89 – 21.33	13.44	0.061 (1.37)	0.966
Total Fat	2.11 (0.12) 1.72 – 2.67	2.09 (0.12) 1.03 – 2.94	1.91	0.016 (0.10)	0.877
Ash	12.30 (1.06) 10.14 – 15.27	14.03 (1.06) 9.78 – 20.13	10.35	-1.74 (1.25)	0.237
Carbohydrates by Calculation	71.79 (1.87) 58.00 – 78.01	70.08 (1.87) 61.07 – 81.08	20.01	1.71 (2.46)	0.525
Crude Fiber	9.11 (0.40) 6.47 – 12.35	9.56 (0.40) 6.32 – 12.39	6.07	-0.45 (0.47)	0.352

[1]dw = dry weight
[2]Mean (S.E.) = least-square mean (standard error)
[3]Maximum value minus minimum value for the conventional near-isogenic control sugar beet.

Table 41. Summary of Sugar Beet Root Protein and Amino Acids for KWS20-1 Sugar Beet and Its Conventional Near-Isogenic Control

				Difference (Test minus Control)		
Component (% dw)[1]	KWS20-1 sugar beet Mean (S.E.)[2] Range	Control Mean (S.E.) Range	Control Range Value[3]	Mean (S.E.)	p-Value	% Relative[4]
Protein	5.63 (0.54) 3.71 - 11.67	6.06 (0.54) 4.57 - 9.87	5.30	-0.43 (0.57)	0.495	-7.05
Alanine	0.18 (0.012) 0.13 - 0.25	0.18 (0.012) 0.14 - 0.27	0.13	-0.00082 (0.0063)	0.897	-0.46
Arginine	0.12 (0.0034) 0.10 - 0.15	0.13 (0.0034) 0.12 - 0.15	0.029	-0.0047 (0.0026)	0.085	-3.67
Aspartic Acid	0.44 (0.028) 0.33 - 0.60	0.46 (0.028) 0.38 - 0.69	0.31	-0.023 (0.016)	0.161	-4.96
Cystine	0.039 (0.0010) 0.029 - 0.048	0.040 (0.0010) 0.034 - 0.047	0.012	-0.00066 (0.0013)	0.622	-1.67
Glutamic Acid	0.73 (0.094) 0.46 - 1.25	0.75 (0.094) 0.52 - 1.19	0.67	-0.026 (0.047)	0.600	-3.50
Glycine	0.13 (0.0030) 0.12 - 0.15	0.14 (0.0030) 0.12 - 0.16	0.033	-0.0046 (0.0023)	0.061	-3.42

Table 41. Summary of Sugar Beet Root Protein and Amino Acids for KWS20-1 Sugar Beet and Its Conventional Near-Isogenic Control (Continued)

				Difference (Test minus Control)		
Component (% dw)[1]	KWS20-1 sugar beet Mean (S.E.)[2] Range	Control Mean (S.E.) Range	Control Range Value[3]	Mean (S.E.)	p-Value	% Relative[4]
Histidine	0.080 (0.0020) 0.066 - 0.097	0.083 (0.0020) 0.072 - 0.10	0.028	-0.0023 (0.0019)	0.248	-2.80
Isoleucine	0.13 (0.0060) 0.11 - 0.18	0.14 (0.0060) 0.11 - 0.18	0.071	-0.0045 (0.0043)	0.349	-3.26
Leucine	0.19 (0.0042) 0.17 - 0.23	0.20 (0.0042) 0.17 - 0.26	0.083	-0.0076 (0.0046)	0.114	-3.82
Lysine	0.19 (0.0051) 0.16 - 0.22	0.20 (0.0051) 0.17 - 0.22	0.055	-0.0091 (0.0038)	0.025	-4.64
Methionine	0.041 (0.0013) 0.034 - 0.059	0.043 (0.0013) 0.036 - 0.050	0.013	-0.0019 (0.0015)	0.234	-4.36
Phenylalanine	0.10 (0.0031) 0.084 - 0.12	0.10 (0.0031) 0.093 - 0.12	0.030	-0.003 (0.0019)	0.134	-2.88

Table 41. Summary of Sugar Beet Root Protein and Amino Acids for KWS20-1 Sugar Beet and Its Conventional Near-Isogenic Control (Continued)

				Difference (Test minus Control)		
Component (% dw)[1]	KWS20-1 sugar beet Mean (S.E.)[2] Range	Control Mean (S.E.) Range	Control Range Value[3]	Mean (S.E.)	p-Value	% Relative[4]
Proline	0.12 (0.0025) 0.10 - 0.14	0.12 (0.0025) 0.11 - 0.15	0.035	-0.0048 (0.0022)	0.046	-3.82
Serine	0.16 (0.0054) 0.14 - 0.20	0.17 (0.0054) 0.14 - 0.22	0.073	-0.01 (0.0043)	0.027	-6.13
Threonine	0.13 (0.0028) 0.12 - 0.16	0.14 (0.0028) 0.12 - 0.15	0.031	-0.0053 (0.0025)	0.048	-3.88
Tryptophan	0.055 (0.0021) 0.045 - 0.080	0.055 (0.0021) 0.047 - 0.077	0.031	0.000080 (0.0025)	0.977	0.14
Tyrosine	0.11 (0.0032) 0.085 - 0.14	0.11 (0.0032) 0.11 - 0.13	0.026	-0.0045 (0.0022)	0.056	-3.87
Valine	0.17 (0.0036) 0.15 - 0.21	0.18 (0.0036) 0.16 - 0.21	0.047	-0.0074 (0.0041)	0.088	-4.04

[1]dw = dry weight

[2] Mean (S.E.) = least-square mean (standard error)

[3]Maximum value minus minimum value for the conventional near-isogenic control sugar beet.

[4]The relative magnitude of the difference in mean values between KWS20-1 sugar beet and its conventional near-isogenic control, expressed as a percent of the control.

Table 42. Summary of Sugar Beet Root Sucrose and Fiber for KWS20-1 Sugar Beet and Its Conventional Near-Isogenic Control

				Difference (Test minus Control)	
Component (% dw)[1]	KWS20-1 sugar beet Mean (S.E.)[2] Range	Control Mean (S.E.) Range	Control Range Value[3]	Mean (S.E.)	p-Value
Crude Fiber	5.39 (0.20) 4.00 - 6.74	5.27 (0.20) 2.80 - 6.84	4.04	0.11 (0.26)	0.664
Pectin	2.95 (0.10) 2.13 - 3.62	3.14 (0.10) 2.69 - 3.56	0.87	-0.19 (0.13)	0.232
Sucrose	80.10 (0.83) 72.38 - 85.48	79.85 (0.83) 73.46 - 84.09	10.63	0.25 (1.16)	0.842

[1]dw = dry weight
[2]Mean (S.E.) = least-square mean (standard error)
[3]Maximum value minus minimum value for the conventional near-isogenic control sugar beet.

Table 43. Summary of Sugar Beet Root Fat and Carbohydrates by Calculation for KWS20-1 Sugar Beet and Its Conventional Near-Isogenic Control

				Difference (Test minus Control)	
Component (%dw)[1]	KWS20-1 sugar beet Mean (S.E.)[2] Range	Control Mean (S.E.) Range	Control Range Value[3]	Mean (S.E.)	p-Value
Total Fat	0.60 (0.048) 0.21 - 1.11	0.46 (0.048) 0.20 - 0.82	0.63	0.14 (0.042)	0.027
Carbohydrates by Calculation	91.55 (0.61) 84.85 - 94.66	90.84 (0.61) 86.21 - 92.93	6.72	0.72 (0.66)	0.335

[1]dw = dry weight
[2]Mean (S.E.) = least-square mean (standard error)
[3]Maximum value minus minimum value for the conventional near-isogenic control sugar beet.

Table 44. Summary of Sugar Beet Root Ash and Minerals for KWS20-1 Sugar Beet and Its Conventional Near-Isogenic Control

				Difference (Test minus Control)	
Component (% dw)[1]	KWS20-1 sugar beet Mean (S.E.)[2] Range	Control Mean (S.E.) Range	Control Range Value[3]	Mean (S.E.)	p-Value
Ash	2.29 (0.14) 1.16 - 3.25	2.61 (0.14) 1.62 - 3.91	2.29	-0.32 (0.14)	0.036
Phosphorus	0.088 (0.0090) 0.049 - 0.12	0.10 (0.0090) 0.051 - 0.16	0.11	-0.013 (0.0049)	0.014
Potassium	0.95 (0.045) 0.78 - 1.24	1.06 (0.045) 0.87 - 1.32	0.45	-0.11 (0.028)	<0.001

[1]dw = dry weight
[2]Mean (S.E.) = least-square mean (standard error)
[3]Maximum value minus minimum value for the conventional near-isogenic control sugar beet.
The following component with more than 50% of observations below the assay LOQ was excluded from statistical analysis: sodium.

Table 45. Summary of Sugar Beet Root Secondary Metabolite for KWS20-1 Sugar Beet and Its Conventional Near-Isogenic Control

				Difference (Test minus Control)	
Component (% dw)[1]	KWS20-1 sugar beet Mean (S.E.)[2] Range	Control Mean (S.E.) Range	Control Range Value[3]	Mean (S.E.)	p-Value
Oleanolic Acid	0.12 (0.014) 0.066 - 0.16	0.12 (0.014) 0.060 - 0.21	0.14	-0.0046 (0.0065)	0.517

[1]dw = dry weight
[2]Mean (S.E.) = least-square mean (standard error)
[3]Maximum value minus minimum value for the conventional near-isogenic control sugar beet.

B.5(b) Information on the range of natural variation for each constituent measured to allow for assessment of biological significance should any statistically significant difference be identified

Table 46. Conventional Reference Varieties and the AFSI Database for Components in Sugar Beet Tops and Root

Tissue Components[1]	Reference Range[2]	AFSI Range[3]
Tops Nutrients		
Proximates		
protein (% dw)	8.52 - 26.13	8.42-27.52
total fat (% dw)	1.31 - 3.88	0.91-10.07
ash (% dw)	9.43 - 22.95	10.809-24.219
Carbohydrates By Calculation		
carbohydrates by calculation (% dw)	53.66 - 79.25	48.75-74.26
Fiber		
crude fiber (% dw)	5.36 - 18.04	7.24138-15.20408
Root Nutrients		
Proximates		
protein (% dw)	2.84 - 11.07	2.52511-7.06587
total fat (% dw)	0.21 - 0.98	0.44156-1.68868
ash (% dw)	0.86 - 3.64	0.898-7.530
Amino Acids		
alanine (% dw)	0.12 - 0.30	0.094-0.233
arginine (% dw)	0.10 - 0.16	0.077-0.194
aspartic acid (% dw)	0.27 - 0.71	0.22009-0.56954
cystine (% dw)	0.029 - 0.062	0.04696-0.10452
glutamic acid (% dw)	0.38 - 1.46	0.31370-1.79641
glycine (% dw)	0.10 - 0.17	0.09177-0.21149
histidine (% dw)	0.061 - 0.10	0.05446-0.12644
isoleucine (% dw)	0.096 - 0.20	0.076-0.234
leucine (% dw)	0.15 - 0.26	0.129-0.337
lysine (% dw)	0.15 - 0.26	0.145-0.335
methionine (% dw)	0.031 - 0.057	0.043-0.071
phenylalanine (% dw)	0.081 - 0.13	0.076-0.209
proline (% dw)	0.093 - 0.16	0.050-0.153
serine (% dw)	0.12 - 0.26	0.119-0.229
threonine (% dw)	0.10 - 0.17	0.092-0.201
tryptophan (% dw)	0.043 - 0.073	NA
tyrosine (% dw)	0.082 - 0.14	0.069-0.162
valine (% dw)	0.13 - 0.23	0.104-0.279
Carbohydrates By Calculation		
carbohydrates by calculation (% dw)	84.62 - 95.52	87.85-95.91

Table 46. Conventional Reference Varieties and the AFSI Database for Components in Sugar Beet Tops and Root (Continued)

Tissue Components[1]	Reference Range[2]	AFSI Range[3]
Fiber and Sucrose		
crude fiber (% dw)	2.81 - 7.55	3.31276-6.03448
pectin (% dw)	1.97 - 3.78	-
sucrose (% dw)	53.97 - 90.50	-
Minerals		
phosphorus (% dw)	0.043 - 0.28	-
potassium (% dw)	0.51 - 1.93	-
Root Other		
Secondary Metabolite		
oleanolic acid (% dw)	0.037 - 0.20	0.075-0.363

[1]dw = dry weight
[2]Range of values for conventional sugar beet reference varieties grown and analyzed concurrently with the KWS20-1 and control sugar beet.
[3]AFSI range is from AFSI CCDB, 2020 (Accessed October 27, 2020).

B.5(c) The levels of any other constituents that may potentially be influenced by the genetic modification.

Considering mode of action of KWS20-1 sugar beet described in B.1(a), and composition analysis in B.5(b), it is not anticipated that any other constituents would be influenced by the genetic modification.

C. INFORMATION RELATED TO THE NUTRITIONAL IMPACT OF THE FOOD PRODUCED USING GENE TECHNOLOGY

There are no nutritional impacts on the food derived from KWS20-1 sugar beet. This product is developed to confer herbicides tolerance. It is not a nutritionally altered product.

D. OTHER INFORMATION

The data and information presented in this submission demonstrate that the food derived from KWS20-1 sugar beet are as safe and nutritious as those derived from commercially-available, conventional sugar beet for which there is an established history of safe consumption. No additional studies are considered necessary to demonstrate the safety of KWS20-1 sugar beet.

PART 3 STATUTORY DECLARATION – AUSTRALIA

STATUTORY DECLARATION pursuant to Statutory Declarations Act 1959

I, [redacted] Regulatory Affairs Manager at Bayer CropScience Pty Ltd, Level 4, 109 Burwood Road, Hawthorn, Vic. 3122, make the following declaration under the Statutory Declarations Act 1959:

1. the information provided in this application fully sets out the matters required,

2. the information provided in this application is true to the best of my knowledge and belief,

3. no information has been withheld that might prejudice this application, to the best of my knowledge and belief.

I understand that a person who intentionally makes a false statement in a statutory declaration is guilty of an offence under section 11 of the Statutory Declarations Act 1959, and I believe that the statements in this declaration are true in every particular.

[redacted]

Signature of person making the declaration

Declared at Hawthorn on 22 of February 2024

Before me

[redacted]

Level 4, 109 Burwood Road, Hawthorn, Vic. 3122, an Australian Legal Practitioner within the meaning of the Legal Profession Uniform Law (Victoria)

//////////////////

22 February 2024

Bayer CropScience Pty Ltd
ABN 87 000 226 022

Level 4, 109 Burwood Road
Hawthorn VIC 3122
Australia

Tel. +61 3 9248 6888

crop.bayer.com.au

PART 4 REFERENCES

UNPUBLISHED REPORTS BEING SUBMITTED

Appendix 1. M-811949-01-1. Summary of Molecular Characterization of T-DNA Insertion in Herbicide-Tolerant Sugar Beet KWS20-1 by Southern Blot Analysis.

Appendix 2. M-831595-01-1. Determination of the T-DNA Insert Stability in Two Generations of the Herbicide-Tolerant Sugar Beet KWS20-1 by Southern Blot Analysis.

Appendix 3. M-823019-01-1. Updated Bioinformatics Evaluation of the T-DNA in Herbicide-Tolerant Sugar Beet KWS20-1 Utilizing the AD_2022, TOX_2022, and PRT_2022 Databases.

Appendix 4. M-823015-01-1. Updated Bioinformatics Evaluation of Putative Flank-Junction Peptides in Herbicide-Tolerant Sugar Beet KWS20-1 Utilizing the AD_2022, TOX_2022, and PRT_2022 Databases.

Appendix 5. M-831661-01-1. Two-Generation Segregation Analysis to Determine the Inheritance Pattern of T-DNA Insertion in Herbicide-Tolerant Sugar Beet KWS20-1.

Appendix 6. M-820110-01-1. Amended Report for TRR0001005: Demonstration of the Presence of CP4 EPSPS, DMO+27.1 and PAT Proteins Across 3 Generations of Herbicide-Tolerant Sugar Beet KWS20-1.

Appendix 7. M-822452-02-1. Characterization of the Dicamba Mono-Oxygenase Protein Purified from Leaf Tissue of Herbicide-Tolerant Sugar Beet KWS20-1 and Comparison of the Physicochemical and Functional Properties of the Plant-Produced and *Escherichia coli* (*E. coli*) Produced KWS20-1 Dicamba Mono-Oxygenase Proteins.

Appendix 8. M-822068-01-1. Amended Report for TRR0001154: Characterization of the PAT Protein Purified from Leaf Tissue of Herbicide-Tolerant Sugar Beet KWS20-1 and Comparison of the Physicochemical and Functional Properties of the Plant-Produced and *Escherichia coli* (*E. coli*) Produced PAT (*pat*) Proteins.

Appendix 9. M-822059-01-1. Characterization of the CP4 EPSPS Protein Purified from Leaf Tissue of Herbicide-Tolerant Sugar Beet KWS20-1 and Comparison of the Physicochemical and Functional Properties of the Plant-Produced and *Escherichia coli* (*E. coli*) Produced CP4 EPSPS Proteins.

Appendix 10. M-821856-01-1. Assessment of CP4 EPSPS, DMO, and PAT Protein Levels in Tissues Collected from Treated Herbicide-Tolerant Sugar Beet KWS20-1 Produced in United States Field Trials During 2020.

Appendix 11. M-823018-01-1. Updated Bioinformatics Evaluation of DMO in Herbicide-Tolerant Sugar Beet KWS20-1 Utilizing the AD_2022, TOX_2022, and PRT_2022 Databases.

Appendix 12. M-816143-01-1 Updated Bioinformatics Evaluation of PAT Utilizing the AD_2022, TOX_2022, and PRT_2022 Database.

Appendix 13. M-814116-01-1. Updated Bioinformatics Evaluation of CP4 EPSPS Utilizing the AD_2022, TOX_2022, and PRT_2022 Databases.

Appendix 14. M-820284-01-1. Assessment of the *in vitro* Digestibility of *Escherichia coli*-produced DMO+27.1 Protein by Pepsin and Pancreatin.

Appendix 15. M-786726-02-1. Amended Summary for Assessment of the in vitro Digestibility of Phosphinothricin N-Acetyltransferase Protein by Pepsin and Pancreatin.

Appendix 16. M-792416-01-1. Assessment of the *in vitro* Digestibility of Purified *E. coli*-produced CP4 EPSPS Protein in Simulated Gastric Fluid.

Appendix 17. M-788006-01-1. Assessment of the *in vitro* Digestive Fate of CP4 EPSP Synthase.

Appendix 18. M-820277-01-1. The Effect of Heat Treatment on the Functional Activity of *Escherichia coli* (*E. coli*)-produced DMO+27.1 Protein.

Appendix 19. M-786722-01-1. Effect of Heat Treatment on the Functional Activity of *Escherichia coli*-Produced Phosphinothricin N-acetyltransferase Protein.

Appendix 20. M-798507-01-1. Amended Report for MSL0022432: Effect of Temperature Treatment on the Functional Activity of CP4 EPSPS.

Appendix 21. M-840756-01-1. Summary of the Magnitude of Dicamba Residues in Herbicide-Tolerant Sugar Beet KWS20-1 Raw Agricultural Commodities Following Application of a Dicamba-Based Formulation – 2020 U.S. Trials.

Appendix 22. M-840758-01-1. Summary of the Magnitude of Glufosinate Residues in Herbicide-Tolerant Sugar Beet KWS20-1 Raw Agricultural Commodities Following Application of a Glufosinate-Based Formulation – 2020 U.S. Trials.

Appendix 23. M-820249-01-1. Amended Report for TRR0000674: Compositional Analyses of Herbicide-Tolerant Sugar Beet KWS20-1 Tops and Root Tissues Grown in the United States During the 2020 Season.

PUBLISHED REFERENCES

ACSC. 2022. Proudly making life a little sweeter. American Crystal Sugar Company, Moorhead, Minnesota. https://www.crystalsugar.com/media/abmbkah2/american-crystal-sugar-company-brochure.pdf [Accessed February 3, 2022].

Adrian-Romero, M., G. Blunden, B.G. Carpenter and E. Tyihák. 1999. HPLC quantification of formaldehyde, as formaldemethone, in plants and plant-like organisms. Chromatographia 50:160-166.

AFSI. 2020. Crop Composition Database, Version 8.0. Agriculture & Food Systems Institute, Washington, D.C. www.cropcomposition.org [Accessed January 4, 2020].

Alibhai, M.F. and W.C. Stallings. 2001. Closing down on glyphosate inhibition - With a new structure for drug discovery. Proceedings of the National Academy of Sciences of the United States of America 98:2944-2946.

An, S.-q. and G. Berg. 2018. *Stenotrophomonas maltophilia*. Trends in Microbiology 26:637-638.

Anderson, J.E., J.-M. Michno, T.J.Y. Kono, A.O. Stec, B.W. Campbell, S.J. Curtin and R.M. Stupar. 2016. Genomic variation and DNA repair associated with soybean transgenesis: A comparison to cultivars and mutagenized plants. BMC Biotechnology 16:41.

Barker, R.F., K.B. Idler, D.V. Thompson and J.D. Kemp. 1983. Nucleotide sequence of the T-DNA region from the *Agrobacterium tumefaciens* octopine Ti plasmid pTi15955. Plant Molecular Biology 2:335-350.

Barry, G.F., G.M. Kishore, S.R. Padgette and W.C. Stallings. 2001. Glyphosate-tolerant 5-enolpyruvylshikimate-3-phosphate synthases. Patent 6,248,876, U.S. Patent Office, Washington, D.C.

Behrens, M.R., N. Mutlu, S. Chakraborty, R. Dumitru, W.Z. Jiang, B.J. LaVallee, P.L. Herman, T.E. Clemente and D.P. Weeks. 2007. Dicamba resistance: Enlarging and preserving biotechnology-based weed management strategies. Science 316:1185-1188.

Berg, G. and J.L. Martinez. 2015. Friends or foes: Can we make a distinction between beneficial and harmful strains of the *Stenotrophomonas maltophilia* complex? Frontiers in Microbiology 6:241.

Bradshaw, R.A., W.W. Brickley and K.W. Walker. 1998. N-terminal processing: The methionine aminopeptidase and N^{α}-acetyl transferase families. Trends in Biochemical Sciences 23:263-267.

Brooke, J.S., G. Di Bonaventura, G. Berg and J.-L. Martinez. 2017. Editorial: A multidisciplinary look at *Stenotrophomonas maltophilia*: An emerging multi-drug-resistant global opportunistic pathogen. Frontiers in Microbiology 8:1511.

Brune, P., S. Chakravarthy, G. Graser, C.A. Mathesius, S. McClain, J.S. Petrick, A. Sauve-Ciencewicki, B. Schafer, A. Silvanovich, K. Brink, K. Burgin, D. Bushey, M.L. Cheever, T.

Edrington, H. Fu, V. Habex, R. Herman, E. Islamovic, E.A. Lipscomb, S. Motyka, L. Privalle, R. Ranjan, J. Roper, P. Song, G. Tilton, J. Zhang, S. Waters, A. Ramos, A.H. Culler, P. Hunst, R. Gast, D. Mahadeo and L. Goodwin. 2021. Core and supplementary studies to assess the safety of genetically modified (GM) plants used for food and feed. Journal of Regulatory Science 9:45-60.

Buchanan, B.B., W. Gruissem and R.L. Jones. 2000. Phenylpropanoid and phenylpropanoid-acetate pathway metabolites. Pages 1286-1289 in Biochemistry and Molecular Biology of Plants. American Society of Plant Biologists, Rockville, Maryland.

Caetano-Anollés, G., M. Wang, D. Caetano-Anollés and J.E. Mittenthal. 2009. The origin, evolution and structure of the protein world. Biochemical Journal 417:621-637.

CFIA. 2012. The biology of *Beta vulgaris* L. (Sugar beet). Canadian Food Inspection Agency, Ottawa, Ontario. http://www.inspection.gc.ca/english/plaveg/bio/dir/bio0201e.shtml [Accessed July 22, 2021].

Chakraborty, S., M. Behrens, P.L. Herman, A.F. Arendsen, W.R. Hagen, D.L. Carlson, X.-Z. Wang and D.P. Weeks. 2005. A three-component dicamba *O*-demethylase from *Pseudomonas maltophilia*, strain DI-6: Purification and characterization. Archives of Biochemistry and Biophysics 437:20-28.

Christ, B., R. Hochstrasser, L. Guyer, R. Francisco, S. Aubry, S. Hörtensteiner and J.-K. Weng. 2017. Non-specific activities of the major herbicide-resistance gene *BAR*. Nature Plants 3:937-945.

Clark, S.E. and G.K. Lamppa. 1992. Processing of the precursors for the light-harvesting chlorophyll-binding proteins of photosystem II and photosystem I during import and in an organelle-free assay. Plant Physiology 98:595-601.

Codex Alimentarius. 2009. Foods derived from modern biotechnology. Second Edition. Codex Alimentarius Commission, Joint FAO/WHO Food Standards Programme, Food and Agriculture Organization of the United Nations, Rome, Italy.

Cross, T. 1989. Other genera. Pages 2586-2615 in Bergey's Manual of Systematic Bacteriology. Volume 4. S.T. Williams and M.E. Sharpe (eds.). Williams & Wilkins, Balitmore, Maryland.

D'Ordine, R.L., T.J. Rydel, M.J. Storek, E.J. Sturman, F. Moshiri, R.K. Bartlett, G.R. Brown, R.J. Eilers, C. Dart, Y. Qi, S. Flasinski and S.J. Franklin. 2009. Dicamba monooxygenase: Structural insights into a dynamic Rieske oxygenase that catalyzes an exocyclic monooxygenation. Journal of Molecular Biology 392:481-497.

della-Cioppa, G., S.C. Bauer, B.K. Klein, D.M. Shah, R.T. Fraley and G.M. Kishore. 1986. Translocation of the precursor of 5-*enol*pyruvylshikimate-3-phosphate synthase into chloroplasts of higher plants *in vitro*. Proceedings of the National Academy of Sciences of the United States of America 83:6873-6877.

Depicker, A., S. Stachel, P. Dhaese, P. Zambryski and H.M. Goodman. 1982. Nopaline synthase: Transcript mapping and DNA sequence. Journal of Molecular and Applied Genetics 1:561-573.

Dong, H., C. Zhu, J. Chen, X. Ye and Y.-P. Huang. 2015. Antibacterial activity of S*tenotrophomonas maltophilia* endolysin P28 against both gram-positive and gram-negative bacteria. Frontiers in Microbiology 6:1299.

Dumitru, R., W.Z. Jiang, D.P. Weeks and M.A. Wilson. 2009. Crystal structure of dicamba monooxygenase: A Rieske nonheme oxygenase that catalyzes oxidative demethylation. Journal of Molecular Biology 392:498-510.

FAO-WHO. 1991. Strategies for assessing the safety of foods produced by biotechnology. Report of joint FAO/WHO consultation. World Health Organization, Geneva, Switzerland.

FAO-WHO. 2011a. Pesticide residues in food 2010: Joint FAO/WHO meeting on pesticide residues. FAO Plant Production and Protection Paper 200. Food and Agriculture Organization of the United Nations, World Health Organization, Rome, Italy.

FAO-WHO. 2011b. Summary report: Acceptable daily intakes, acute reference doses, short-term and long-term dietary intakes, recommended maximum residue limits and supervised trials median residue values recorded by the 2011 meeting. Food and Agriculture Organization of the United Nations, World Health Organization, Geneva, Switzerland.

Ferraro, D.J., L. Gakhar and S. Ramaswamy. 2005. Rieske business: Structure-function of Rieske non-heme oxygenases. Biochemical and Biophysical Research Communications 338:175-190.

Fling, M.E., J. Kopf and C. Richards. 1985. Nucleotide sequence of the transposon Tn*7* gene encoding an aminoglycoside-modifying enzyme, 3"(9)-*O*-nucleotidyltransferase. Nucleic Acids Research 13:7095-7106.

Fluhr, R., P. Moses, G. Morelli, G. Coruzzi and N.-H. Chua. 1986. Expression dynamics of the pea *rbcS* multigene family and organ distribution of the transcripts. The EMBO Journal 5:2063-2071.

Franz, J.E., M.K. Mao and J.A. Sikorski. 1997. Glyphosate's molecular mode of action. Pages 521-535 in Glyphosate: A Unique Global Herbicide. American Chemical Society, Washington, D.C.

Frottin, F., A. Martinez, P. Peynot, S. Mitra, R.C. Holz, C. Giglione and T. Meinnel. 2006. The proteomics of N-terminal methionine cleavage. Molecular & Cellular Proteomics 5:2336-2349.

Giglione, C., A. Boularot and T. Meinnel. 2004. Protein N-terminal methionine excision. Cellular and Molecular Life Sciences 61:1455-1474.

Giza, P.E. and R.C.C. Huang. 1989. A self-inducing runaway-replication plasmid expression system utilizing the Rop protein. Gene 78:73-84.

Goodfellow, M. and S.T. Williams. 1983. Ecology of actinomycetes. Annual Review of Microbiology 37:189-216.

Gribble, G.W. 2010. Occurrence. Pages 9-348 in Naturally Occurring Organohalogen Compounds - A Comprehensive Update. Volume 91. Springer-Verlag, New York, New York.

Gruys, K.J., M.C. Walker and J.A. Sikorski. 1992. Substrate synergism and the steady-state kinetic reaction mechanism for EPSP synthase from *Escherichia coli*. Biochemistry 31:5534-5544.

Ha, S.-B. and G. An. 1988. Identification of upstream regulatory elements involved in the developmental expression of the *Arabidopsis thaliana cab1* gene. Proceedings of the National Academy of Sciences of the United States of America 85:8017-8021.

Harayama, S., M. Kok and E.L. Neidle. 1992. Functional and evolutionary relationships among diverse oxygenases. Annual Review of Microbiology 46:565-601.

Harrigan, G.G., K.C. Glenn and W.P. Ridley. 2010a. Assessing the natural variability in crop composition. Regulatory Toxicology and Pharmacology 58:S13-S20.

Harrigan, G.G., D. Lundry, S. Drury, K. Berman, S.G. Riordan, M.A. Nemeth, W.P. Ridley and K.C. Glenn. 2010b. Natural variation in crop composition and the impact of transgenesis. Nature Biotechnology 28:402-404.

Harrigan, G.G., W.P. Ridley, K.D. Miller, R. Sorbet, S.G. Riordan, M.A. Nemeth, W. Reeves and T.A. Pester. 2009. The forage and grain of MON 87460, a drought-tolerant corn hybrid, are compositionally equivalent to that of conventional corn. Journal of Agricultural and Food Chemistry 57:9754-9763.

Harrison, L.A., M.R. Bailey, M.W. Naylor, J.E. Ream, B.G. Hammond, D.L. Nida, B.L. Burnette, T.E. Nickson, T.A. Mitsky, M.L. Taylor, R.L. Fuchs and S.R. Padgette. 1996. The expressed protein in glyphosate-tolerant soybean, 5-enolypyruvylshikimate-3-phosphate synthase from *Agrobacterium* sp. strain CP4, is rapidly digested in vitro and is not toxic to acutely gavaged mice. Journal of Nutrition 126:728-740.

Haslam, E. 1993. Introduction, commentary and overview. Pages 1-16 in Shikimic Acid: Metabolism and Metabolites. John Wiley and Sons, Inc., Chichester, England.

Heller, D., E.J. Helmerhorst, A.C. Gower, W.L. Siqueira, B.J. Paster and F.G. Oppenheim. 2016. Microbial diversity in the early *in vivo*-formed dental biofilm. Applied and Environmental Microbiology 82:1881-1888.

Herman, P.L., M. Behrens, S. Chakraborty, B.M. Chrastil, J. Barycki and D.P. Weeks. 2005. A three-component dicamba *O*-demethylase from *Pseudomonas maltophilia*, strain DI-6: Gene isolation, characterization, and heterologous expression. The Journal of Biological Chemistry 280:24759-24767.

Hernandez-Garcia, C.M. and J.J. Finer. 2014. Identification and validation of promoters and cis-acting regulatory elements. Plant Science 217-218:109-119.

Hérouet, C., D.J. Esdaile, B.A. Mallyon, E. Debruyne, A. Schulz, T. Currier, K. Hendrickx, R.-J. van der Klis and D. Rouan. 2005. Safety evaluation of the phosphinothricin acetyltransferase proteins encoded by the *pat* and *bar* sequences that confer tolerance to glufosinate-ammonium herbicide in transgenic plants. Regulatory Toxicology and Pharmacology 41:134-149.

Herrmann, K.M. 1995. The shikimate pathway: Early steps in the biosynthesis of aromatic compounds. The Plant Cell 7:907-919.

Hochuli, E., W. Bannwarth, H. Döbeli, R. Gentz and D. Stüber. 1988. Genetic approach to facilitate purification of recombinant proteins with a novel metal chelate adsorbent. Nature Biotechnology 6:1321-1325.

Hunt, A.G. 1994. Messenger RNA 3' end formation in plants. Annual Review of Plant Physiology and Plant Molecular Biology 45:47-60.

Illergård, K., D.H. Ardell and A. Elofsson. 2009. Structure is three to ten times more conserved than sequence - A study of structural response in protein cores. Proteins 77:499-508.

ILSI-CERA. 2011. A review of the environmental safety of the PAT protein. International Life Sciences Institute, Center for Environmental Risk Assessment, Washington, D.C.

Itoh, Y., J.M. Watson, D. Haas and T. Leisinger. 1984. Genetic and molecular characterization of the *Pseudomonas* plasmid pVS1. Plasmid 11:206-220.

Janas, K.M., M. Cvikrová, A. Palągiewicz and J. Eder. 2000. Alterations in phenylpropanoid content in soybean roots during low temperature acclimation. Plant Physiology and Biochemistry 38:587-593.

Kämpfer, P. 2006. The family *Streptomycetaceae*, Part I: Taxonomy. Pages 538-604 in The Prokaryotes. A Handbook on the Biology of Bacteria: Archaea. Bacteria: Firmicutes, Actinomycetes. Volume 3. M.Dworkin, S. Falkow, E. Rosenberg, K.-H. Schleifer, and E. Stackebrandt (eds.). Springer+ Business Media, LLC., New York, New York.

Kishore, G., D. Shah, S. Padgette, G. della-Cioppa, C. Gasser, D. Re, C. Hironaka, M. Taylor, J. Wibbenmeyer, D. Eichholtz, M. Hayford, N. Hoffmann, X. Delannay, R. Horsch, H. Klee, S. Rogers, D. Rochester, L. Brundage, P. Sanders and R.T. Fraley. 1988. 5-enolpyruvylshikimate 3-phosphate synthase. From biochemistry to genetic engineering of gIyphosate tolerance. Pages 37-48 in Biotechnology for Crop Protection. P.A. Hedin, J.J. Menn, and R.M. Hollingworth (eds.). American Chemical Society, Washington, D.C.

Klee, H.J., Y.M. Muskopf and C.S. Gasser. 1987. Cloning of an *Arabidopsis thaliana* gene encoding 5-enolpyruvylshikimate-3-phosphate synthase: Sequence analysis and manipulation to obtain glyphosate-tolerant plants. Molecular and General Genetics 210:437-442.

Klein, J., J. Altenbucher and R. Mattes. 1998. Nucleic acid and protein elimination during the sugar manufacturing process of conventional and transgenic sugar beets. Journal of biotechnology 60:145-153.

Krueger, J.P., R.G. Butz, Y.H. Atallah and D.J. Cork. 1989. Isolation and identification of microorganisms for the degradation of dicamba. Journal of Agricultural and Food Chemistry 37:534-538.

Kuluev, B.R. and A.V. Chemeris. 2007. Amplification and cloning of dahlia mosaic virus and carnation etched ring virus promoters. Russian Journal of Genetics 43:1413-1414.

Kutzner, H.J. 1981. The family streptomycetaceae. Pages 2028-2090 in The Prokaryotes: A Handbook on Habitats, Isolation, and Identification of Bacteria. Volume 2. M.P. Starr, H. Stolp, H.G. Trüper, A. Balows, and H.G. Schlegel (eds.). Springer-Verlag, Berlin, Germany.

Lege, K.E., J.T. Cothren and C.W. Smith. 1995. Phenolic acid and condensed tannin concentrations of six cotton genotypes. Environmental and Experimental Botany 35:241-249.

Lindsey, K. and P. Gallois. 1990. Transformation of sugarbeet (*Beta vulgaris*) by *Agrobacterium tumefaciens*. Journal of Experimental Botany 41:529-536.

Lira, F., G. Berg and J.L. Martínez. 2017. Double-face meets the bacterial world: The opportunistic pathogen *Stenotrophomonas maltophilia*. Frontiers in Microbiology 8:2190.

Locci, R. 1989. Streptomycetes and related genera. Pages 2451-2508 in Bergey's Manual of Systematic Bacteriology. Volume 4. S.T. Williams and M.E. Sharpe (eds.). Williams & Wilkins, Baltimore, Maryland.

Maeda, H. and N. Dudareva. 2012. The shikimate pathway and aromatic amino acid biosynthesis in plants. Annual Review of Plant Biology 63:73-105.

Manderscheid, R. and A. Wild. 1986. Studies on the mechanism of inhibition by phosphinothricin of glutamine synthetase isolated from *Triticum aestivum* L. Journal of Plant Physiology 123:135-142.

McGinnis, R.A. 1982. Beet-sugar technology. Third Edition. Beet Sugar Development Foundation, Denver, Colorado.

Mehrotra, S. and V. Goyal. 2012. *Agrobacterium*-mediated gene transfer in plants and biosafety considerations. Applied Biochemistry and Biotechnology 168:1953-1975.

Meier, U. 2001. BBCH Monograph. Second Edition. Growth stages of mono-and dicotyledonous plants. U. Meier (ed.). Federal Biological Research Centre for Agriculture and Forestry, Bonn, Germany.

Meinnel, T. and C. Giglione. 2008. Tools for analyzing and predicting N-terminal protein modifications. Proteomics 8:626-649.

Mukherjee, P. and P. Roy. 2016. Genomic potential of *Stenotrophomonas maltophilia* in bioremediation with an assessment of its multifaceted role in our environment. Frontiers in Microbiology 7:967.

Nester, E.W. 2015. *Agrobacterium*: Nature’s genetic engineer. Frontiers in Plant Science 5:730.

OECD-FAO. 2021. Table C.23.2 - Sugar projections: Consumption, per capita. OECD-FAO agricultural outlook 2021-2030. Organisation for Economic Co-operation and Development, Food Agriculture Organization of the United Nations, Paris, France. https://www.oecd-ilibrary.org/agriculture-and-food/sugar-projections-consumption-per-capita_4ad4cf3a-en [Accessed February 16, 2023].

OECD. 1999. Consensus document on general information concerning the genes and their enzymes that confer tolerance to phosphinothricin herbicide. ENV/JM/MONO(99)13. Series on Harmonization of Regulatory Oversight in Biotechnology No.11. Organisation for Economic Co-operation and Development, Paris, France.

OECD. 2001. Consensus document on the biology of *Beta vulgaris* L. (Sugar beet). ENV/JM/MONO(2001)11. Organisation for Economic Co-operation and Development, Paris, France.

OECD. 2002a. Consensus document on compositional considerations for new varieties of sugar beet: Key food and feed nutrients and antinutrients. ENV/JM/MONO(2002)4. Organisation for Economic Co-operation and Development, Paris, France.

OECD. 2002b. Report of the OECD workshop on the toxicological and nutritional testing of novel foods. SG/ICGB(1998)1/FINAL. Organisation for Economic Co-operation and Development, Paris, France.

OECD. 2002c. Module II: Herbicide biochemistry, herbicide metabolism and the residues in glufosinate-ammonium (Phosphinothricin)-tolerant transgenic plants. ENV/JM/MONO(2002)14. Series on Harmonization of Regulatory Oversight in Biotechnology No. 25. Organisation for Economic Co-operation and Development, Paris, France.

Okuno, N.T., I.R. Freire, R.T.R.S. Segundo, C.R. Silva and V.A. Marin. 2018. Polymerase chain reaction assay for detection of *Stenotrophomonas maltophilia* in cheese samples based on the *smeT* gene. Current Microbiology 75:1555-1559.

Padgette, S.R., D.B. Re, G.F. Barry, D.E. Eichholtz, X. Delannay, R.L. Fuchs, G.M. Kishore and R.T. Fraley. 1996. New weed control opportunities: Development of soybeans with a Roundup Ready™ gene. Pages 53-84 in Herbicide-Resistant Crops: Agricultural, Environmental, Economic, Regulatory and Technical Aspects. S.O. Duke (ed.). CRC Press, Inc., Boca Raton, Florida.

Palleroni, N.J. and J.F. Bradbury. 1993. *Stenotrophomonas*, a new bacterial genus for *Xanthomonas maltophilia* (Hugh 1980) Swings et al. 1983. International Journal of Systematic Bacteriology 43:606-609.

Rademacher, T.W., R.B. Parekh and R.A. Dwek. 1988. Glycobiology. Annual Review of Biochemistry 57:785-838.

Ridley, W.P., G.G. Harrigan, M.L. Breeze, M.A. Nemeth, R.S. Sidhu and K.C. Glenn. 2011. Evaluation of compositional equivalence for multitrait biotechnology crops. Journal of Agricultural and Food Chemistry 59:5865-5876.

Salomon, S. and H. Puchta. 1998. Capture of genomic and T-DNA sequences during double-strand break repair in somatic plant cells. The EMBO Journal 17:6086-6095.

Schmelz, E.A., J. Engelberth, H.T. Alborn, P. O'Donnell, M. Sammons, H. Toshima and J.H. Tumlinson. 2003. Simultaneous analysis of phytohormones, phytotoxins, and volatile organic compounds in plants. Proceedings of the National Academy of Sciences of the United States of America 100:10552-10557.

Sikorski, J.A. and K.J. Gruys. 1997. Understanding glyphosate's molecular mode of action with epsp synthase: Evidence favoring an allosteric inhibitor model. Accounts of Chemical Research 30:2-8.

Silvanovich, A., M.A. Nemeth, P. Song, R. Herman, L. Tagliani and G.A. Bannon. 2006. The value of short amino acid sequence matches for prediction of protein allergenicity. Toxicological Sciences 90:252-258.

Steinrücken, H.C. and N. Amrhein. 1980. The herbicide glyphosate is a potent inhibitor of 5-enolpyruvylshikimic acid-3-phosphate synthase. Biochemical and Biophysical Research Communications 94:1207-1212.

Sutcliffe, J.G. 1979. Complete nucleotide sequence of the *Escherichia coli* plasmid pBR322. Cold Spring Harbor Symposia on Quantitative Biology 43:77-90.

Tashkov, W. 1996. Determination of formaldehyde in foods, biological media and technological materials by headspace gas chromatography. Chromatographia 43:625-627.

Thomas, K., M. Aalbers, G.A. Bannon, M. Bartels, R.J. Dearman, D.J. Esdaile, T.J. Fu, C.M. Glatt, N. Hadfield, C. Hatzos, S.L. Hefle, J.R. Heylings, R.E. Goodman, B. Henry, C. Herouet, M. Holsapple, G.S. Ladics, T.D. Landry, S.C. MacIntosh, E.A. Rice, L.S. Privalle, H.Y. Steiner, R. Teshima, R. van Ree, M. Woolhiser and J. Zawodny. 2004. A multi-laboratory evaluation of a common in vitro pepsin digestion assay protocol used in assessing the safety of novel proteins. Regulatory Toxicology and Pharmacology 39:87-98.

Thomas, K., G. Bannon, S. Hefle, C. Herouet, M. Holsapple, G. Ladics, S. MacIntosh and L. Privalle. 2005. In silico methods for evaluating human allergenicity to novel proteins: International Bioinformatics Workshop Meeting Report, 23-24 February 2005. Toxicological Sciences 88:307-310.

Thompson, C.J., N.R. Movva, R. Tizard, R. Crameri, J.E. Davies, M. Lauwereys and J. Botterman. 1987. Characterization of the herbicide-resistance gene *bar* from *Streptomyces hygroscopicus*. The EMBO Journal 6:2519-2523.

Todaro, M., N. Francesca, S. Reale, G. Moschetti, F. Vitale and L. Settanni. 2011. Effect of different salting technologies on the chemical and microbiological characteristics of PDO Pecorino Siciliano cheese. European Food Research and Technology 233:931-940.

Torres, M., O. Palomares, J. Quiralte, G. Pauli, R. Rodríguez and M. Villalba. 2015. An enzymatically active β-1,3-glucanase from ash pollen with allergenic properties: A particular member in the Oleaceae family. PLoS ONE 10:e0133066.

Tzin, V., S. Malitsky, M.M.B. Zvi, M. Bedair, L. Sumner, A. Aharoni and G. Galili. 2012. Expression of a bacterial feedback-insensitive 3-deoxy-D-arabino-heptulosonate 7-phosphate synthase of the shikimate pathway in *Arabidopsis* elucidates potential metabolic bottlenecks between primary and secondary metabolism. New Phytologist 194:430-439.

U.S. EPA. 1997. Phosphinothricin acetyltransferase and the genetic material necessary for its production in all plants; Exemption from the requirement of a tolerance on all raw agricultural commodities. Federal Register 62:17717-17720.

U.S. EPA. 2009. Reregistration eligibility decision for dicamba and associated salts. June 8, 2006, as amended June 17, 2009. U.S. Environmental Protection Agency, Washington, D.C.

Venkatesh, T.V., M.L. Breeze, K. Liu, G.G. Harrigan and A.H. Culler. 2014. Compositional analysis of grain and forage from MON 87427, an inducible male sterile and tissue selective glyphosate-tolerant maize product for hybrid seed production. Journal of Agricultural and Food Chemistry 62:1964-1973.

Walton, J. 2022. The 5 countries that produce the most sugar. Investopedia, New York, New York.

Wang, C., K.C. Glenn, C. Kessenich, E. Bell, L.A. Burzio, M.S. Koch, B. Li and A. Silvanovich. 2016. Safety assessment of dicamba mono-oxygenases that confer dicamba tolerance to various crops. Regulatory Toxicology and Pharmacology 81:171-182.

Wang, K., Y. Yuan, H. Li, J.-H. Cho, D. Huang, L. Gray, S. Qin and D.J. Galas. 2013. The spectrum of circulating RNA: A window into systems toxicology. Toxicological Sciences 132:478-492.

Wang, X.-Z., B. Li, P.L. Herman and D.P. Weeks. 1997. A three-component enzyme system catalyzes the O demethylation of the herbicide dicamba in *Pseudomonas maltophilia* DI-6. Applied and Environmental Microbiology 63:1623-1626.

Wehrmann, A., A.V. Vliet, C. Opsomer, J. Botterman and A. Schulz. 1996. The similarities of *bar* and *pat* gene products make them equally applicable for plant engineers. Nature Biotechnology 14:1274-1278.

Wild, A. and R. Manderscheid. 1984. The effect of phosphinothricin on the assimilation of ammonia in plants. Zeitschrift für Naturforschung C 39:500-504.

Wohlleben, W., W. Arnold, I. Broer, D. Hillemann, E. Strauch and A. Pühler. 1988. Nucleotide sequence of the phosphinothricin *N*-acetyltransferase gene from *Streptomyces viridochromogenes* Tü494 and its expression in *Nicotiana tabacum*. Gene 70:25-37.

Zambryski, P., A. Depicker, K. Kruger and H.M. Goodman. 1982. Tumor induction by *Agrobacterium tumefaciens*: Analysis of the boundaries of T-DNA. Journal of Molecular and Applied Genetics 1:361-370.

Zhou, J., K.H. Berman, M.L. Breeze, M.A. Nemeth, W.S. Oliveira, D.P.V. Braga, G.U. Berger and G.G. Harrigan. 2011. Compositional variability in conventional and glyphosate-tolerant

soybean (*Glycine max* L.) varieties grown in different regions in Brazil. Journal of Agricultural and Food Chemistry 59:11652-11656.